Durham University

Durham E-Theses

Interactions of water and calcium ions with food components, studied by NMR

Khaliq, Abdul

How to cite:

Khaliq, Abdul (1995) *Interactions of water and calcium ions with food components, studied by NMR*, Durham theses, Durham University. Available at Durham E-Theses Online: http://etheses.dur.ac.uk/4884/

Use policy

The full-text may be used and/or reproduced, and given to third parties in any format or medium, without prior permission or charge, for personal research or study, educational, or not-for-profit purposes provided that:

- a full bibliographic reference is made to the original source
- a link is made to the metadata record in Durham E-Theses
- the full-text is not changed in any way

The full-text must not be sold in any format or medium without the formal permission of the copyright holders.

Please consult the full Durham E-Theses policy for further details.

Academic Support Office, The Palatine Centre, Durham University, Stockton Road, Durham, DH1 3LE
e-mail: e-theses.admin@durham.ac.uk Tel: +44 0191 334 6107
http://etheses.dur.ac.uk

The copyright of this thesis rests with the author.
No quotation from it should be published without
his prior written consent and information derived
from it should be acknowledged.

Interactions of Water and Calcium Ions with Food Components, Studied by NMR.

By Abdul Khaliq

A Thesis submitted in partial fulfilment of the requirements for the degree of Doctor of Philosophy at the University of Durham.

Department of Chemistry
University of Durham
January, 1995

UNIV DUNELM
14 JUN 1995

ABSTRACT

NMR studies of water oxygen-17 relaxation in aqueous sucrose and lysozyme solutions have been carried out to investigate the interactions of water with sucrose and lysozyme. The effect of sucrose and lysozyme concentration on water oxygen-17 relaxation has been studied in detail. The dependence of relaxation on frequency and pH has also been analysed. The existing model, describing the relaxation of water oxygen-17 in aqueous protein solutions suggested by Halle in 1981, is tested to see whether it gives a true representation. It is found that at low concentrations of sucrose and lysozyme, the experimental data give good agreement with the model. However, at saturated sucrose concentration the agreement is not so good. An extra contribution to the transverse relaxation rate is seen. A possible explanation for the extra contribution to the transverse relaxation rate at high sucrose content is discussed. The effect of ionic charge on oxygen-17 relaxation in lysozyme solutions is also investigated. It is observed that both the ionic charge of lysozyme as well as lysozyme aggregation strongly affect the relaxation of water oxygen-17. A method for analysing the experimental data for water oxygen-17 relaxation in aqueous sucrose and lysozyme solutions using Halle's model is presented and employed to calculate the various parameters of the model.

The relaxation and chemical shift of calcium-43 in simple calcium salts, calcium acetate and calcium ascorbate have been studied as a function of concentration and pH. The complexation of calcium to sucrose and to lysozyme has also been investigated. In almost all cases, a significant calcium-43 chemical shift has been detected. The direct measurement of complexation and binding of calcium by relaxation time and chemical shift measurements has been of particular interest.

ACKNOWLEDGEMENTS

I would like to take this opportunity to thank my supervisor, Prof. R.K. Harris, for his constant help, support and encouragement throughout this study. I am indebted to Prof. P.S. Belton and Dr. B.P. Hills, Institute of Food Research, Norwich, for many helpful discussions, ideas and valuable contributions. I am also grateful to Dr. Ray Matthews, Barry Say (University of Durham) and Dr. John Parkinson (University of Edinburgh) for their help and expertise in using the various NMR spectrometers.

It is with great pleasure that I thank all the colleagues of the NMR group for their friendship and for providing a pleasant working environment. Many thanks to Graham Almond for his help with computers and for many interesting discussions, not necessarily on NMR.

The funding and financial support provided by AFRC and the Institute of Food Research is greatly appreciated.

MEMORANDUM

The research presented in this thesis has been carried out in the Department of Chemistry, University of Durham, and in the AFRC Institute of Food Research, Norwich, between October 1991 and September 1994. It is the original work of the author unless stated otherwise. None of this work has been submitted for any other degree.

The copyright of this thesis rests with the author. No quotation from it should be published without his prior written consent and any information derived from it should be acknowledged.

CONTENTS

Chapter 1	**NMR Theory**	**1**
1.1)	General	1
1.2)	Larmor Precession	2
1.3)	NMR Signal Intensity	3
1.4)	Relaxation	6
1.5)	Spectral Density	8
Chapter 2	**Quadrupolar Relaxation**	**13**
2.1.1)	Quadrupole Moment	13
2.1.2)	Electric Field Gradient	14
2.2)	Model for ^{17}O Relaxation in Biological Systems	20
2.3)	Halle's Model	20
2.4)	Mathematical Form of Halle's Model	21
2.5)	^{17}O Quadrupole Coupling Constant	23
2.6)	Order Parameter	25
2.7)	Asymmetry Parameter	26
Chapter 3	**^{17}O NMR Literature Review**	**29**
3.1)	Water Studies in Food	29
3.2)	Water Relaxation	30
3.3)	Simple Sugar Solutions	32
3.4)	Protein Solutions	33
3.5)	Heterogeneous Food Systems	35
3.6)	Plant Tissue Solutions	36
3.7)	Muscle Tissue	37

Chapter 4	Water ^{17}O Study in Sucrose Solutions	42
4.1)	Relaxation of ^{17}O	43
4.2)	Relaxation of Water ^{17}O in Sucrose Solutions	45
4.3)	Sucrose Solution Preparation	46
4.4)	Sample Temperature	49
4.5)	Spectrometer Performance	49
4.5.1)	Tuning	49
4.5.2)	Shimming	49
4.6)	Measurement of Spin-Lattice Relaxation Time, T_1	50
4.7)	Measurement of Spin-Spin Relaxation Time, T_2	52
4.8)	Analysis of Experimental Data	53
4.9)	pH Effect on ^{17}O Relaxation	60
4.10)	Effect of Sucrose Concentration on ^{17}O Relaxation	68
4.11)	Protocol for the Analysis of Relaxation Data	74
4.11.1)	Halle's Model	75
4.11.2)	Calculation of τ_s	76
4.11.3)	Calculation of $P_{bw}S^2$ and Hence S	79
4.11.4)	Alternative Method for Calculating τ_s and S	80
4.11.5)	Calculation of R^f_{bw} and τ_f	82
4.11.6)	Calculation of P_{bw} at Low Concentrations of Sucrose	85
4.11.7)	Summary of Analysis	88
4.12)	Frequency Dependence of ^{17}O Relaxation	91
4.12.1)	Frequency Dependence of ^{17}O Relaxation in Lysozyme	102
4.12.2)	Possible Explanation for Unexpected Frequency Dependence	104
4.13)	^{17}O Sucrose Conclusion	116

Chapter 5	**^{17}O Study in Lysozyme**	**119**
5.1)	Lysozyme Experiments	119
5.2)	Lysozyme Sample Preparation	121
5.3)	Lysozyme Results	122
5.3.1)	Absence of Salt	122
5.3.2)	Presence of Salt	136
5.4)	Lysozyme Discussion	145
5.4.1)	Absence of Salt	146
5.4.2)	Presence of Salt	147
5.5)	^{17}O Lysozyme Conclusion	151
Chapter 6	**Calcium-43 Studies**	**157**
6.1)	Aim	158
6.2)	Introduction	160
Chapter 7	**^{43}Ca Literature Review**	**163**
7.1)	Simple Salts	164
7.2)	Complex Formation with Low Molecular Weight Ligands	166
7.3)	Binding to Polyions	168
7.4)	Binding to Proteins	170
7.5)	NMR Studies Using Substitution Probes for Calcium	175
7.6)	^{1}H and ^{19}F NMR Studies to Investigate Calcium Binding to Biological Molecules	175
Chapter 8	**^{43}Ca Results and Discussion**	
8.1)	Experimental	180
8.2)	Results	184
8.2.1)	Calcium Chloride	188

8.2.2) Calcium Bromide 192
8.2.3) Calcium Iodide 195
8.2.4) Calcium Nitrate 198
8.2.5) Calcium Acetate 201
8.2.6) Calcium Ascorbate 204
8.2.7) Calcium-Sucrose 207
8.2.8) Calcium-Lysozyme 210
8.3) ^{43}Ca Discussion 211
8.3.1) ^{43}Ca Relaxation 211
8.3.2) Concentration Dependence of Relaxation 212
8.3.3) Chemical Shift 221
8.3.4) pH Effect 227
8.4) ^{43}Ca Conclusion 235

Appendix

NMR Theory

1.1) General

Nuclei with an odd mass number or those with an even mass number but an odd charge number possess the property of spin, characterised by the quantum number, I. These nuclei behave like bar magnets which when placed in an external magnetic field, B_O, will interact with that field. Quantum theory allows a nucleus to exist in 2I+1 states, characterised by the azimuthal quantum number m_I, which can take the values -I, -I+1, ..., +I. This quantum number determines the spin angular momentum component, p_Z

$$p_z = m_I.(h/2\pi) \qquad \text{eqn 1.1}$$

The possession of both spin and charge confers on the nucleus a magnetic moment, μ. The magnitude of μ is determined by the value of p

$$\mu_z = \gamma.p_z \qquad \text{eqn 1.2}$$

The gyromagnetic ratio, γ, is a characteristic of the nucleus and may be either positive or negative.

The energies of the quantised states are given by

$$U = \mu.B_o \qquad \text{eqn 1.3}$$

In the absence of an external magnetic field the states are degenerate. However, the degeneracy of the states is lifted by a magnetic field, whereby the energy of separation is proportional to the strength of the field B_O. At equilibrium, the lowest energy state will be the more highly populated according to Boltzmann distribution. Transitions

UNIV DUNELM

between energy levels can be stimulated by external radiation. A spectral line in an NMR spectrum corresponds to resonance between two energy states at the so called Larmor frequency, given by

$$\nu_L = (\gamma/2\pi).B_o.\Delta m_I \qquad \text{eqn 1.4}$$

The selection rule governing NMR transitions is $\Delta m_I = \pm 1$. Hence equation 1.4 can be written as

$$\nu_L = (\gamma/2\pi).B_o \qquad \text{eqn 1.5}$$

1.2) Larmor Precession

In the presence of an applied magnetic field, B_O, the magnetic moment experiences a torque which tends to align the magnetic moment perpendicular to the field. Since, this torque can only alter the component of angular momentum, p, which is perpendicular to B_O and μ, the net result corresponds to a rotation of μ about B_O in a cone-like shape, Fig 1.1. Such a movement is known as precession and at the Larmor frequency is referred to as Larmor precession. The induced angular velocity of the Larmor precession is given by $\omega_o = -\gamma B_o$

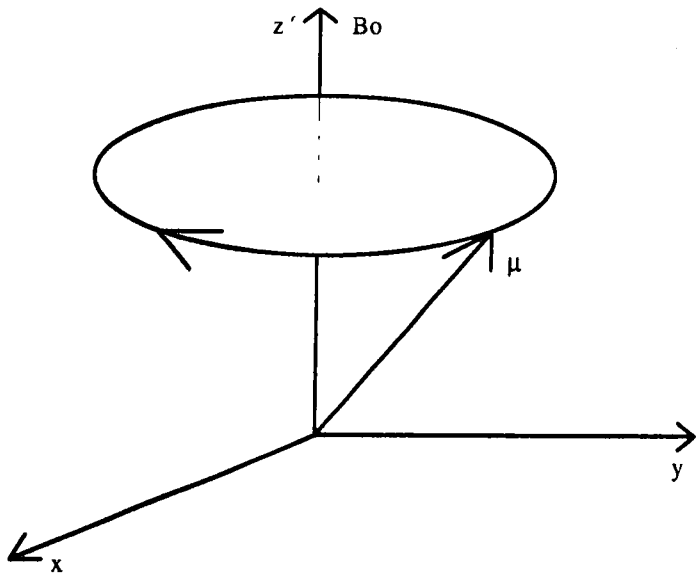

Fig 1.1 Precession of a magnetic moment μ about an applied B_0

1.3) NMR Signal Intensity

The low frequency of nuclear magnetic resonance absorption (radio-frequency range) indicates that the energy separation between spin states is quite small. In fact, the energy difference between two states, $\Delta U = \gamma\hbar B_0$, at normal temperatures is much less than the thermal energy kT.

According to the Boltzmann distribution, more spins are expected to reside in the lowest energy state at equilibrium. For two spin states, Boltzmann distribution gives

$$n_h/n_l = e^{-\Delta U/kT} \qquad \text{eqn 1.6}$$

where n_h and n_l are the number of nuclei in the high and low energy states respectively, ΔU is the energy separation between the two states, k is the Boltzmann constant, and T is the temperature.

From Boltzmann distribution, the population difference between the two states is calculated to be

$$n_l - n_h = \Delta n_0 = N\Delta U/2kT \qquad \text{eqn 1.7}$$

where N is the total number of nuclei in the sample, and the subscript zero refers to the equilibrium situation.

The total magnetic moment or magnetisation, M, of a sample is given by the resultant of the individual magnetic moments. At equilibrium M is expected to be along the +z direction. For a two spin state system (I = 1/2), the magnitude of M at equilibrium is given by

$$M_o = n_l\mu_{zl} + n_h\mu_{zh} = \Delta n_o\mu_{zl} = \tfrac{1}{2}\gamma\hbar\Delta n_o \qquad \text{eqn 1.8}$$

here, $\mu_{zh} = -\mu_{zl}$, and $\mu_{zl} = \frac{1}{2}\gamma\hbar$ (where $m_l = \frac{1}{2}$)

Substitution for Δn_o gives the expression

$$M_o = \tfrac{1}{4}N\gamma\hbar\,\Delta U/kT = \tfrac{1}{4}N(\gamma\hbar)^2\,B_o/kT \qquad \text{eqn 1.9}$$

Thus, the intensity of an NMR signal is proportional to N, γ^2, and B_O.

Transitions between the energy states are induced by a sinusoidally oscillating magnetic field, B_1. In practice, B_1 is a radio frequency (RF) field oscillating in the x-direction. Resonance is attained when the frequency of B_1 is equal to the Larmor frequency, ν_L

$$\nu_L = (\gamma/2\pi).B_o \qquad \text{eqn 1.10}$$

The RF field can be thought of as stimulating both absorption and emission of energy by the spin system (i.e. as stimulating upward and downward spin transitions), but resulting in a net absorption of energy because an excess of spins occupy the low energy state which can be promoted to the high energy state.

All the above is, of course, very elementary where only the basic ideas behind the NMR technique have been outlined. A more considerable and detailed study of NMR theory can be found in many textbooks.[1 - 6]

1.4) Relaxation

If after perturbing a spin system from its equilibrium state, the perturbation influence is removed, the system will tend to return to its original equilibrium condition. Such a process is known as relaxation. However, the spin system does not return instantaneously, but takes a finite time, T, to readjust to the changed conditions. Relaxation can occur by two processes.

Relaxation along the direction of the applied field (i.e. along the z-direction) is known as the spin-lattice or longitudinal relaxation, and is characterised by a time T_1. In fact, longitudinal relaxation describes the approach of the z-component of the nuclear magnetisation, M_Z, towards equilibrium. The process of longitudinal relaxation involves the transfer of energy from the spin system to the lattice (i.e. surroundings) and thus involves transitions between the energy levels. In many circumstances the relaxation is considered to be exponential with a first-order rate constant where the return of the magnetisation to equilibrium occurs according to the equation

$$M_z(t) - M_\infty = [M_z(0) - M_\infty]e^{-t/T_1} \qquad \text{eqn 1.11}$$

Relaxation can also occur perpendicular to the applied field, *i.e.* in the x-y plane. This involves an entropy change rather than an energy change, where the spins lose their coherence and are dephased. The spread of spins causes relaxation which is known as spin-spin relaxation or transverse relaxation and is characterised by a time T_2. For solutions transverse relaxation is also often considered to be exponential with a first-order rate constant. The magnetisation is expected to fall according to the equation

$$M_y(t) = M_y(0)e^{-t/T_2} \qquad \text{eqn 1.12}$$

In order to achieve either type of relaxation, a fluctuating magnetic field is required to cause transitions between the spin states. In solutions a fluctuating magnetic field is produced by molecules undergoing rapid Brownian motion, i.e. diffusing and rotating randomly so that the nuclear magnets in the system are continually moving relative to each other and thus producing chaotic fluctuating magnetic fields at all points within the sample. Over the long term these fields average out to zero but at any instant will contain a component of random intensity and phase at the Larmor frequency, and it is this component which effects interchange of nuclear energy between the spin system and the surroundings (i.e. changes the spin populations between the states until Boltzmann equilibrium is re-established) and gives rise to the T_1 relaxation mechanism. Since the internal field due to Brownian motion has different values for each nucleus at each instant of time, then a range of precession frequencies will be produced and T_2 relaxation also occurs. Thus, fluctuations which cause transitions between states result in both the changes of population associated with T_1 relaxation and dephasing of spins associated with T_2 relaxation. However, transverse relaxation can also occur at zero frequency, unlike longitudinal relaxation, because it does not require a fluctuating field at the Larmor frequency to cause a transition.

Often in mobile liquids $T_1 = T_2$ because the interactions causing relaxation contain a complete range of frequencies (equivalent to white noise).

1.5) Spectral Density, J(ω)

If a pair of spins, originally infinitely far apart from each other, are brought together to a normal internuclear distance in a molecule, then an energy of interaction between the two spins will exist. For a particular molecular arrangement, the energy of interaction will be constant. If, however, the energy of interaction is time dependent due to the random motion of the spins with respect to each other, then the interaction energy will be distributed in both frequency and time. The frequency dependence is called the spectral density, $J(\omega)$, and represents the power available from the fluctuations at the relevant frequency, ω. Its value at the transition frequency, $J(\omega_L)$, can cause a transition (i.e. an interaction between the nuclear magnets with the surroundings to allow energy exchange) and thus facilitate longitudinal relaxation.
The time dependence term, f(t), is expressed in terms of an *auto-correlation function*, $G(\tau)$, defined as

$$G(\tau) = \overline{f(t)f^*(t+\tau)} \qquad \text{eqn 1.13}$$

The horizontal bar indicates an overall average for all the spins. This function is independent of t but indicates how f(t) changes with time τ (i.e. it represents the differences between f(t) values over short intervals of time τ). As τ increases, this function is often assumed to decay exponentially according to

$$G(\tau) = \exp\left(-|\tau|/\tau_c\right) \qquad \text{eqn 1.14}$$

where τ_c is the *correlation time* for a particular motion involved.

For small values of τ, f^* at $t + \tau$ is highly correlated with the initial value of f, whereas for longer τ values, f and f^* become independent variables which are no longer correlated. Hence, the correlation function decreases with increasing τ.

In fact $G(\tau)$ is the time domain function of $J(\omega)$ in the frequency domain. The two functions are related by Fourier transformation.

$$J(\omega) = \int_{-\infty}^{\infty} G(\tau)\exp(-i\,\omega\tau)d\tau \qquad \text{eqn 1.15}$$

$$G(\omega) = \frac{1}{2\pi}\int_{-\infty}^{\infty} J(\omega)\exp(i\,\omega\tau)d\omega \qquad \text{eqn 1.16}$$

Substituting eqn 1.14 into eqn 1.15, followed by integration gives a Lorentzian form of $J(\omega)$

$$J(\omega) = \frac{2\tau_c}{1+\omega^2\tau_c^2} \qquad \text{eqn 1.17}$$

In simple cases the spin-lattice relaxation rate, $1/T_1$, is directly related to the value of the spectral density function at the Larmor precession frequency of the nucleus.

$$1/T_1 \propto J(\omega)$$

$$\text{i.e.} \quad 1/T_1 \propto 2\tau_c/(1+\omega^2\tau_c^2) \qquad \text{eqn 1.18}$$

In Fig 1.2 a plot of $J(\omega)$ vs log ω is shown. The flat portion represents the *extreme narrowing region* for which fast motion occurs and $\omega^2\tau_c^2 << 1$. Outside the extreme narrowing region a sudden drop in the $J(\omega)$ occurs with increasing log ω. However, for most non-viscous solutions τ_c is of the order of ps. Thus the extreme narrowing condition is expected to be applicable.

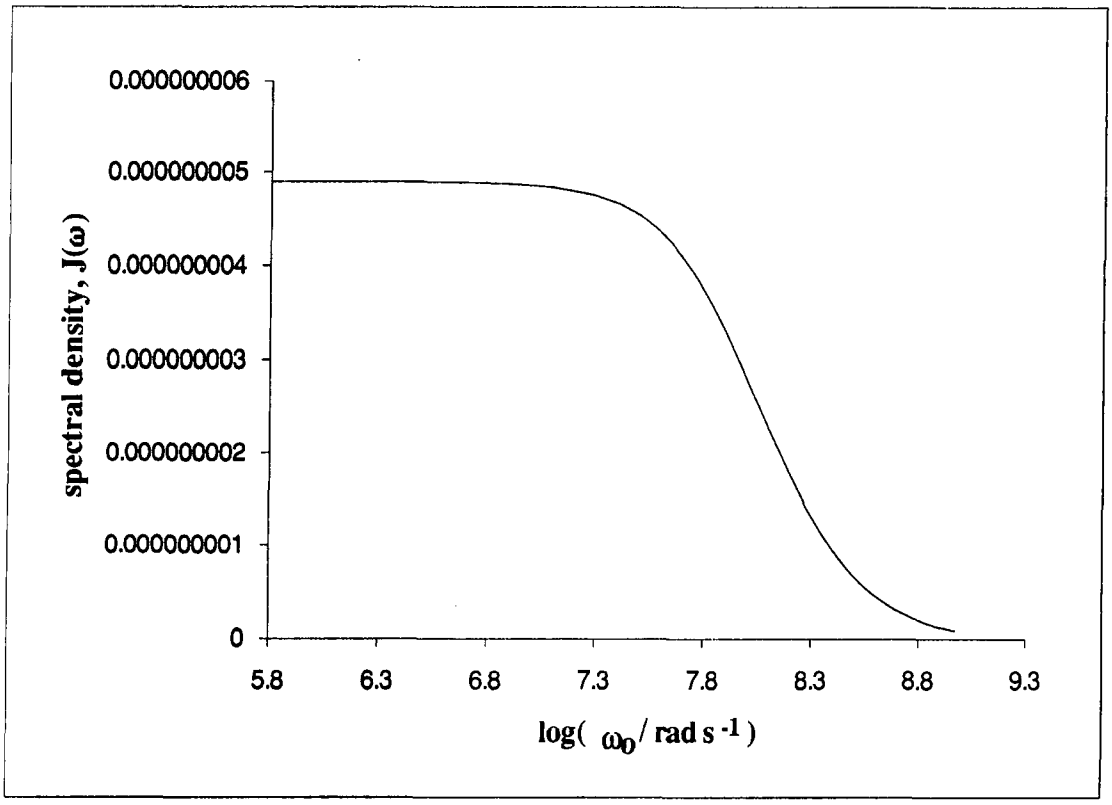

Fig 1.2 The dependence of spectral density, J(ω), on frequency

The full form of J(ω) predicts a minimum in T_1 as a function of τ_c, Fig 1.3. The T_1 minimum occurs when the sudden drop in J(ω) as a function of log ω corresponds to the resonance frequency i.e. $\tau_c = 1/\omega$

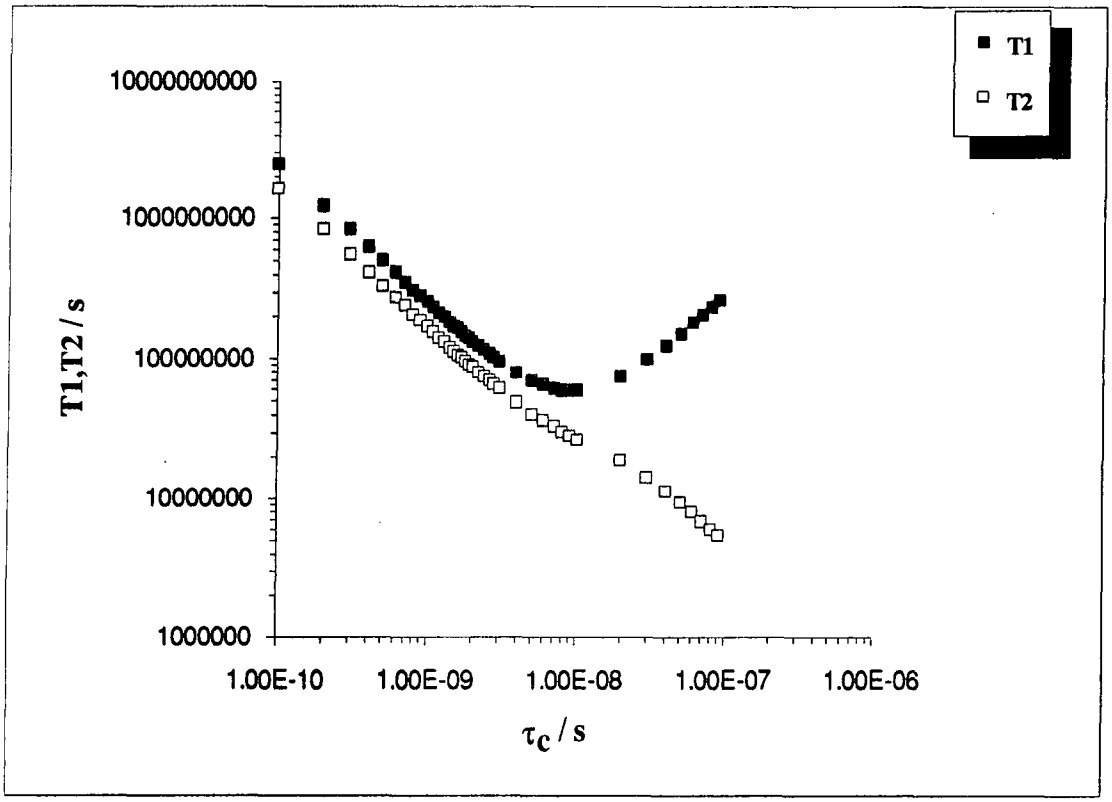

Fig 1.3 The dependence of T_1 and T_2 on correlation time, τ_c

The T_1 minimum is dependent on the frequency and is expected to increase with increasing frequency.

In Fig 1.3 the transverse relaxation time is seen to decrease continuously with increasing correlation time. This continuous decrease is the result of the dependence of transverse relaxation on the zero frequency term. Since transverse relaxation is a dephasing process which does not require a transition, relaxation can occur at zero frequency, unlike longitudinal relaxation which requires a transition and thus a fluctuating field at the resonance frequency.

REFERENCES

1) R. K. Harris, *NMR Spectroscopy*, Longman Scientific & Technical, 1986

2) J. Mason, *Multinuclear NMR*, Plenum Press, 1987

3) A. E. Derome, *Modern NMR Techniques for Chemistry Research*, Pergamon Press, **6**, 1987

4) E. Fukushima and S. B. W. Roeder, *Experimental Pulse NMR - A Nuts and Bolts Approach*, Addison - Wesley Publishing Co., 1981

5) J. W. Akitt, *NMR and Chemistry - An Introduction to the FT Multinuclear Era*, Chapman and Hall, **2**, 1983

6) H. Gunther, *NMR Spectroscopy - An Introduction*, Wiley, 1980

2) Quadrupolar relaxation

All nuclei with a spin greater than I = 1/2 possess a nuclear quadrupole moment due to a non-spherical distribution of positive charge at the nucleus. The quadrupolar moment can interact with a fluctuating, time-dependent, electric field gradient, produced by the electric environment at the nucleus and gives rise to quadrupolar relaxation. This is the only case where a fluctuating magnetic field is not required for relaxation, and it is effective because the quadrupole moment is coaxial with the spin. Since both oxygen-17 and calcium-43 have a spin greater than 1/2 (for ^{17}O, I = 5/2, and for ^{43}Ca, I = 7/2) then quadrupolar relaxation is expected for these nuclei. The magnitude of the quadrupole moment and the electric field gradient determine the efficiency of quadrupolar relaxation. Generally, for quadrupolar nuclei relaxation by other mechanisms can be neglected.

2.1.1) quadrupole moment

A non-spherical distribution of positive charge at the nucleus gives rise to a quadrupole moment, Q. The charge distribution in such a case is usually ellipsoidal with two types. The distribution is either slightly flattened (oblate — discus-shape) or slightly elongated (prolate — rugby ball shape). Since, there are two types of charge distribution, quadrupole moments possess a sign. A prolate quadrupole is denoted by a positive sign, whereas an oblate quadrupole is given a negative sign.

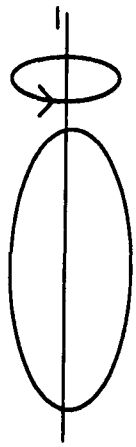

prolate charge distribution

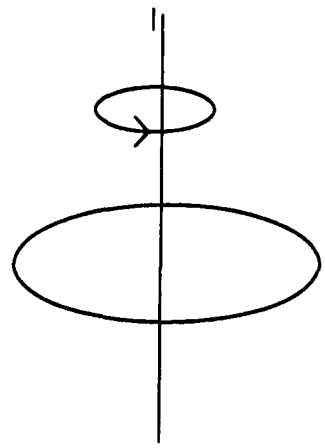

oblate charge distribution

2.1.2) electric field gradient (EFG)

The electric field gradient, eq, is related to the electronic environment at the nucleus as it is determined by the configuration of the electrons near to the nucleus. All filled electronic energy levels are symmetric and so do not contribute to the EFG (s-levels are usually full and have no contribution, whereas, partially full p-levels do contribute to the EFG). The electric field gradient is a tensor quantity and can be transformed into diagonal form described by the three components

$$V_{xx} = \frac{\partial^2 V}{\partial x^2}, \quad V_{yy} = \frac{\partial^2 V}{\partial y^2}, \quad \text{and} \quad V_{zz} = \frac{\partial^2 V}{\partial z^2} \qquad \text{eqn 2.1}$$

where V is the electrostatic potential and x, y, z are the axis

According to Laplace's equation Vxx + Vyy + Vzz = 0 — the sum of the diagonal components is equal to zero — only two quantities are then required to specify the field gradient completely, because the three parameters Vxx, Vyy, Vzz are not independent.

The maximum component of the field gradient, Vzz = eq, in the chosen principal axis system, Fig 2.1, is one of the quantities and the asymmetry parameter, η, is the other quantity. η is defined as

$$\eta = \left| \frac{V_{xx} - V_{yy}}{V_{zz}} \right| \qquad \text{eqn 2.2}$$

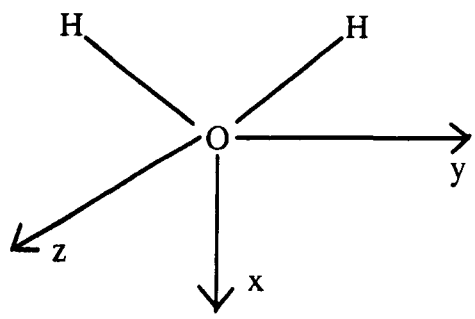

Fig 2.1 principal axis system for the electric field gradient tensor at the oxygen nucleus in an isolated water molecule. The water nuclei lie in the plane of the paper as do the x and y axes, whereas, the z axis is perpendicular to the plane of paper[1,2]

The principal axes are chosen such that Vzz ≥ Vxx ≥ Vyy. Therefore η lies between zero and one (i.e. $0 \leq \eta \geq 1$). The value of η represents the deviation from axial symmetry for a nucleus — for axial symmetry of the field gradient tensor, i.e. Vxx = Vyy, the asymmetry parameter, η, is equal to zero.

The electric field gradient is strongly dependent on the electronic environment at the nucleus. If the electronic environment is of tetrahedral, octahedral, cubic or spherical symmetry, then the electric field gradient will vanish, thus cancelling out any quadrupolar interactions.

When the electric field gradient has axial symmetry ($\eta = 0$) the nuclear quadrupolar interaction energy is given by

$$E = \frac{e^2qQ}{4I(2I-1)}\left[3m_I^2 - I(I+1)\right] \qquad \text{eqn 2.3}$$

The quantity $\frac{e^2qQ}{h}$ has dimensions of frequency (i.e. Hz) and is defined as the nuclear quadrupole coupling constant, χ. It represents the magnitude of the interaction between the quadrupole moment and the electric field gradient.

In a static homogeneous magnetic field (applied field) and an asymmetric electric field, a quadrupolar nucleus will experience at least two forces. One arises from the interaction of the magnetic moment with the magnetic field (described by the Zeeman energy) and the other from the interaction of the quadrupole moment with the electric field gradient (described by the quadrupolar energy). The resulting behaviour of the quadrupolar nucleus will depend on the relative strengths of these two forces, where the total energy of interaction is given by

$$E = E_{ZEEMAN} + E_{QUADRUPOLAR} \qquad \text{eqn 2.4}$$

thus,

$$E.h^{-1} = \underbrace{-\nu_L m_I}_{\text{Zeeman term}} + \underbrace{\chi\frac{3m_I^2 - I(I+1)}{8I(2I-1)}\left(3\cos^2\theta - 1\right)}_{\text{Quadrupolar term}} \qquad \text{eqn 2.5}$$

where θ is the angle between the applied field, B_O, and the maximum component of the electric field gradient, Vzz.

When the magnetic effect is negligible compared to the electric quadrupole effect then the nuclear states are degenerate and pure quadrupole resonance is observed (NQR experiment). However, when the quadrupole effect is negligible in comparison to the magnetic effect, then the 2I+1 energy levels are equally spaced out in energy and only one transition is observed (NMR experiment), Fig 2.2.

Usually the presence of even a small electric field gradient at the nucleus perturbs the Zeeman energy levels (created by the interactions of the magnetic moments with the static magnetic field) according to the azimuthal quantum number, m_I, so that these levels are no longer equally spaced. For first order perturbation and a static electric field gradient, for example in a single crystal or a powder, the NMR spectrum consists of 2I equidistant lines. If, however, the electric field gradient is time-dependent, then changes in both orientation and magnitude of the field gradient have to be considered — the electric field gradient is usually fixed within the framework of the molecule such that any movement of the molecule would cause the interaction between the electric field gradient and the magnetic field B_O to change. The characteristics of the spectrum then vary according to the rate of change of the field gradient (correlation time, τ, dependent). The orientation dependent part of the quadrupolar interaction is controlled by θ.

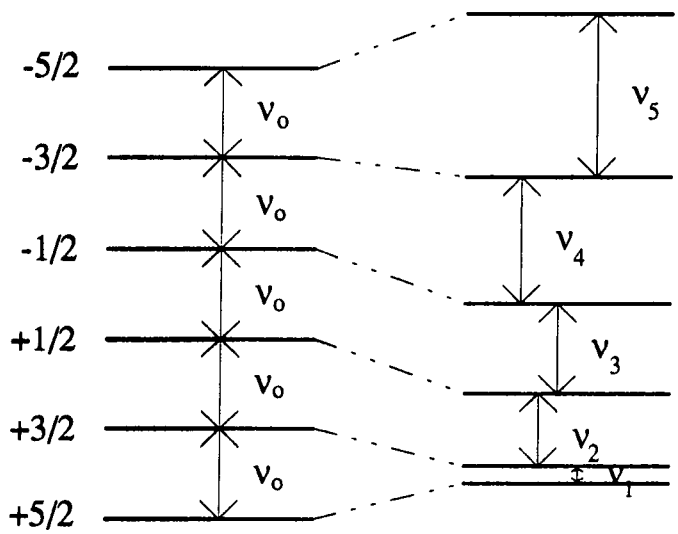

Fig 2.2 Zeeman levels -no quadrupolar effects 1st Order Quadrupolar effect

When the electric field gradient is fluctuating rapidly and isotropically such that $\omega\tau \ll 1$ (within the validity of the extreme narrowing condition, where ω is the resonant frequency) the lifetime of the individual quadrupole levels is so short that quadrupolar splitting cannot be observed and only one line is seen. The quadrupole interaction then serves its purpose as a relaxation mechanism and is generally more efficient than any other type of mechanism. Within the validity of the extreme narrowing condition, longitudinal and transverse relaxation rates are equal and single exponential, and can be described by the equation:

$$\frac{1}{T_1} = \frac{1}{T_2} = \frac{3\pi^2(2I+3)}{10I^2(2I-1)}\chi^2\left(1+\eta^2/3\right)\tau \qquad \text{eqn 2.6}$$

When the extreme narrowing condition does not hold, i.e.$\omega\tau \geq 1$ (slow motion), the relaxation behaviour is more complex. Since quadrupolar relaxation can lead to the emission of a single or double quantum of energy, i.e. $\Delta m_I = \pm 1$ or $\Delta m_I = \pm 2$, the overall relaxation process is expected to be very complex due to the possibility of different relaxation pathways.

For a non-extreme narrowing situation, the longitudinal and transverse relaxation rates are no longer expected to be equal and may even be multiexponential.

However, multiexponential relaxation behaviour of calcium-43 and oxygen-17 have not been encountered in the literature for any solution state system. A single Lorentzian line, broadened to some extent by quadrupolar relaxation, is observed in most cases. Similarly, in this study, only single lines were observed for all systems studied. But, the possibility of multiexponential relaxation behaviour for quadrupolar nuclei should not be discarded in all cases. A further discussion is given in section 4.12.

Christopher[10] observed multiexponential behaviour of water oxygen-17 relaxation in a liquid crystal system. If multiexponential relaxation occurs for oxygen-17 and calcium-43 then this is expected to yield 5 and 7 lines (2I lines) respectively. The intensities of the lines are proportional to $A^2 = I(I+1) - m(m-1)$. Thus, for oxygen-17 the intensity ratio of the lines is expected to be 5:8:9:8:5. The separation between the lines is given by

$$\Delta\nu = \frac{3\chi}{4I(2I-1)}\left(3\cos^2\theta - 1\right) \qquad \text{eqn 2.7}$$

2.2) Model for Oxygen-17 Relaxation in Biological systems

The study of water interactions with biological systems using NMR has been hindered by the lack of theoretical models to describe the relaxation phenomena of water in these systems.

In 1981, a model explaining the relaxation of water oxygen-17 in aqueous biological (or protein) systems was described by Halle.[3] This model is considered to be the most consistent with experiment so far and is still widely used. A brief description and discussion of the model is given here.

2.3) Halle's model

In Halle's model there are two types of water — bound water, via hydrogen bonding with the –OH groups of the protein (or other substrate) molecule, and free water. The motion of free water, described by a single correlation time, is assumed to be unaffected by the presence of protein. Therefore, free water is expected to undergo simple quadrupolar relaxation. However, bound water is considered to have anisotropic reorientational motion, the anisotropy being introduced by the protein (or substrate). Fast motion of bound water, characterised by a correlation time τ_f, refers to the reorientational motion of a water molecule around a hydrogen bond and/or the reorientational motion of a water molecule attached to a fast moving side chain of the protein. The slow reorientational motion of bound water, characterised by a correlation time τ_s, is assumed to be strongly dependent on the reorientational motion of the protein molecule. Thus for bound water, two relaxation rates are expected as a result of the anisotropic reorientational motion.

The averaging of the quadrupolar interaction is considered a two step process. In the first step, the quadrupolar interaction is partially averaged out by the fast, slightly anisotropic, reorientational motion of the bound water, whereas, the remaining part of

the quadrupolar interaction is completely averaged to zero by the slower motion of the bound water. Since the quadrupolar interaction is completely averaged to zero over a short period of time, then splitting of the oxygen-17 signal is not expected.

Halle's model is sometimes referred to as a *two-step model* (TSM)[4], as an *anisotropic, dual motion model* with *fast exchange*[11] or as a *three-state model.*[6]

2.4) Mathematical form of Halle's model

Halle's model can be represented by two terms corresponding to bound and free water. Thus, the general mathematical expression for such a model is given by

$$R_i = \underbrace{P_{bw}\left(R^s_{ibw} + R^f_{ibw}\right)}_{\text{bound water term}} + \underbrace{\left(1 - P_{bw}\right)R_{iw}}_{\text{free water term}} \qquad (i = 1, 2) \qquad \text{eqn 2.8}$$

where P_{bw} is the fraction of oxygen-17 nuclei in bound water; R^s_{bw} and R^f_{bw} are the relaxation rates of the slow and fast components of bound water respectively, and R_w is the relaxation rate of pure water.

From spectral density calculations and analytical expressions obtained for I = 5/2 multi-exponential relaxation, Halle and Wennerström[11] have reported that for first order quadrupolar relaxation

$$R^s_{1bw} = \frac{3\pi^2(2I+3)}{10I^2(2I-1)} S^2\chi^2\tau_s\left(\frac{0.2}{1+\omega^2\tau_s^2} + \frac{0.8}{1+4\omega^2\tau_s^2}\right) \qquad \text{eqn 2.9}$$

$$R^{s}_{2bw} = \frac{3\pi^2(2I+3)}{10I^2(2I-1)} S^2\chi^2\tau_s\left(0.3+\frac{0.5}{1+\omega^2\tau_s^2}+\frac{0.2}{1+4\omega^2\tau_s^2}\right) \qquad \text{eqn 2.10}$$

and

$$R^{f}_{ibw} = \frac{3\pi^2(2I+3)}{10I^2(2I-1)} \chi^2\tau_f\left(1+\frac{\eta^2}{3}-S^2\right) \qquad \text{eqn 2.11}$$

where χ is the quadrupolar coupling constant, and S is the order parameter (see section 2.6).

The relaxation of the fast component of bound water is considered to be under extreme narrowing condition, such that $R^{f}_{1bw} = R^{f}_{2bw}$.

In Fig. 2.3 the basic features of Halle's model for a water-substrate system are illustrated.

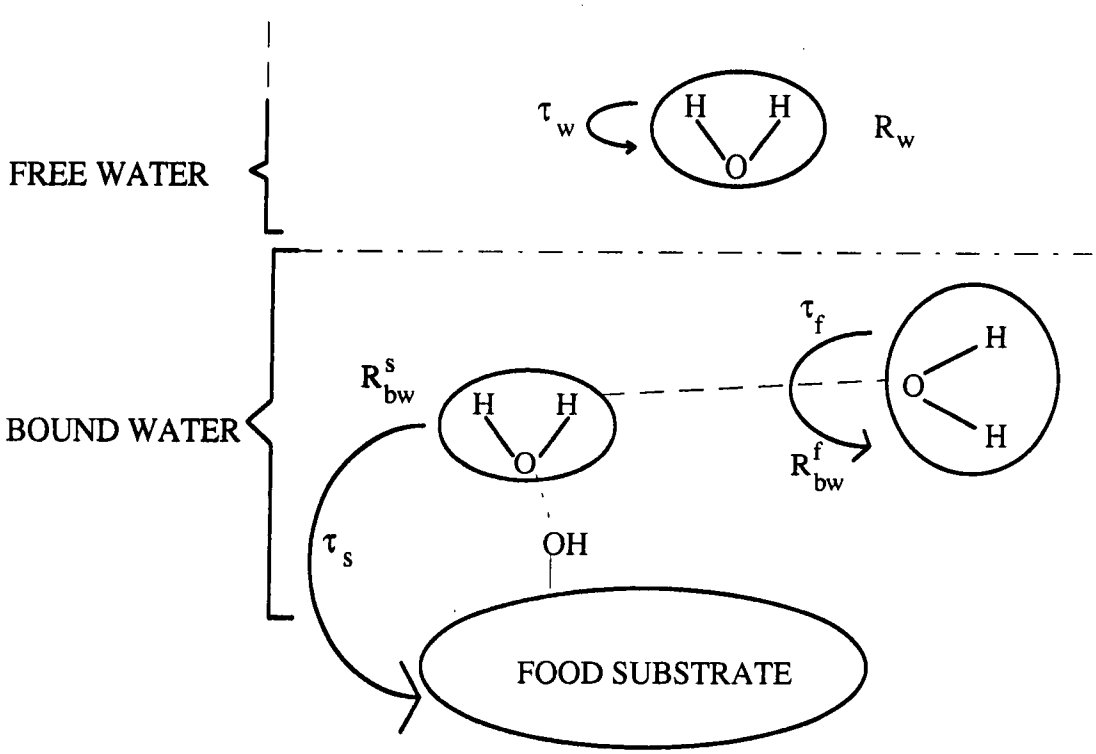

Fig. 2.3 Halle's model for a water-substrate system. The various symbols and terms are explained in text.

2.5) Oxygen-17 Quadrupolar coupling constant, χ

The Quadrupolar Coupling Constant (QCC) gives a measure of the strength of interaction between the quadrupole moment and a fluctuating electric field gradient of a nucleus. QCC for water oxygen-17 was calculated by Halle[3] from the relaxation rate of pure water, given by

$$R_w = \frac{3\pi^2(2I+3)}{10I^2(2I-1)}\chi^2\left(1+\eta^2/3\right)\tau_c \qquad \text{eqn 2.12}$$

In order to calculate the value of QCC (χ), Halle had to determine the values of the relaxation rate of pure water, R_w, the asymmetry parameter, η, and the rotational correlation time of pure water, τ_w.

The value of τ_w was obtained from the macroscopic dielectric relaxation time, τ_{diel}. The exact form of the relationship between τ_w and τ_{diel} is reported to be a controversial issue by Halle. However, according to Halle the most reliable relationship is[3]

$$\tau_w = \tau_{diel} K^{-1/(2K+1)} \qquad \text{eqn 2.13}$$

where $K = \varepsilon_s/\varepsilon_\infty$. ε_s is the static relative permittivity and ε_∞ is the same quantity in the high frequency limit.

The oxygen-17 relaxation rate in water was experimentally found to be 131.0 ±2.0 s^{-1} at 27 °C by Halle. The measurement was done at low pH value to eliminate any effects of exchange broadening, From dielectric data, τ_{diel} was estimated to be 7.79 ps using ε_s = 77.85 and ε_∞ = 77.23 for water at 27 °C. Substituting these parameters into the above equations, Halle found that the factor $\chi\sqrt{\left(1+\eta^2/3\right)} = 7.58$ MHz for water. The asymmetry parameter for liquid water is assumed to be the same as in ice[7,8] i.e. η = 0.93. With this value, Halle estimated the oxygen-17 quadrupolar

coupling constant in water to be 6.67 ± 0.20 MHz, almost the same as the value calculated for H_2O ice[8] (6.525 ± 0.015 MHz) and D_2O ice[7] (6.66 ± 0.01 MHz). The good agreement of χ for ^{17}O between the liquid and solid states of water indicates the powerful role played by hydrogen bonding in the solid state (considerable hydrogen bonding occurs in the liquid state).[7] As the molecular charge distribution of any nucleus in a liquid or solid state system is expected to be the same (i.e. the symmetry of electrons close to the nucleus and the distribution of positive charge within a nucleus are not affected by the type of bonding), then the values of χ and η for oxygen-17 in liquid water are expected to be the same as those found in ice.[1]

The value of χ for oxygen-17 is reported to be temperature independent in the range 5 to 95 °C.[3]

Throughout this study, the value of water oxygen-17 χ is taken to be 6.67 MHz.

However, by using the value of χ determined for pure water, then any influence from the charge on a protein surface on the oxygen-17 quadrupolar coupling constant is neglected. To examine this effect, Halle[3] studied the system $Li^+(H_2O)$ and investigated the effect of O-Li^+ distance on χ and η. At an equilibrium distance of 0.185 nm, it was found that the value of χ reduced by about 5 %, whereas the value of η decreased by less than 10 % compared to the values obtained from pure water. Very small changes in χ and η for other charged water systems (Na^+–OH_2 and Cl^-–OH_2)[1] were also calculated. Such small changes justify the conclusion that the charge on a protein surface has very little effect on the value of χ and η for water oxygen-17.

2.6) Order Parameter, S

The order parameter reflects the degree of water ordering around the protein binding site. As mentioned before, in Halle's model, the averaging of the quadrupolar interaction is considered a two-step process. The fast reorientational motion of the bound water averages out the majority of the quadrupolar interaction, whereas, the reorientational motion for the slow relaxation component of bound water is responsible for averaging the residual quadrupolar interaction. In fact, the residual quadrupolar interaction is related to the local ordering effect of the slow component of bound water. The greater the local ordering, the bigger the magnitude of the residual anisotropy.

When the motion of the slow component of bound water is very slow the water oxygen-17 signal is then split into five (2I lines) equidistant peaks with a frequency separation of

$$\Delta = \frac{3}{40} P |S| \chi \qquad \text{eqn 2.14}$$

where P is the mole fraction of hydrated water, S is the order parameter, and χ is the oxygen-17 quadrupolar coupling constant.

For a water-sodium octanoate-decanol system (liquid crystal system), Halle[3] found the value of water oxygen-17 S = 0.06 at 27 °C using the above relationship. However, in determining the value of S, Halle approximated the value for P by assuming that there are 2 to 6 water molecules attached to a carboxylate group and 1 to 3 water molecules attached to a hydroxyl group. The validity of these assumptions is not tested and remains open to criticism.

Kakalis and Baianu[5] have assumed a value of S for water oxygen-17 to be in the range 0.12 to 0.15 in their relaxation study of aqueous lysozyme solutions. Clearly the exact value of the order parameter, S, for water oxygen-17 is debatable.

2.7) Asymmetry Parameter, η

As mentioned before, the asymmetry parameter is dependent on the electric field gradient and is given by

$$\eta = \left| \frac{V_{xx} - V_{yy}}{V_{zz}} \right|$$

The principal axes of the electric field gradient are chosen such that $V_{zz} \geq V_{xx} \geq V_{yy}$. Therefore η is expected to lie in the range $1 \geq \eta \geq 0$.

Edmonds and Zussman[8] attempted to calculate the asymmetry parameter for oxygen-17 in H_2O ice by pure quadrupolar resonance (NQR). In NQR , the energy levels are split by the quadrupolar interaction at zero applied field (i.e. no Zeeman splitting). Any transitions between these energy levels, as a result of absorbing the radio frequency energy, lead to a NQR signal.

For oxygen-17, Edmonds and Zussman observed three lines of different intensities and at frequencies of 1.65; 1.75, and 3.39 MHz. The authors assumed that these frequencies corresponded to transitions between the energy levels $\pm 3/2 \leftrightarrow \pm 1/2$; $\pm 5/2 \leftrightarrow \pm 3/2$, and $\pm 5/2 \leftrightarrow \pm 1/2$, respectively. By using the equations of Bersohn[9] which express the energy level dependence for $I = 5/2$ on η as a power series of η^2, Edmonds and Zussman were able to calculate a value for $\eta = 0.92 \pm 0.02$.

The asymmetry parameter for oxygen-17 in D_2O ice was calculated by Spiess *et al.*[7] They recorded spectra at different frequencies for two crystal orientations of D_2O — one where the chosen principal axis of D_2O is parallel to the applied field and the other where the principal axis is perpendicular to the applied field. Only the central transition ($+1/2 \rightarrow -1/2$) of the oxygen-17 spectrum was observed. Both the parallel and the perpendicular lines were observed to be split. Waldstein and Rabideau[12] have found that in hexagonal ice the oxygen atoms tend to be arranged in a tetrahedron.

The authors designated the axes of the tetrahedron α; β; γ, and δ. Water molecules are assumed to be located with the oxygen atom at the centre of the tetrahedron and the deuterium atoms positioned along two of the four tetrahedron axes. Depending upon which pair of axes is occupied by deuterium atoms, the water molecules can be grouped into six orientational classes $\alpha\beta$; $\alpha\gamma$; $\alpha\delta$; $\beta\gamma$; $\beta\delta$, and $\gamma\delta$.

For the parallel case, the orientations $\alpha\beta$; $\alpha\gamma$, and $\alpha\delta$ are assumed to be the same because they produce the same angle with the externally applied magnetic field, B_0. As a result these orientations give rise to the same spectrum. On the other hand, the orientations $\beta\gamma$, $\beta\delta$, and $\gamma\delta$ are equal. Therefore, for the parallel situation two lines are expected as are observed experimentally by Spiess.[7]

For the perpendicular case four lines can be expected. The orientations $\alpha\gamma$ and $\alpha\delta$ are assumed to be equal, $\beta\gamma$ and $\beta\delta$ are equal, whereas $\alpha\beta$ and $\beta\delta$ are different and unique. However, experimentally Spiess *et al.*[7] only observed three lines.

From the observed splitting of the oxygen-17 signal in the two orientations, and using second order perturbation theory (first order perturbation theory has no effect on the central transition $+1/2 \rightarrow -1/2$) Spiess *et al* obtained $\eta = 0.95$

The values of the asymmetry parameter calculated by Spiess *et al.*[7] and Edmonds *et al.*[8] were in good agreement. Hence, throughout this study, the value for the asymmetry parameter, η, of oxygen-17 is taken to be 0.93

REFERENCES

1) B. Halle and H. Wennerström, *J. Chem. Phy.*, 1981, **75(4)**, 1928 - 1943

2) B. Halle, S. Engström, P. L. Cummins, G. B. Backsay and N. S. Hush, *J. Chem. Phy.*, 1985, **82(4)**, 2002 - 2013

3) B. Halle, T. Anderson, S. Forsén and B. Lindman, *J. Am. Chem. Soc.*, 1981, **103**, 500 - 508

4) L. Piculell and B. Halle, *J. Chem. Soc., Faraday Trans. 1*, 1986, **82**, 401 - 414

5) L. T. Kakalis and I. C. Baianu, *Archs. Biochem. Biophy.*, 1988, **267**, 2, 829 - 841

6) T. F. Kumosinski and H. Pessen, *Archs. Biochem. Biophy.*, 1982, **218**, 286 - 302

7) H. W. Spiess, B. B. Garrett and R. K. Sheline, *J. Chem. Phy.*, 1969, **51**, 1201 - 1205

8) D. T. Edmonds and A. Zussman, *Phy. Lett.*, 1972, **41A**, 2, 167 - 169

9) R. Bersohn, *J. Chem. Phy.*, 1952, **20**, 1505 - 1509

10) D. J. Christopher, *PhD Thesis*, University of Durham, 1992

11) B. Halle and H. Wennerström, *J. Mag. Res.*, 1981, **44**, 89 - 100

12) P. Waldstein and S. W. Rabideau, *J. Chem. Phy.* 1967, **47**, 5338 - 5342

Applications of Oxygen-17 NMR to Food Studies

It has long been recognised that NMR can be of use to food studies. One of the earliest references to the use of NMR in foods is dated 1957.[1] However, it is only within the last decade that there has been a consistent and widespread use of NMR in the food industry. This is probably due to the increasing development and relative ease of use of NMR instrumentation. The possibility of performing new experiments, for example 2D experiments and multinuclear studies, has proved to be very informative and enhanced the understanding of food molecules. Generally, NMR has been utilised to extract structural and chemical information from highly complex food systems. Another advantage with NMR (solid-state) is its property of being a non-invasive technique. The requirement of non-invasiveness in food studies is very important in that it allows to preserve the food whilst it is being examined.

In this chapter an attempt is made to review the activity of food studies using NMR. Most of the work in this field has been carried out in the latter half of the decade. The recent publication of two books[2,3] dealing with the NMR applications in food and agricultural studies has generated great interest in this field and as a result has dramatically increased the pace of the subject.

3.1) Water Studies in Food

Water is very important to food. It is the medium in which most food chemistry occurs and can have a profound affect on food texture, quality and preservation properties.

Recently attempts have been made to use NMR water relaxation times in order to obtain information on water availability. Several papers[4-10] have appeared relating water proton, deuterium and oxygen-17 relaxation to solute and water activity in casein[4-8], lysozyme[8], starch[9] and wheat flour[10].

3.2) Water Relaxation

Relaxation of water in the presence of food systems has recently been reviewed by Belton[11,23] and Hills *et al.*[12] The theoretical basis of relaxation in food systems is fairly well understood. Water proton transverse relaxation in dilute solutions of proteins and carbohydrates is thought to be dominated by proton exchange with solute protons[12-17], whereas longitudinal proton relaxation is assumed to be dominated by both proton exchange and dipolar cross relaxation[18-19]. Theories for these phenomena have been presented and shown to account quantitatively for water proton relaxation both for carbohydrates and proteins. The exchange process was shown to give rise to a significant transverse relaxation dispersion when the pulse spacing in the CPMG pulse sequence is varied for dilute sugar solutions[13,17], Fig 3.1. At short pulse spacing insufficient time is available for exchange to take place. Thus, exchange has no effect on relaxation, resulting in slow transverse relaxation. However, at long pulse spacing enough time is available for exchange to occur and have a considerable effect on relaxation. As a result the transverse relaxation rate is observed to increase with pulse spacing.

Chemical exchange of deuterium between water and solute deuteroxyl groups also plays a significant role in deuterium relaxation.[17,25] A large CPMG pulse spacing dispersion has also been observed for water deuterium transverse relaxation.

Only water oxygen-17 relaxation reports selectively on the behaviour of water and is free from any exchange effects. Belton[20] studied the relaxation of water oxygen-17 for a sugar solution in water enriched in oxygen-17 . No difference in water relaxation was found between the oxygen-17 enriched sugar sample and the sugar sample with natural abundance oxygen-17. Hence, it was concluded that exchange of oxygen-17 between the sugar and the water did not take place and that the relaxation of water oxygen-17 was free from any exchange effects. A strong bond between the sugar chain and oxygen prevents oxygen from participating in any exchange with the water.

A paper on oxygen-17 water relaxation in dilute protein solutions was published in 1981 by Halle *et al.*[21] The results were analysed and interpreted using the model described in chapter 1.

Although water relaxation in the dilute regime is considered to be well understood, with a firm theoretical basis (Halle's model), this is not the case for concentrated, water-poor regimes appropriate to most foods. Very little NMR literature is available for systems with low water content. No model is described which specifically considers the relaxation of water in water-poor regimes. Relaxation of water is expected to behave similarly in dilute and concentrated systems although this may not be the case. For example, relaxation of oxygen-17 in concentrated samples may be multiexponential, whereas in dilute solutions relaxation is expected to be single-exponential due to averaging by fast motion.[21-24]

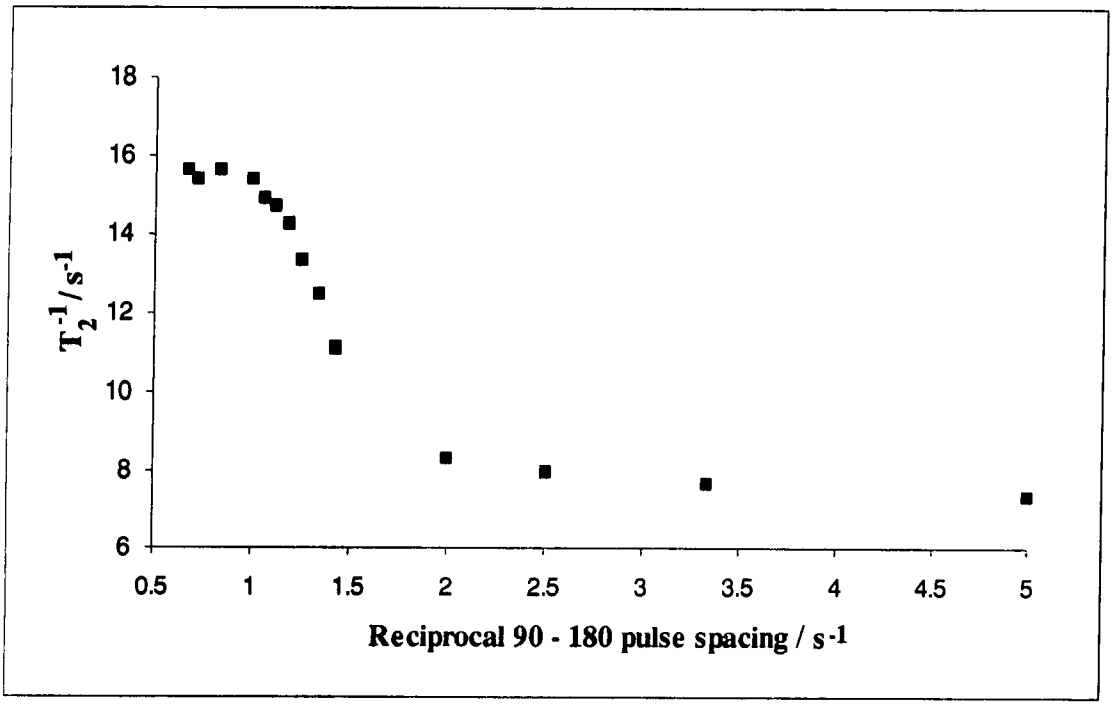

Fig 3.1 The dependence of water proton T_2^{-1} on the reciprocal of 90-180 ° CPMG pulse spacing for a sucrose solution. Concentration = 65.8 % w/w sucrose, pH = 2.8, temperature = 298 K

Since this work mainly involves the relaxation of water oxygen-17 rather than the relaxation of water proton or deuterium, this chapter will be concerned with the importance of oxygen-17 and the studies performed on food systems using this nucleus.

3.3) Simple Sugar Solutions

A non-linear increase of water oxygen-17 relaxation rate in sucrose solutions with increasing sucrose concentration has been reported by Richardson[26] and Baianu.[27] They explained the results in terms of water-sucrose and sucrose-sucrose hydrogen bonding. Recently, Belton *et al.*[22] presented a quantitative theory, based on Halle's model, which gave reasonable fits to water oxygen-17 relaxation in sucrose as well as in other carbohydrates at room temperature. Their work clearly showed a non-linear relaxation dependence on concentration. Belton *et al.*[22] attributed this non-linear dependence to increasing slow bound-water correlation time, τ_S, due to increasing solution viscosity. A similar theory has been shown to account for the concentration dependence of deuterium water relaxation in glucose solutions up to saturation.[17]

3.4) Protein Solutions

Since Halle's paper,[21] much attention has been paid to the relaxation of water in protein systems. Halle's paper concerned the study of water oxygen-17 relaxation of various proteins. Halle reported the relaxation to be concentration, pH, and frequency dependent. Like sugar solutions, oxygen-17 relaxation for aqueous solutions of lysozyme and human plasma albumin were found to increase non-linearly, especially at the higher protein concentrations. Halle predicted a similar trend for other proteins, although the variation of relaxation with concentration for other proteins was not examined. Halle concluded that the non-linearity was an effect of increasing τ_S with increasing protein concentration, i.e. an increase in solution viscosity.

The relaxation was found to be frequency dependent in the range 4-35 MHz. The relaxation rate was reported to decrease with increasing frequency.

pH was also found to affect the relaxation of water oxygen-17. Halle studied the dependence of such relaxation for the proteins human plasma albumin (HPA) and human immunoglobin G (IgG) in D_2O as an effect of pD. Transverse relaxation was found to be strongly dependent on pD. An increase in relaxation rate was observed between a pD of 4 and 10.

The extent of hydration of the various proteins was also examined by Halle. It was found that charged residues, particularly carboxylates, are more extensively hydrated than uncharged residues. This finding was in good agreement with the proton NMR work[28,29] on proteins and polypeptides, giving hydration numbers of 6 - 7.5 for anionic, 3 - 4.5 for cationic, and 2 - 3 for polar charged residues.

Kakalis and Baianu also studied the relaxation of water oxygen-17 in lysozyme solutions.[30] Halle, as well as Kakalis and Baianu, attempted to calculate the correlation time of the slow component of bound water, τ_S, for oxygen-17 in the presence of lysozyme. Halle found the value of τ_S to be 19 ns assuming that the order parameter, S, has a value of 0.06 for a 8.3 % w/w lysozyme solution. On the other hand, Kakalis and Baianu[30] assumed that the order parameter for oxygen-17 was

0.12 - 0.15. Using this value they calculated a τ_S of 7.4 ns for a lysozyme solution of the same concentration as Halle's sample. Clearly the choice of order parameter has a big effect on the value of τ_S. The exact value of S is an important factor and is still very much in doubt.

Water oxygen-17 relaxation studies for lysozyme solutions have also been carried out by Lioutas *et al.*[31] The results were analysed by a series of straight lines where each line was thought to represent a different population of water. The relaxation rates of the various populations were calculated from the slope of the line. Lioutas *et al.*[32] analysed their water proton relaxation data for lysozyme using five lines and claimed to have identified five populations of water. However, Fullerton *et al.*[33] explained their water proton relaxation data on lysozyme using three straight lines and, hence, three water populations.

Differences of opinion exist between Belton *et al.*[34] and Myer-Betts and Baianu[8] in interpreting the results of lysozyme studies. In both cases, the relaxation of water oxygen-17 is considered to increase linearly up to a concentration of about 10% w/w lysozyme. At higher concentrations, the relaxation rate is reported to increase non-linearly. At very high concentrations of lysozyme, the relaxation rate is seen to level out and remain constant.

Myer-Betts and Baianu[8] attempted to interpret the non-linearity of relaxation with a theory proposed by Kumosinski and Pessen, who tried to explain a similar non-linearity in the deuterium water relaxation of milk caseins.[4-7] According to these authors the fraction of bound water should be replaced by an activity term $n_H a_P$, where a_P is the protein activity and n_H is the hydration expressed as g H_2O / g dry protein. However, according to Belton *et al.*[34] there seems to be no satisfactory theoretical justification for replacing a bound water fraction term by a thermodynamic activity term. Furthermore, the fitting procedure adopted from Kumosinski-Pessen theory assumes that the bound water correlation times are independent of protein concentration. This is certainly not the case according to Halle's model[21] and is also

not the case for sugar solutions.[17,22] Despite the defects in Kumosinski-Pessen theory highlighted by Belton *et al.*, it is still widely used in food studies.[4,5,7-10]

The possible explanation given by Belton *et al.* to describe the variation of relaxation rate with concentration agrees with the ideas expressed by Halle. The non-linear increase in relaxation is thought to be caused by an increasing slow bound-water correlation time, τ_S, with increasing protein concentration, i.e. an increase in viscosity. Both the ionic strength and the charge on the protein have been observed to affect the relaxation of water oxygen-17 in solutions of lysozyme[35] and muscle proteins.[35]

3.5) Heterogeneous Food Systems

Most powders, pastes and suspensions can be classified as heterogeneous food systems. Examples would include lysozyme powder, starch suspensions and powder, wheat starch-sugar mixture, wheat flour suspension, and so on. However, much attention has been given to the starch-water system since starch is widely used as a thickener, texturiser, and as an emulsifier aid in the food industry.

Richardson and co-workers[9,36] have reported water oxygen-17 and deuterium transverse relaxation rates for corn starch suspensions over a wide concentration range. The observation of single exponential oxygen-17 relaxation by Richardson *et al.*[9] suggested that diffusive exchange of water between the bulk and water inside the starch granules is fast compared to the difference in their intrinsic relaxation rates. As the concentration of starch is increased, the relaxation rate is observed to increase linearly, then non-linearly, eventually levelling off to some extent, but not completely. This behaviour is almost a repeat of that for lysozyme, hence the same explanation, in terms of concentration dependence on solution viscosity (or bound-water slow correlation time τ_S), can probably be used here. However, unlike the case for lysozyme solution, the relaxation data for the starch-water system show a second increase in relaxation rate above a concentration of about 60% starch. The increase in relaxation rate above a concentration of 70% starch was reported by Richardson and

co-workers.[36] A possible explanation for this second increase was given by Belton *et al.*[34] It was suggested that the increase is associated with a morphological change accompanying the transition from a water-saturated paste at about 60% starch to an increasingly unsaturated microporous powder which contains only adsorbed water (i.e. bound water) but no bulk water. Assuming that the morphological interpretation is correct, then it is possible to obtain information about the state of the bound water directly for a concentrated (>70% w/w starch) starch sample. Such a study was reported by Tanner *et al.*[37] using proton NMR. To the surprise of these authors, the so-called bound water was found to be quite mobile. The fast (τ_f) and slow (τ_s) correlation times of bound water were found to be ~ 10^{-9} s and ≥ 6×10^{-5} s respectively. In fact, three distinct correlation times were calculated from the relaxation data, which corresponded to the lifetime of a water molecule at a particular site on the starch powder (*ca.* 10^{-7} s), the fast (τ_f) and slow (τ_s) correlation times of bound water.

The relaxation of water oxygen-17 in wheat flour has been studied by d'Avignon *et al.*[38]

3.6) Plant Tissue solutions

Diffusion of water between the different compartments of plant tissue (e.g. wheat cells; courgettes; onions; apples etc.) is a very important factor in determining the relaxation of water. Unfortunately, very little literature was found for the relaxation studies of water for these systems. The small amount of literature that is available is mainly concerned with the relaxation of water protons[14,39,40] and not oxygen-17. Since the various compartments of plant tissue are associated with different water relaxation rates, the overall relaxation of the whole tissue sample is expected to be multi-exponential and extremely complicated. The development of theoretical models for such complicated systems is not an easy task.

A packed suspension of Sephadex beads is one of the simplest two-compartment systems with multi-exponential relaxation. The relaxation of Sephadex beads has been studied by Hills and Duce[39] and found to be multi-exponential. In this system the relaxation of water inside the Sephadex beads was found to be dominated by proton exchange. Consequently, for small-sized Sephadex beads, the relaxation of deuterated water was reported to be single exponential by Hills[13] despite the fact that Sephadex beads are heterogeneous with two distinct compartments. The small size of the Sephadex beads allows a deuterium oxide molecule (D_2O) to diffuse so rapidly between the inside and outside water compartments that it experiences only an average relaxation rate. Thus, the small-bead suspension appears to be homogeneous (i.e. only one compartment) from the viewpoint of deuterium relaxation.

3.7) Muscle Tissue

Muscle tissue is considered to consist of three compartments. Water oxygen-17 longitudinal relaxation in muscle is reported to be multi-exponential.[41,42] This suggests that slow exchange of water molecules between the different compartments takes place and that each compartment has different relaxation properties. The water proton[43] and deuterium[44] transverse relaxations were also found to be multi-exponential. The data have been analysed by fitting to three relaxation times with three fractional populations of water.[40] But for these nuclei chemical exchange of protons between water and exchangeable groups in muscle is expected to contribute significantly to relaxation.

A list of recent reviews relevant to NMR studies in food is presented in table 3.1. For further information readers are referred to the references given in this table.

Table 3.1 List of recent references for the study of interactions of water with food systems using NMR.

SUBJECT	YEAR	REFERENCE
1. General Review of NMR Applications	1984 / 90 / 93	45, 26, 34
2. Water		
general review of NMR theory & applications	1990 / 93	11, 34
literature review	1987	47
3. Proteins	1989 / 93	48, 34
4. Carbohydrate NMR	1986 / 93	49, 34

REFERENCES

1) T.F. Conway, R.F. Cohee and R.J. Smith, *Manufacturing Confectioner*, 1957, **37**, 27

2) J.W. Finlay, S.J. Schmidt and A. Serianni (Eds.), NMR *Applications to Biopolymers*, Plenum Press, New York, 1990

3) P.E. Pfeffer and W.V. Gerasimowicz (Eds.), *NMR in Agriculture*, CRC Press, Boca Raton, USA, 1989

4) T.F. Kumosinski and H. Pessen, in *NMR in Agriculture* (ed. P.E. Pfeffer and W.V. Gerasimowicz), p . 219, CRC Press, Boca Raton, USA, 1989

5) T.F. Kumosinski and H. Pessen, *Methods Enzymol.*, 1985, **117**, 219

6) T.F. Kumosinski, H. Pessen, S.J. Prestrelski and H.M. Farrell Jr., *Arch. Biochem. Biophys.*, 1987, **257**, 259

7) T.F. Kumosinski, H. Pessen and H.M. Farrell Jr., *J. Ind. Microbiol.*, 1988, **3**, 147

8) P.A. Myers-Betts and I.C. Baianu, *J. Agric. Food Chem.*, 1990, **38**, 1171

9) S.J. Richardson, I.C. Baianu and M.P. Steinberg, *Starch*, 1987, **39**, 79

10) S.J. Richardson, I.C. Baianu and M.P. Steinberg, *J. Agric. Food Chem.*, 1986, **34**, 117

11) P.S. Belton, *Comments Agric. Food Chem.*, 1990, **2**, 179

12) B.P. Hills, S.F. Takacs and P.S. Belton, *Food Chem.*, 1990, **37**, 95

13) B.P. Hills, *Spectrosc. Int. J.*, 1990, **8**, 149

14) B.P. Hills, K.M. Wright and P.S. Belton, *Mol. Phys.*, 1989, **67**, 1309

15) B.P. Hills, S.F. Takacs and P.S. Belton, *Mol. Phys.*, 1989, **67**, 903

16) B.P. Hills, S.F. Takacs and P.S. Belton, *Mol. Phys.*, 1989, **67**, 919

17) B.P. Hills, *Mol. Phys.*, 1991, **72**, 1099

18) B.P. Hills, *Mol. Phys.*, 1992, **76**, 489

19) B.P. Hills, *Mol. Phys.*, 1992, **76**, 509

20) P.S. Belton and K.M. Wright, *J. Chem. Soc., Faraday Trans. 1*, 1986, **82**, 451

21) B. Halle, T. Andersson, S. Forsén and B. Lindman, *J. Am. Chem. Soc.*, 1981, **103**, 500

22) P.S. Belton, S.G. Ring, R.L. Botham and B.P. Hills, *Mol. Phys.*, 1991, **72**, 1123

23) P.S. Belton, *Prog. Biophys. Molec. Biol.*, 1994, **61**, 61

24) L. Piculell, *J. Chem. Soc., Faraday Trans 1*, 1986, **82**, 387

25) B.P. Hills and F.A. Favret, *J. Mag. Res., Series B*, 1994, **103**, 142

26) S.J. Richardson, I.C. Baianu and M.P. Steinberg, *J.Food Science*, 1987, **52**, 806

27) I.C. Baianu and A. Mora-Gutierrez, *J. Agric. Food Chem.*, 1989, **37**, 1459

28) I.D. Kuntz Jr. and W. Kanzmann, *Adv. Protein Chem.*, 1974, **28**, 239

29) I.D. Kuntz Jr., T.S. Brassfield, G.D. Law and G.V. Purcell, *Science*, 1969, **163**, 1329

30) L.T. Kakalis and I.C. Baianu, *Arch. Biochem. Biophys.*, 1988, **267**, 829

31) T.S. Lioutas, I.C. Baianu and M.P. Steinberg, *Arch. Biochem. Biophys.*, 1986, **247**, 68

32) T.S. Lioutas, I.C. Baianu and M.P. Steinberg, *J. Agric. Food Chem.*, 1987, **35**, 133

33) G.D. Fullerton, M.F. Finnie, K.E. Hunter, V.A. Ord and I.L. Cameron, *Magn. Reson. Imaging*, 1987, **5**, 353

34) P.S. Belton, I.J. Colquhoun and B.P. Hills, *Ann. Rep. NMR Spec.*, (ed. G.A. Webb), 1993, **26**, chap.1

35) I.C. Baianu, T.F. Kumosinski, P.J. Bechtel, P.A. Myers-Betts, P. Yakubu and A. Mora, in *NMR Applications to Biopolymers* (ed. J.W. Finlay, S.J. Schmidt and A. Serianni), p.361, Plenum Press, New York, 1990

36) S.J. Richardson, I.C. Baianu and M.P. Steinberg, *Starch*, 1987, **39**, 198

37) S.F. Tanner, B.P. Hills and R. Parker, *J. Chem. Soc. Faraday Trans. 1*, 1991, **87**, 2613

38) D.A. d'Avignon, C.C. Hung, M.T.L. Pagel, B. Hart, G.L. Bretthorst and J.H. Ackerman, in *NMR Applications to Biopolymers* (ed. J.W. Finlay, S.J. Schmidt and A. Serianni), p.391, Plenum Press, New York, 1990

39) B.P. Hills and S.L. Duce, *Magn. Reson. Imaging*, 1990, **8**, 321

40) P.S. Belton and R.G. Ratcliffe, *Prog. NMR Spectr.*, 1985, **17**, 241

41) M.M. Civan and M. Shporer, *Biochim. Biophys. Acta*, 1974, **343**, 399

42) M.M. Civan, A.M. Achlama and M. Shporer, *Biophys. J.*, 1978, **21**, 127

43) P.S. Belton, R.R. Jackson and K.J. Packer, *Biochim. Biophys. Acta*, 1972, **286**, 16

44) B.M. Fung and P.S. Puon, *Biophys. J.*, 1981, **33**, 27

45) I. Horman, in *Analysis of Foods and Beverages : Modern Techniques* (ed. G. Charalambous), p.205, Academic Press, London, 1984

46) P.S. Belton and I.J. Colquhoun, *Spectrosc. Int.*, 1990, **2**, 22

47) S.J. Richardson and M.P. Steinberg, in *Water Activity : Theory and Applications*, (ed. L.B. Rockland and L.R. Beuchat), p.235, Marcel Dekker, New York, 1987

48) I.C. Baianu, in *NMR in Agriculture* (ed. P.E. Pfeffer and W.V. Gerasimowicz), p.167, CRC Press, Boca Raton, USA, 1989

49) E.B. Rathbone, in *Analysis of Food Carbohydrate* (ed. G.G. Birch), p.149, Elsevier Applied Science, London, 1985

Water Oxygen-17 Results and Discussion

4.1) Relaxation of Oxygen-17

Oxygen-17 has a spin of 5/2 and a quadrupolar moment of -0.026×10^{-28} m^2, therefore, it is expected to undergo quadrupolar relaxation. In the literature[1, 2], it is reported that quadrupolar relaxation plays the major role in the relaxation process of oxygen-17. Other relaxation mechanisms are considered to have a negligible contribution.

In the extreme narrowing regime the quadrupolar contribution to the relaxation rate ($R_1 = R_2$) is given by

$$R_Q = \frac{3\pi^2(2I+3)}{10I^2(2I-1)}\chi^2\left(1+\eta^2/3\right)\tau_c \qquad \text{eqn 4.1}$$

Quadrupolar relaxation strongly depends on the quadrupolar coupling constant, χ. This parameter represents the magnitude of the interaction between the quadrupolar moment and the electric field gradient produced at the nucleus.

However, scalar interactions between the oxygen and the protons in a water molecule can also have an important contribution to oxygen-17 relaxation, especially the transverse relaxation, if the exchange of protons between different proton environments is slow compared to the NMR relaxation timescale.

Scalar interactions involve a magnetic field produced by the protons acting on the oxygen nucleus (and vice-versa), causing the oxygen to relax. The scalar interaction is an electron mediated interaction between the nuclear magnetic moments of the two nuclei and is modulated by the exchange of protons between different proton sites. This type of relaxation is known as scalar relaxation of the first kind. Scalar relaxation is only expected to significantly affect the transverse relaxation. It is strongly dependent on the field (frequency of the nuclei) and the exchange rate of

either of the two water protons. The contribution of scalar relaxation is given by the equations

$$R_{2sc} = \frac{4\pi^2}{3} J^2 I_H (I_H + 1) \left[\tau_{ex} + \frac{\tau_{ex}}{1 + (\omega_H - \omega_O)^2 \tau_{ex}^2} \right] \qquad \text{eqn 4.2}$$

$$R_{1sc} = \frac{8\pi^2}{3} J^2 I_H (I_H + 1) \left[\frac{\tau_{ex}}{1 + (\omega_H - \omega_O)^2 \tau_{ex}^2} \right] \qquad \text{eqn 4.3}$$

where J is the coupling constant between ^1H — ^{17}O in Hz. In pure water $J_{O—H}$ is given to be 81.1 Hz by Halle and Karlström;[3] τ_{ex} is the lifetime of a proton at a water molecule, *i.e.* it is related to the exchange rate of protons; I_H = 1/2 (spin number of proton), and ω_H and ω_O are the resonance frequencies (in angular units) of proton and oxygen respectively.

The scalar relaxation contribution to oxygen-17 relaxation is strongly dependent on the exchange of the protons directly attached to the oxygen nucleus. If the exchange is fast *i.e.* a small value for τ_{ex}, then the scalar relaxation will have a negligible effect on the overall relaxation process. If, however, the exchange of protons is slow, *i.e.* large value of τ_{ex}, such that $(\omega_H - \omega_O)\tau_{ex} >> 1$, then scalar relaxation will have a considerable effect on transverse relaxation but not on longitudinal relaxation. The reason why scalar relaxation affects transverse relaxation and not longitudinal relaxation can be seen from the above equations.

4.2) Relaxation of Water Oxygen-17 in Sucrose Solutions

Relaxation of water oxygen-17 in the presence of sucrose is assumed to occur according to Halle's model.[1] Two categories of water are present, namely bound water and free water. Bound water is considered to have anisotropic motion described by two correlation times of different magnitudes. Exchange of water molecules or protons between the bound and free water states is expected to occur.

Sucrose is a relatively small molecule compared to other food molecules and has a molecular mass of 342.30 g. The formula for sucrose is $C_{12}H_{22}O_{11}$

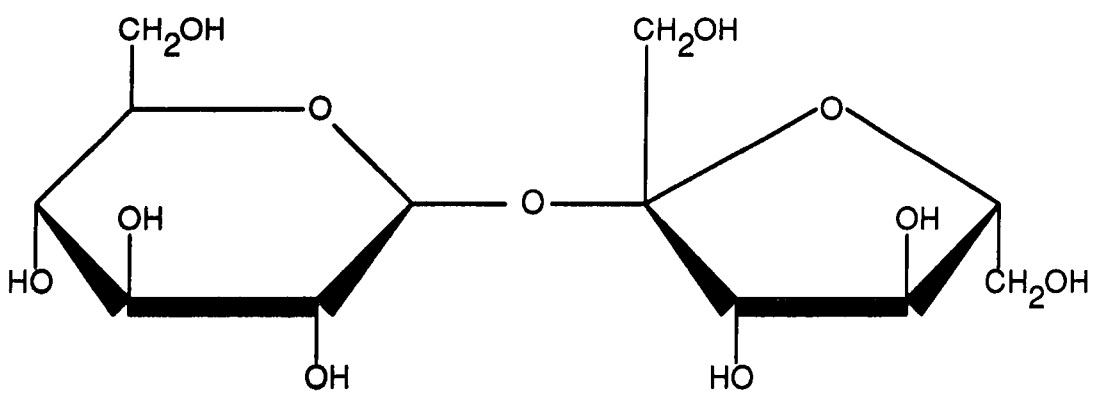

Fig.4.1 Displayed formula of sucrose

4.3) Sucrose Sample Preparation

The natural abundance of the oxygen-17 nucleus is approximately 0.037 %. Thus, for water oxygen-17 studies it was necessary to use enriched water samples in order to record reasonable oxygen-17 spectra. 21.8 % enriched oxygen-17 water was purchased from CK Gas Products. At low spectrometer frequencies (13.557 and 40.671 MHz) it was almost impossible to observe a signal without the enrichment. However, at the higher frequencies (67.789 & 81.330 MHz) a water oxygen-17 signal could be observed with a reasonable signal to noise ratio after about 32 transients without the enrichment. Similarly, for the spectrometer frequency of 33.909 MHz (Bruker AC-250) a reasonable signal could be observed with natural abundance of water at low concentrations of sucrose, but, for the higher concentrated samples, enriched water was necessary. The signal to noise ratio dramatically increased when using the enriched material. Why a signal was observed at a frequency of 33.909 MHz and not at 40.671 MHz at natural abundance for low concentrated sucrose solutions remains a mystery.

Sucrose was purchased from Sigma Chemical Ltd and used without any further treatment. Various concentrations of sucrose were prepared by adding a calculated amount of sucrose to 1 g of 21.8 % oxygen-17 enriched water and shaking. The pH of the water was in all cases altered with 1 mol dm^{-3} HCl to less than 3 before the addition of sucrose. A small volume of HCl was required to alter the pH, delivered using a micro-pipette.

The addition of HCl had an insignificant effect on the mass of water which was still assumed to be 1 g. The pH of water was measured by both litmus paper and an electronic pH meter (Jenway 3020 meter). For all solutions, the pH of water was measured before and after the addition of sucrose. It was found that sucrose had very little effect on the pH of acidified water.

For Bruker MSL-100 and MSL-300 spectrometers the concentration of sucrose was incremented by adding known amounts of sucrose to the NMR tube. Initially the least concentrated sample was prepared and to this was added more sucrose to increase the sucrose concentration. Each sample was analysed on both spectrometers before the addition of the next sucrose increment. For Bruker AC-250; AMX-500, and the Varian VXR-600 spectrometers, new samples were prepared at natural abundance of water and analysed on all three spectrometers.

However, for all spectrometers, the same saturated sucrose sample was analysed which contained 1 g of enriched water. The concentration of this sample was 73 % w/w sucrose at 25 °C and a pH of 2.8.

When preparing the saturated sucrose concentrated sample, it was necessary to heat the sample in order to dissolve the sugar. This was achieved by using a hot plate and heating around 70 °C for approximately one hour with continuous magnetic stirring. Care had to be taken to avoid excessive heating and to prevent evaporation of water.

The saturated sucrose sample was also de-gassed and sealed under vacuum to remove the effect of oxygen in air. The paramagnetic properties of oxygen in air are expected to affect the relaxation of water oxygen-17. Degassing of oxygen under vacuum was achieved by the freeze-pump-thaw-freeze method in order to make sure that complete degassing had occurred. The sample was frozen in liquid nitrogen and care had to be taken not to crack the NMR tube during the freezing period.

The degassed sample was analysed on the Bruker AC-250 and AMX-500 spectrometers only. Surprisingly, the relaxation properties of water oxygen-17 in the degassed sample did not change significantly from those of the non-degassed sample at both frequencies. This effect was also observed by Belton.[4]

Since the oxygen in air had very little effect on water oxygen-17 relaxation, then degassing and sealing under vacuum before analysing was not necessary. Thus, all samples were analysed without removing the air.

All measurements were done at a temperature of 298 K using a 10 mm probe.

4.4) Sample Temperature

The temperature of the sample was controlled by passing thermostatted air through the probe head. The temperature was measured by a thermocouple. The tip of the thermocouple was placed very close to the sample. The desired temperature and the rate of heating for the system were set. It was suggested and recommended by the regular users of the various spectrometers that a low to medium rate of heating and a degree of patience were more effective in achieving the desired temperature than was a faster rate of heating. The temperature unit was in all cases calibrated by the frequent users with an accuracy of ±0.5 K or better.

For all measurements the temperature was set to 298 K on each spectrometer and assumed to be homogeneous throughout the sample.

4.5) Spectrometer Performance

4.5.1) Tuning

The overall spectrometer performance is greatly enhanced by tuning so that the individual components (transmitter, probe, and the pre-amplifier) are optimised to work at their best in order to observe a signal. The spectrometers were, in each case, tuned to the oxygen-17 nucleus frequency by reducing the reflection from the tuning box to a minimum. For the oxygen-17 nucleus, the tuning procedure was an easy and relatively quick task to carry out on all spectrometers.

4.5.2) Shimming

The magnetic field homogeneity can be achieved by shimming the probe, *i.e.* by adjusting the current flowing through the shim coils around the probe. The field

homogeneity is independent of the nucleus under study. Thus, any nucleus can be used to shim the probe. Shimming can be achieved by two ways:

1) shimming using the lock — if the sample under study contains deuterium, then shimming can be done on the deuterium lock. Once the deuterium lock signal is found, shimming is achieved by maximising the lock signal
2) shimming can also be achieved by optimising the area or the length of an FID after a single transient.

If, however, the probe is not properly shimmed, broadening of the signal would result. To avoid spurious line broadening of the water oxygen-17 signal, shimming was done on the FID of a water proton signal. The shimming procedure was carried out until the linewidth at half-height for the water protons was approximately 1-2 Hz. The linewidth at half-height due to the magnetic field inhomogeneity is proportional to the gyromagnetic ratio, γ, of the nucleus. Since the gyromagnetic ratio of oxygen-17 is much smaller than that of the proton, then a linewidth of 1 Hz for protons indicates a reasonably well shimmed probe for studying oxygen-17.

4.6) Measurement of Spin-Lattice Relaxation Time, T_1

Spin-lattice relaxation involves the transfer of energy from the spin system to the surroundings (lattice). The relaxation time can be measured by using the inversion recovery method which involves the pulse sequence

$$[180° - \tau - 90° - \text{acquire} - T_d]_n$$

Here T_d is the relaxation delay which is set approximately to $5 \times T_1$, so that the magnetisation has sufficient time to reach equilibrium before the next 180° pulse is applied. The signal is sampled after the 90° pulse, the purpose of which is to flip the

magnetisation from the -z axis to the -y axis (*i.e.* the direction in which the detector is placed in the hardware set up)

The time τ is varied so that the signal is sampled at different times throughout the experiment. A diagrammatic explanation of an inversion recovery experiment is given in Fig 4.2

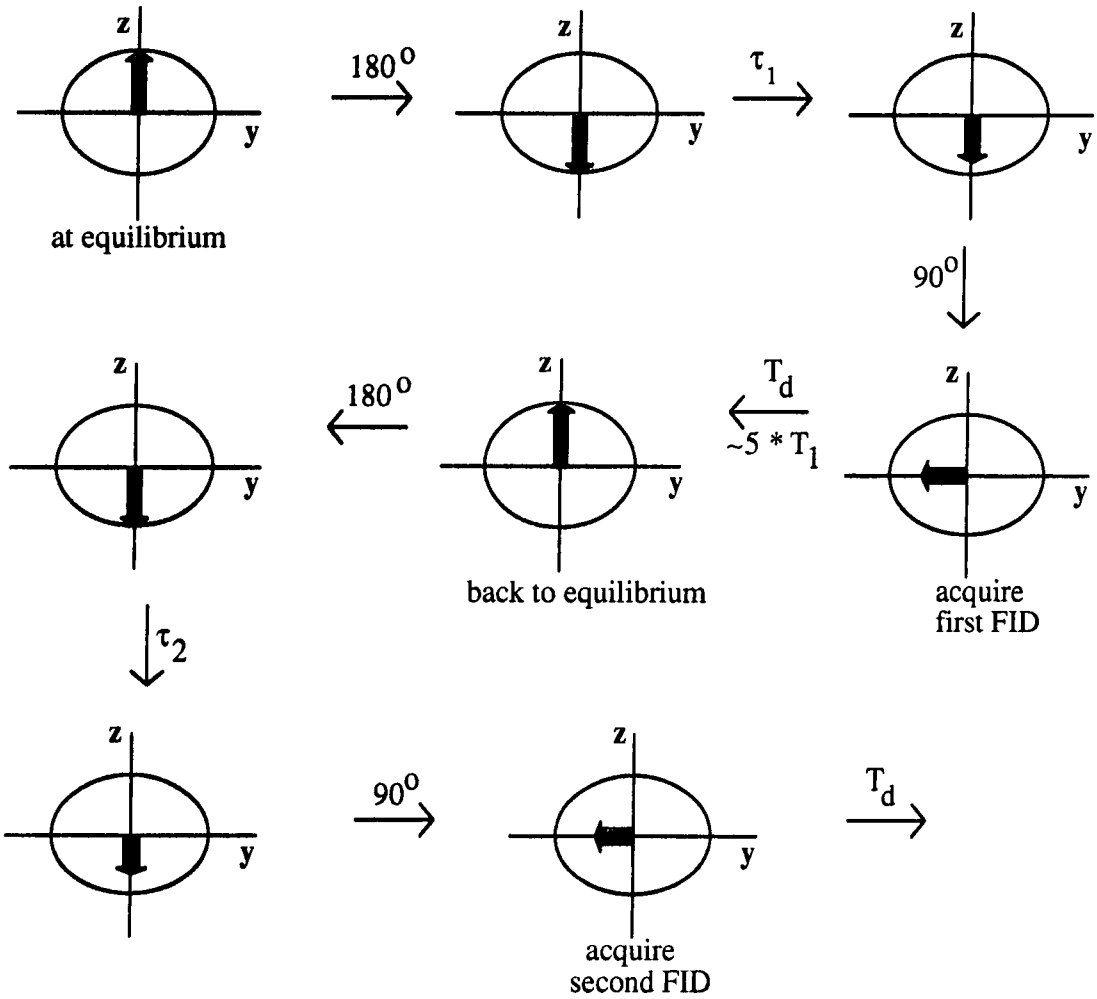

Fig 4.2 A diagrammatic representation of the pulse sequence for an inversion recovery experiment used to measure the spin-lattice relaxation time, T_1

4.7) Measurement of Spin-Spin Relaxation Time, T_2

Spin-spin relaxation (also known as transverse relaxation) is the relaxation process which occurs in a perpendicular direction to the applied magnetic field and involves an entropy change whereby the spins are dephased after a 90° pulse. The relaxation time can be measured using the Carr-Purcell-Meiboom-Gill (CPMG) pulse sequence and/or from the linewidth at half-height of the signal. The CPMG pulse sequence involves a repetition of 180° pulses after the initial 90° pulse. The CPMG pulse sequence can be described as:

$$90° - [\tau - 180° - \tau - \text{acquire(echo)}]_n$$

The signal is acquired after every 2τ time value. The successive echoes lead to an exponential decay that can be characterised by the transverse relaxation time, T_2. In most cases, the CPMG pulse sequence only samples the first point of the echo FID. In some cases, the heights of the echo FID are stored and Fourier transformed to give an exponential decay.

However for water oxygen-17 relaxation studies, the CPMG pulse sequence could not be used to measure the transverse relaxation time. The short relaxation time, T_2, combined with the long repetitive 180° pulses created electronic problems that could not be avoided. The CPMG pulse sequence was attempted on the Varian VXR-600 spectrometer on numerous occasions for water oxygen-17 samples, but each time interference from the electronics occurred and incorrect results were encountered.

As mentioned before, transverse relaxation results from the loss of phase coherence of the spins in the x-y plane. Dephasing can also occur as a result of magnetic field inhomogenities within the sample, which can cause some nuclei to precess faster than others, thus producing a frequency spread for the spin system (i.e. the spins precess at different frequencies). The frequency spread is related to the linewidth at half-height

of the signal. For isotropically rotating molecules and single exponential relaxation, transverse relaxation is related to the linewidth at half-height by the equation

$$\Delta \nu_{1/2} = \frac{1}{\pi T_2} \qquad \text{eqn 4.4}$$

where $\Delta\nu_{1/2}$ is the linewidth at half-height

However, since magnetic field inhomogeneities influence the relaxation in the x-y plane, then transverse relaxation is usually characterised by a time constant time T_2^* which does not represent the true T_2 process. In fact, the linewidth at half-height gives a measure of T_2^*, eqn 4.5. It is found that the contribution from magnetic field inhomogeneity enhances the transverse relaxation process such that $T_1 > T_2$ in almost all cases.

$$1/T_2^* = 1/T_2 + 1/T_{2\,\text{field inhomogeneity}} \qquad \text{eqn 4.5}$$

4.8) Analysis of Experimental Data

For Bruker MSL-100 and MSL-300 spectrometers, unpeeling programs were used to analyse the data. For the inversion recovery experiment a SIMFIT program was used to fit the FID data to a single exponential. The program handled a maximum of 128 data points. Initially an estimate of T_1 had to be supplied. An iterative fitting procedure was used by the program to obtain an accurate value of T_1, Fig 4.3. The spin-spin relaxation was observed following a single 90° pulse. Analysis of data was carried out using a program called QUICKFIT. This program fitted the on-resonance FID data to a single exponential Lorentzian line. QUICKFIT produced a plot of the log of FID data points against time, Fig 4.4, the relaxation time being obtained from the gradient.

For the Bruker AC-250 spectrometer, T_1 was obtained by fitting the experimental data points to a single exponential relaxation equation, Fig 4.5. However, values of T_2 were obtained from a line fitting program, part of the spectrometer software, the output of which gave a value of the linewidth at half-height. This program only allowed a fit to up to 300 data points of the spectrum. Fig 4.28 (section 4.12) shows a fit to the experimentally observed signal for oxygen-17 using the line-fitting program. For Bruker AMX-500 and Varian VXR-600 spectrometers, the inversion recovery relaxation times were obtained by fitting the experimental data points to a single exponential relaxation equation, Fig 4.6. The spin-spin relaxation times were obtained from the linewidth at half-height of the Fourier transformed spectrum, Fig 4.7.

Fig 4.3 Simfit plot for water oxygen-17 spin-lattice relaxation in an aqueous sucrose solution. Concentration = 26.4 % w/w sucrose, SF = 13.557 MHz, temperature = 298 K.

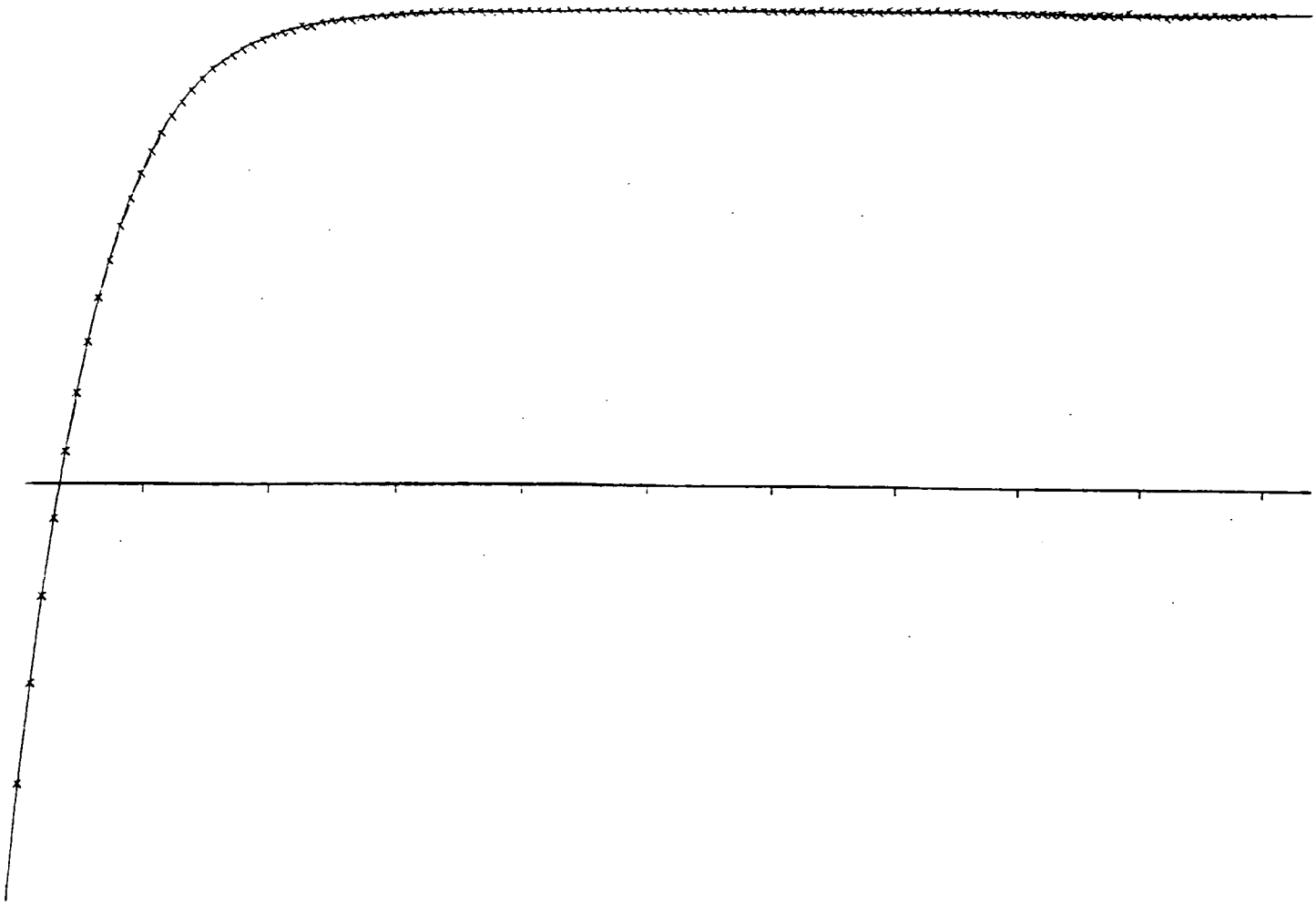

Fig 4.4 Quickfit plot for water oxygen-17 on-resonance FID in an aqueous sucrose solution. Concentration = 26.4 % w/w sucrose, SF = 13.557 MHz, temperature = 289 K.

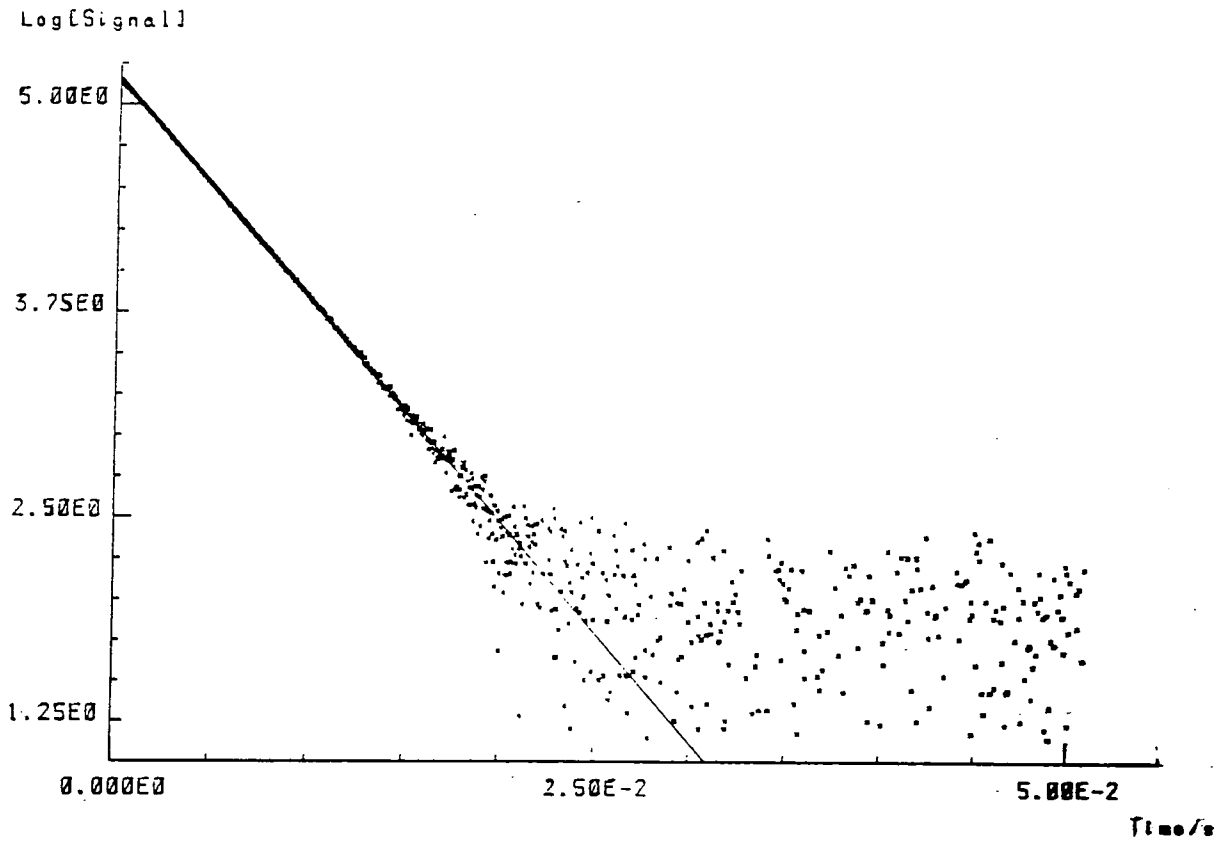

Fig 4.5 Magnetisation recovery after an inversion recovery experiment for water oxygen-17 spin-lattice relaxation for an aqueous sucrose solution. Concentration = 53.2 % w/w sucrose, temperature = 298 K SF = 33.909 MHz.

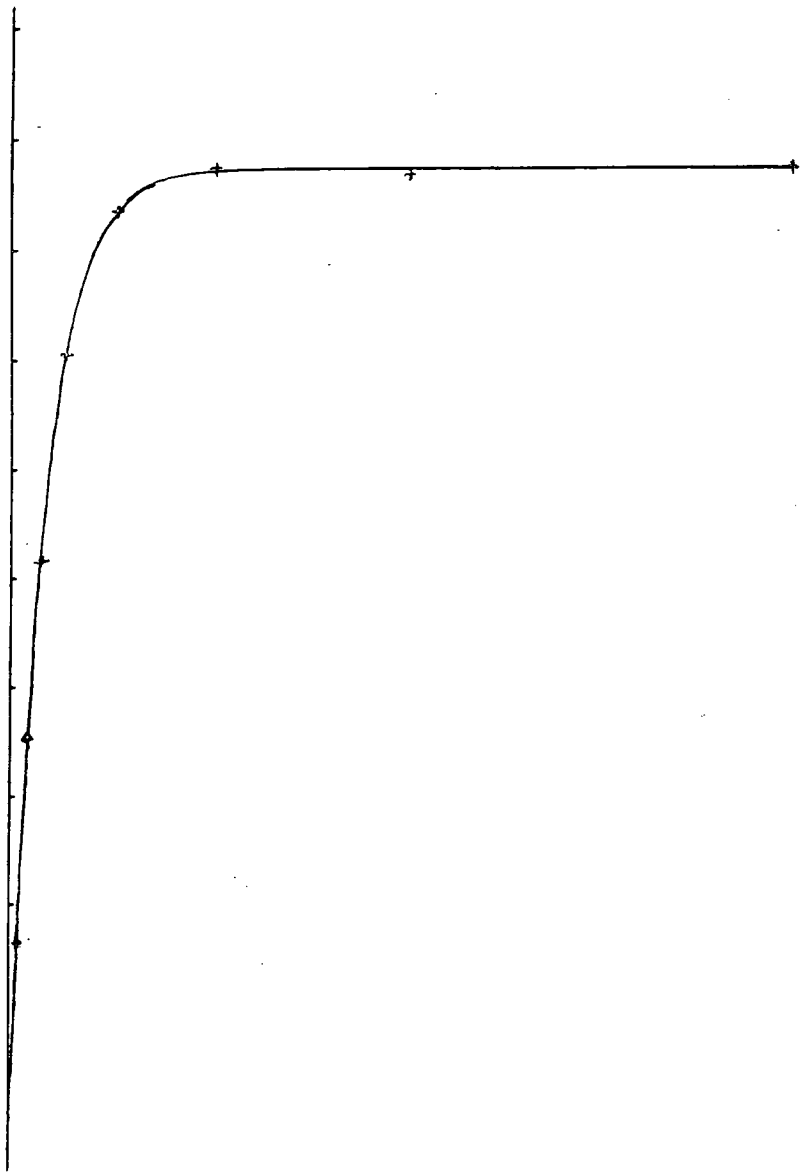

Fig 4.6 Magnetisation recovery after an inversion recovery experiment for water oxygen-17 spin-lattice relaxation in an aqueous sucrose solution. SF = 81.330 MHz, temperature = 298 K.

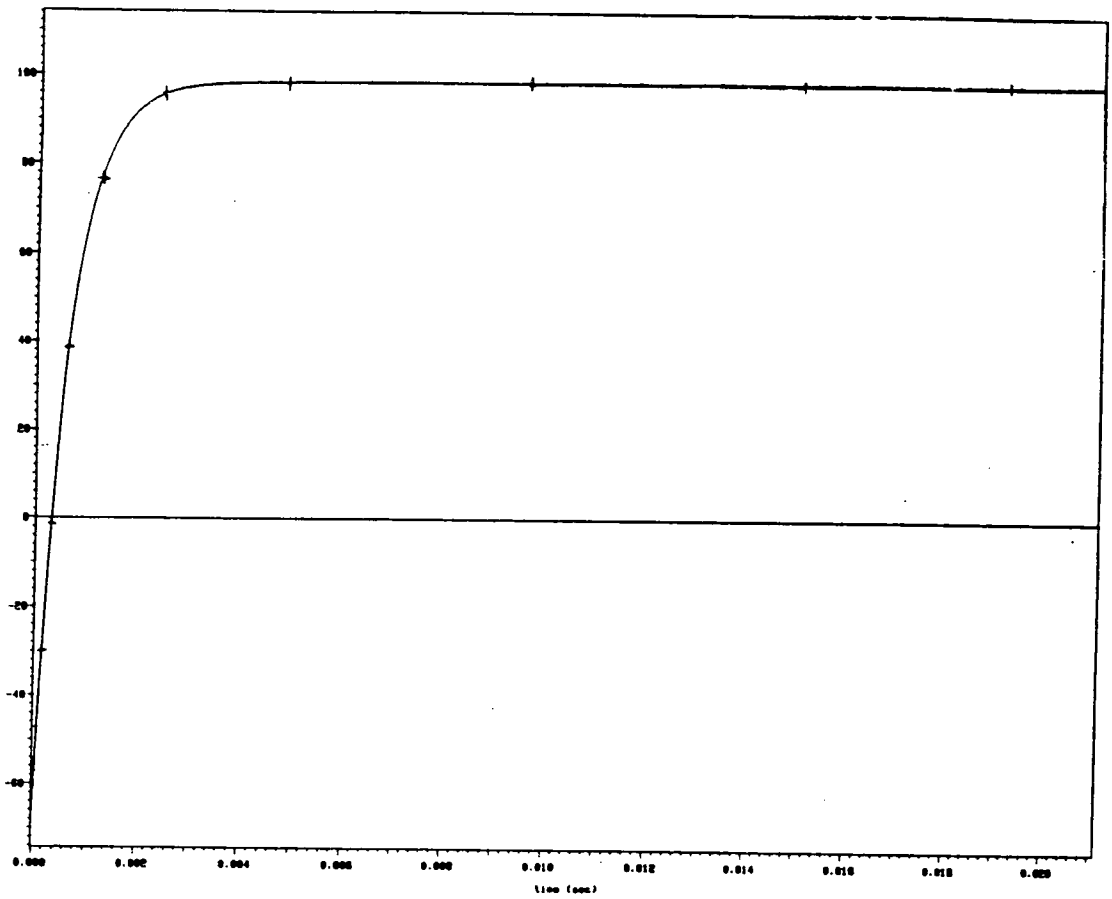

Fig 4.7 Lorentzian line-fitting to a water oxygen-17 signal in an aqueous sucrose solution. SF = 81.330 MHz.

The 'individual components fit' can be ignored in this case. It is only important when there are two overlapping peaks, in which case the 'individual components fit' gives a fit to each peak

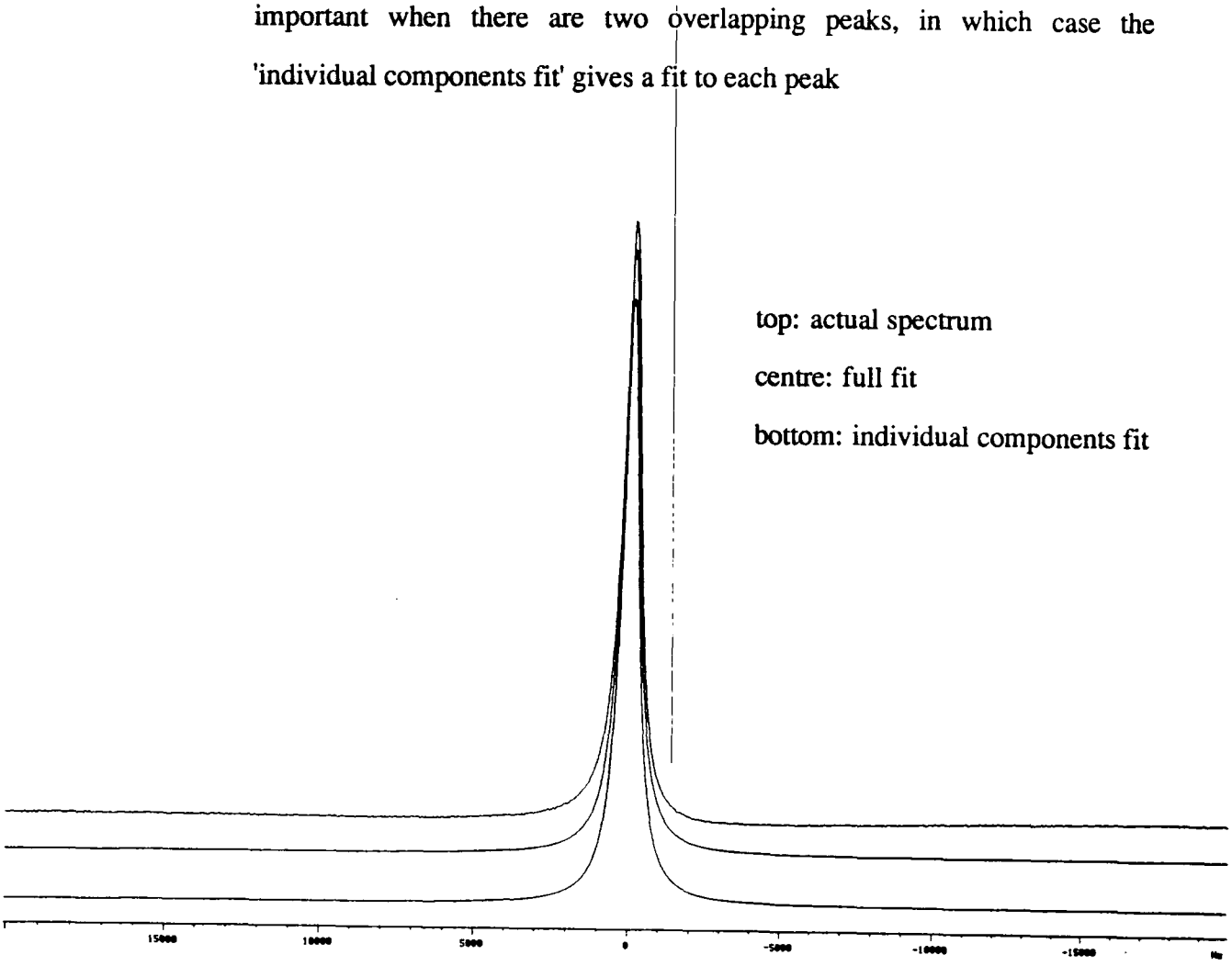

With the oxygen-17 enriched water samples, a signal was observed very quickly and easily. In almost all cases, a signal could be seen after a single transient. The signals were quite broad but easily observable. For all sucrose solutions studied, only a single water oxygen-17 signal was observed implying that sufficiently fast water exchange between the two water states takes place, Fig 4.8.

In Fig 4.9 a simple water - substrate diagram for Halle's model, showing exchange of water molecules between the two water states is shown.

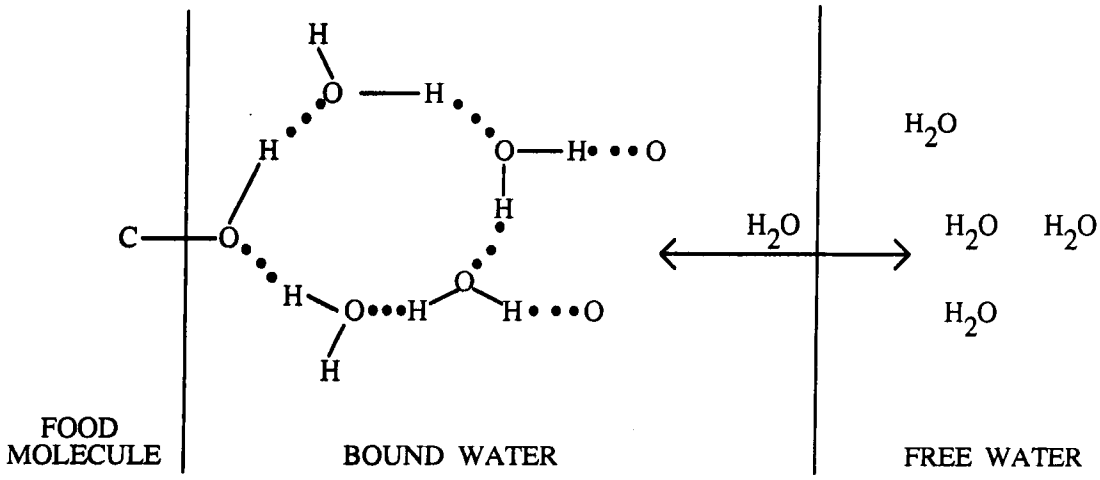

Fig 4.9 A simple model for a water - substrate interface showing bound and free water states.

The relaxation of oxygen-17 was seen to be extremely fast, i.e. ms region — an advantage allowing many experiments to be carried out in a short time scale. Quadrupolar relaxation is expected to be the dominant relaxation mechanism. For all concentrations of sucrose the exchange of protons between water molecules is considered to be so fast that the scalar interaction between the proton and the oxygen in a water molecule has negligible effect on the overall oxygen-17 relaxation process.

Fig 4.8 A water oxygen-17 signal for an aqueous sucrose solution. Concentration = 60 % w/w sucrose, SF = 81.330 MHz, pH = 2.9, temperature = 298 K.

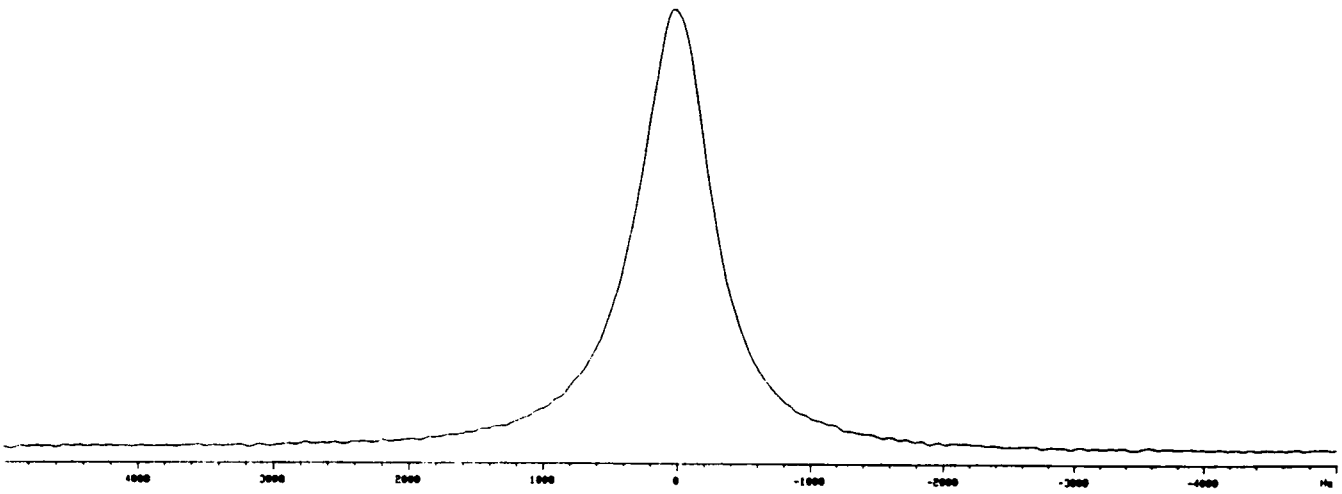

4.9) pH Effect on Oxygen-17 Relaxation

The pH dependence of both the transverse and longitudinal relaxation rates was studied for a constant concentration of sucrose. Fig 4.10 shows the variation of both the transverse and longitudinal relaxation rates as a function of pH. In Fig 4.11, the linewidth at half-height of the oxygen-17 signal is shown as a variation of pH.

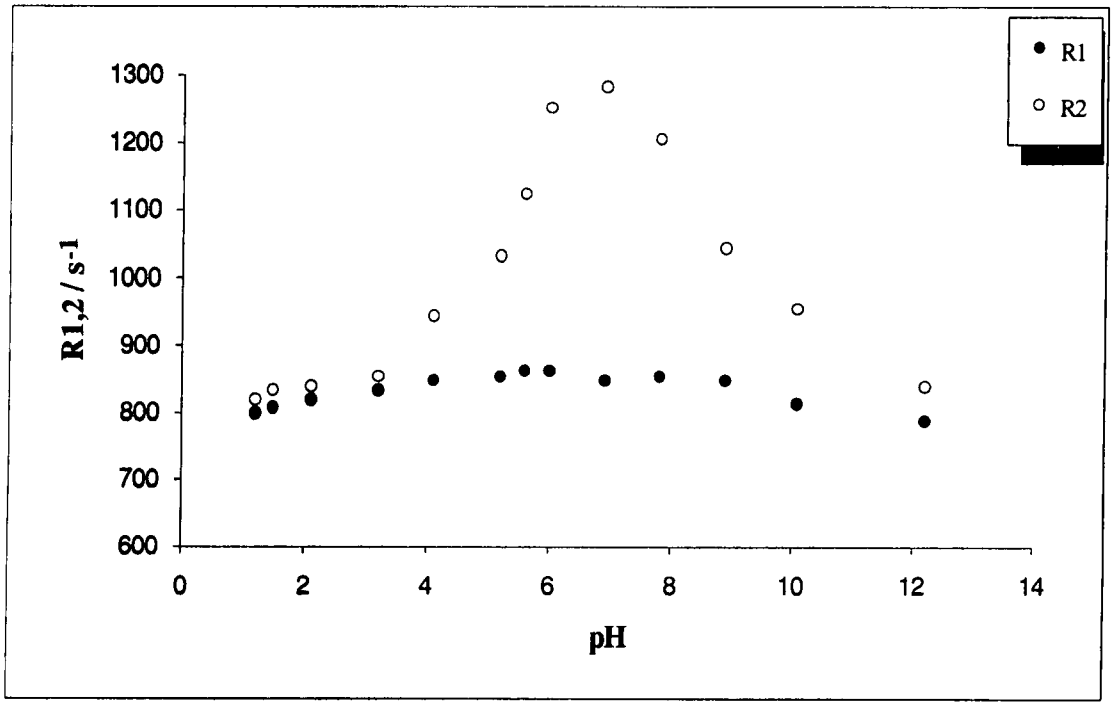

Fig 4.10 The dependence of water oxygen-17 relaxation rates on pH for a constant sucrose solution. Concentration = 52 % w/w sucrose, SF = 33.909 MHz, temperature = 298 K.

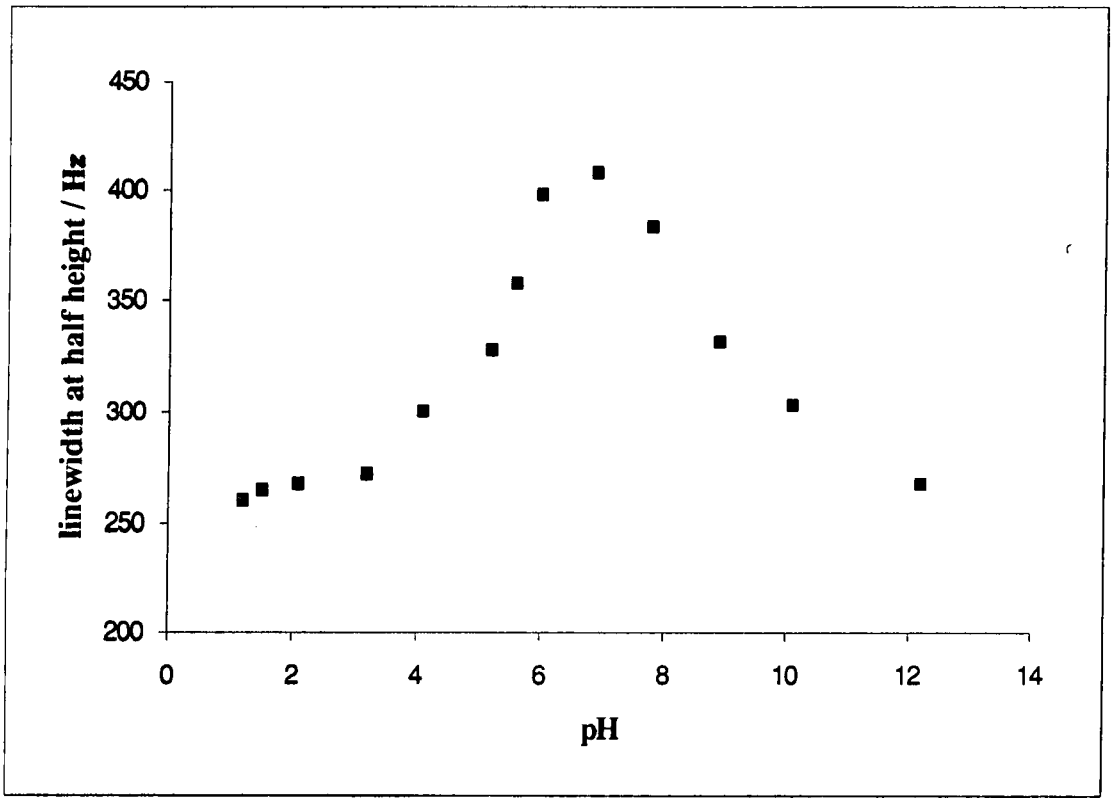

Fig 4.11 The dependence of water oxygen-17 linewidth on pH for a constant concentration of sucrose.

Concentration = 52 % w/w sucrose, temperature = 298 K.

It can be seen that the longitudinal relaxation is almost independent of pH in the range studied. However, the transverse relaxation is strongly pH dependent. Proton exchange between water molecules is considered to have a significant contribution to water oxygen-17 linewidth, and thus to transverse relaxation. The proton exchange process is considered to be acid-base catalysed[5] *i.e.* pH dependent. For $5 \leq pH \leq 9$ relatively slow proton exchange occurs, thus a large increase in the linewidth is observed. At pH values of less than 4 and greater than 10, the proton exchange process is so fast that the exchange broadening effect is eliminated and the oxygen-17 signal becomes progressively narrower.

However, to be absolutely sure that in all the experiments performed, the proton exchange contribution to the oxygen-17 linewidth is completely removed by pH alteration, "gated and inverse gated proton decoupling" experiments were also carried out to see if any further narrowing of the oxygen signal could be achieved. Both the pH and proton decoupling methods were tested to find out which one was more effective in eliminating the effect of proton exchange. The question of which method to use was explored experimentally. The pulse sequences for both gated decoupling and inverse gated decoupling experiments are shown in Fig 4.12

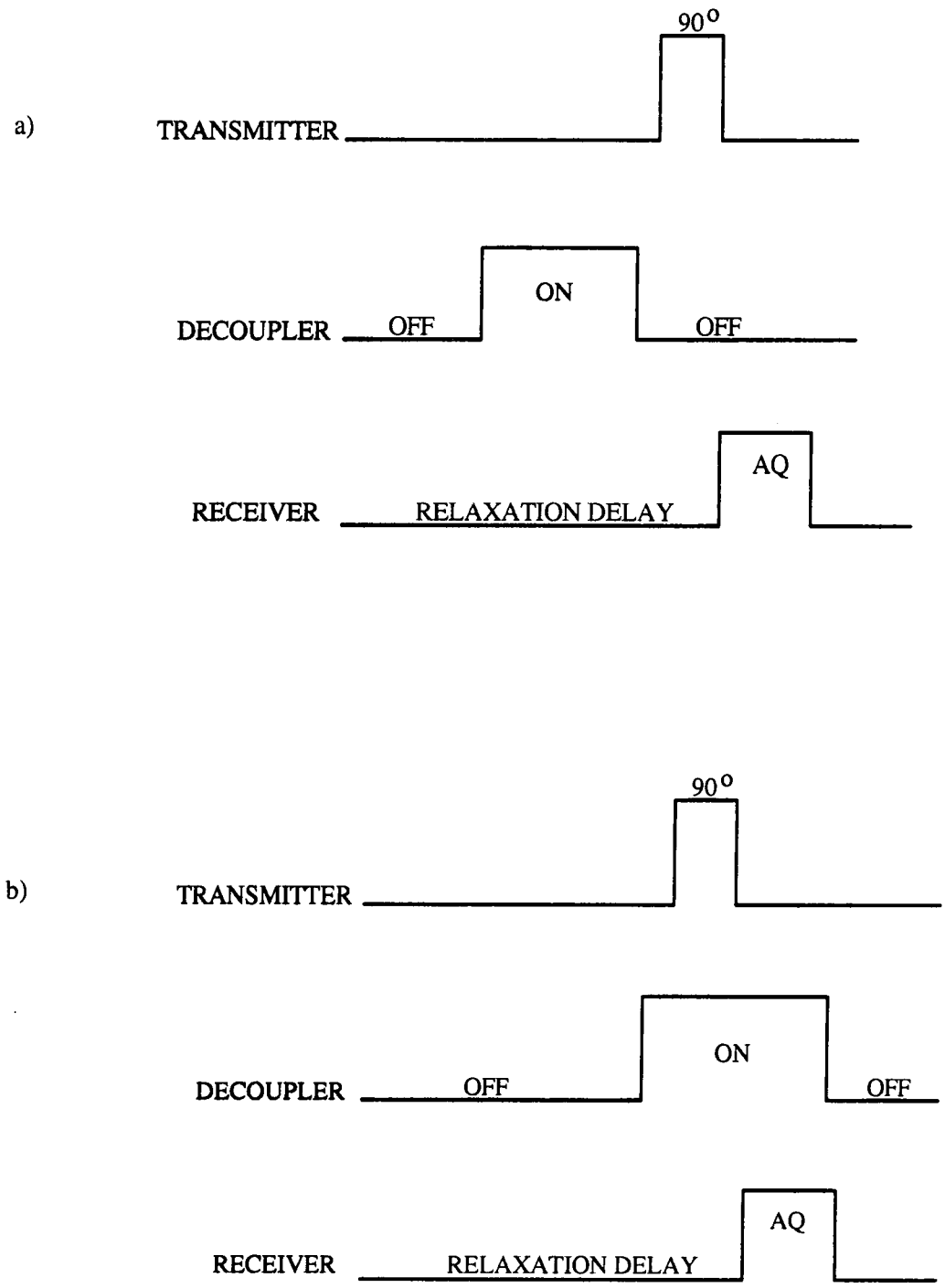

Fig 4.12 Pulse sequences for a) inverse gated decoupling and b) gated decoupling experiments

The results of the decoupling study were compared to the results obtained by altering the pH. Table 4.1 gives a comparison of the oxygen-17 linewidth at various sucrose concentrations for gated decoupling, inverse-gated decoupling, and pH alteration experiments.

Concentration	Gated Decoupling		Inverse Gated Decoupling		pH Experiment	
% w/w sucrose	pH	$\Delta V_{1/2}$ / Hz	pH	$\Delta V_{1/2}$ / Hz	pH	$\Delta V_{1/2}$ / Hz
distilled water	6.6	50 ± 5	6.6	51 ± 5	2.6	53 ± 5
13.1	6.5	61 ± 7	6.5	61 ± 5	2.5	67 ± 5
26.3	6.5	85 ± 10	6.5	85 ± 7	2.5	96 ± 10
39.4	6.4	140 ± 20	6.4	133 ± 10	2.2	147 ± 15
52.6	6.4	296 ± 20	6.4	305 ± 30	2.4	320 ± 30

Table 4.1 Experimental data for water oxygen-17 linewidth at half-height for gated decoupling, inverse gated decoupling and pH experiments for aqueous sucrose solutions. SF = 33.909 MHz, temperature = 298 K.

The results show that the proton exchange contribution to the oxygen-17 linewidth can be eliminated by either proton decoupling or by altering the pH of the solution. Very little difference in the linewidth of the signal is seen between the three experiments, Fig 4.13. Therefore, it was concluded that altering the pH of the solutions under study

to less than 3 was adequate enough to remove the effect of proton exchange broadening on the oxygen-17 signal.

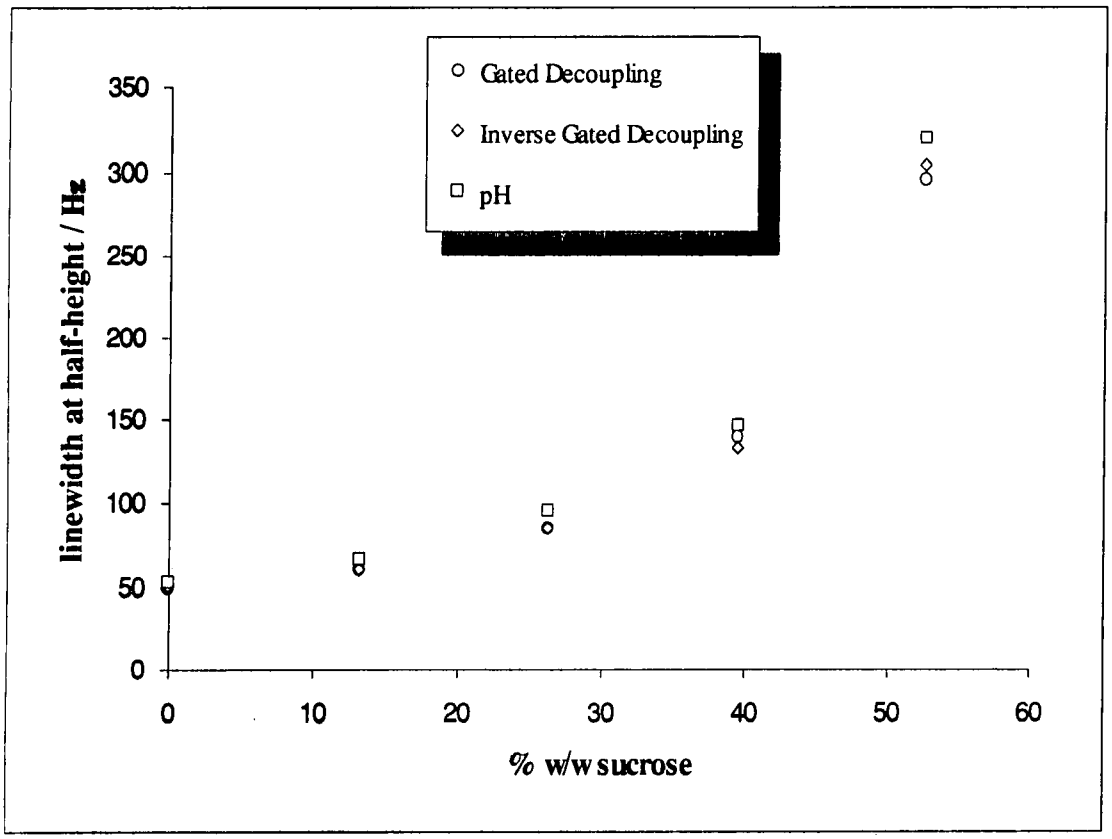

Fig 4.13 The variation of water oxygen-17 linewidth at half-height with sucrose concentration for gated decoupling (o), inverse gated decoupling (◊) and pH (□) experiments. SF = 33.909 MHz, temperature = 298 K.

4.10) Effect of Sucrose Concentration on Water Oxygen-17 Relaxation

The relaxation of water oxygen-17 was initially studied for aqueous sucrose solutions. In Table 4.2 the results for water oxygen-17 relaxation as an effect of sucrose concentration at various spectrometer frequencies are presented. All samples were prepared as mentioned earlier (section 4.3). Data for both longitudinal and transverse relaxation are given. For each case, three measurements were made and the average value of these measurements taken. As indicated earlier, the longitudinal relaxation time was measured using the inversion-recovery method, whereas the transverse relaxation time was obtained from the linewidth at half-height of the signal.

TABLE 4.2 Experimental data for water oxygen-17 longitudinal and transverse relaxation times as a function of sucrose concentration for aqueous sucrose solutions at various spectrometer frequencies. The errors represent repetition of results.

Concentration	pH	SF=13.557 / MHz		SF=33.909 / MHz		SF=40.671 / MHz		SF=67.789 / MHz		SF=81.330 / MHz	
% w/w sucrose		T1 / ms	T2 / ms	T1 / ms	T2 / ms	T1 / ms	T2 / ms	T1 / ms	T2 / ms	T1 / ms	T2 / ms
acidified water	2.9	6.8	5.9	7.2	6.1	6.4	5.2	6.9	6.3		
		±0.5	±0.6	±0.7	±0.6	±0.6	±0.8	±0.7	±0.7		
13.3	2.9	5.1	4.5	5.2	4.8	5.0	4.2	5.8	4.8		
		±0.2	±0.1	±0.5	±0.3	±0.3	±0.3	±0.4	±±0.3		
26.4	2.8	3.5	3.2	3.6	3.3	3.4	3.0	4.0	2.7		
		±0.2	±0.2	±0.2	±0.3	±0.2	±0.2	±0.1	±0.3		
39.4	2.8	2.0	1.9	2.0	1.9	2.0	1.9	2.6	2.0		
		±0.1	±0.1	0.1	±0.2	±0.1	±0.1	±0.1	±0.2		
52.5	2.7	0.8	0.7	0.8	0.75	0.8	0.7	1.4	1.2		
		±0.1	±0.1	±0.1	±0.1	±0.1	±0.1	±0.1	±0.1		
60.1	2.5	0.5	0.4	0.6	0.5	0.6	0.4	0.5	0.45	0.6	0.5
		±0.1	±0.1	±0.1	±0.1	±0.1	±0.2	±0.1	±0.1	±0.2	±0.1

TABLE 4.2 CONTINUED

Concentration	pH	SF=13.557 / MHz		SF=33.909 / MHz		SF=40.671 / MHz		SF=67.789 / MHz		SF=81.330 / MHz	
% w/w sucrose		T1 / ms	T2 / ms	T1 / ms	T2 / ms	T1 /ms	T2 / ms	T1 / ms	T2 / ms	T1 / ms	T2 / ms
65.6	2.6	0.23	0.2	0.25	0.22	0.29	0.26	0.26	0.24	0.28	0.26
		±0.01	±0.01	±0.02	±0.01	±0.02	±0.02	±0.01	±0.01	±0.02	±0.01
73.05	2.6	0.06	0.03	0.09	0.05	0.1	0.06	0.12	0.08	0.12	0.09
		±0.01	±0.02	±0.01	±0.01	±0.02	±0.01	±0.01	±0.01	±0.01	±0.02

In Fig 4.14 the effect of sucrose concentration on water oxygen-17 relaxation rate can be seen.

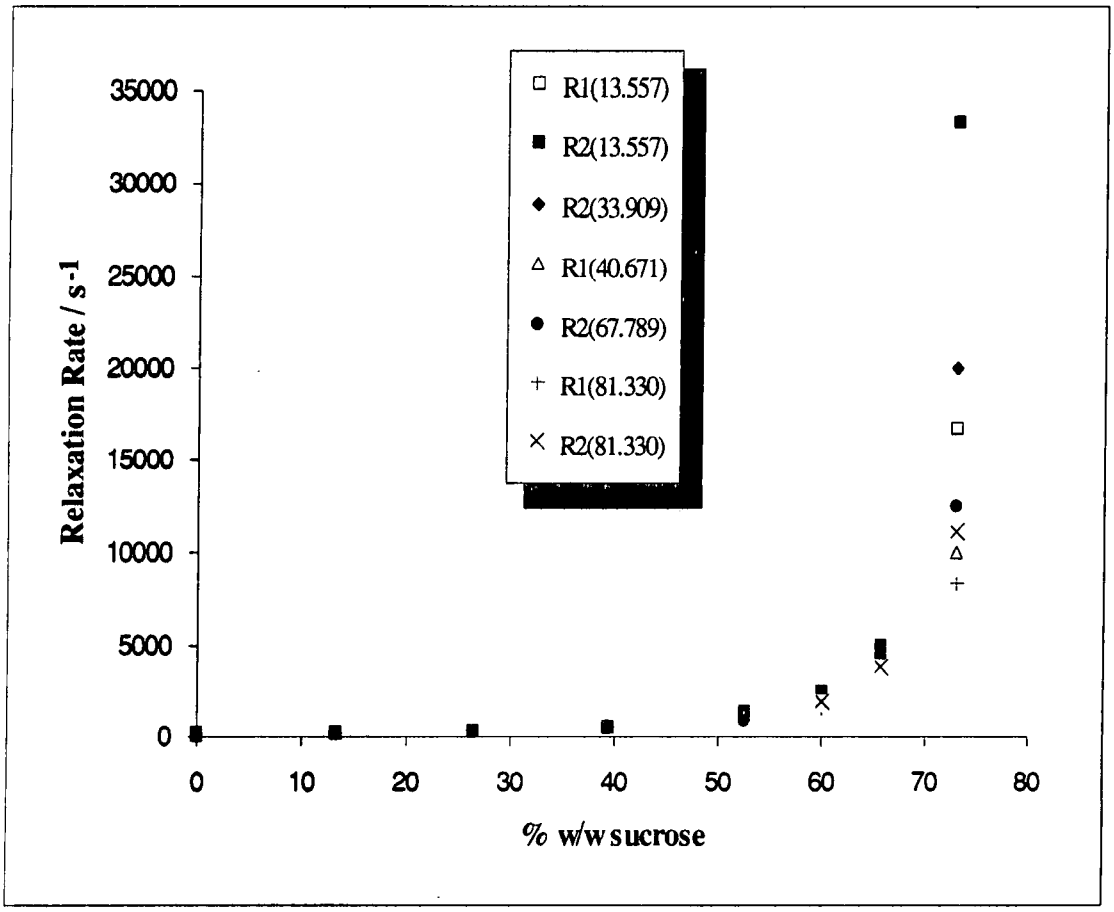

Fig 4.14 The dependence of water oxygen-17 relaxation rates, R_1 and R_2, on sucrose concentration at different spectrometer frequencies.

Both the transverse and longitudinal relaxation rates increase with increasing sucrose concentration. The increase in relaxation with concentration is a result of increasing the fraction of bound water, P_{bw}, and the viscosity of the solution. As the viscosity of the solution increases, the motion of the solution decreases, resulting in an increase in the relaxation rate. In Fig 4.15 the variation of sucrose viscosity[6] as a function of sucrose concentration is shown.

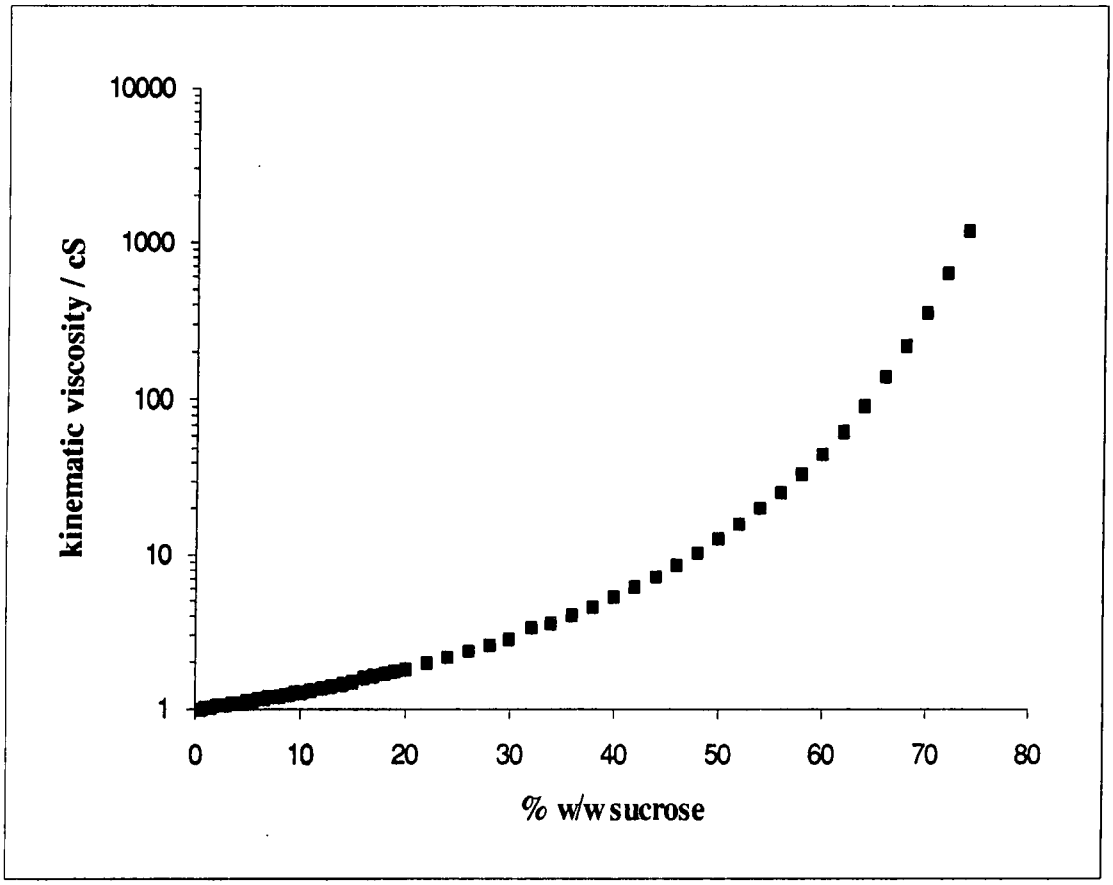

Fig 4.15 The dependence of kinematic viscosity on sucrose concentration.

The variation of the viscosity curve is seen to be similar to the relaxation rate curve, Figs 4.14 and 4.15. This shows that the increase in relaxation rate, as a function of sucrose concentration, is strongly dependent on the change in viscosity with concentration.

At low concentrations of sucrose, the longitudinal and transverse relaxation rates are equal and independent of frequency, Fig 4.14. At low sucrose content, the extreme narrowing condition is expected to be valid, such that the fast motion averages out the interactions causing relaxation and hence, an equality of longitudinal and transverse relaxation rates which are independent of frequency. It is observed that for sucrose solutions, the extreme narrowing condition is valid up to a concentration of 60 % w/w sucrose. Above this concentration, the extreme narrowing condition is no longer valid, and both the longitudinal and transverse relaxation rates become frequency dependent,

see section 4.12. In the non-extreme narrowing regime $R_1 \neq R_2$. In fact, R_2 is always greater than R_1 as may be expected.

4.11) Protocol for the Analysis of Relaxation Data

In this section, a method for analysing the water oxygen-17 relaxation data for sucrose/water system using Halle's model is presented. Relaxation times, measured at various frequencies, are utilised to calculate the various parameters of Halle's model. In the past, calculations have been based on single frequency measurements[1, 7]. The use of a range of frequencies to analyse the relaxation data is presented here. An entirely different approach to that of Halle[1] for calculating the parameters τ_s, S, τ_f, P_{bw}, R^s_{bw}, and R^f_{bw} is presented which may be justified providing a few assumptions, also made by Halle, are valid.

Generally, this method can be used for any sugar/water system for which there are two states of water (bound and free) in order to analyse water oxygen-17 relaxation data

4.11.1) Halle's Model

The mathematical form of Halle's model is summarised in eqns 4.6 — 4.10

$$R_1 = P_{bw}(R^s_{1bw} + R^f_{1bw}) + (1 - P_{bw})R_{1w} \qquad \text{eqn 4.6}$$

$$R_2 = P_{bw}(R^s_{2bw} + R^f_{2bw}) + (1 - P_{bw})R_{2w} \qquad \text{eqn 4.7}$$

where

$$R^s_{1bw} = KS^2\chi^2\tau_s\left(\frac{0.2}{1+\omega^2\tau_s^2} + \frac{0.8}{1+4\omega^2\tau_s^2}\right) \qquad \text{eqn 4.8}$$

$$R^s_{2bw} = KS^2\chi^2\tau_s\left(0.3 + \frac{0.5}{1+\omega^2\tau_s^2} + \frac{0.2}{1+4\omega^2\tau_s^2}\right) \qquad \text{eqn 4.9}$$

and

$$R^f_{1,2bw} = K\chi^2\tau_f\left(1 + \frac{\eta^2}{3} - S^2\right) \qquad \text{eqn 4.10}$$

χ = quadrupolar coupling constant, ^{17}O = 6.67 MHz

η = asymmetry parameter, ^{17}O = 0.93

S = order parameter

$$K = \frac{3\pi^2(2I+3)}{10I^2(2I-1)}$$

4.11.2) Calculation of τ_S (saturated sucrose case)

— Assumptions

a) R^f_{1bw} is independent of ω (extreme narrowing)

b) R_{1w} is independent of ω (extreme narrowing)

thus for measurements at three frequencies (ω_1, ω_2 and ω_3) :

$$\underbrace{\frac{R_1(\omega_1)-R_1(\omega_2)}{R_1(\omega_1)-R_1(\omega_3)}}_{\text{let this be A}}=\frac{R^s_{1bw}(\omega_1)-R^s_{1bw}(\omega_2)}{R^s_{1bw}(\omega_1)-R^s_{1bw}(\omega_3)} \qquad \text{eqn 4.11}$$

Therefore, using eqn 4.8 one obtains

$$A=\frac{\left(\frac{0.2}{1+\omega_1^2\tau_s^2}+\frac{0.8}{1+4\omega_1^2\tau_s^2}\right)-\left(\frac{0.2}{1+\omega_2^2\tau_s^2}+\frac{0.8}{1+4\omega_2^2\tau_s^2}\right)}{\left(\frac{0.2}{1+\omega_1^2\tau_s^2}+\frac{0.8}{1+4\omega_1^2\tau_s^2}\right)-\left(\frac{0.2}{1+\omega_3^2\tau_s^2}+\frac{0.8}{1+4\omega_3^2\tau_s^2}\right)} \qquad \text{eqn 4.12}$$

where in the cases presented here ω_1 = 13.557 MHz and ω_2 = 81.330 MHz are the lowest and highest frequencies used, respectively, while ω_3 takes the values 33.909, 40.671 and 67.789 MHz

This procedure eliminates the constant factor $KS^2\chi^2P_{bw}$ as well as R^f_{1bw} and R_{1w}.

The experimental ratios, A, calculated for the three ω_3 frequencies are reported in table 4.3.

From a theoretical plot of A vs τ_S for each spectrometer frequency ω_3 and the experimental relaxation data the value of τ_S can be obtained. Knowing the experimental ratio A for each ω_3 frequency the value of τ_S can be estimated by interpolation as is shown in Fig 4.16. For the saturated sucrose solution (73 % w/w sucrose) the values of τ_S for the three ω_3 frequencies were estimated to be

ω_3 / MHz	A	τ_S / ns
33.909	1.6 ± 0.1	4.9
40.671	1.3 ± 0.1	4.9
67.789	1.1 ± 0.1	2.8

Table 4.3 Values of ratio A, calculated from experimental longitudinal relaxation data, and the corresponding τ_S values estimated for the spectrometer frequencies ω_3.

The value of τ_S at ω_3 = 67.789 MHz is slightly different from the τ_S values at the other two frequencies because the accuracy of the plot for 67.789 MHz measurement is very low due to the nature of the plot.

A similar approach could be used with R_2, but there is evidence (see below) that Halle's proposed model is not adequate in this case for the saturated sucrose solution. Moreover, only the saturated case has sufficient dependence of R_1 on spectrometer frequency to make the detailed approach feasible.

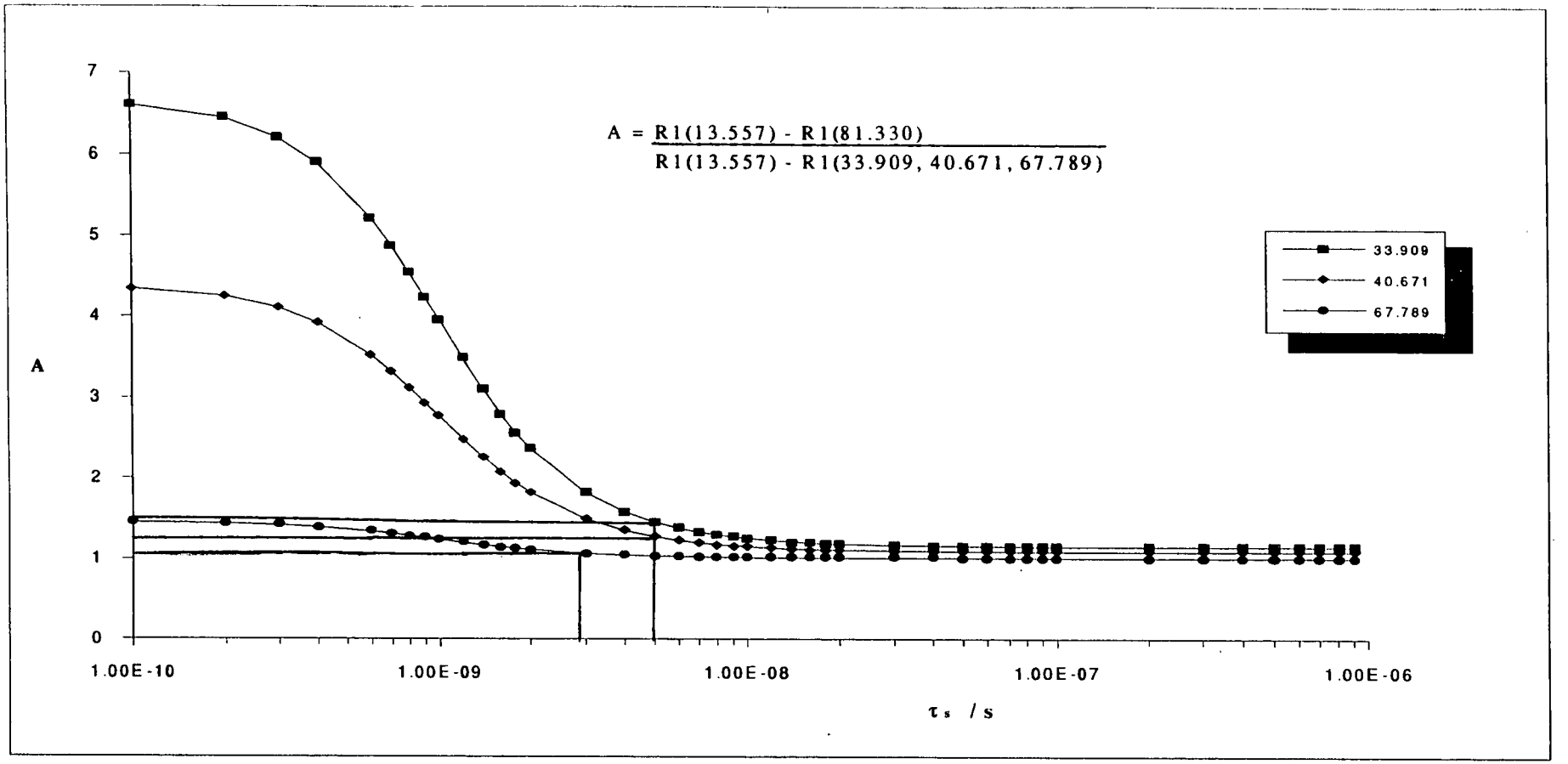

Fig 4.16 Plot of the theoretical ratio, A, against the correlation time of the slow component of bound water, τ_S, using Halle's model. The value of τ_S is estimated for saturated sucrose solution at three frequencies.

4.11.3) Calculation of $P_{bw}S^2$ and Hence S

Assuming that

$$R^{f}_{1bw} = R^{f}_{2bw}$$
$$R_{1w} = R_{2w}$$

and using eqns 4.6 & 4.7, it can be shown that

$$R_2 - R_1 = P_{bw}\left(R^{s}_{2bw} - R^{s}_{1bw}\right) \qquad \text{eqn 4.13}$$

Using equations 4.8, 4.9, and 4.13, the product $P_{bw}S^2$ can be calculated.

If it is assumed that for the saturated sucrose concentration, $P_{bw} = 1$, then the value of S (order parameter) can be calculated. In table 4.4, the calculated values of $P_{bw}S^2$ and S are given. However, for the saturated sucrose solution an anomalous R_2 - R_1 dependence on frequency was observed (see section 4.12). This anomaly is expected to affect $P_{bw}S^2$ and hence S. Thus, an alternative method to calculate S is described below.

ω / MHz	$P_{bw}S^2$	S (P_{bw} = 1)
33.909	0.12	0.34
40.671	0.1	0.32
67.789	0.11	0.32

Table 4.4 Relaxation parameters calculated for water oxygen-17 relaxation in a saturated sucrose sample using Halle's model. The calculations are based on both spin-lattice and spin-spin relaxation data.

4.11.4) Alternative Method for Calculating τ_S and S^2

The order parameter, S^2, and τ_S can be estimated by using the extrapolated value of the longitudinal relaxation rate at zero frequency, $R_1(0)$. From Fig 4.31 (see section 4.12.2), $R_1(0)$ is estimated to be 2.55×10^4 s^{-1}.

According to eqn's 4.6 and 4.8, assuming that $R^f_{1bw}(0) = R^f_{1bw}(\omega)$

$$R_1(0) - R_1(\omega) = P_{bw} K \chi^2 S^2 \tau_s \left(1 - \frac{0.2}{1+\omega^2\tau_s^2} - \frac{0.8}{1+4\omega^2\tau_s^2}\right) \qquad \text{eqn 4.14}$$

The two unknown variables, S^2 and τ_S, can be estimated by iteratively fitting the experimental data $R_1(0)$ - $R_1(\omega)$ as a function of ω using equation 4.14. The result of the fitting analysis is shown in Fig 4.17.

The value of τ_S was found to be 4.8 ns. This agreed closely with the calculated value of 4.9 ns based on the method described in section 4.11.2. On the other hand, the value of S^2 from the iterative fitting method was found to be 0.0729. Therefore, S was calculated to be 0.27. This was slightly less than the value of 0.32 calculated

using the method described in section 4.11.3. The iterative fitting method has the advantage that it uses only R_1 data to calculate S, whereas the method described in section 4.11.3 uses the data R_2 - R_1, which is found to be dubious due to the anomalous dependence on frequency. Another advantage of the iterative fitting method is that it uses the R_1 data from all five frequencies together.

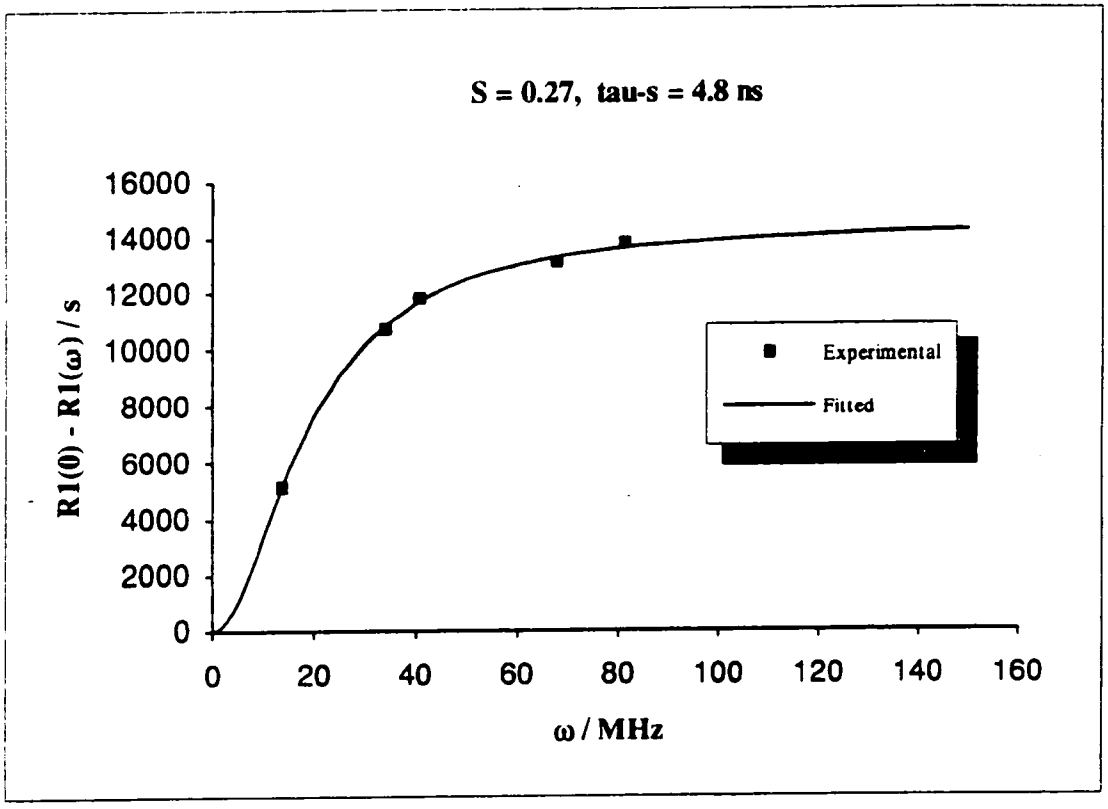

Fig 4.17 Comparison of the experimental and theoretical $R_1(0)$ - $R_1(\omega)$ data as a function of ω for saturated sucrose solution. $R_1(0)$ was estimated by extrapolating the experimental data to zero frequency. From the iterative fitting procedure S and τ_S were found to be 0.27 and 4.8 ns, respectively

4.11.5) Calculation of R^f_{bw} and τ_f

Assuming that for the saturated sucrose concentration $P_{bw} = 1$ is valid, and using eqns 4.6 and 4.7 one obtains

$$R_1 = R^s_{1bw} + R^f_{1bw}$$
$$R_2 = R^s_{2bw} + R^f_{2bw}$$

respectively.

Knowing S, τ_s, ω, and χ, the values of R^s_{1bw} and R^s_{2bw} can be found. Thence, knowing R_1 and R_2 from the experimental data, it is possible to calculate R^f_{1bw} and R^f_{2bw}, which should be equal.

Knowing R^f_{bw}, S, χ, and η and using eqn 4.10, the value of τ_f can be calculated.

In table 4.5, the calculated values of R^s_{1bw}, R^s_{2bw}, R^f_{1bw} and R^f_{2bw} are given for both the method described in sections 4.11.2 and 4.11.3 (for which τ_s = 4.9 ns and S = 0.32 - 0.34) and the iterative fitting method, section 4.11.4 (τ_s = 4.8 ns, S = 0.26). The values of τ_f, calculated from R^f_{1bw} and R^f_{2bw}, are reported in table 4.6 for both approaches to S and τ_s.

	Calculation Method		Iterative Fitting Method	
ω / MHz	τ_f / ps (R^f_{1bw})	τ_f / ps (R^f_{2bw})	τ_f / ps (R^f_{1bw})	τ_f / ps (R^f_{2bw})
13.557	-	-	136	325
33.909	103	122	133	195
40.671	105	102	128	168
67.789	122	74	131	126
81.330	-	-	125	94

Table 4.6 Values of τ_f obtained from R^f_{1bw} and R^f_{2bw} data for both methods.

	Calculation Method (sections 4.11.2 and 4.11.3)				Iterative Fitting Method (section 4.11.4)			
ω / MHz	R^s_{1bw} / s^{-1}	R^s_{2bw} / s^{-1}	R^f_{1bw} / s^{-1}	R^f_{2bw} / s^{-1}	R^s_{1bw} / s^{-1}	R^s_{2bw} / s^{-1}	R^f_{1bw} / s^{-1}	R^f_{2bw} / s^{-1}
13.557	-	-	-	-	8900	11601	7799	18698
33.909	5181	12194	5918	7005	3448	7973	7651	11226
40.671	3974	11045	6025	5854	2651	7223	7348	9676
67.789	1708	8549	6991	4250	1145	5577	7554	7222
81.330	-	-	-	-	826	5187	7173	5412

Table 4.5 Values of R^s_{1bw}, R^s_{2bw}, R^f_{1bw} and R^f_{2bw} for water oxygen-17 relaxation in saturated sucrose concentration obtained from both approaches to S and τ_S as described in text. An error of ±10 % is estimated for each value.

From the calculated results for both approaches to S and τ_s (tables 4.5 and 4.6), the following conclusions can be drawn

a) R^s_{1bw} and R^s_{2bw} are strongly dependent on frequency. With increasing frequency, both R^s_{1bw} and R^s_{2bw} decrease.

b) R^s_{2bw} is always greater than R^s_{1bw}.

c) For the iterative fitting method, R^f_{1bw} is found to be independent of frequency. Any slight variation is probably due to experimental error. A small but unexpected increase in R^f_{1bw} is found with increasing frequency for the method described in sections 4.11.2 and 4.11.3.

d) R^f_{2bw} shows an unexpected dependence on frequency. With increasing frequency R^f_{2bw} is calculated to decrease for both approaches. The unexpected variation with frequency is attributed to the extra contribution to transverse relaxation (see section 4.12) which is also frequency dependent.

e) For all cases $R^f_{2bw} \neq R^f_{1bw}$. Again, the extra contribution to transverse relaxation rate is thought to be responsible for the unexpected inequality.

f) τ_f values calculated from R^f_{1bw} are found to be independent of frequency, within experimental error, especially for the iterative fitting method. However, the values of τ_f calculated from R^f_{2bw} are frequency dependent as a result of the frequency dependence shown by R^f_{2bw}.

The calculations based on longitudinal relaxation are thought to be more reliable than those from transverse relaxation. The extra contribution to transverse relaxation (see section 4.12.2) makes all calculations based on transverse relaxation dubious. The frequency dependence of R^f_{2bw}, τ_f, and the fact that $R^f_{2bw} \neq R^f_{1bw}$ are all attributed to the extra contribution to transverse relaxation. Furthermore, the calculations based on longitudinal relaxation are in good agreement with the assumptions proposed by Halle (R^f_{1bw} and τ_f are independent of frequency).

Comparing the results between the two approaches to S and τ_S reveals that the calculations based on the iterative fitting method are probably more reliable because of the constancy shown by the terms R^f_{1bw} and τ_f.

4.11.6) Calculation of P_{bw} at Low Concentrations of Sucrose

Assuming that for sugar/water systems the Debye-Stokes relationship is applicable such that the correlation time is directly proportional to the viscosity of the solution, *i.e.*

$$\tau_s = C \times (\eta/\rho) \qquad \text{eqn 4.15}$$

where C = constant, η = viscosity, and ρ = density

it is possible to calculate the correlation time of the slow component of bound water for all concentrations of sucrose studied. The variation of viscosity for an aqueous sucrose solution with sucrose concentration can be found tabulated in physical and chemical data handbooks.[6]

Knowing τ_S for each sucrose concentration and using equation 4.8, the relaxation rate of the slow component of bound water, R^s_{bw}, can be calculated for each different sucrose sample assuming that both S and R^f_{bw} are independent of frequency.

In table 4.7, the calculated values of τ_S, R^s_{1bw} and R^s_{2bw} are given for various concentrations of sucrose.

% w/w sucrose	τ_s / ps	R^s_{1bw} / s^{-1}	R^s_{2bw} / s^{-1}
13.3	8.2	23.4	23.4
26.4	13.7	39.0	39.0
39.4	29.2	83.2	83.2
52.5	95.1	270.1	271.0
60.1	265.4	754.9	755.7
65.6	717.5	2018.9	2034.7

Table 4.7 Calculated values of τ_s, R^s_{1bw} and R^s_{2bw} for water oxygen-17 relaxation as a function of sucrose concentration for aqueous sucrose solutions. ω = 13.557 MHz and S = 0.26.

For low concentrations of sucrose R^s_{1bw} and R^s_{2bw} are equal and independent of frequency. Thus for dilute sucrose solutions, transverse and longitudinal relaxation rates are expected to be equal and independent of frequency as is observed experimentally, see Fig 4.14.

By simple re-arrangement of eqn 4.6 or eqn 4.7 one finds that for low concentrated samples (i.e. $P_{bw} < 1$):

$$P_{bw} = \frac{R - R_w}{R^s_{bw} + R^f_{bw} - R_w} \qquad \text{eqn 4.16}$$

Knowing the longitudinal relaxation rate, R_1, from experimental data; the relaxation rates of the fast and slow components of bound water, R^f_{1bw} and R^s_{1bw} respectively, and the relaxation rate of pure water, R_{1w}, it is possible to calculate the fraction of bound water, P_{bw}, for each sucrose concentration using eqn 4.16, table 4.8.

% w/w sucrose	P_{bw}
13.3	0.01
26.4	0.02
39.4	0.06
52.5	0.17
60.1	0.27
65.6	0.51

Table 4.8 The calculated variation of the fraction of bound water, P_{bw}, as a function of sucrose concentration.

ω = 13.557 MHz, τ_f = 123 ps, S = 0.26, χ = 6.67 MHz and η = 0.93

4.11.7) Summary of Analysis

The correlation time of the slow component of bound water, τ_S, calculated from the spin-lattice relaxation data is found to be 4.9 ns. According to the literature τ_S is of the expected region, *i.e.* ns. From a theoretical point of view, Belton *et al.*[7] have reported the value of τ_S for sucrose solutions to be in the region of ns. Halle and co-workers[1] have also reported the magnitude of τ_S to be of ns for the systems that they studied. Thus in this study, the value of τ_S is taken to be 4.9 ns for the saturated sucrose solution (73 % w/w sucrose).

The product $P_{bw}S^2$ is constant and independent of frequency. This is expected as neither P_{bw} and the order parameter, S, are dependent on frequency. Unfortunately, the value of P_{bw} or S cannot be calculated independently from Halle's model. Only the product of these terms can be determined. To calculate S an assumption has to be made regarding P_{bw} or vice-versa.

Assuming that at the saturated sucrose concentration there is no free water, *i.e.* $P_{bw} = 1$, the value of S is calculated to be approximately 0.26. This value is greater than the value calculated by Halle[1] and twice the value reported by Kakalis and Baianu.[8] The possibility of a strong interaction between sucrose and water molecules could result in a greater ordering effect of water molecules around the sucrose binding site, thus increasing the value of S.

The average value for the correlation time of the fast component of bound water, τ_f, is calculated to be 123 ps. This value is approximately nine times greater than the theoretical value calculated by Belton *et al.*[7] The τ_f value calculated by Belton *et al.* for aqueous sucrose solutions was approximately 14 ps. Overall the motion of the fast component of bound water is calculated to be 47 times slower than that of bulk water (free water), for which the correlation time, τ_c, is on average calculated to be 2.4 ps.[9] However, compared to the slow component of bound water, the correlation time of the fast component is greater by approximately 46 times.

With increasing sucrose concentration, the correlation time of the slow component of bound water also increases, Fig 4.19. Increasing sucrose concentration results in an increase in the fraction of bound water, as reported in table 4.8 and shown in Fig 4.18, and an increase in the viscosity of the solution. Hence, a slower motion and an increase in correlation time are expected, Fig 4.19. Within the extreme narrowing regime (*i.e.* dilute solutions of sucrose), the transverse and the longitudinal relaxation rates are equal and independent of frequency because R^s_{1bw} and R^s_{2bw} are equal and independent of frequency as has been calculated and reported in table 4.7. However, for concentrated sucrose solutions (*i.e.* non-extreme narrowing regime), R^s_{1bw} and R^s_{2bw} are no longer equal and show a strong dependence on frequency. With increasing frequency both R^s_{1bw} and R^s_{2bw} are calculated to decrease. Thus, with increasing frequency both the transverse and the longitudinal relaxation rates are expected to decrease as has been observed experimentally for the saturated sucrose solution, see Fig 4.20.

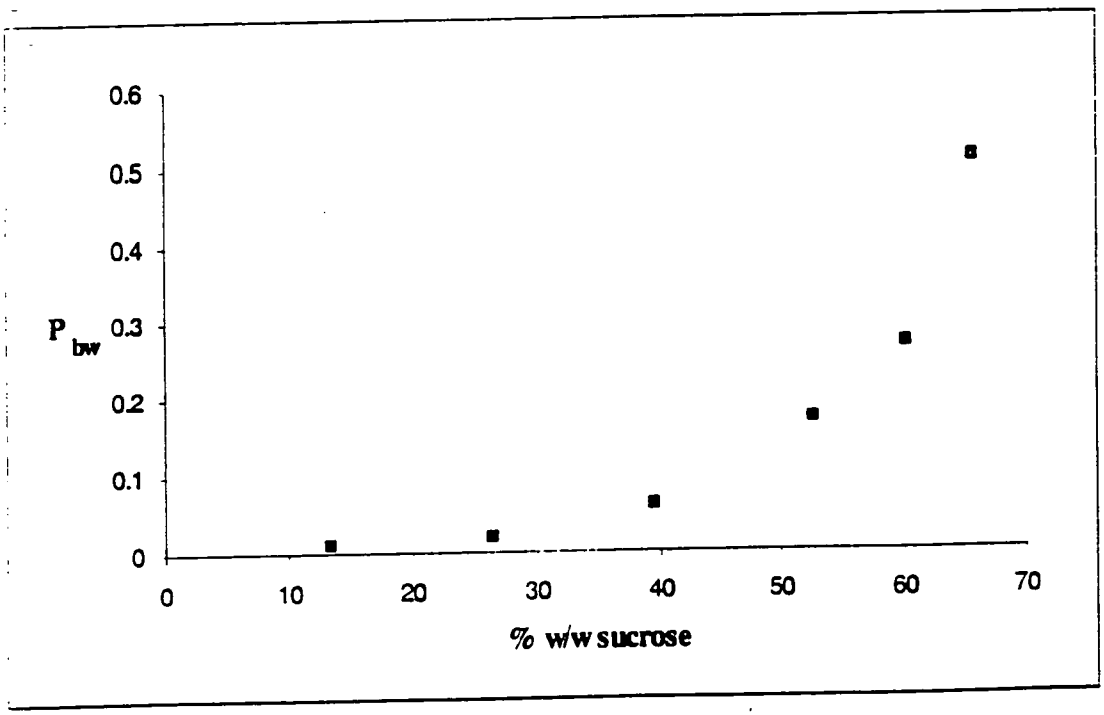

Fig 4.18 The variation of the fraction of bound water, P_{bw}, with sucrose concentration. ω = 13.557 MHz, S = 0.26, τ_f = 123 ps

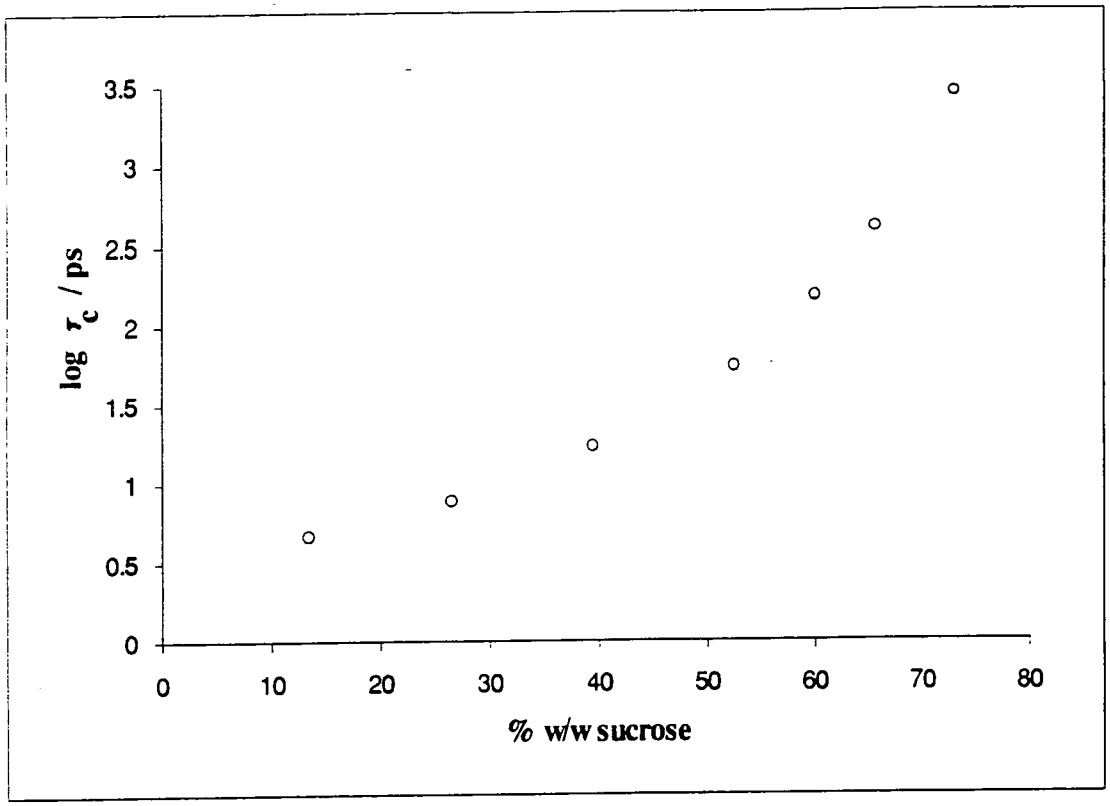

Fig 4.19 The dependence of the correlation time of the slow component of bound water, τ_S, on sucrose concentration. ω = 13.557 MHz, S = 0.26

4.12) Frequency Dependence of ^{17}O Relaxation

The frequency dependence on relaxation and the inequality between longitudinal and transverse relaxation rates can be clearly seen for the saturated sucrose solution (73 % w/w sucrose), Fig 4.20

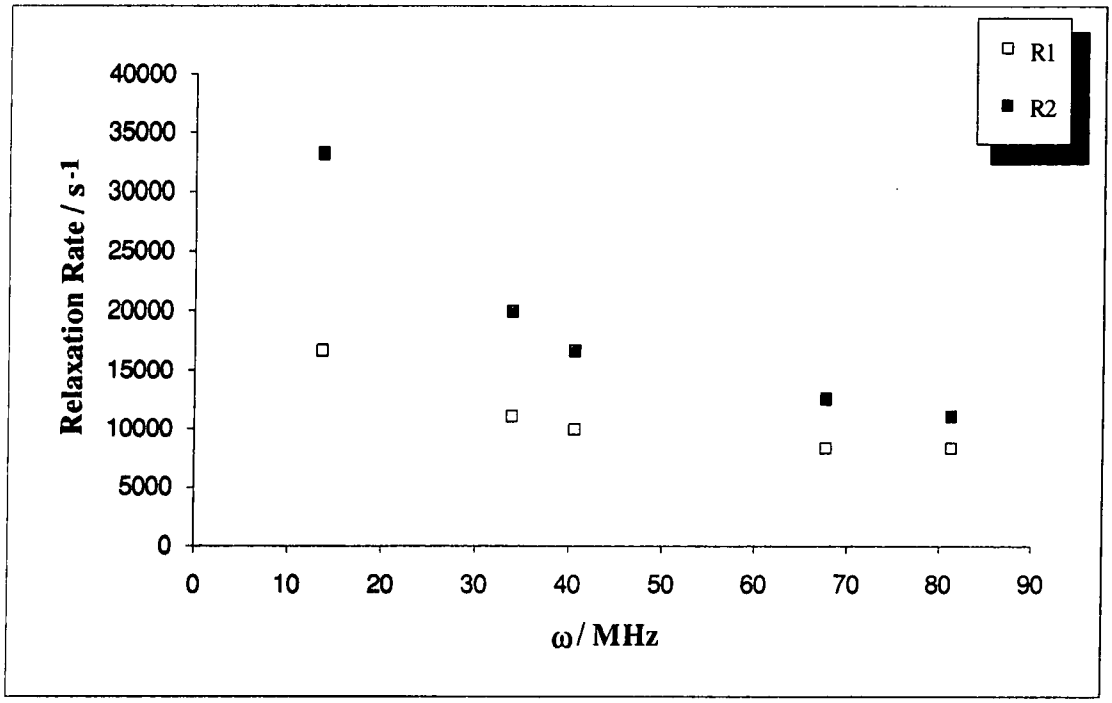

Fig 4.20 The variation of water oxygen-17 longitudinal and transverse relaxation rates on spectrometer frequency for a concentrated sucrose solution. Concentration = 73 % w/w sucrose, temp = 298 K, pH = 2.6

Surprisingly for water oxygen-17, the difference between the transverse and longitudinal relaxation rates was seen to decrease with increasing frequency in the non-extreme narrowing region. Fig 4.20 shows a bigger difference between the two relaxation rates at the lower frequency end which clearly decreases with increasing spectrometer frequency for the saturated sucrose solution. This observation was

reproducible as the whole experiment was repeated at least twice and the same trend for frequency dependence was observed. According to the spectral density function, J(ω), relaxation is independent of frequency as long as the extreme narrowing condition is applicable, but, outside the extreme narrowing range the relaxation decreases with increasing frequency, Fig 4.21. This was observed experimentally. However, the spectral density function also predicts an increase in the difference between the two relaxation rates with frequency, Fig 4.22. Clearly there is a discrepancy with the experimental observation.

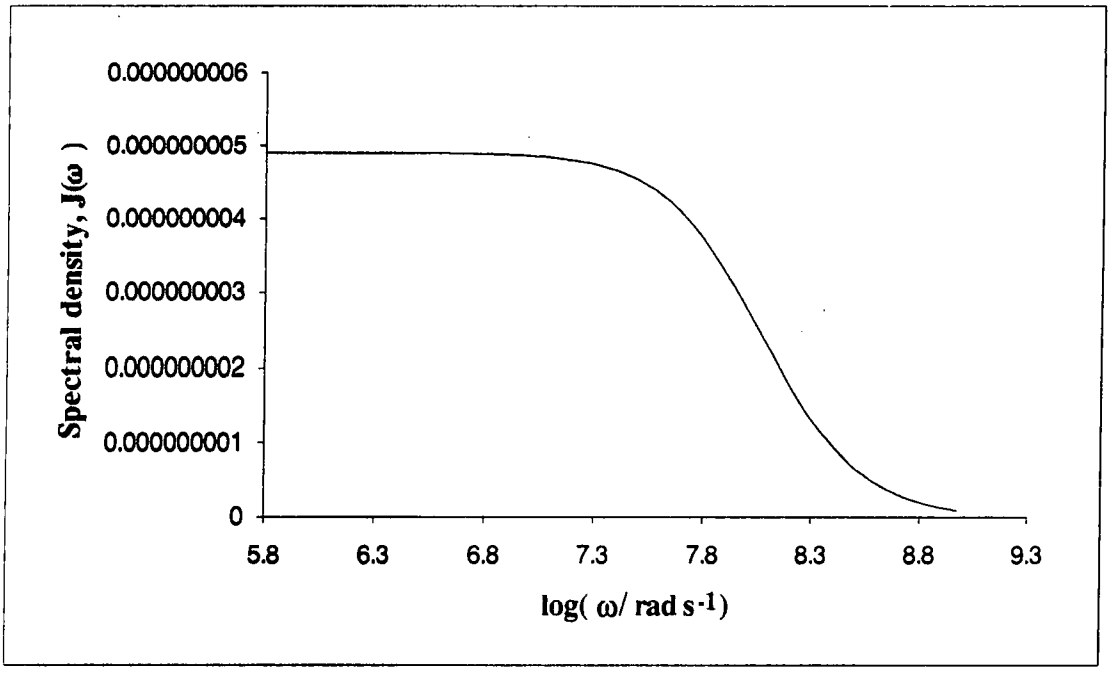

Fig 4.21 The dependence of spectral density, J(ω), on frequency, ω

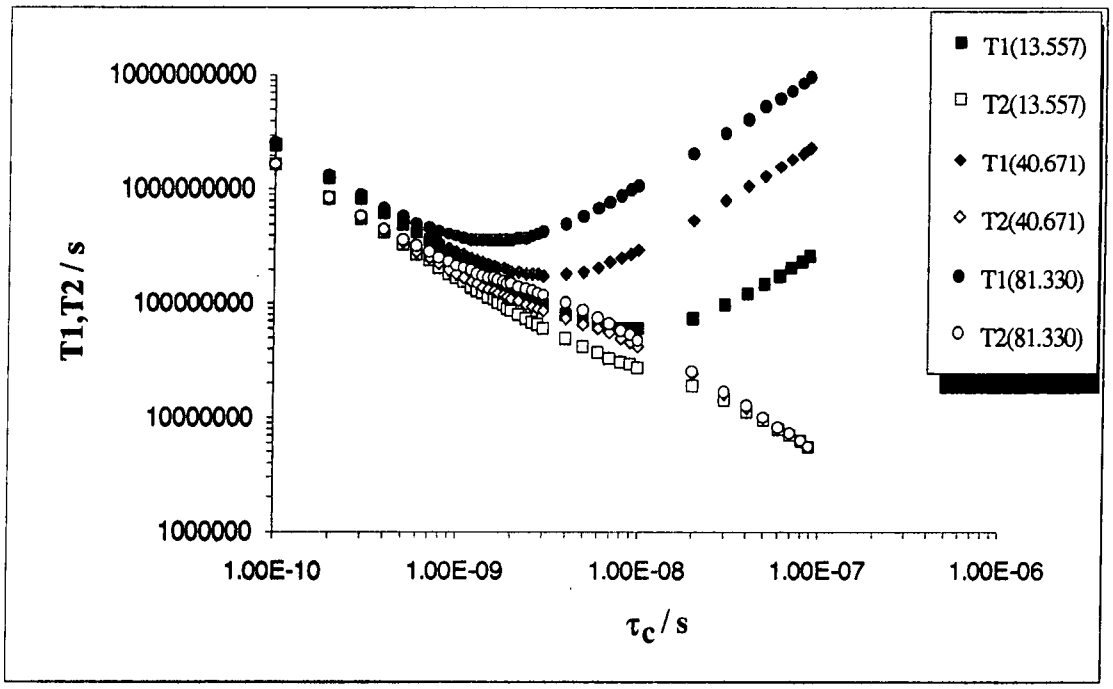

Fig 4.22 The dependence of T_1 and T_2 on τ_c for different spectrometer frequencies.

According to Halle *et al.*[1], water oxygen-17 relaxation in aqueous protein systems is frequency dependent outside the extreme narrowing region. Both the transverse and the longitudinal relaxation rates are expected to decrease with increasing frequency, as is observed experimentally. However, Halle predicted the difference between the two relaxation rates to increase with increasing frequency, Fig 4.23.

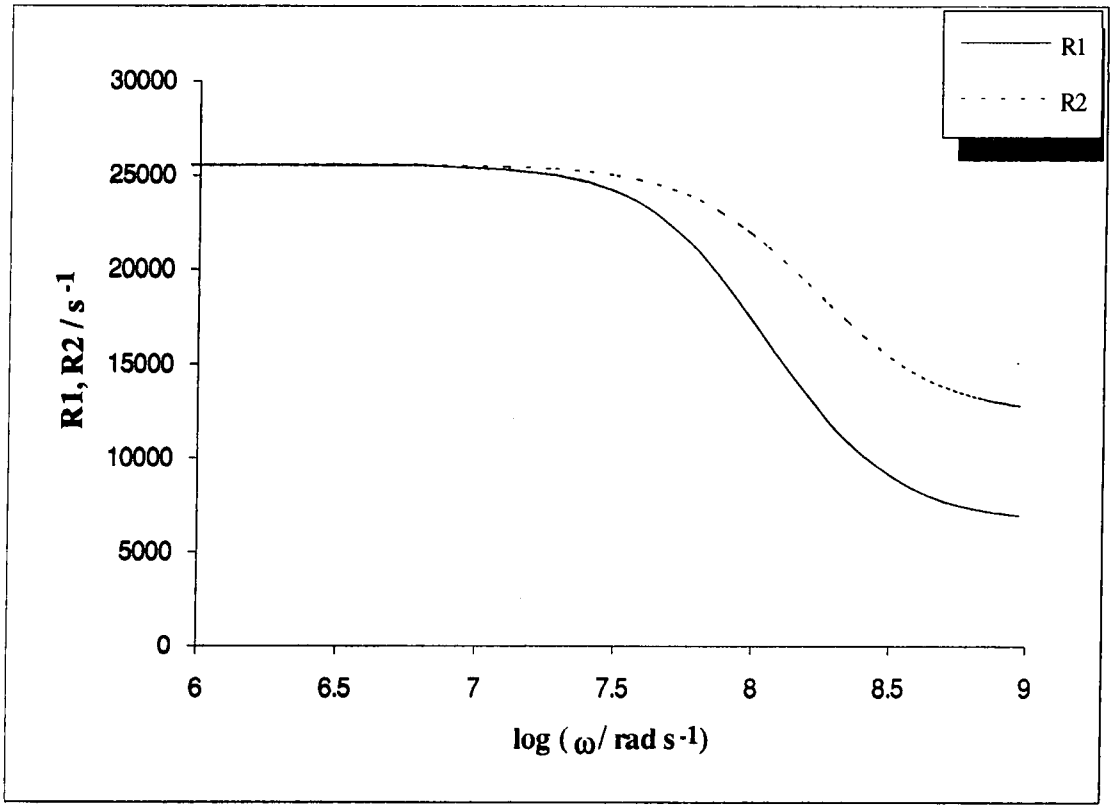

Fig 4.23 Theoretical dependence of water oxygen-17 relaxation rates on frequency according to Halle's model

Clearly, Halle's prediction is in disagreement with the experimentally observed trend for the saturated sucrose case as mentioned above.

For quadrupolar nuclei, like oxygen-17, the concept of relaxation is no longer single exponential once outside the extreme narrowing region. In fact, both the longitudinal and transverse relaxations are each expected to be the sum of I + 1/2 components (3 for oxygen-17, since I = 5/2). Bull *et al.*[10] studied the relaxation of spin I = 5/2 and 7/2 for a two-state model (similar to Halle's model), under conditions where the probability of finding the nucleus in one site, say B — which may be considered as a macromolecule binding site — is very much smaller than that of the other site, say A, the free site. They assumed that site A was in the extreme narrowing limit, where

$\omega_0\tau_c=10^{-3}$, whereas for the nuclei in the less abundant site, B, $\omega_0\tau_c$ was chosen to be 5.0 (non-extreme narrowing region). Fast exchange of nuclei between the two sites was considered. Bull *et al.*[10] showed that for such a system, the longitudinal relaxation is dominated by a single exponential term to a very high degree. However, for transverse relaxation all three relaxing components were considered to be of importance and multiexponential relaxation was a possibility, although this was not observed experimentally. Halle and Wennerström[11] have also reported the relaxation of spin I = 5/2 and 7/2 nuclei in the non-extreme narrowing regime. Longitudinal and transverse relaxation rates were found to be unequal, but both were observed to be single exponential. Deviations from single exponential decay and Lorentzian absorption line shape, a pre-requisite for non-exponential relaxation, have to the author's knowledge only been observed for sodium-23.[12] More commonly, the relaxation appears to be exponential, even when the contribution from the bound state in a two-state system is considerable and when the longitudinal and transverse relaxation rates are unequal and frequency dependent. Halle and Wennerström[11] have argued that, in systems where fast exchange is occurring between sites of extreme motional narrowing and sites with slower fluctuations, transverse relaxation for spin with I = 5/2 and 7/2 will be very nearly exponential. Belton and Ratcliffe[13] have also reported that both longitudinal and transverse relaxation for oxygen-17 in biological systems are observed to be single exponential to a high degree of approximation. However, importantly, they have pointed out that transverse relaxation may be multiexponential and that it is very dangerous to assume a *priori* that transverse relaxation will always be single exponential, especially for concentrated macromolecule systems.

The possibility of multiexponential behaviour for oxygen-17 transverse relaxation was investigated as a possible cause of the unexpectedly observed difference between the transverse and longitudinal relaxation rates as a function of frequency for the saturated sucrose solution. This hypothesis was tested to see if, first of all, multiexponential transverse relaxation could be detected, and secondly whether this was the cause of the

unusual frequency dependence. Figs 4.24 and 4.25 show plots of the transverse relaxation FID data at frequencies of 40.671 and 67.789 MHz respectively.

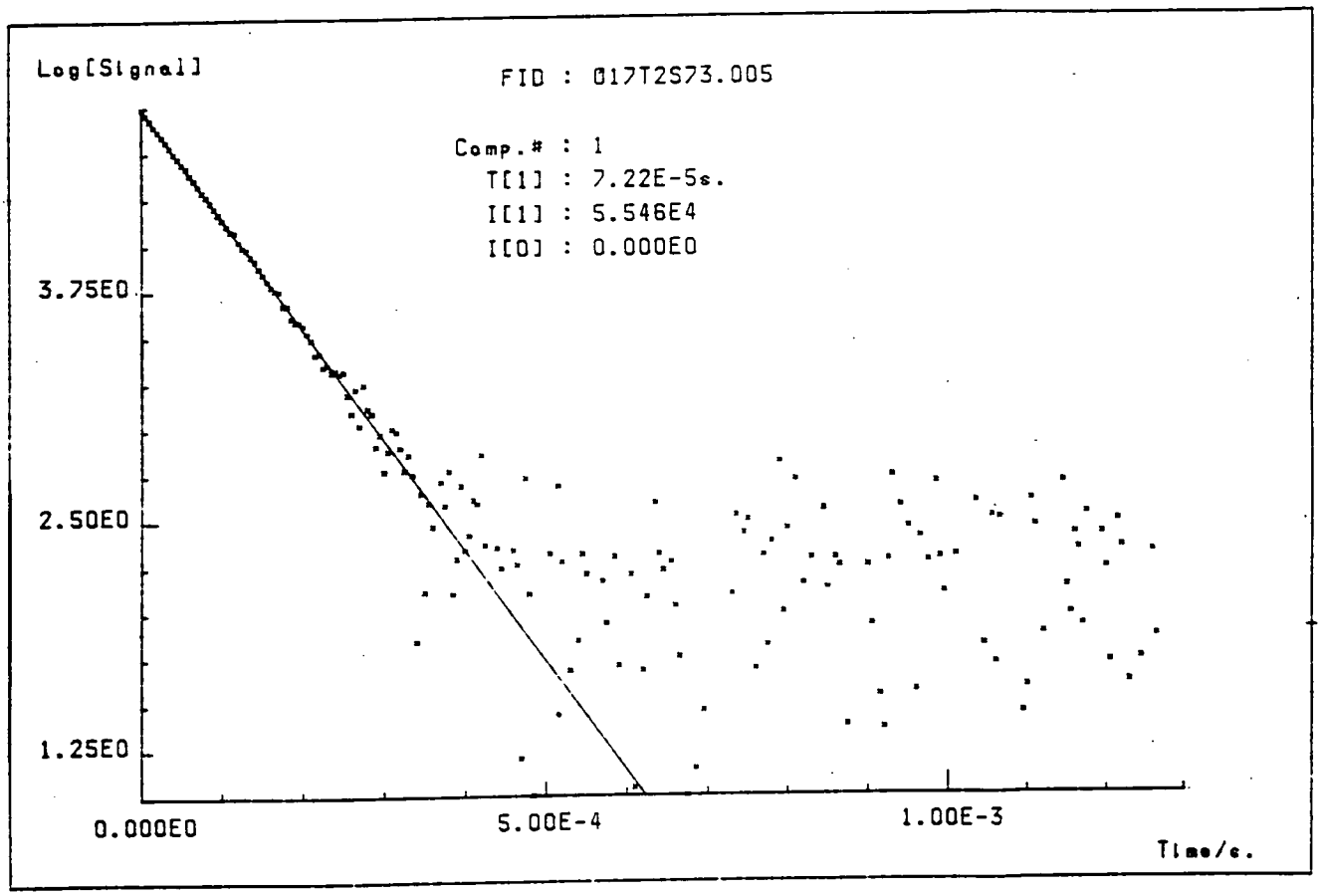

Fig 4.24 Quickfit plot for water oxygen-17 FID in a concentrated sucrose solution. Concentration = 73 % w/w sucrose, SF = 40.671 MHz, pH = 2.6, temperature = 298 K

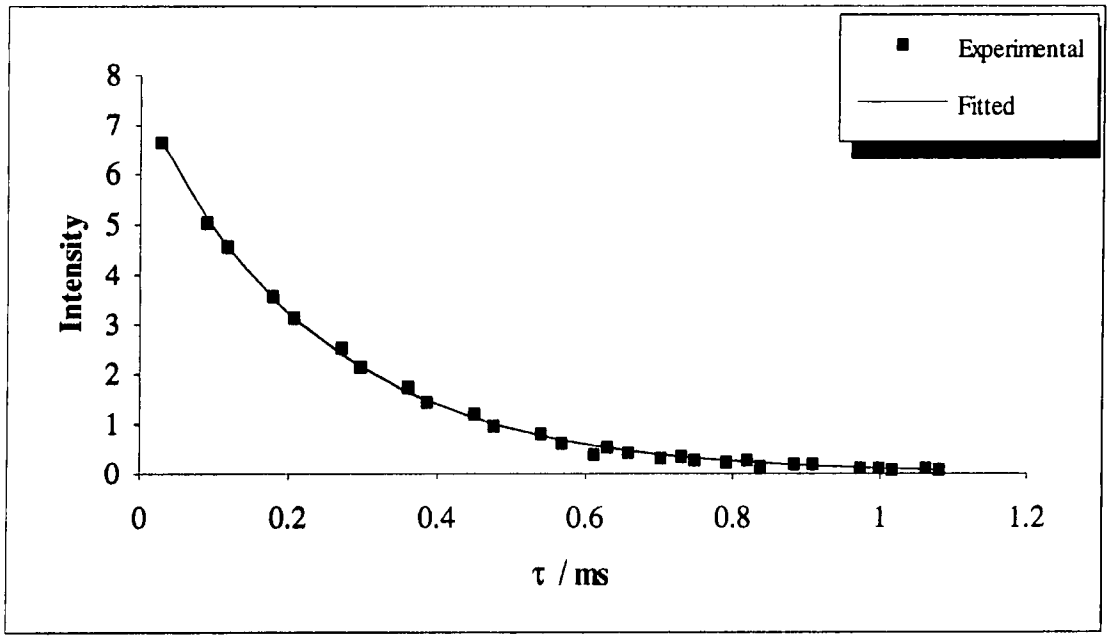

Fig 4.25 Plot of water oxygen-17 FID data to a single exponential transverse relaxation model for an aqueous sucrose solution. SF = 67.789 MHz, temperature = 298 K, pH = 2.6

The transverse relaxation data is seen in both cases to fit well to a single decay, implying that transverse relaxation is single exponential. No signs of multiexponential behaviour could be observed. In fact, for all cases the FID data were in good agreement to a single exponential fit.

In Figs 4.26 and 4.27, the water oxygen-17 longitudinal relaxation FID data are shown fitted to a single exponential equation. As expected, the longitudinal relaxation is single exponential.

Figs 4.28 and 4.29 show Lorentzian line fits to the oxygen-17 signal at spectrometer frequencies of 33.909 and 81.330 MHz. Very reasonable fits are observed, indicating that the water oxygen-17 signal for aqueous sucrose solutions is Lorentzian to a high degree.

Fig 4.26 Simfit plot for water oxygen-17 spin-lattice relaxation data in a concentrated sucrose solution.

Concentration = 73 % w/w sucrose, pH = 2.6, temperature = 298 K.

(x = experimental point, solid line = fitted line)

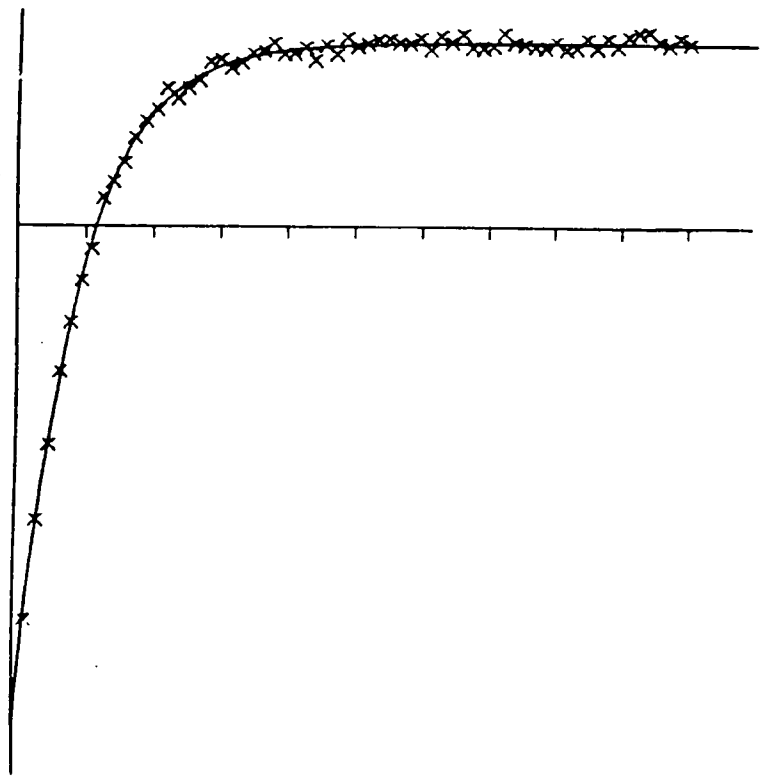

Fig 4.27 Magnetisation recovery after an inversion recovery experiment for water oxygen-17 spin-lattice relaxation in a concentrated sucrose solution. Concentration = 73 % w/w sucrose, SF = 81.330 MHz, pH = 2.6, temperature = 298 K

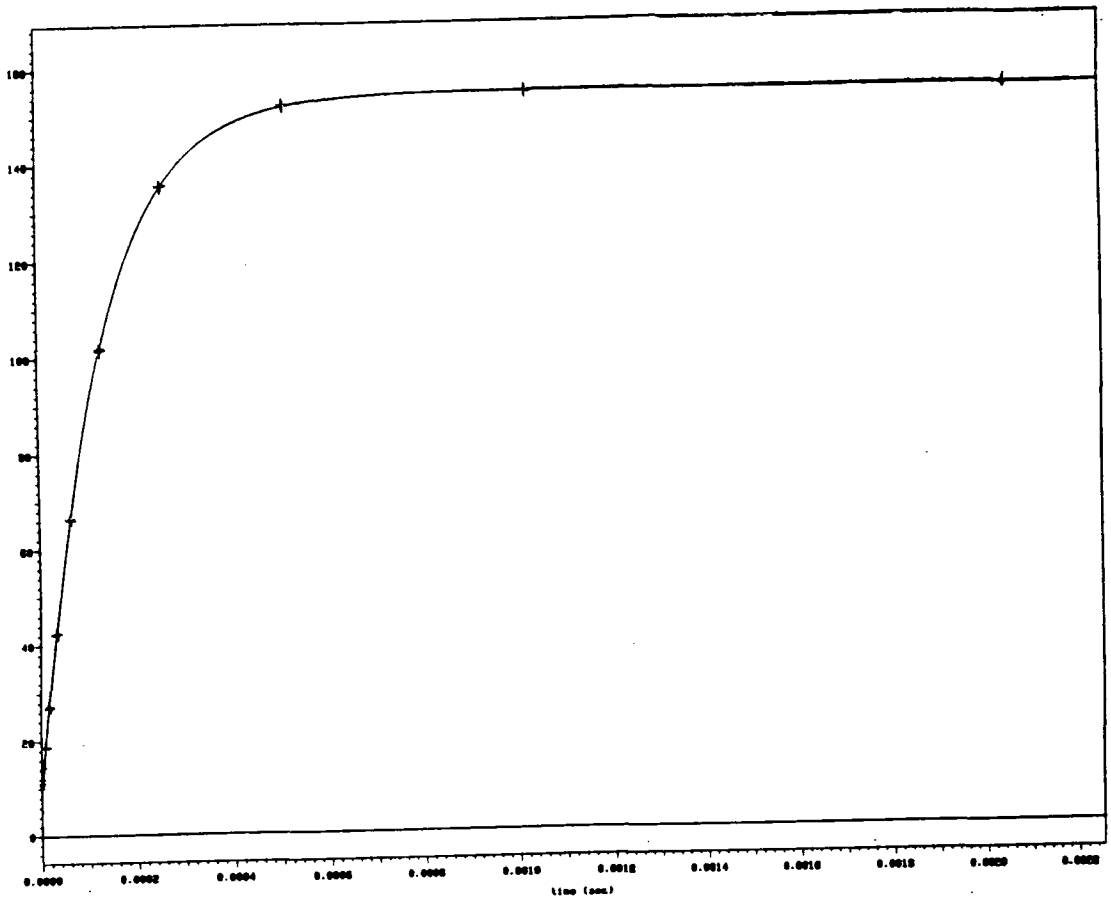

Fig 4.28 Lorentzian line fitting to an oxygen-17 signal for a concentrated sucrose solution. Concentration = 73 % w/w sucrose, SF = 33.909 MHz, pH = 2.6, temperature = 298 K

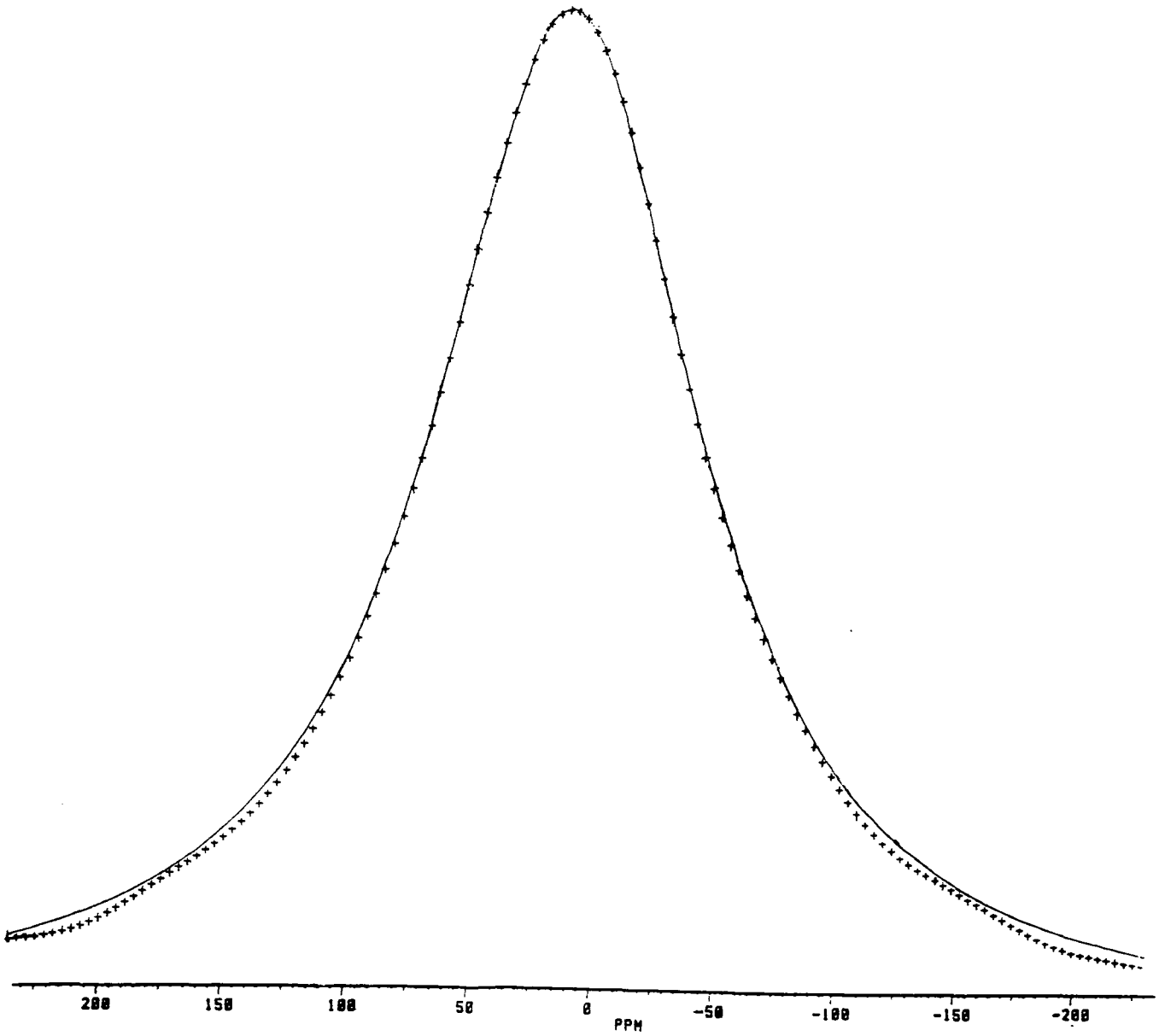

Fig 4.29 Lorentzian line fitting to an oxygen-17 signal for a concentrated sucrose solution. Concentration = 73 % w/w sucrose, pH = 2.6, SF = 81.330 MHz, temperature = 298 K

The 'individual components fit' can be ignored in this case. This is only relevant when there are two overlapping peaks. In such a case, the 'individual components fit' gives a fit to each peak

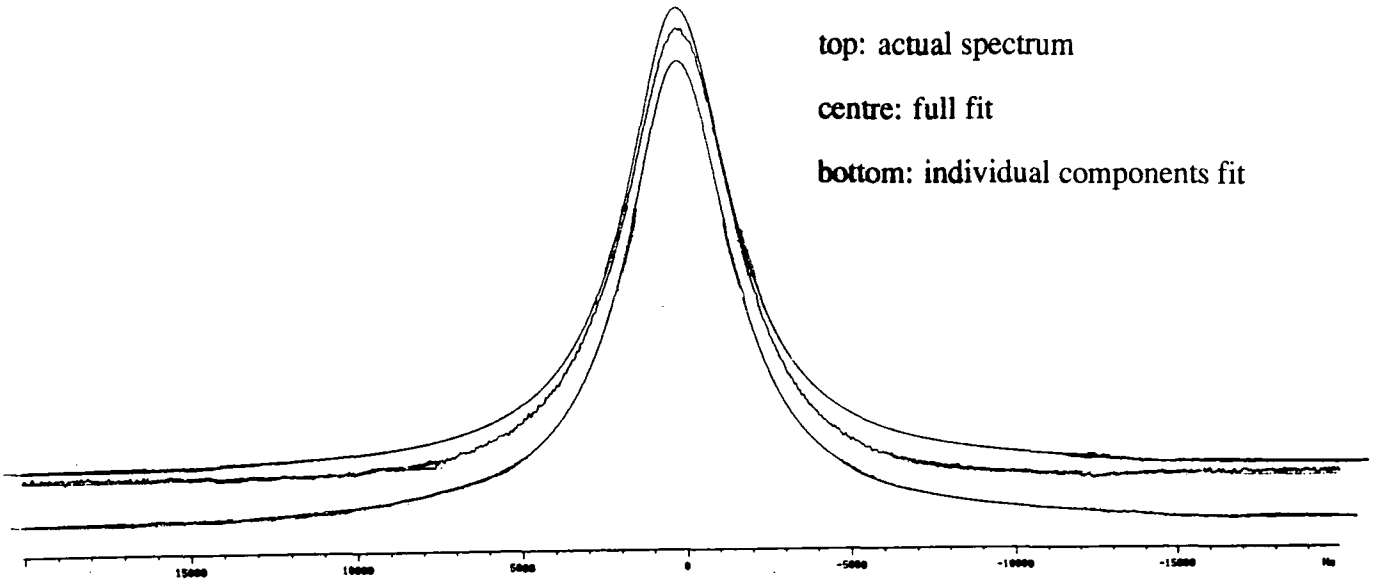

4.12.1) Frequency Dependence of ^{17}O Relaxation for Lysozyme solutions

As expected, according to the literature[10,11,13], multiexponential relaxation behaviour for oxygen-17 could not be detected or observed for either transverse or longitudinal relaxation. Hence, the idea that the unexpected difference in relaxation rates as a function of frequency was a result of multiexponential relaxation was discarded.

To be absolutely sure that the frequency dependence effect on sucrose data is real, an independent study of water oxygen-17 relaxation in aqueous lysozyme solutions as a function of frequency was also carried out. The same experiments for lysozyme were carried out as for sucrose on all spectrometers using the same pulse programs. This allowed the effect of frequency on lysozyme data to be compared to the sucrose data. Any errors from spectrometers would be expected to produce a similar, but unexpected, trend for the difference between the two relaxation rates with increasing frequency for lysozyme as compared to the sucrose data. However, Fig 4.30 shows that the difference between the two relaxation rates for lysozyme increases slightly with increasing frequency. More importantly, the lysozyme data do not show a decrease. Thus, it can be assumed quite confidently that the effect of spectrometer frequency on the relaxation of water oxygen-17 in aqueous sucrose solutions is real.

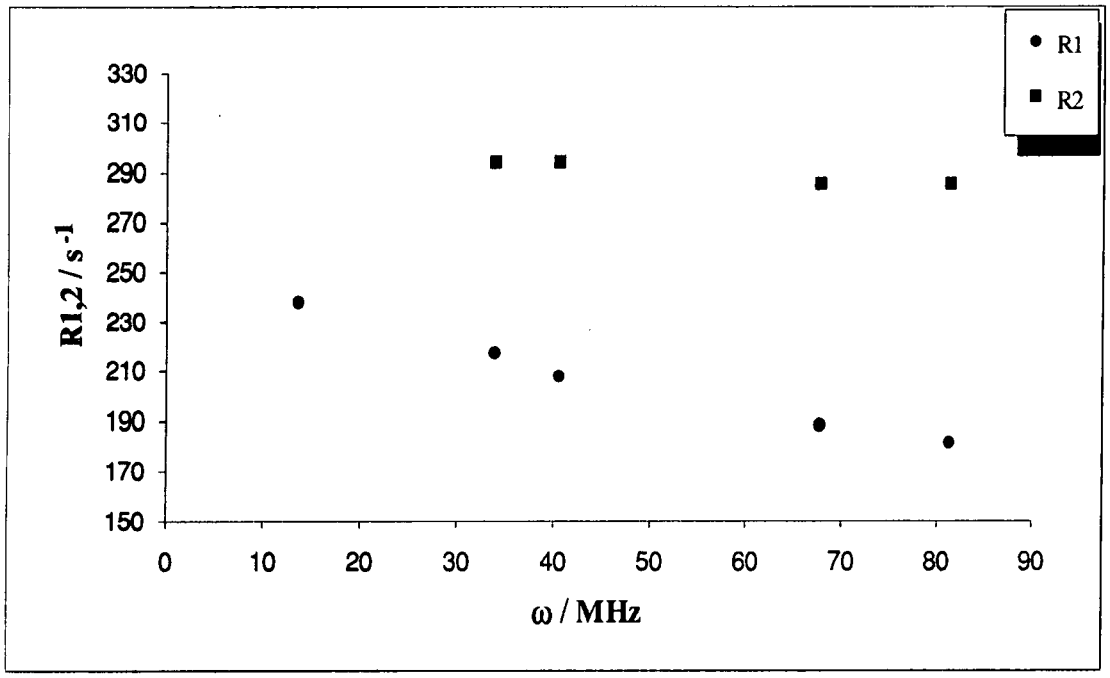

Fig 4.30 Variation of water oxygen-17 relaxation rates for an aqueous lysozyme solution with frequency. Concentration = 8.29 % w/w lysozyme, temperature = 298 K

4.12.2) Possible Explanation for Unexpected Frequency Dependence

Fitting the experimentally observed data for sucrose to Halle's model reveals a very good fit to the longitudinal relaxation data, but, not so good for transverse relaxation. An extra contribution to transverse relaxation is seen for all cases, except at the highest two frequencies, Fig 4.31.

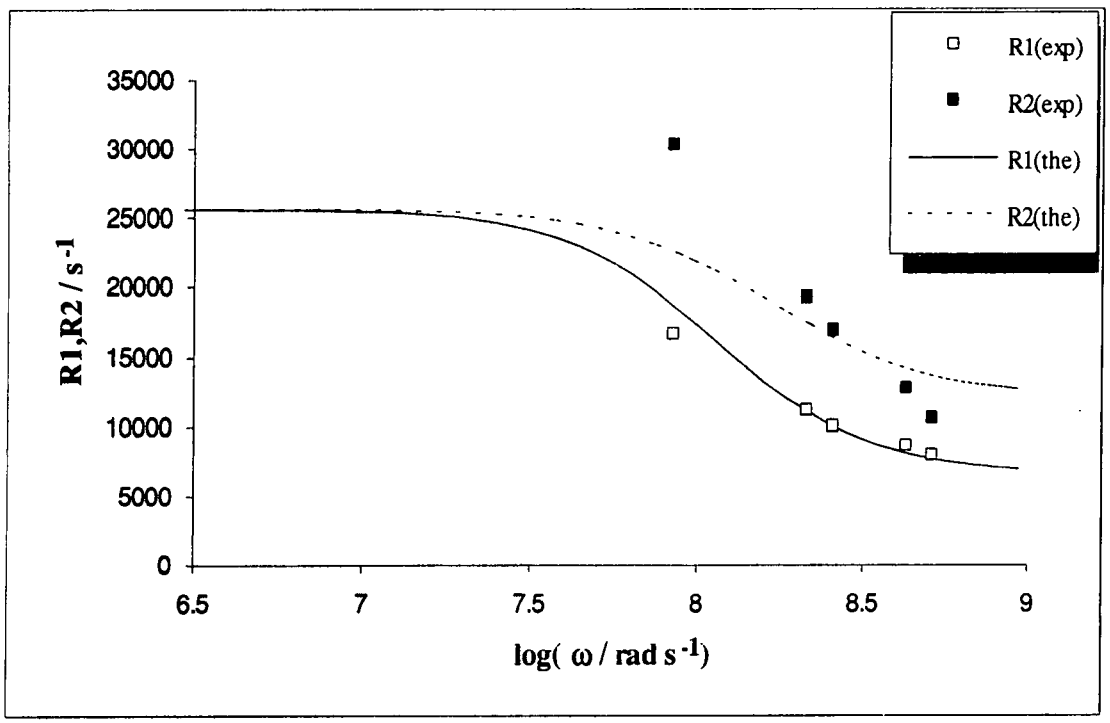

Fig 4.31 Experimental data for water oxygen-17 relaxation for a saturated sucrose solution fitted to Halle's model as a function of frequency.

At high concentrations of sucrose, the exchange of water molecules between the bound and free water may not be rapid, contrary to the assumption made by Halle. In his studies[1], Halle has looked at very low concentrations of proteins for which the exchange of water between the bound and free water states is considered to be fast.

Hence, the exchange process is considered to have a negligible effect on relaxation and is ignored by Halle.

However, the concentration of the protein can be an important factor in controlling the exchange of water between the bound and free water states. With increasing protein concentration, the exchange rate is expected to decrease, such that at high concentrations, the exchange is slow enough that it could possible play an important role for transverse relaxation, by broadening the signal, but not for longitudinal relaxation.

In fact, at high sucrose content, the lifetime of water molecules in the bound state is expected to increase such that the concentration of free water is assumed to be low or negligible. For such a situation, the exchange of water molecules between the bound and free water states is expected to be very slow. Thus, for saturated sucrose solution, the assumption that $P_{bw} = 1$ is expected to be valid. Hence, according to Halle's model, only bound water is expected to be present at high sucrose concentration with slow anisotropic reorientational motion.

However, according to Hills and Pardoe[14], some water still retains a high degree of rotational and translational motion even in the glassy state for sugars. For a 10 % w/w maltose glass, proton NMR studies[14] clearly showed two signals — a narrow signal on top of a much broader signal, Fig 4.32. The broad component was thought to be associated with the rigid maltose CH and OH protons, whilst the narrow component was assumed to be associated with the water protons. The assignment was proved by repeating proton experiments on the 10 % maltose-D_2O solution, for which the amplitude of the narrow central component was greatly reduced. It was not totally removed due to the small quantity of HDO present in the system. However, importantly, Hills and Pardoe showed that even in the glassy-state, where there is no bulk (free) water, the water is still very mobile, as evidenced by its narrow spectral line width. Thus, the prediction based on Halle's model that only one state of water, namely bound water, exists in the absence of free water is not entirely true. In fact,

even when there is no free water, at least two states of water, a mobile state and a rigid state, are expected according to the proton NMR study of Hills.[14]

From the transverse relaxation studies of the rigid and mobile states of water as a function of temperature, Hills observed that, at the glass transition temperature, a considerable change in the dynamic state of both the water and maltose molecules was evident. A drop in $T_{2(rigid)}$ was observed, reflecting the loss of mobility of the maltose molecules as they formed the 3-dimensional network associated with the glassy-state. A similar decrease in $T_{2(mobile)}$ associated with mobility of the water molecules was also observed.

Importantly, the observed narrow component for the glassy-state spectrum at all temperatures indicated that the motion of the water was not associated with that of the maltose. Hills and Pardoe explained the motion of water as being decoupled from that of the sugar. The conclusion from the proton NMR results that water is still highly mobile even in the glassy state was tested by Hills and Pardoe using deuterium NMR on a 10 % maltose-D_2O glass.[14] The broad peak, arising from maltose protons in the proton spectrum, was expected to be absent in the corresponding deuterium spectrum so that only the narrow water, D_2O, component is observed. Any signal from the maltose-deuteroxyl groups is expected to have a short transverse relaxation time as a result of efficient quadrupolar relaxation, so that it is assumed to be broadened into the baseline.

In Fig 4.33 the deuterium spectrum, acquired by Hills and Pardoe, for the 10 % maltose-D_2O glass at the glass transition temperature is shown. Only a narrow single peak for deuterium is observed. This confirmed the earlier assignment of the narrow component in the proton spectrum to water molecules with high mobility in the glassy-state.

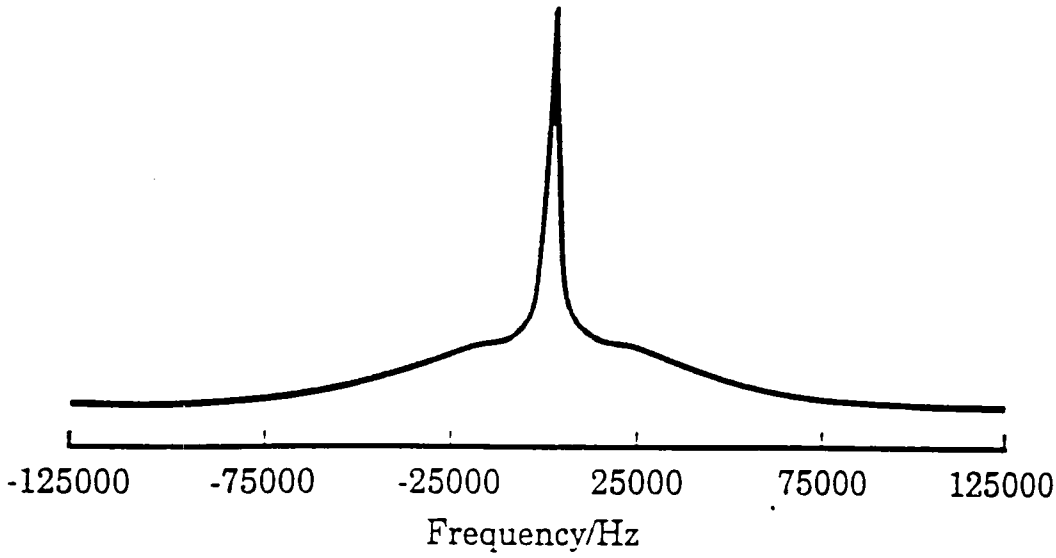

Fig 4.32 Proton spectrum for a 10 % maltose - water glass (from Hills & Pardoe)

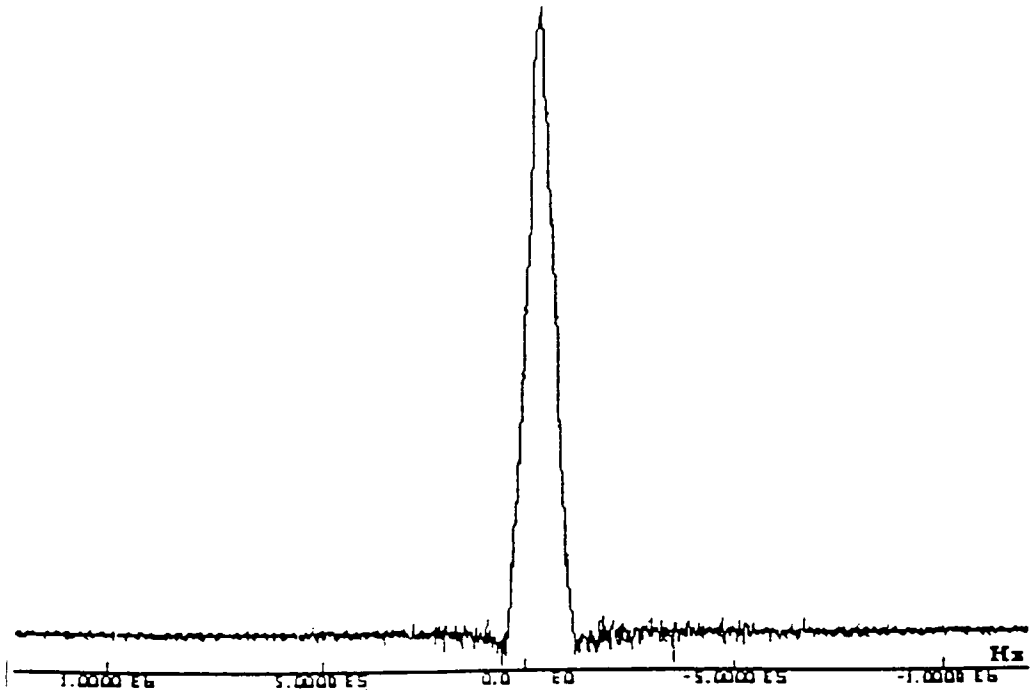

Fig 4.33 Deuterium spectrum for a 10 % maltose - D_2O glass at 258 K (from Hills & Pardoe)

From their study, Hills and Pardoe[14] established a picture for the interaction of water with sugar molecules in glassy-state sugars, Fig 4.34. The picture is one where water is assumed to diffuse into the channels located between the sugar molecules held in a rigid glass matrix. Water is assumed to 'hop' off the various sugar-OH groups, thus undergoing exchange between the sugar molecules. The average distance that water molecules 'hop' in the maltose glassy-state was calculated to be 10 Å by Hills and Pardoe which is reported to be of the order of magnitude of the distance expected between neighbouring maltose molecules.[14] An estimate of 10^{-5} sec. for the average lifetime of a water molecule at a particular site on the maltose glass matrix is quoted by the authors. Within the located channels the water is thought to retain a high degree of rotational and translational motion and as a result a narrow signal is observed.

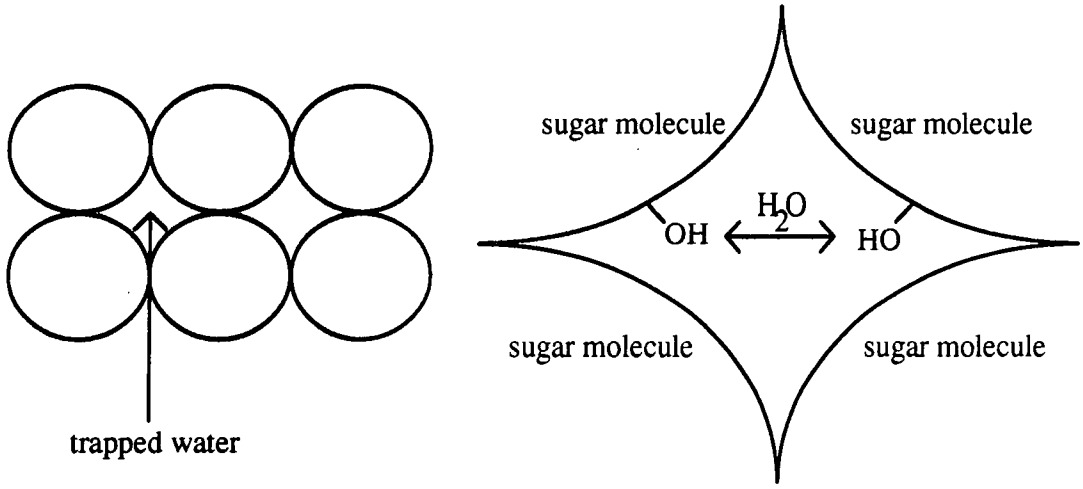

(a) rigid sugar molecules held in a matrix (b) channel in sugar matrix

Fig 4.34 (a) The picture established by Hills and Pardoe[14] for the interaction of water with sugar molecules in the glassy-state, (b) a water molecule hopping (exchanging) between -OH groups of neighbouring sugar molecules within the located channel of the sugar matrix.

Assuming that the picture based on the study of Hills and Pardoe[14] is correct we have to introduce at least two states of water to describe the relaxation of water at saturated sucrose concentration for which there is no free bulk water. One state is the hydrogen bonded, "bound", water molecules to sucrose, with an anisotropic reorientational motion described by two correlation times. The other state is assumed to be that of water molecules trapped by rigid sucrose molecules. It is important to note that the trapped water state is not the same as the free bulk water state. In fact, it is assumed that for saturated sucrose concentration $P_{bw} = 1$, so that there is no free water present in the system.

However, it is reasonable to assume that

$$P_h + P_t = P_{bw} = 1 \qquad \text{eqn 4.17}$$

where P_h and P_t are the fractions of water in the hydrogen bonded and trapped water states, respectively. The trapped water molecules are expected to contribute to the overall relaxation of water. Thus, Halle's model can now be modified to take into account the effect of the trapped water molecules on water oxygen-17 relaxation at high sugar content for which it is assumed that $P_{bw} = 1$. The transverse and longitudinal relaxation rates can be written as

$$R_2 = P_h\left(R^s_{2bw} + R^f_{2bw}\right) + P_t R_{2t} \qquad \text{eqn 4.18}$$

$$R_1 = P_h\left(R^s_{1bw} + R^f_{1bw}\right) + \underbrace{P_t R_{1t}}_{\text{new terms due to trapped water}} \qquad \text{eqn 4.19}$$

Since the sucrose molecules are essentially rigid on the time scale of the water motion, the trapped water molecules are thought to be in the channels located between sucrose

molecules held in a rigid matrix . It is suggested that the interaction of sucrose with trapped water is anisotropic such that the presence of sucrose introduces a local ordering effect on these water molecules around the binding site. As a result quadrupolar splitting of water oxygen-17 may occur. However as reported by Hills and Pardoe[14], the trapped water molecules have a high degree of rotational and translational mobility within the located channels. Thus, the quadrupolar interaction is expected to be averaged out to zero. Therefore, we may expect the trapped water molecules to produce a "powder spectrum" which is the sum of the oriented five-peak sub-spectra, Fig 4.35

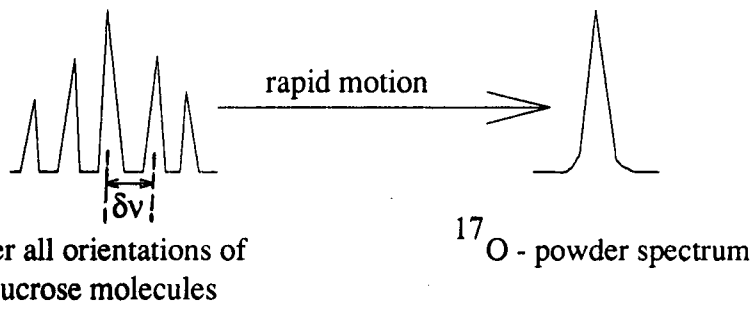

Fig 4.35 Averaging of the five-peak sub-spectra for oxygen-17 to produce a powder spectrum

According to the experimental observation, Fig 4.31, the extra contribution to relaxation only affects transverse and not longitudinal relaxation. The effect on transverse relaxation is observed to be frequency dependent, such that a greater contribution occurs at the lower frequency.

The trapped water molecules are thought to be responsible for the extra contribution to transverse relaxation. Why the trapped water state only affects transverse relaxation and not longitudinal relaxation is not clearly understood. It may be suggested that the exchange ('hopping') process of water molecules between neighbouring sucrose

molecules is only expected to affect transverse relaxation and not longitudinal relaxation. Also, since the powder spectrum is essentially a line broadening mechanism, it is only expected to contribute significantly to transverse relaxation.

Analysing the experimental data reveals that the extra contribution to transverse relaxation may be written empirically in the form

$$R_{2t} = \frac{A(\delta\nu)^2 \tau_t}{1+\omega^2\tau_t^2} \qquad \text{eqn 4.20}$$

where A = constant and incorporates P_t.

The correlation time for trapped water, τ_t, is

$$\frac{1}{\tau_t} = \frac{1}{\tau_{\substack{\text{exchange}\\ \text{lifetime}}}} + \frac{1}{\tau_{\text{rotation}}} \qquad \text{eqn 4.21}$$

where $\tau_{\substack{\text{exchange}\\ \text{lifetime}}}$ = lifetime of a water molecule at a particular site on the sugar molecule

It is expected that

$$\tau_{\substack{\text{exchange}\\ \text{lifetime}}} >> \tau_{\text{rotation}}$$

Therefore,

$$\tau_t = \tau_{\text{rotation}} \qquad \text{eqn 4.22}$$

According to the experimental observation, the extra contribution to relaxation does not affect longitudinal relaxation. Therefore, eqn 4.19 may be simplified to

$$R_1 = P_h\left(R^s_{1bw} + R^f_{1bw}\right) \qquad \text{eqn 4.23}$$

Assuming that R^f_{1bw} is independent of frequency, it is possible to derive eqn 4.24 from eqn 4.23.

$$R_1(0) - R_1(\omega) = P_h\left[R^s_{1bw}(0) - R^s_{1bw}(\omega)\right] \qquad \text{eqn 4.24}$$

Using the extrapolated value of $R_1(0) \approx 2.55\times10^4\ s^{-1}$ at zero frequency obtained from Fig 4.31 (section 4.12.2) and knowing χ and τ_s (τ_s = 4.9 ns, see section 4.11.2) it is possible to calculate the product P_hS^2 at all frequencies studied using eqn 4.24.

Knowing P_hS^2 it is possible to calculate the product $P_hR^s_{1bw}$. Using eqn 4.23 and the experimental value R_1, the product $P_hR^f_{1bw}$ can now be calculated at all frequencies..

The results of the calculation are summarised in table 4.9

ω / MHz	P_hS^2	$P_hR^s_{1bw}$ / s^{-1}	$P_hR^f_{1bw}$ / s^{-1}
13.557	0.08	10604	6095
33.909	0.09	4553	6546
40.671	0.09	3492	6507
67.789	0.08	1501	7198
81.330	0.08	1081	6918

Table 4.9 Calculation of various products for water oxygen-17 longitudinal relaxation in saturated sucrose solution at different spectrometer frequencies. The method of calculation and the various parameters are explained in text.

Re-arranging eqn 4.18 reveals that

$$R_{2t} = \frac{R_2 - P_h\left(R^s_{2bw} + R^f_{2bw}\right)}{P_t} \qquad \text{eqn 4.25}$$

Inserting eqn 4.20 into eqn 4.25 results in

$$\frac{A(\delta\nu)^2\tau_t}{1+\omega^2\tau_t^2} = R_2 - P_h\left(R^s_{2bw} + R^f_{2bw}\right) \qquad \text{eqn 4.26}$$

Eqn 4.26 has two unknown parameters, $A(\delta\nu)^2$ and τ_t. The constant A is assumed to incorporate P_t. Knowing R_2, χ, τ_s, P_hS^2 ($P_hR^s_{2bw}$) and assuming that $P_hR^f_{2bw}$ = $P_hR^f_{1bw}$ it is possible to fit eqn 4.26 as a function of ω to estimate the values of these unknown parameters by using the measurements of T_2 for the five different spectrometer frequencies.

The results of the calculation and fitting are tabulated in table 4.10

Concentration	$A(\delta\nu)^2$	P_hS^2	τ_t / ns
73 % w/w sucrose	1.72×10^{12}	0.08	9

Table 4.10 Calculated and fitted parameters for the extra contribution to transverse relaxation.

The extra contribution to transverse relaxation, in the form of the relationship given in eqn. 4.20, explains the unexpected difference observed between the two relaxation rates as a function of frequency, Fig 4.36. There remains a small discrepancy at the

highest spectrometer frequency. However, it can be seen that the calculated value of τ_t is not unreasonable.

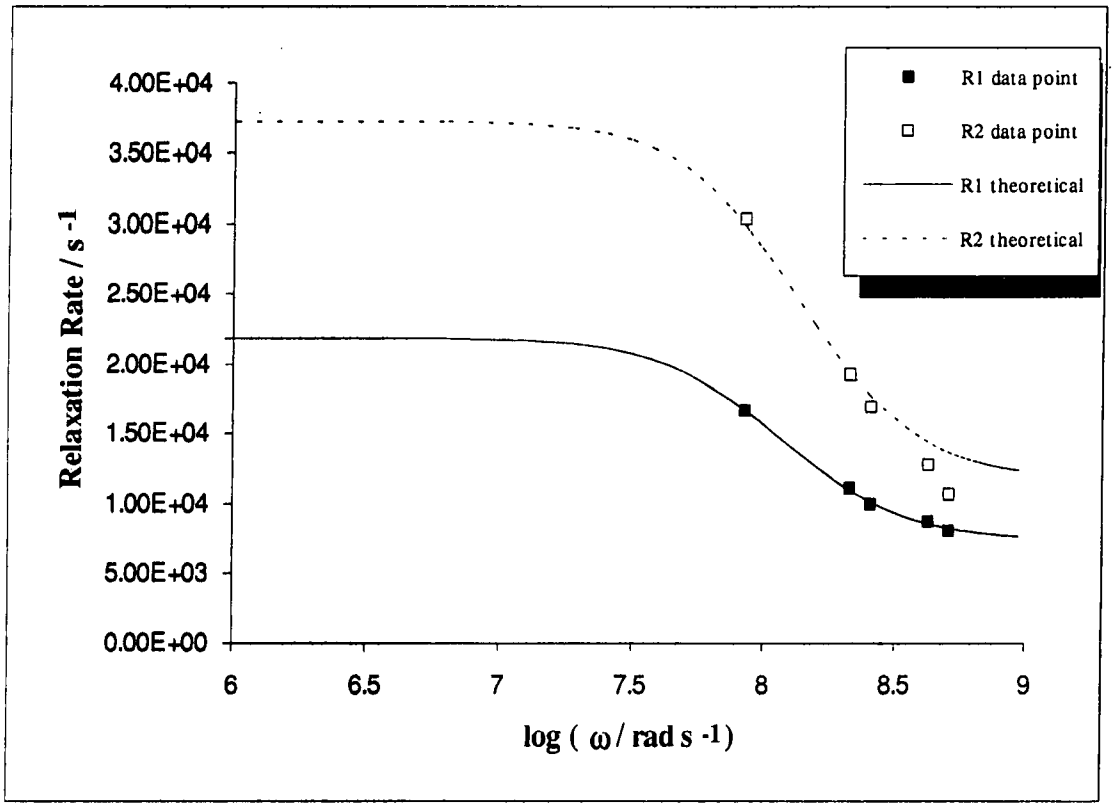

Fig 4.36 Comparison between the experimental and theoretical data for water oxygen-17 R_1 and R_2 in aqueous sucrose solution. The theoretical data are derived using Halle's model. The theoretical curve for transverse relaxation data includes the extra contribution.
Concentration = 73 % w/w sucrose, temperature = 298 K

Assuming that the extra state of water is due to trapped water molecules, then the results obtained in this study agree quantitatively with the model proposed by Hills and Pardoe[14] in order to explain their water proton results for a 10 % maltose-H_2O glass.

The extra contribution to transverse relaxation is only expected at high sucrose content for which there is no free, bulk, water. It is not expected at low concentrations of sucrose because at these concentrations there is a considerable amount of free water present in the system and no trapped water. The exchange of water molecules between bound and free water states is assumed to be sufficiently rapid that it does not contribute to transverse relaxation. In fact, it was found that both the transverse and the longitudinal relaxation of water oxygen-17 at low concentrations of sucrose agreed reasonably well with the model proposed by Halle.

The high value of the order parameter, S, calculated for the saturated sucrose solution may also be explained as a result of the trapped water state. A strong interaction between the trapped water molecules and sucrose is assumed to be present. As a consequence the sucrose molecules exert a high local ordering effect on these water molecules. Thus, the water molecules are expected to be highly ordered within a small confined space — in agreement with the high order parameter calculated in the present research compared to the value estimated by Halle[1].

4.13) CONCLUSION

From the relaxation study of water oxygen-17 in aqueous sucrose solutions, it can be assumed that the theoretical model proposed by Halle[1] for water oxygen-17 relaxation is only reliable at low concentrations of sucrose. The model is based on the assumption that fast exchange of water molecules takes place between the bound and free water states , which is strictly only valid at low concentrations of sucrose. A significant amount of free water is present in the system at low concentrations of sucrose, and therefore rapid exchange of water molecules between the two water states is expected. Thus, the two-state fast-exchange model gives good agreement with the experimental data.

However, with increasing concentration of sucrose, the lifetime of a water molecule in the bound state is expected to increase, such that at high sucrose content the assumption that rapid exchange of water molecules takes place between the two water states is no longer valid. At high concentrations of sucrose, the experimental data for transverse relaxation is observed to disagree with Halle's model. In fact, an extra contribution to transverse relaxation is observed which surprisingly has no effect on longitudinal relaxation. Even at high sucrose concentration, longitudinal relaxation is observed to give good agreement with Halle's model . Unfortunately, the exact origin of the extra contribution remains a mystery. However, it is suggested that the extra contribution to transverse relaxation may be due to water molecules being trapped in a rigid matrix of sucrose molecules, which undergo exchange (or 'hop') between sucrose hydroxyl groups on adjacent sucrose monomers, in agreement with the model proposed by Hills and Pardoe[14] . These authors suggested that the trapped water state, in conjunction with the bound water state, explained the observation of two proton signals (a narrow signal and a broad signal) for a 10 % maltose glass. Furthermore, the trapped water molecules are suggested to be associated with considerable rotational and translational motion and as a result a powder spectrum for water oxygen-17, which is the sum of five peak sub-spectra, is produced.

It may be suggested that, since the trapped water molecules undergo exchange and because the powder spectrum is essentially a line broadening mechanism, then these water molecules only contribute significantly to transverse relaxation and not to longitudinal relaxation.

Importantly, the present research shows that for high concentrations of sucrose or any other macromolecule the relaxation of water oxygen-17 cannot be explained in terms of Halle's model but it is necessary to modify this model to take into consideration the extra contribution to transverse relaxation.

For low concentrations of macromolecule, Halle's model importantly highlights the point that the motion of bound water must be considered to be anisotropic, which can only be described by two correlation times of differing magnitudes. In studies where the bound water is described by only one correlation time,[15-17] great difficulty was encountered in correlating the experimental data to the theoretical model. In such cases, data interpretation is considered to be in serious error. Therefore, as Halle has shown, it is important to consider anisotropic motion of the bound water.

REFERENCES

1) B. Halle, T. Andersson, S. Forsén and B. Lindman, *J. Am. Chem. Soc.*, 1981, **103**, 500

2) L. Piculell, *J. Chem. Soc., Faraday Trans. 1*, 1986, **82**, 387

3) B. Halle and G. Karlström, *J. Chem. Soc., Faraday Trans. 2*, 1983, **79**, 1031

4) P.S. Belton and K.M. Wright, *J. Chem. Soc., Faraday Trans. 1*, 1986, **82**, 451

5) B.P. Hills, *Mol. Phys.*, 1991, **72**, 1099

6) R.C. Weast, *CRC Handbook of Chemistry and Physics*, 1983 - 1984, p.D-266, 64th Ed., CRC Press, Boca Raton, Florida

7) P.S. Belton, S.G. Ring, R.I. Botham and B.P. Hills, *Mol. Phys.*, 1991, **72**, 1123

8) L.T. Kakalis and I.C. Baianu, *Arc. Biochem. Biophys.*, 1988, **267**, 829

9) B. Halle and H. Wennerström, *J. Chem. Phys.*, 1981, **75**, 1928

10) T.E. Bull, S. Forsén and D.L. Turner, *J. Chem. Phys.*, 1979, **70**, 3106

11) B. Halle and H. Wennerström, *J. Mag. Res.*, 1981, **44**, 89

12) H. Gustavsson, B. Lindman and T. Bull, *J. Am. Chem. Soc.*, 1978, **100**, 4655

13) P.S. Belton and R.G. Ratcliffe, *Prog. NMR Spectrosc.*, 1985, **17**, 241

14) B.P. Hills and K. Pardoe, private communication

15) S.J. Richardson, I.C. Baianu and M.P. Steinberg, 1987, *J.F. Sci.*, **52**, 806

16) T.F. Kumosinski and H. Pessen, 1982, *Arc. Biochem. Biophys.*, **218**, 286

17) J.R. Zimmerman and W.E. Brittin, 1957, *J. Phys. Chem.*, **61**, 1328

5.1) Lysozyme Experiments

Relaxation of water oxygen-17 in aqueous lysozyme solutions was studied as a function of lysozyme concentration at different spectrometer frequencies. The effect of ionic strength on water oxygen-17 relaxation was examined in detail for lysozyme solutions. To a constant concentration of lysozyme, different amounts of NaCl were added and oxygen-17 relaxation studied.

Halle *et al.*[1] studied the effect of frequency on water oxygen-17 relaxation for aqueous protein solutions. Both the longitudinal and transverse relaxation rates were reported to decrease with increasing frequency, Fig 5.1. However, as can be observed from Fig 5.1, Halle's data seem to be insufficient to predict a frequency variation. A poor correlation between the experimental data and the theoretical curves is observed for most cases. In fact, looking at Halle's data it seems to be very difficult to draw any reasonable conclusion from only a few data points. Thus, it was considered worthwhile to analyse the variation of water oxygen-17 relaxation rates with frequency for aqueous lysozyme solutions to confirm whether or not Halle's prediction and conclusions are valid. The effect of frequency on water oxygen-17 relaxation for lysozyme solutions with and without the presence of NaCl was analysed.

The longitudinal relaxation time for water oxygen-17 was measured using the inversion-recovery pulse sequence, whereas the transverse relaxation time was measured from the linewidth at half-height or the on-resonance FID. For Bruker MSL-100 and MSL-300 spectrometers the on-resonance FID was used. For other spectrometers, the linewidth at half-height of the Fourier transformed spectrum was used to calculate the transverse relaxation time.

In fact, the experimental methods described for sucrose solution analysis (see section 4.8) were repeated for lysozyme analysis, with the addition of proton decoupling.

All measurements were carried out at a temperature of 298 K using a 10 mm probe.

Fig 5.1 Water oxygen-17 longitudinal (filled symbols, solid curves) and transverse (open symbols, dashed curves) relaxation rates normalised to unit protein concentration W_{PR} (mass %) for aqueous protein solutions at 27 °C as a function of frequency (Fig 3, reference 1). Symbols represent experimental data, whereas the lines represent the fits according to Halle's model.

HPA = Human Plasma Albumin, PA = Parvalbumin, Lys = Lysozyme

Cyt C = Cytochrome C and Hb = Human Oxyhemoglobin

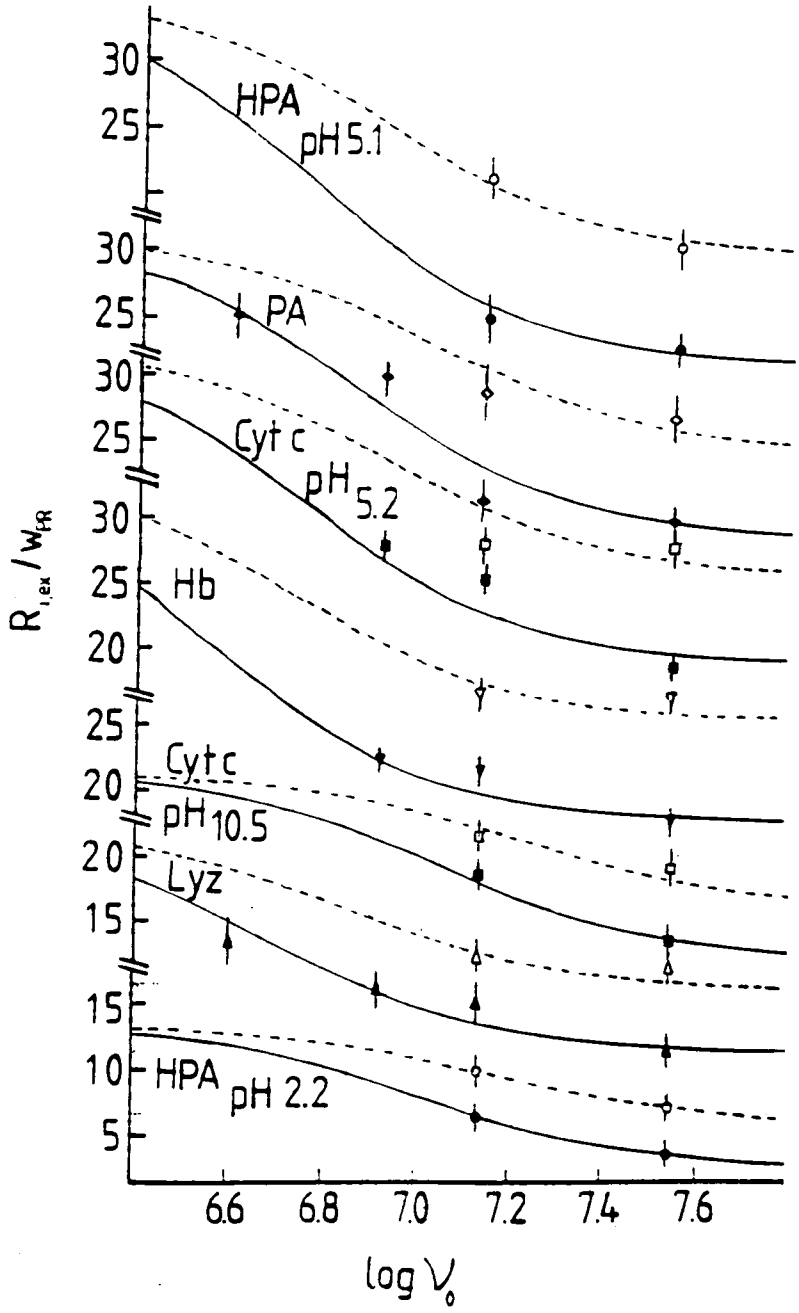

5.2) Lysozyme Sample Preparation

Lysozyme solutions were prepared by following the procedure used for sucrose solution preparation. To 1 g of approximately 21 % oxygen-17 enriched water successive additions of lysozyme were made to increase the lysozyme concentration. Initially the least concentrated sample was prepared. Each sample was analysed before the next increment of lysozyme. Unlike sucrose solutions, the pH of water was not altered to less than three when preparing lysozyme solutions . An attempt was made to perform lysozyme experiments using the same conditions as Halle. In Halle's study,[1] the pH of the lysozyme solutions was approximately 5.1. In the present research, pH measurements were done by using both litmus paper and a pH meter (Jenway 3020 meter). To remove the effect of proton exchange broadening on the oxygen-17 signal, proton decoupling experiments were performed for all cases.

When studying the effect of sodium chloride on water oxygen-17 relaxation in aqueous lysozyme solutions, a constant concentrated lysozyme solution (8.29 % w/w lysozyme) was prepared. To this was added different amounts of sodium chloride to increase the salt concentration.

Chicken egg white lysozyme was purchased from Sigma Chemical Co. Ltd and used without any further treatment. Sodium chloride was purchased from BDH Chemicals and also used without any further treatment

5.3) Results

5.3.1) Absence of Salt

For all solutions of lysozyme a single water oxygen-17 signal was observed. The relaxation of water oxygen-17 was found to be very fast due to a very efficient relaxation mechanism, predominantly quadrupolar.

In table 5.1 the relaxation of water oxygen-17 in aqueous lysozyme solutions is reported for various concentrations of lysozyme at different spectrometer frequencies.

The relaxation of water oxygen-17 in the presence of lysozyme can be considered to follow Halle's model.[1] As mentioned before, Halle's model considers two states of water, bound and free. Furthermore, the bound water is considered to have anisotropic motion, described by two relaxation rates. With increasing lysozyme concentration the relaxation rates, R_1 and R_2, are seen to increase, Fig 5.2. It is known that lysozyme self-associates with increasing concentration to form dimers and higher oligomers[2-4] (which only become important at high protein concentrations). With increasing lysozyme concentration the amount of bound water is also expected to increase. Both the lysozyme association and the increase in bound water are expected to decrease the overall motion of the lysozyme-water system. Hence, with increasing lysozyme concentration, the reorientational motion of bound water is expected to increase, resulting in an increase in relaxation rate as is observed experimentally, Fig 5.2. A detailed discussion can be found in section 5.4.

The concentration effect of lysozyme on water oxygen-17 relaxation in aqueous lysozyme solutions has also been studied by Halle *et al.*[1] at spectrometer frequencies of 4.0, 8.13, 13.56 and 33.9 MHz. The relaxation rates were reported to increase with increasing lysozyme concentration, Fig 5.2. Similarly, Lioutas *et al.*[6] have studied the

effect of lysozyme concentration on water oxygen-17 transverse relaxation for lysozyme-D_2O solutions at pD 7 and 20 °C at a frequency of 33.9 MHz. An increase in transverse relaxation rate was observed with increasing protein concentration as can be seen from Fig 5.2. Furthermore, Fig 5.2 shows that at low concentrations of lysozyme the transverse relaxation rate measured by Lioutas and Baianu[6] is greater than that measured in the present research and that of Halle *et al.*[1] This is attributed to the fact that D_2O has a greater viscosity than H_2O and as result the relaxation rate in D_2O is expected to be greater than in H_2O.

	SF = 13.557 MHz		SF = 33.909 MHz		SF = 40.671 MHz		SF = 67.789 MHz		SF = 81.330 MHz	
% w/w lysozyme	T1 / ms	T2 / ms	T1 / ms	T2 / ms	T1 / ms	T2 / ms	T1 / ms	T2 / ms	T1 / ms	T2 / ms
1.04	7.5		7.4	6.3	7.3	6.5	7.4	6.4	7.3	6.4
3.01	6.8		6.8	5.6	6.7	5.7	6.7	5.7	6.8	5.7
4.98	6.1		6	4.7	5.9	4.8	6	4.8	6.1	4.8
6.00	5.8		5.6	4.2	5.7	4.2	5.7	4.3	5.9	4.3
6.45	5.3		5.4	3.9	5.4	4	5.5	4	5.6	4.1
6.96	5		5.2	3.8	5.3	3.8	5.4	3.9	5.6	4
8.29	4.2		4.6	3.4	4.8	3.4	5.3	3.5	5.5	3.5

Table 5.1 Experimental data for water oxygen-17 longitudinal and transverse relaxation in aqueous lysozyme solutions as a function of lysozyme concentration at 298 K for different spectrometer frequencies.

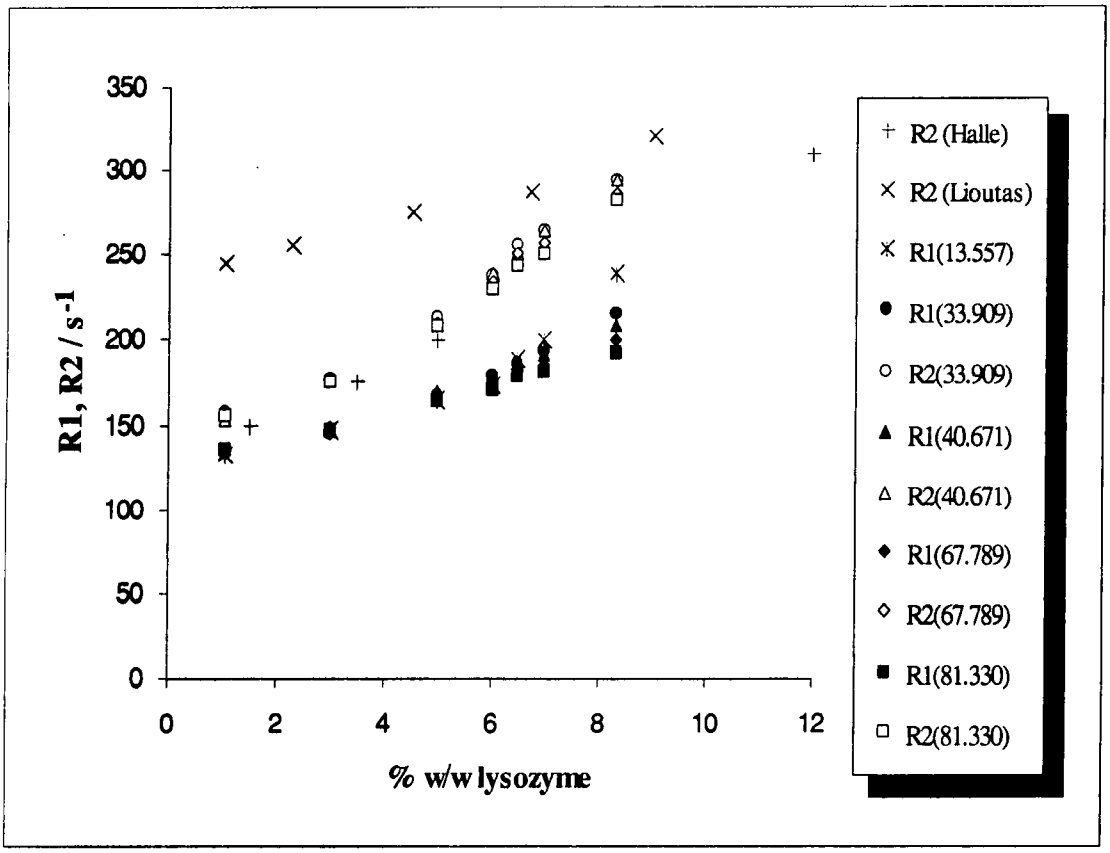

Fig 5.2 The dependence of water oxygen-17 longitudinal and transverse relaxation rates on lysozyme concentration for aqueous lysozyme solutions at various spectrometer frequencies. Filled symbols correspond to longitudinal and open symbols to transverse relaxation data obtained in this research. × represents R_2 data from Lioutas and Baianu's work at 34 MHz in D_2O solutions (from Fig 3, reference 6), whereas + represents R_2 data from Halle's work at 13.56 MHz (from Fig 6, reference 1)

The transverse relaxation rate is always observed to be greater than the longitudinal relaxation rate as may be expected. The difference between the two relaxation rates is seen to increase with increasing concentration and frequency (see section 4.12.1).

Fig 5.2 shows that at low concentrations of lysozyme, both the longitudinal and the transverse relaxation rates are independent of frequency. However, at high concentrations of protein, a frequency dependence can be observed for T_1 but

apparently not for T_2 as can be seen from Fig 5.3. A possible explanation for this is given below. With increasing frequency, the longitudinal relaxation rate is observed to decrease as would be expected from Halle's model.

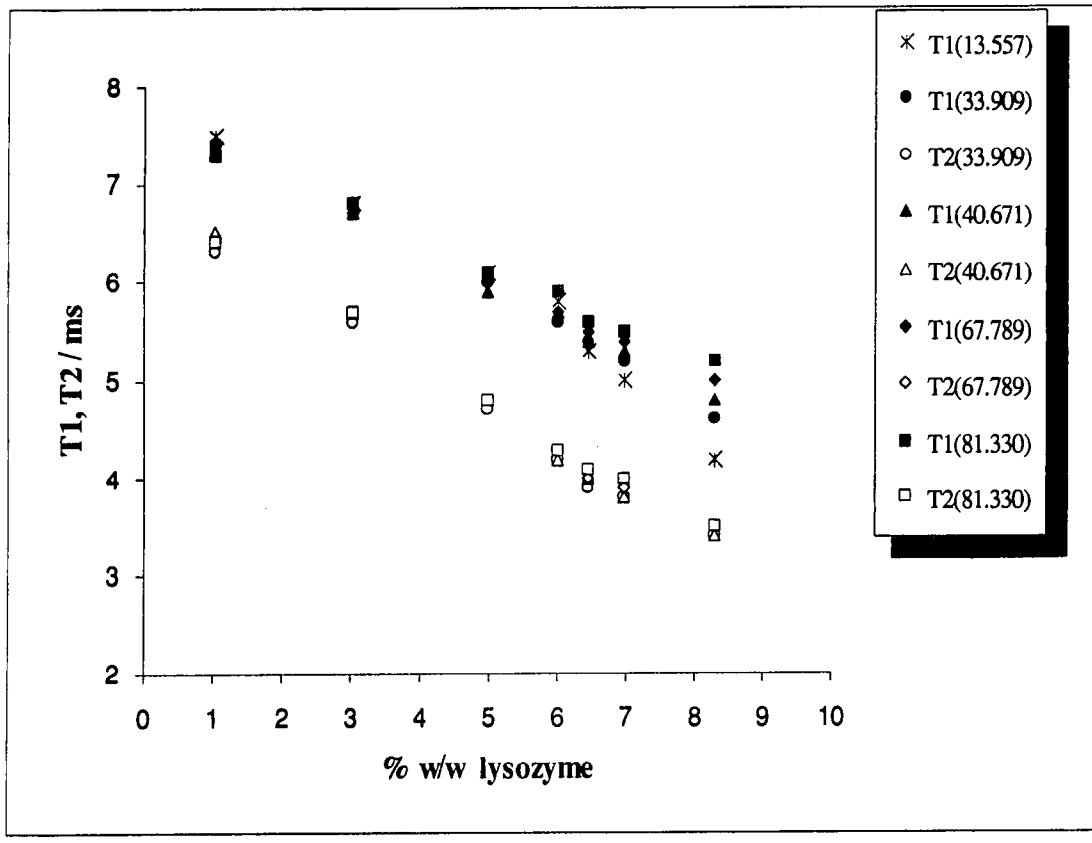

Fig 5.3 The dependence of water oxygen-17 longitudinal and transverse relaxation times on lysozyme concentration for aqueous lysozyme solutions at various spectrometer frequencies.

At high concentrations of lysozyme, the process of self association and the increase in solution viscosity decrease the motion of the lysozyme-water system such that the system is no longer in the extreme narrowing region and becomes frequency-dependent.

When analysing their data, Lioutas *et al.*[6] claimed to have identified five different populations of water or five distinct regions of water. Straight lines were drawn to identify the different populations, Fig 5.4. The authors believed that the experimental data in Fig 5.4 could not be fitted to a simple two-state model which considers only bound and free water with fast exchange of water molecules between the two states. In fact, the authors believed that for concentrations above 0.5 % w/w lysozyme, *i.e.* regions II - IV in Fig 5.4, a slope instead of a plateau is observed for each different region, which justifies the assumption that there are more than two populations of water. The relaxation rates were calculated from the intercepts and slopes for these straight lines. However, according to Belton *et al.*[2] this seems to be a very dubious exercise because an arbitrary number of lines can be drawn for the experimental data presented in Fig 5.4. It is suggested by Belton *et al.* that this is an entirely empirical exercise and does not justify the assumption that there are more than two distinct water states in an aqueous lysozyme solution.

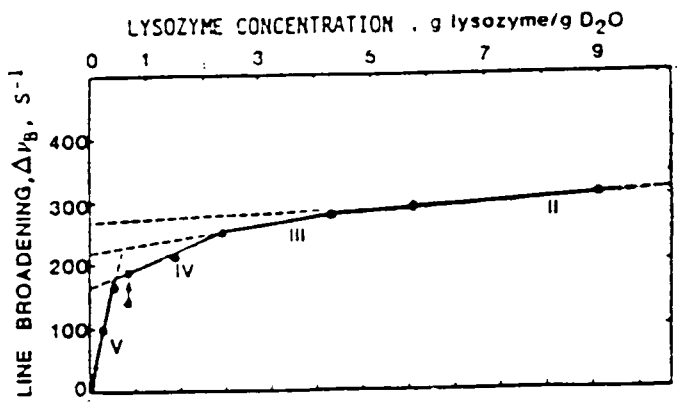

Fig 5.4 Water oxygen-17 NMR line broadening as a function of lysozyme concentration (data from Lioutas *et al.*[6])

Fig 5.5 shows that for a lysozyme solution the longitudinal relaxation rate decreases with increasing frequency, whereas the transverse relaxation rate is observed to be independent of frequency.

The variation of the longitudinal relaxation rate is in agreement with Halle's prediction and experimental observation that relaxation rate decreases with increasing frequency, Fig 5.5. The constancy of transverse relaxation rate with frequency can be explained by assuming that the zero frequency term of the spectral density function, *i.e.* J(0), dominates transverse relaxation at the studied lysozyme concentration (8.29 % w/w lysozyme). Lysozyme is a considerably large molecule (MW = ~ 14000), therefore the aggregation of lysozyme is expected to reduce the motion of the lysozyme - water system such that the rigid-lattice condition applies. Within the non-extreme narrowing regime, transverse relaxation is expected to be dominated by the J(0) term. Since J(0) is frequency independent, then transverse relaxation is also expected to be frequency independent.

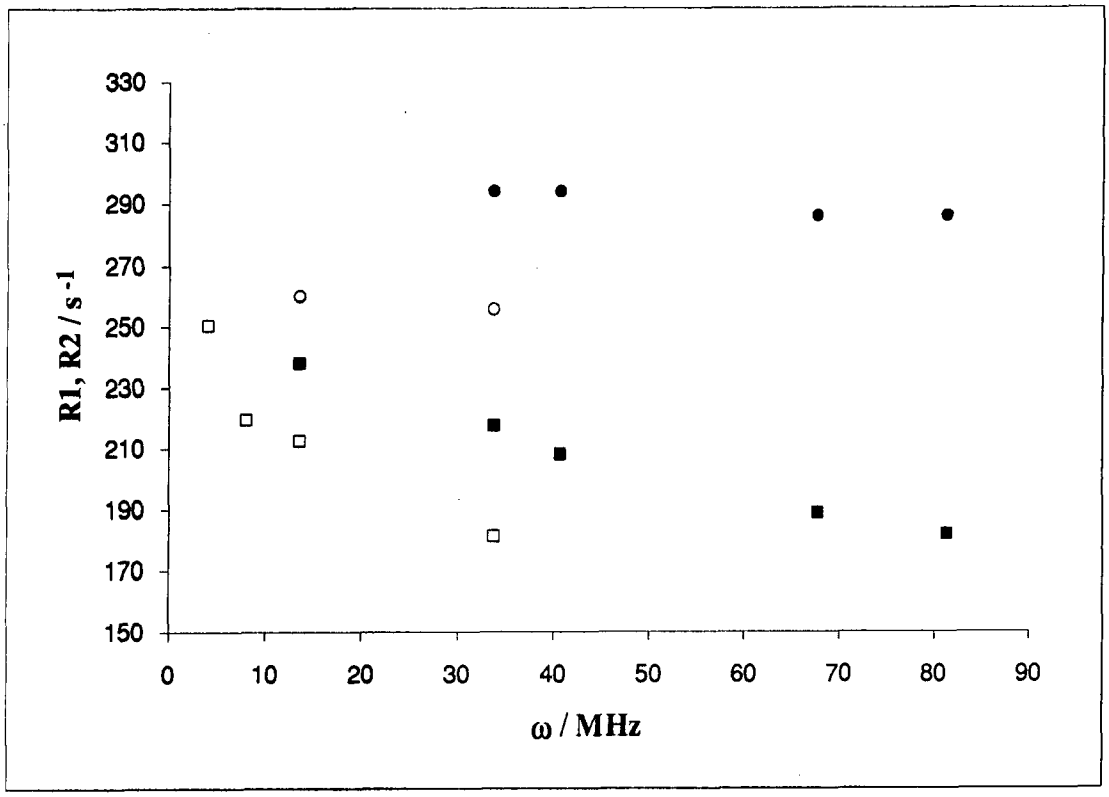

Fig 5.5 The variation of water oxygen-17 longitudinal and transverse relaxation rates for an aqueous lysozyme solution with frequency.
Concentration = 8.29 % w/w lysozyme, pH = 5.0 and temperature = 298 K. Squares represent longitudinal and circles represent transverse relaxation rates. The open symbols show Halle's data (from Fig 3, reference 1) at 300 K

The frequency dispersion for a lysozyme solution, *i.e.* the difference in relaxation rate between the lowest and the highest frequency, for longitudinal relaxation is observed to be quite small. Similarly, a relatively small dispersion, compared to other proteins, has been observed for lysozyme by Hallenga and Koenig[7] from water proton longitudinal relaxation rate studies, Fig 5.6. The magnitude of the dispersion differs according to the molecular weight of the protein. High molecular weight proteins are expected to produce a much bigger dispersion.

Fig 5.6 Dispersion of water proton longitudinal relaxation rate for 50 mg/ml solutions of proteins with a range of molecular weights, at 298 K (Fig 2, reference 7). The approximate molecular weight of each protein is given. The abbreviations are HC = Hemocyanin, IG = γ-immunoglobin, AD = Alcohol dehydrogenase, Hb = Human hemoglobin, CA = Carbonic anhydrase and LY = Lysozyme

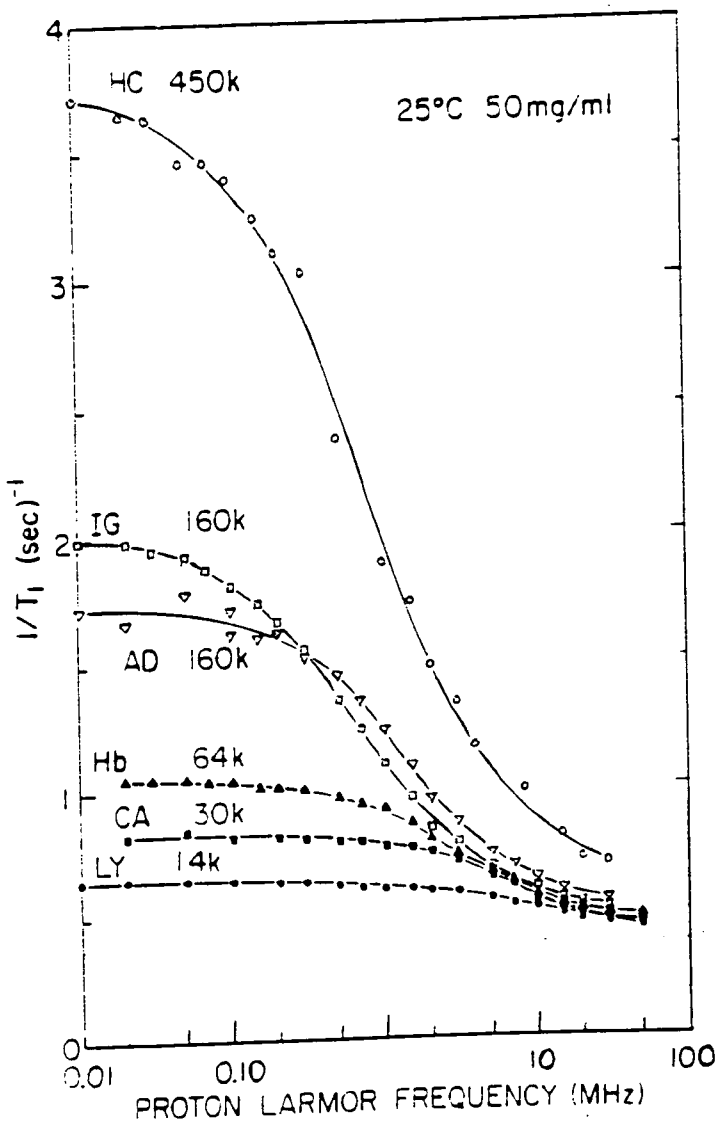

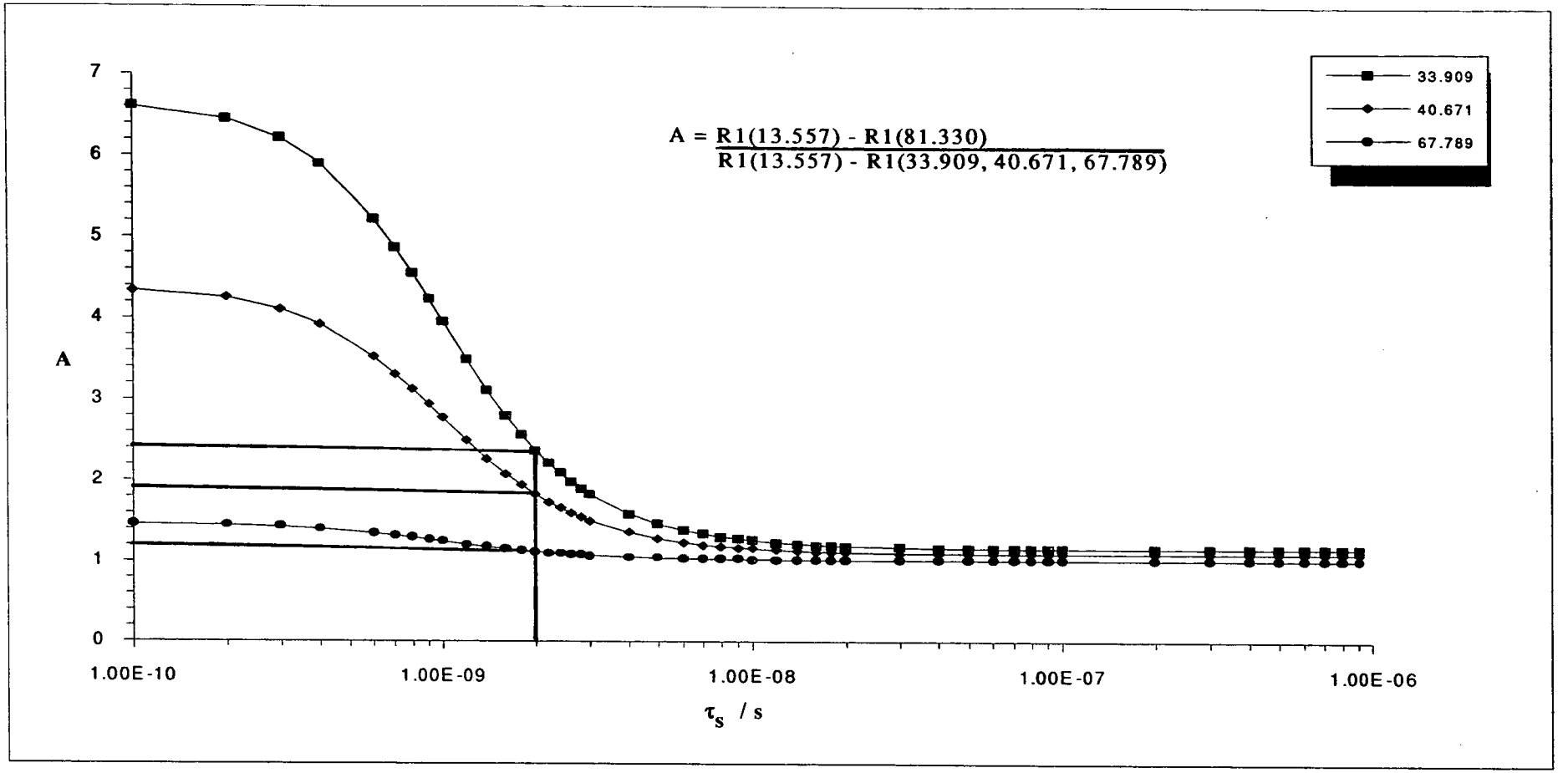

Fig 5.7 Plot of the theoretical ratio, A, against the correlation time of the slow component of bound water, τ_S, using Halle' model. The value of τ_S is estimated for 8.29 % w/w lysozyme solution in the absence of salt.

Unfortunately, for the highest lysozyme concentration studied (8.29 % w/w lysozyme) only the product $P_{bw}S^2$ could be evaluated. At this concentration, a significant amount of free water is still present in the system, and therefore it is incorrect to assume that at this concentration the fraction of bound water, P_{bw}, is equal to unity. Since it is not possible to determine either P_{bw} or S independently from Halle's model, then the parameters τ_f and R^f_{bw} could not be calculated.

However in the absence of salt, the correlation time of the slow component of bound water, τ_s, was determined by following the procedure described in section 4.11. 2 and making use of equation 4.12, as is shown in Figs 5.7 From the value of τ_s, it was possible to calculate the product $P_{bw}S^2$. The results are summarised in table 5.2.

		Absence of salt	
ω / MHz	A	τ_s / ns	$P_{bw}S^2$
33.909	2.4 ± 0.2	2	0.002
40.671	1.9 ± 0.2	2	0.002
67.789	1.2 ±0.1	2	0.002

Table 5.2 Calculation of the experimental ratio A from longitudinal relaxation data and estimation of τ_s and the product $P_{bw}S^2$ for water oxygen-17 relaxation in an aqueous lysozyme solution. Concentration = 8.29 % w/w lysozyme,

pH = 5.0 and temperature = 298 K.

Both the parameters $P_{bw}S^2$ and τ_s are independent of frequency. Good agreement is obtained at the three frequencies for both parameters as would be expected.

Halle *et al.*[1] also attempted to determine the value of τ_s for an aqueous 8.29 % w/w lysozyme solution by fitting their experimental data to the two-state model with three unknown parameters R^f_{bw}; $(P_{bw}(S\chi)^2$, and τ_s. As can be seen from Fig 5.1 the experimental data is insufficient to obtain a reasonable fit. As a consequence, the fits are not very good for the proteins studied. However, from the attempted fitting procedure, Halle estimated the value of τ_s to be 19 ns.

Kakalis and Baianu[5] also calculated τ_s for 8.3 % w/w lysozyme solution by using a similar procedure to the one described in section 4.11 of the present study. Kakalis and Baianu made use of the literature data given by Halle in combination with new measurements of longitudinal and transverse relaxation rates at frequencies of 40.671 and 67.789 MHz to calculate the correlation time. The value of τ_s for 8.29 % w/w lysozyme solution was calculated to be approximately 7 ns.[5]

In table 5.3, the results of the three studies to calculate τ_s for water oxygen-17 relaxation in 8.29 % w/w lysozyme solution are summarised.

	Present Research	Kakalis & Baianu	Halle's Study
% w/w lysozyme	τ_s / ns	τ_s / ns	τ_s / ns
8.29	2	7	19

Table 5.3 Comparison of the calculated values of τ_s between the present research, Kakalis and Baianu's study[5] and Halle's study[1] for water oxygen-17 relaxation in 8.29 % w/w lysozyme solution at pH 5.0 and 298 K.

The value of τ_s calculated by Halle is greater than the τ_s values calculated in this study and that of Kakalis and Baianu. Fitting to only three or four data points with three unknown parameters suggests that the analysis method employed by Halle is liable to

errors. However, when analysing Halle's T_1 data from Fig 5.1 using the method described in section 4.11, a τ_s value of 7.4 — 12 ns was obtained, Fig 5.8. The results of the analysis are given in table 5.4 It is suggested that the τ_s value of 19 ns estimated by Halle is associated with significant errors.

A possible explanation for the difference in τ_s calculated from the present research and that of Kakalis and Baianu[5] is given later, see section 5.4.1

ω / MHz	A	τ_s / ns
8.13	2.3	12
13.56	1.8	7.4

Table 5.4 Calculation of the experimental ratio A and estimation of τ_s for water oxygen-17 longitudinal relaxation data supplied by Halle[1], for a lysozyme solution of concentration 8.29 % w/w lysozyme at pH 5.1 and 300 K.

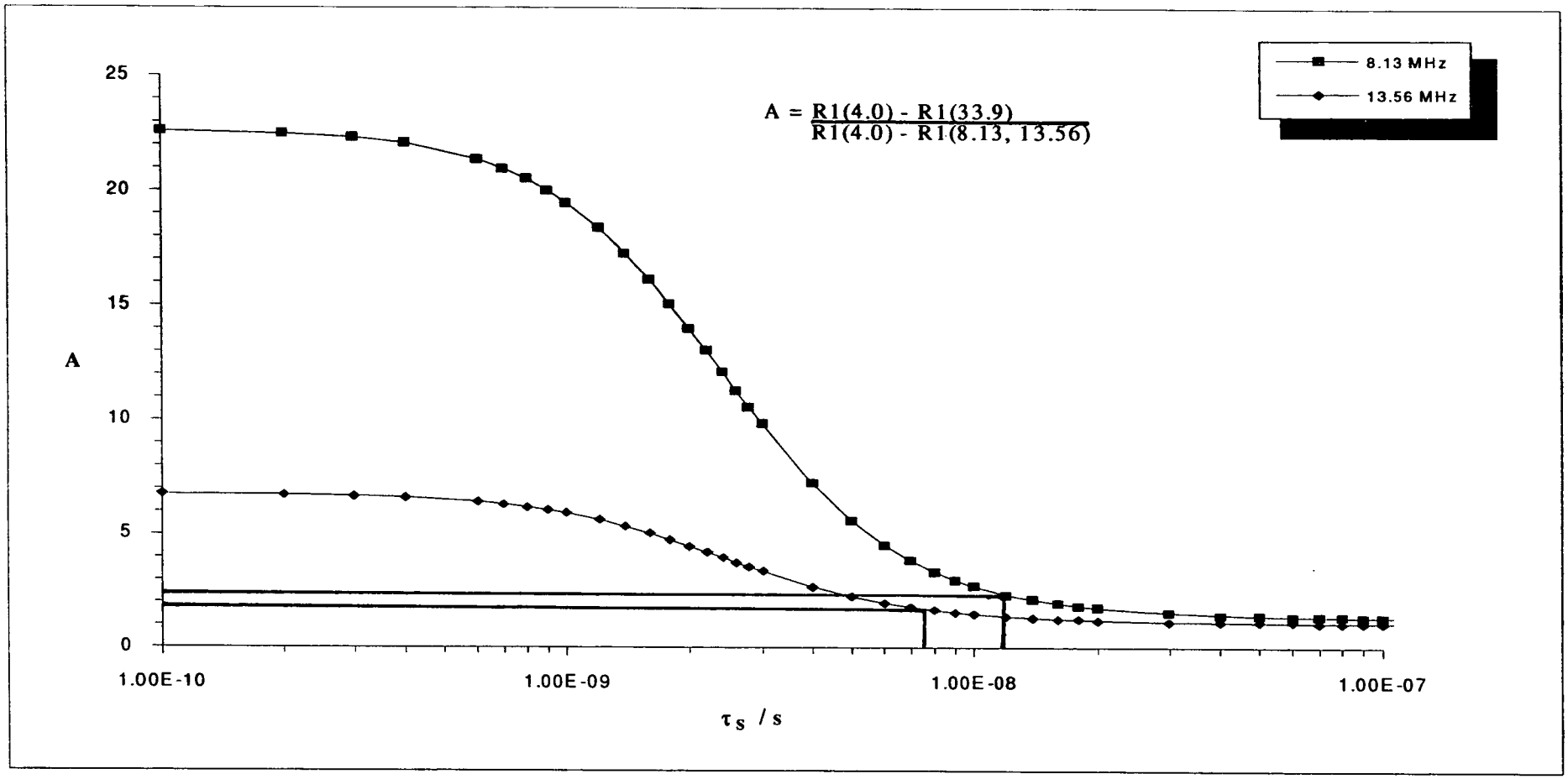

Fig 5.8 Plot of the theoretical ratio, A, against the correlation time of the slow component of bound water, τ_S, using Halle's model. The value of τ_S is estimated for Halle's data (from Fig 3, reference 44

5.3.2) Presence of Salt

As well as the protein concentration, the ionic strength of lysozyme is also expected to affect water oxygen-17 relaxation. For a lysozyme solution of concentration 8.29 % w/w lysozyme, the effect of ionic strength on water oxygen-17 relaxation was analysed at different spectrometer frequencies. In the presence of salt, relaxation of water oxygen-17 is seen to be slower than in the absence of salt, compare tables 5.1 and 5.5.

As the concentration of the salt increases, the longitudinal relaxation time is seen initially to decrease and then to increase, whereas, the transverse relaxation time shows a consistent increase, Fig 5.9 For all spectrometer frequencies, the longitudinal relaxation data is observed to pass through a minimum. The position of the minimum is observed to be dependent on the frequency. As the frequency increases the T_1 minimum is observed to occur at a different ionic strength. For example, a close inspection of Fig 5.9 reveals that for a spectrometer frequency of 13.557 MHz the T_1 minimum occurs between 0.1 - 0.15 mol dm^{-3} NaCl, whereas for a frequency of 81.330 MHz the T_1 minimum is seen to occur at a higher NaCl concentration of 0.2 - 0.25 mol dm^{-3}. A possible explanation for the variation in T_1 minimum as a function of frequency will be given later.

	SF = 13.557 MHz		SF = 33.909 MHz		SF = 40.671 MHz		SF = 67.789 MHz		SF = 81.330 MHz	
[NaCl] / M	T1 / ms	T2 / ms	T1 / ms	T2 / ms	T1 / ms	T2 / ms	T1 / ms	T2 / ms	T1 / ms	T2 / ms
0.05	4.4		4.5	3.6	4.7	3.6	4.8	3.7	5.2	3.7
0.1	4.3		4.4	4	4.5	4	4.7	4.1	4.8	4.1
0.15	4.3		4.4	4.6	4.4	4.5	4.6	4.5	4.7	4.4
0.2	4.4		4.5	4.6	4.5	4.7	4.5	4.7	4.5	4.7
0.25	5.2		5.2	5.3	5.1	5.2	4.9	5	4.6	5.1

Table 5.5 The dependence of water oxygen-17 longitudinal and transverse relaxation on sodium chloride concentration for 8.29 % w/w lysozyme solution at different spectrometer frequencies. Temperature = 298 K

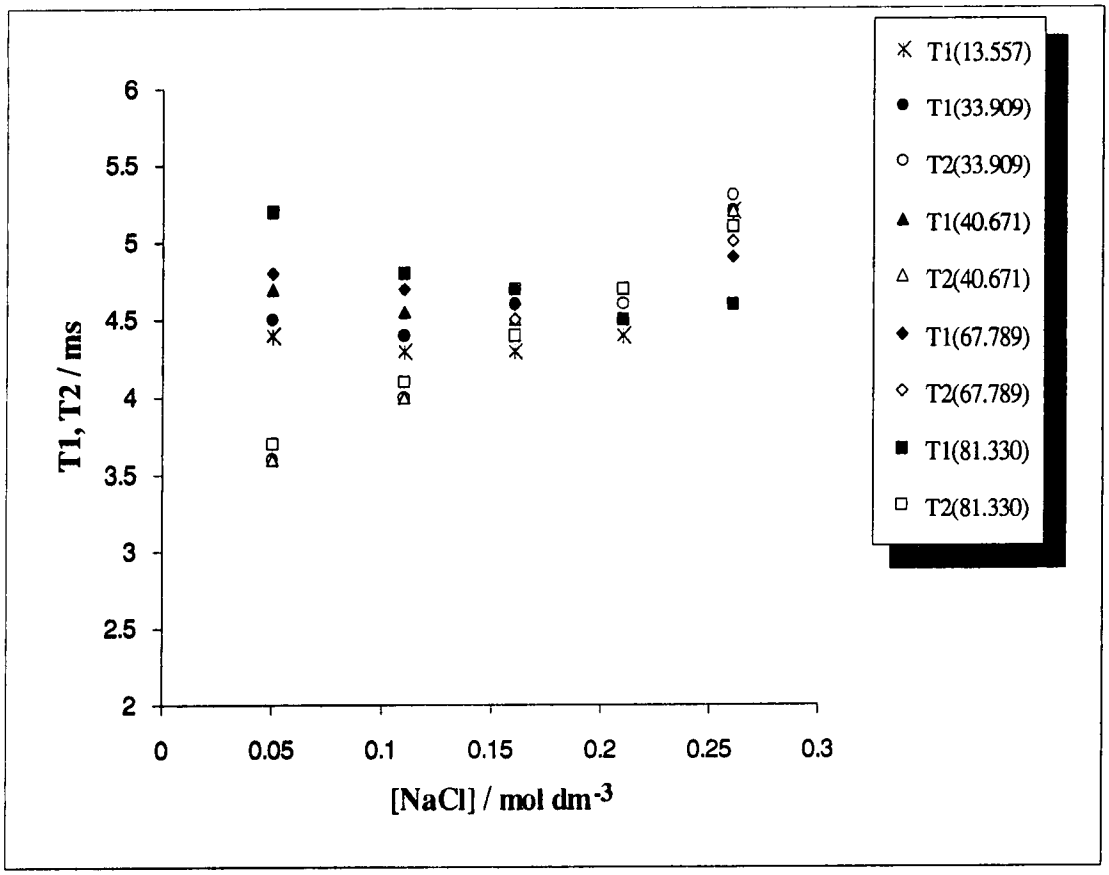

Fig 5.9 The effect of sodium chloride concentration on water oxygen-17 longitudinal and transverse relaxation times for an aqueous lysozyme solution. Concentration = 8.29 % w/w lysozyme, temperature =298 K

At low concentrations of salt, a significant difference between the longitudinal and transverse relaxation times can be observed. However, with increasing salt concentration, the difference is observed to decrease, such that, at high salt concentrations we have a situation where the two relaxation rates are equal, *i.e.* extreme narrowing holds. This observation leads to the conclusion that with increasing salt concentration the system is moving from a non extreme narrowing situation to extreme narrowing, whereby the motion of the solution increases, *i.e.* the reorientational correlation time, τ_c, decreases.

A decrease in τ_c could be expected if the Na^+ ions and Cl^- ions cause electrostatic repulsion between the lysozyme molecules, thus dissociating the lysozyme chain. In such a case, the reorientational motion would correspond to the individual lysozyme monomer rather than the whole lysozyme chain. Since the motion of the monomer is expected to be faster, because of its small size, compared to the whole lysozyme chain, then the correlation time of the system is expected to decrease with increasing salt concentration..

It is assumed that at low concentrations of the salt, only partial suppression of the attractive forces between the lysozyme molecules occurs, whereas, at higher concentrations of salt, the suppression effect is stronger.

Kakalis and Baianu[5] studied the relaxation of water oxygen-17 for lysozyme solutions in the absence and in the presence of sodium chloride. In the presence of 0.1 mol dm^{-3} NaCl the reorientational correlation time of the slow component of bound water was found to be less than the corresponding value obtained in the absence of salt. In the presence of salt, the authors believed that suppression of the attractive forces between the lysozyme monomers was responsible for the decrease in τ_S.

Halle *et al.*[1] have also found that for an aqueous Human Plasma Albumin (HPA) solution the correlation time of the slow component of bound water, in the presence of 0.15 mol dm^{-3} KCl, is less than that in the absence of salt. In a similar way to Kakalis and Baianu[5], Halle *et al.*[1] explained this in terms of electrostatic repulsion between the densely populated and highly charged protein molecules leading to dissociation of the protein chain.

The dependence of the correlation time on salt concentration also explains why the T_1 minimum in Fig 5.9 is observed to occur at a different salt concentration with varying frequency. In Fig 4.22 (see section 4.12), the expected variation of the T_1 minimum as a function of the correlation time for different spectrometer frequencies, predicted from the spectral density function, is shown. With increasing frequency the T_1 minimum moves to a lower correlation time in good agreement with the experimental

observation for lysozyme data where the T_1 minimum is seen to shift towards a higher ionic strength, *i.e.* lower correlation time.

At the lowest concentration of NaCl (0.05 mol dm^{-3}), T_1 is observed to be frequency dependent whereas T_2 is observed to be independent of frequency, as was seen for the highest concentrated lysozyme solution in the absence of NaCl. The constancy of transverse relaxation can be explained by using the same argument as the case in which there is an absence of salt, see section 5.3.1. As expected the longitudinal relaxation rate decreases with increasing frequency. The difference between the two relaxation rates is also frequency dependent. With increasing frequency, the difference between the two relaxation rates is observed to increase, Fig 5.10.

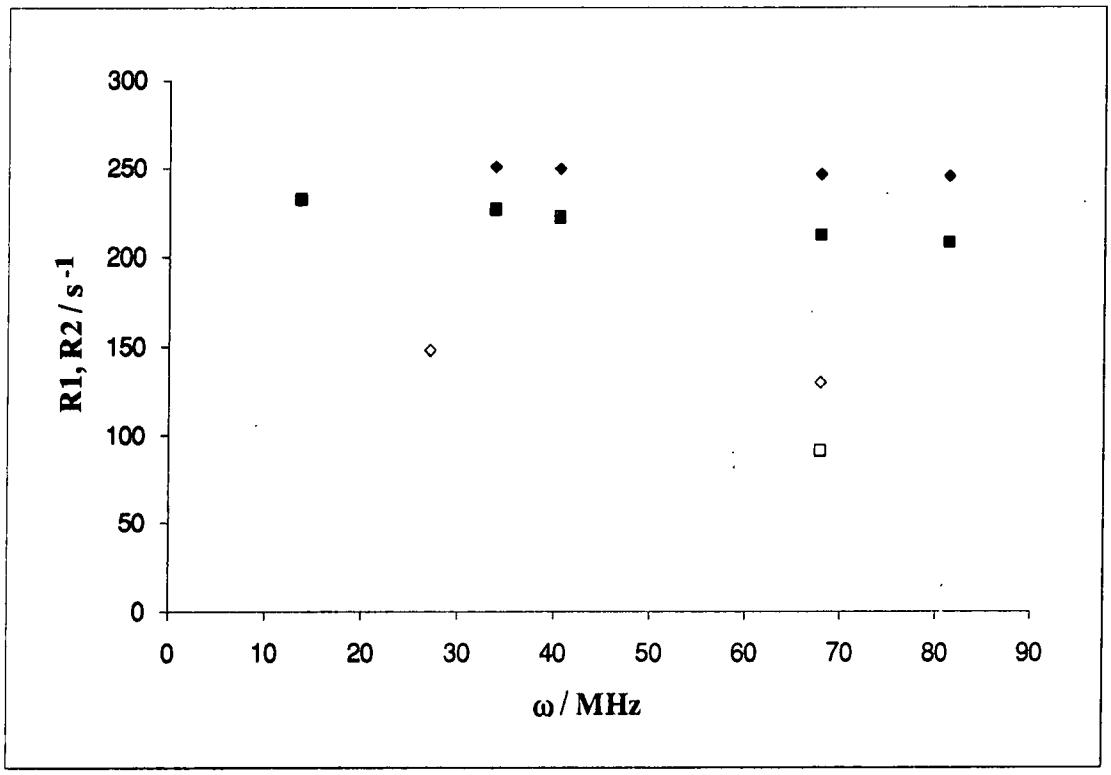

Fig 5.10 Variation of water oxygen-17 relaxation rates with frequency for an aqueous solution in the presence of 0.1 mol dm^{-3} NaCl. Squares represent longitudinal relaxation, whereas diamonds represent transverse relaxation. Filled symbols show data from present study for 8.29 % w/w lysozyme at pH 5.0 and 298 K. Open symbols show Kakalis and Baianu's data[5] for 10 % w/w lysozyme in D_2O at pD 4.5 and 21 °C

By using the procedure described in section 4.11, both the correlation time of the slow component of bound water, τ_s, and $P_{bw}S^2$ were determined in the presence of 0.1 mol dm^{-3} NaCl, Fig 5.11. The results of the analysis are presented in table 5.6

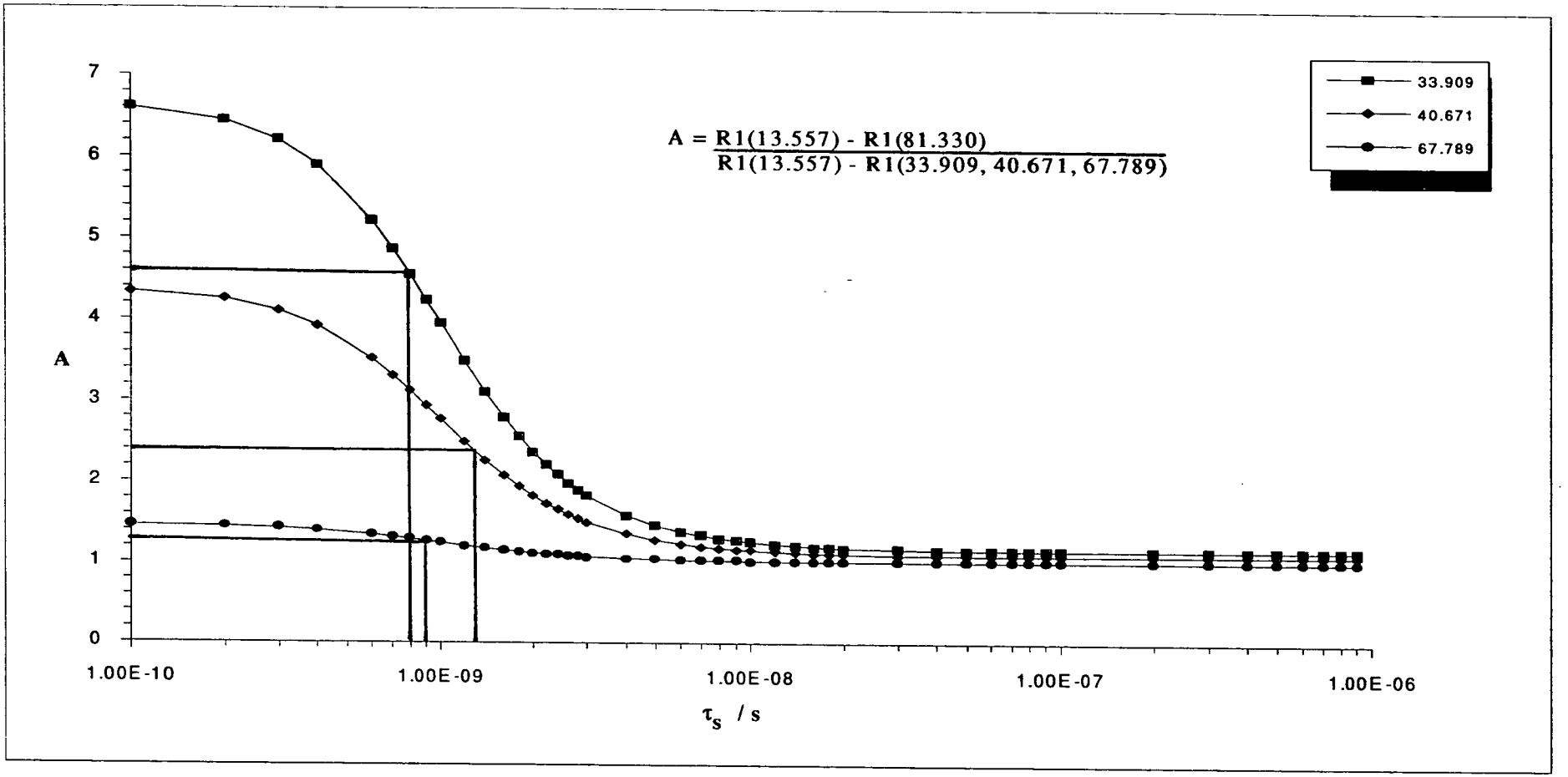

Fig 5.11 Plot of the theoretical ratio, A, against the correlation time of the slow component of bound water, τ_S, using Halle's model. The value of τ_S is estimated for 8.29 % w/w lysozyme solution in the presence of 0.1 mol dm^{-3} NaCl

	Presence of 0.1 mol dm^{-3} NaCl		
ω / MHz	A	τ_s / ns	$P_{bw}S^2$
33.909	4.6 ±0.2	0.8	0.01
40.671	2.4 ± 0.2	1.2	0.01
67.789	1.3 ± 0.1	0.9	0.01

Table 5.6 The calculated values of the experimental ratio A, τ_s, and $P_{bw}S^2$ for 8.29 % w/w lysozyme solution in the presence of 0.1 mol dm^{-3} NaCl at 298 K

Both the parameters τ_s and $P_{bw}S^2$ are independent of frequency as was the case for the absence of salt. Comparing the results between the absence and the presence of salt reveals that in the presence of salt the value of τ_s is less than in the absence of salt as has been predicted from the experimental observation.

Moreover, in the presence of salt, an increase in the product $P_{bw}S^2$ is calculated compared to the absence of salt for all frequencies studied. This can be attributed to the fact that in the presence of salt, the amount of bound water increases. The binding of hydrated ions to lysozyme is expected to increase the charge on lysozyme and the amount of water in the immediate vicinity of the lysozyme surface due to electrostatic interactions. Kakalis and Baianu[5] found that in the presence of 0.1 mol dm^{-3} NaCl the fraction of bound water increases. Halle *et al.*[1] also reported that in the presence of charged particles, proteins are much more hydrated than in the absence of the charge residues. Thus, the findings of the present research are in good agreement with previous studies.

Using a similar approach as described in section 4.11, Kakalis and Baianu[5] calculated τ_s to be approximately 4 ns for a lysozyme solution of concentration 10 % w/w

lysozyme in the presence of 0.1 mol dm^{-3} NaCl in D_2O at pD 4.5 and 21 °C. The τ_s value calculated by Kakalis and Baianu is higher than the value calculated in this study as a result of using a higher lysozyme concentration and using D_2O instead of H_2O. As mentioned before D_2O has a greater viscosity than H_2O, therefore the relaxation rate in D_2O is expected to be greater *i.e.* a higher τ_s value.

Both the present research and the study of Kakalis and Baianu[5] importantly show that in the presence of charged species the correlation time of the slow component of bound water, τ_s, decreases. This can be explained in terms of the electrostatic repulsion between the charges causing the lysozyme association to break down, resulting in an increase in the motion of the lysozyme-water system. It is worth noting that although in the presence of NaCl the fraction of bound water increases, the dissociation of lysozyme into individual monomers increases the overall motion of the lysozyme-water system, hence decreasing the relaxation rate.

5.4) Lysozyme Discussion

Since the relaxation of water oxygen-17 in aqueous lysozyme solutions depends on both the lysozyme concentration and the ionic charge of the system, then an empirical equation of the form

$$D_P = \left(\frac{q_o^2 D_p^o D_s^o}{q_p^2 D_p^o + q_s^2 D_s^2}\right)\left(\frac{h_o}{h}\right)\left(1 + C_p \frac{d\ln\gamma^{\pm}}{dC_p}\right) \qquad \text{eqn 5.1}$$

where

$$q_p^2 = (4\pi/\varepsilon kT)Z_p^2 C_p \qquad \text{eqn 5.2}$$

$$q_s^2 = (4\pi/\varepsilon kT)Z_s^2 C_s \qquad \text{eqn 5.3}$$

$$q_o^2 = q_p^2 + q_s^2 \qquad \text{eqn 5.4}$$

has been given by Belton *et al.*[2] to describe the relaxation of water oxygen-17 in the presence of proteins. It is assumed that $\tau_s \propto D_p^{-1}$.

Here D_p is the rotational diffusion coefficient of the protein, C_p is the concentration of the protein with charge Z_p, and C_s is the concentration of the counterion of charge Z_s, ε is the dielectric constant and h is the viscosity of the solution at concentration C_p, h_o is the pure water viscosity. D_p^o and D_s^o are the diffusion coefficients of the protein and counterion at infinite dilution. $\gamma^{\pm}$ is the mean ionic activity coefficient. Both $\gamma^{\pm}$ and (h_o/h) are dependent on the concentration of the protein.

The viscosity dependence on protein concentration is given empirically by Belton *et al.*[2] to be

$$\log\left(\frac{h}{h_o}\right) = AC_p/(1 - BC_p) \qquad \text{eqn 5.5}$$

where A and B are constants.

It seems reasonable to test equation 5.1 for relaxation of water oxygen-17 in aqueous lysozyme solutions both in the absence and presence of salt.

5.4.1) Absence of Salt

In the absence of salt $q_s^2 = 0$, hence $q_p^2 = q_o^2$. Therefore, equation 5.1 can be written as

$$D_p = D_s^o\left(\frac{h_o}{h}\right)\left(1 + C_p\frac{d\ln\gamma^{\pm}}{dC_p}\right) \qquad \text{eqn 5.6}$$

Assuming that the terms D_s^o and $d\ln\gamma^{\pm}/dC_p$ are constants and independent of lysozyme concentration, then equation 5.6 can be written as

$$D_p = D_s^o\left(\frac{h_o}{h}\right)\left(1 + aC_p\right) \qquad \text{eqn 5.7}$$

where $a = d\ln\gamma^{\pm}/dC_p$.

Substituting equation 5.5 into equation 5.7 results in

$$D_p = D_s^o\left(\frac{1}{\exp\left[\frac{AC_p}{1 - BC_p}\right]}\right)\left(1 + aC_p\right) \qquad \text{eqn 5.8}$$

since $\tau_s \propto D_p^{-1}$ then

$$\frac{1}{\tau_s} = D_s^o \left(\frac{1}{\exp\left[\frac{AC_p}{1-BC_p}\right]} \right) (1 + aC_p) \qquad \text{eqn 5.9}$$

A theoretical plot of τ_s against C_p (lysozyme concentration) using eqn. 5.9 predicts a sharp increase in τ_s with increasing lysozyme concentration which passes through a maximum and then decreases, but only slightly, Fig 5.12.

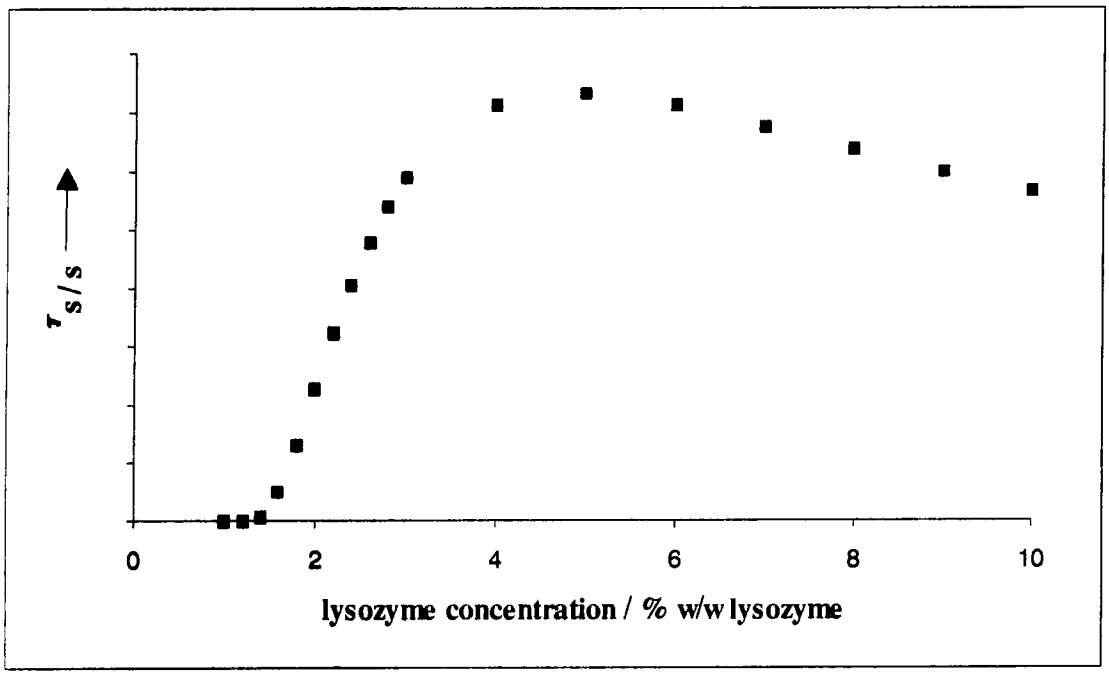

Fig 5.12 Theoretical plot of the correlation time of the slow component of bound water, τ_s, as a function of lysozyme concentration using Gordon's equation[2] (eqn 5.1) in the absence of salt. The ionic activity term, $d\ln\gamma^{\pm}/dC_p$, is assumed to be a constant and independent of lysozyme concentration.

At low concentrations of lysozyme the second term in eqn. 5.9, aC_p, is expected to be negligible such that the relaxation is dominated by the viscosity term, i.e. $AC_p/(1-BC_p)$. With increasing lysozyme concentration this term is expected to increase and as a result the term $1/\exp[AC_p/(1-BC_p)]$ decreases. Hence τ_s^{-1} decreases, *i.e.* τ_s increases as is shown in the initial part of Fig 5.12.

At high concentrations of lysozyme the viscosity of the solution is anticipated to be sufficiently high so that the term $1/\exp[AC_p/(1-BC_p)]$ is considered to be negligible. In such a case, relaxation is expected to be dominated by the second term in eqn 5.9, i.e. by the term aC_p. Thus with increasing lysozyme concentration τ_s^{-1} increases and as a result τ_s decreases as can be observed from Fig 5.12

However, experimentally the correlation time of the slow component of bound water, τ_s, is observed to increase with increasing lysozyme concentration up to a concentration of 8.29 % w/w lysozyme. With increasing lysozyme concentration, the fraction of bound water is expected to increase such that the overall motion of the lysozyme-water system decreases. Thus, a decrease in the rotational diffusion coefficient of the lysozyme-water system is expected and an increase in the rotational correlation time, resulting in an increase in relaxation rate as is observed experimentally, Fig 5.2. The discrepancy between the experimental observation and that predicted by Gordon's equation is probably due to the bound water fraction term. It is suggested that such a term should be incorporated into Gordon's equation in order for this equation to accurately predict the variation of τ_s with lysozyme concentration.

For a lysozyme solution of concentration 8.29 % w/w lysozyme and pH of 5.0 at 25 °C the correlation time of the slow component of bound water, τ_s, was calculated to be 2 ns, which is of the expected magnitude. By making use of the literature data reported by Halle *et al.*[1] combined with new measurements, Kakalis and Baianu[5] calculated τ_s to be 7 ns for a 8.3 % w/w lysozyme solution at pH 5.1 and 27 °C using the same procedure as described in section 4.11. However, Kakalis and Baianu

calculated the experimental ratio A (see eqn 4.12) by combining longitudinal and transverse relaxation data. There seems to be no obvious advantage in using data from both relaxation processes to calculate A. If anything, the accuracy of the ratio A calculated from both longitudinal and transverse relaxation rates is probably less than that of the ratio obtained by using only longitudinal or only transverse relaxation data.

5.4.2) Presence of Salt

In the presence of salt, the diffusion coefficient of lysozyme is expected to be dependent on the terms q_s^2, the charge on lysozyme, solution viscosity and the activity coefficient, see eqn 5.1.

Assuming that the viscosity and activity coefficient terms are constants and independent of added salt concentration then eqn. 5.1 may be written as

$$D_p = \frac{q_o^2 D_p^o D_s^o}{q_p^2 D_p^o + q_s^2 D_s^o} C \qquad \text{eqn 5.10}$$

where $C = \left(\frac{h_o}{h}\right)\left[1 + \frac{C_p d\ln\gamma^{\pm}}{dC_p}\right] = \text{constant}$

Furthermore, assuming that D_p^o and D_s^o are constants and independent of salt concentration and that $\tau_s \propto D_p^{-1}$ then eqn. 5.10 can be simplified to

$$\frac{1}{\tau_s} = \frac{q_o^2 A}{q_p^2 D_p^o + q_s^2 D_s^o} C \qquad \text{eqn 5.11}$$

In Fig 5.13, the effect of salt concentration on τ_s is shown using eqn. 5.11.

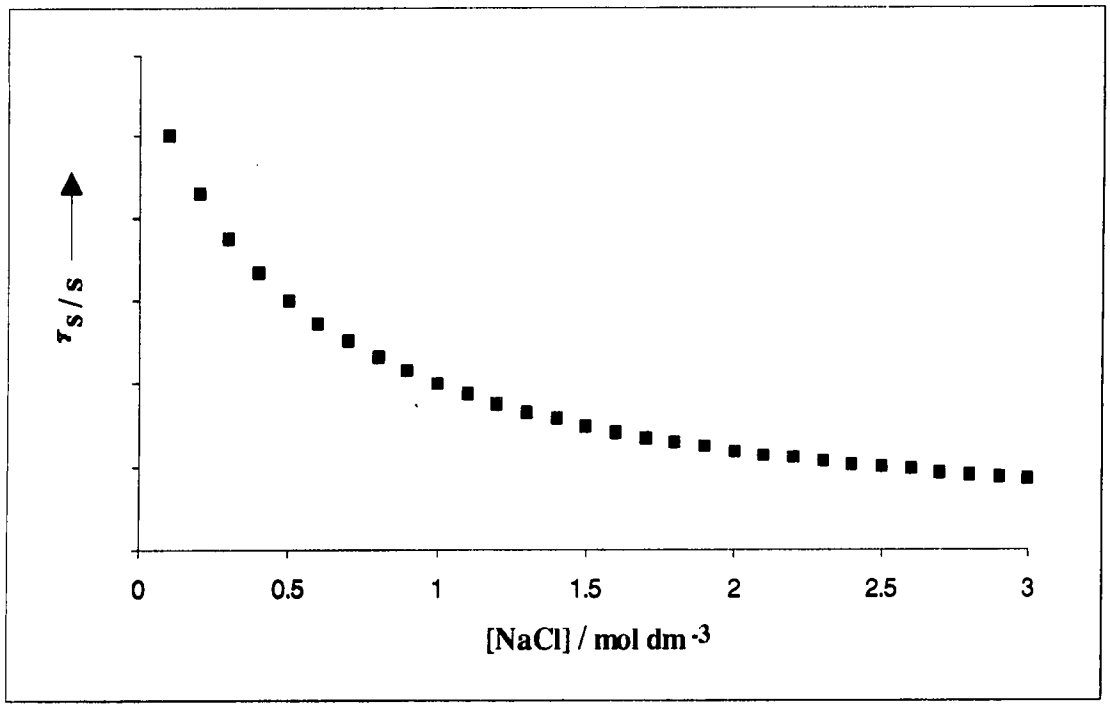

Fig 5.13 Theoretical plot of the correlation time of the slow component of bound water, τ_S, as a function of sodium chloride concentration using Gordon's equation. The viscosity, activity coefficient, D_p^o and D_s^o terms are assumed to be constants and independent of salt concentration.

With increasing salt concentration the factor q_s^2 is expected to increase, which in turn increases the factor q_o^2, eqns 5.3 and 5.4. The charge on the protein is also expected to increase with increasing salt concentration, thus increasing q_p^2 and further increasing q_o^2. Although it has been assumed that the viscosity of the solution is independent of salt concentration, it is known that the addition of salt dissociates the lysozyme chain, thus increasing the motion of the system and decreasing the viscosity. As a result, the term (h_o/h) is expected to increase.

As assumed above the activity coefficient term, $1 + C_p\left(d\ln\gamma^{\pm}/dC_p\right)$, is expected to vary slightly with salt concentration. For an aqueous sodium chloride solutions, the variation of the activity coefficient, $\gamma^{\pm}$, as a function of sodium chloride concentration

is shown in Fig 5.14.[8] Up to a salt concentration of 1.0 mol dm^{-3} the activity coefficient is observed to decrease.

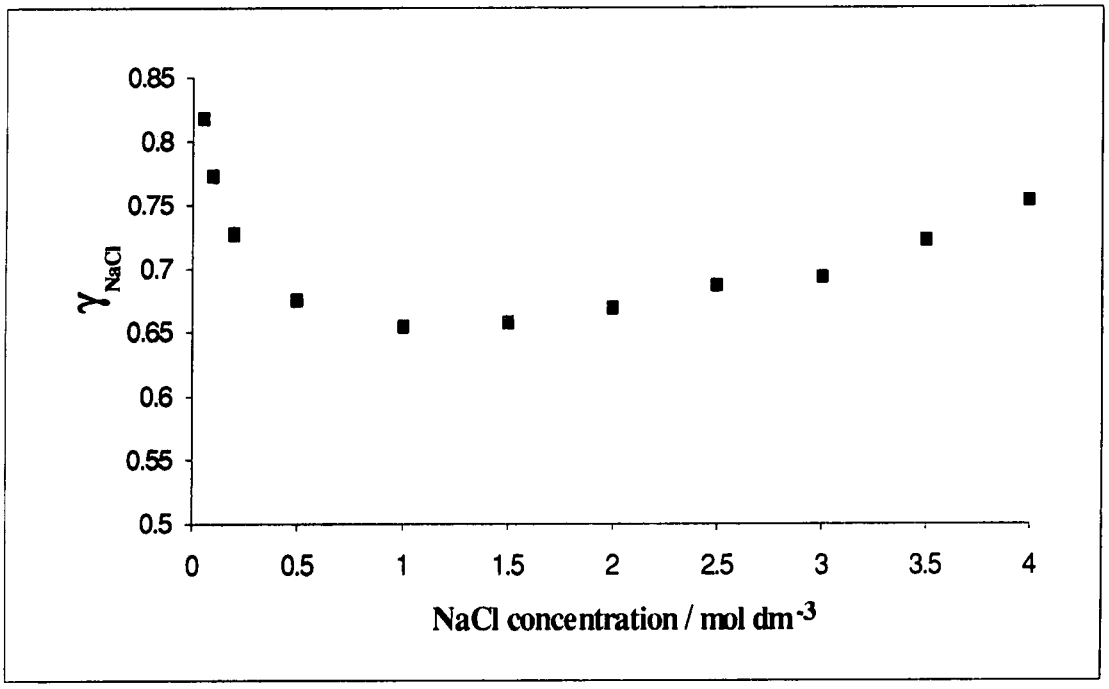

Fig 5.14 The variation of the activity coefficient, $\gamma^{\pm}$, for sodium chloride with concentration. Data from reference 8.

Assuming that in the presence of 8 % w/w lysozyme, the dependence of the activity coefficient on salt concentration shows a similar variation to Fig 5.14, then for the salt concentration range studied, *i.e.* 0 to 0.25 mol dm^{-3}, the activity coefficient is expected to decrease slightly. However, the change in the activity coefficient, $\gamma^{\pm}$, is observed to be sufficiently small that it is expected to have a negligible effect on the term $1+C_p\left(d\ln\gamma^{\pm}/dC_p\right)$.

Overall the increase in salt concentration increases the term q_o^2 (by increasing q_s^2 and q_p^2), thus increasing the rotational diffusion coefficient of lysozyme. Hence, the

rotational correlation time is expected to decrease with increasing salt concentration as is observed experimentally, Fig 5.9, and predicted from Gordon's equation, Fig 5.13.

In the presence of 0.1 mol dm^{-3} NaCl, the correlation time, τ_S, for 8.29 % w/w lysozyme solution at 25 °C was calculated to be approximately 0.9 ns (see section 5.3.2). For a 10 % w/w lysozyme solution in D_2O at pD 4.5 and 21 °C, Kakalis and Baianu[5] calculated τ_S to be 4.7 ns in the presence of 0.1 mol dm^{-3} NaCl using a similar method as described in section 4.11.2. Kakalis and Baianu measured relaxation rates at only two frequencies, 27.13 and 67.80 MHz. They combined data from both relaxation processes to calculate the experimental ratio A in order to obtain τ_S.

Kakalis and Baianu[5] also predicted a relationship which relates the correlation time associated with the protein tumbling in solution, τ_c, with the solution viscosity and the activity coefficient of the protein. A relationship of the form

$$\tau_c = \frac{4\pi r^3}{3kT} \times \eta \times \frac{1}{1 + C(d\ln\gamma/dC)} \qquad \text{eqn 5.12}$$

was given. Here r is the radius of the protein, k is the Boltzmann constant, T is the temperature in °K, η is the solution viscosity and C is the protein concentration.

Furthermore, Kakalis and Baianu[5] reported that the differential term $d\ln\gamma/dC$ is virtually zero in the presence of 0.1 mol dm^{-3} NaCl for lysozyme solutions up to a concentration of 8 % w/w lysozyme. Unfortunately, no explanation was given for the reasoning behind this assumption. However assuming that this is true, then in the presence of 0.1 mol dm^{-3} NaCl eqn 5.7 yields

$$\tau_c = \frac{4\pi r^3}{3kT} \times \eta \qquad \text{eqn 5.13}$$

which is equivalent to the Debye-Stokes relationship. According to eqn 5.13, in the presence of 0.1 mol dm^{-3} NaCl, the correlation time of the slow component of bound water for a lysozyme solution of concentration 8 % w/w lysozyme is dependent on the viscosity of the solution but independent of the concentration or the charge of the added salt. This, however, is not strictly true, because in the present research the concentration of salt is observed to affect τ_s through the factor q_s^2, Fig 5.9.

Unfortunately, Kakalis and Baianu[5] did not consider studying other concentrations of salt in order to analyse the effect of salt concentration on water oxygen-17 relaxation for a constant lysozyme concentration.

At very high concentrations of lysozyme the relaxation of water oxygen-17 levels-off to a constant value. It can be seen from Fig 5.15 that the relaxation rate of water oxygen-17 levels-off at a concentration of approximately 70 % w/w lysozyme. This apparent levelling-off can be explained by the possible aggregation of the lysozyme at high concentrations. Thus, the lysozyme reorientational correlation time becomes very high, essentially infinite. For such a case, Belton *et al.*[2] have reported that the correlation time of the slow component of bound water, τ_s, is probably determined by some other type of motion such as diffusion over the lysozyme surface.

Fig 5.15 Dependence of water oxygen-17 excess transverse relaxation rate on lysozyme concentration in D_2O. $\Delta R_2 = R_{2\ observed} - R_{2\ free\ water}$. (Fig 3, reference 2)

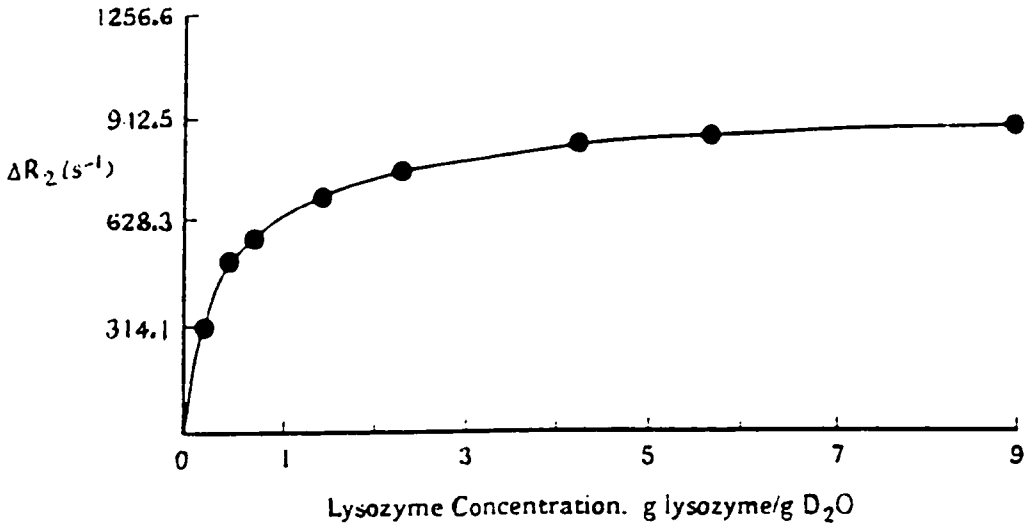

5.5) CONCLUSION

Generally, Gordon's equation (*i.e.* eqn 5.1) seems to give a reasonable description for the relaxation of water oxygen-17 in aqueous protein solutions. The relaxation is observed to be strongly dependent on the ionic strength and the charge on the protein, through the factors q_s^2 and q_o^2, as suggested by Belton *et al.*[2] and observed by Kumosinski *et al.*[9] for solutions of lysozyme. The amount of protein aggregation and the viscosity of the solution, *i.e.* the concentration of protein, are also considered to be of importance. The combined effect of ionic strength, protein charge, protein aggregation, and the solution viscosity is expected to affect the reorientational motion of the protein, which in turn has a considerable effect on the reorientational motion of the slow component of bound water, and hence on water-17 relaxation. However, surprisingly Gordon's equation does not consider the bound water fraction term which is thought to be of significance. It is suggested that the inclusion of the bound water fraction term into Gordon's equation would account for the slight discrepancy observed between the experimental and theoretical data for the variation of τ_S with protein concentration in the absence of salt.

On the other hand, the equation reported by Kakalis and Baianu[5], eqn 5.12, does not consider the effects of protein charge or the ionic strength of the solution. Thus, it is suggested that this equation does not give a true representation of water oxygen-17 relaxation in aqueous protein solutions.

As was the case for solutions of low sucrose content, it is again reasonable to assume that at low concentrations of protein the relaxation of water oxygen-17 can be described by Halle's model.

REFERENCES

1) B. Halle, T. Andersson, S. Forsén and B. Lindman, *J. Am. Chem. Soc.*, 1981, **103**, 500

2) P.S. Belton, I.J. Colquhoun and B.P. Hills, *Ann. Rep. NMR Spec.*, (ed. G.A. Webb), 1993, **26**, chap.1

3) H.H. Raeymaekers, H. Eisendrath, A. Verbeken, Y.V. Haverbeke and R.N. Muller, *J. Mag. Res.*, 1989, **85**, 421

4) O.G. Hampe, *Eur. J. Biochem.*, 1972, **31**, 32

5) L.T. Kakalis and I.C. Baianu, *Arc. Biochem. Biophys.*, 1988, **267**, 829

6) T.S. Lioutas, I.C. Baianu and M.P. Steinberg, *Arc. Biochem. Biophys.*, 1986, **247**, 68

7) K. Hallenga and S.H. Koenig, *Biochemistry*, 1976, **15**, 4255

8) R.H. Stokes and R.A. Robinson, *Trans. Faraday Soc.*, 1949, **45**, 612

9) T.F. Kumosinski, I.C. Baianu, P.J. Bechtel, P.A. Myers-Betts, P. Yakubu and A. Mora, in *NMR Applications to Biopolymers* (ed. J.W. Finlay, S.J. Schmidt and A. Serianni), p.361, Plenum, New York, 1990

CALCIUM - 43 STUDIES

6.1) Aim

Calcium-43 relaxation studies were performed for simple calcium salts in solution. It is known that calcium binds to proteins, and as a result is very important biologically. However, the low natural abundance and the low sensitivity combined with the low receptivity of calcium-43 have been a drawback for NMR studies of calcium-43 in the past.

Improving technology, however, and the availability of high-field NMR spectrometers with FT facilities have made it possible to study nuclei such as calcium-43. Simple salts of calcium were studied initially to investigate whether or not calcium-43 studies at natural abundance are possible. The variation of calcium-43 relaxation, linewidth at half-height of the Fourier transformed signal, and the chemical shift as a function of pH and salt concentration were investigated in detail.

From the available spectrometers, a calcium-43 signal was only observed at the two highest frequencies, Bruker AMX-500 and Varian VXR-600 spectrometers. Great effort was made to observe a signal on Bruker AC-250 and MSL-300 spectrometers. Unfortunately, for these spectrometers a calcium-43 signal could not be observed at natural abundance even for saturated calcium chloride solution.

The results obtained from Bruker AMX-500 and Varian VXR-600 spectrometers were compared to see whether there was any evidence of a frequency dependence for calcium-43 relaxation, linewidth, and chemical shift.

The addition of compounds, important in the food industry, such as ascorbates, to calcium chloride solutions were also investigated to find out if there is any evidence of calcium complexing to these compounds. Of particular interest was the direct measurement of calcium complexation and binding by relaxation time and chemical shift measurements. The possibility of complexation between calcium and sucrose and between calcium and lysozyme were also investigated. The evidence from calcium-43 chemical shift changes reported in the literature for biologically important molecules suggests that there is considerable complexing.[1,2] If this turns out to be

true then it should be possible and straightforward to detect complex formation and binding of calcium to sucrose and lysozyme.

6.2) Introduction

As well as being present in biological systems, calcium also occurs widely in non-biological systems. In table 6.1 the occurrence of calcium in both biological and non-biological systems is summarised

	Ca^{2+}
Igneous rocks	40 000
Sedimentary rocks	30 000
Limestone	300 000
Sea-Water	400
Salmon (whole blood)	240
Man (whole blood)	60
(plasma)	120
(interstitial fluid)	120
(cell fluid)	4
(muscle)	1400
(nerve)	280

Table 6.1 Concentrations (ppm) of calcium ion in rocks, water, and living materials.[1]

Approximately 100 different proteins have been reported to bind calcium ions.[2] Examples of some calcium binding proteins are given in table 7.1. For all cases, the calcium ion is reported to be liganded exclusively by oxygen atoms either in carboxylate groups, in peptide carbonyls, hydroxyl groups, or water molecules[1].

The effect of calcium ions on the structure and function of biological molecules has been of great interest.[3-5] Calcium is found in bone and in biological fluids as the free ion, as well as bound to a large number of proteins where it serves a structural role or as an activator of enzymatic processes. Among important calcium-requiring physiological processes may be mentioned muscle contraction, blood clotting and visual excitation. The details of these physiological processes or changes that occur upon calcium binding are not important in the present research.

REFERENCES

1) S. Forsén and B. Lindman, *Ann. Rep. NMR Spec.*, 1981, **11A**, 183

2) H.J. Vogel, T. Drakenberg and S. Forsén, in *NMR of Newly Accessible Nuclei - Chemical and Biochemical Applications* (ed. P. Laszlo), p.157, Academic Press, New York, 1983

3) R.H. Kretsinger, *Ann. Rev. Biochem.*, 1976, **45**, 239

4) *Calcium in Biological Systems*, Symposia of the Society for Experimental Biology, Symposium XXX, Cambridge University Press, 1976

5) *Calcium Binding Protein and Calcium Function* (ed. F.L. Siegel, E. Carafoli and R.H. Wasserman), Elsevier/North Holland, New York, 1980

Overview of Calcium-43 NMR Studies

As mentioned before, the low natural abundance, low NMR sensitivity and low receptivity of calcium-43 have in the past hindered NMR studies of this nucleus. In the biological field the binding of calcium ion to a large macromolecule excessively increases the linewidth of the calcium-43 signal so that the broadened signal is beyond the limits of detection. So far, the reported NMR studies for calcium-43 in the biological field have utilised enriched calcium-43 material and low concentrations of the biological molecule. It is assumed that without the enrichment most of the studies would not have been possible. Unfortunately the cost of using biological material enriched in calcium-43 is very high, therefore the NMR literature for calcium-43 is limited to a small quantity.

However in this chapter an attempt is made to review the available NMR literature on calcium-43. Studies of simple calcium salts as well as biological-calcium systems are considered and summarised.

7.1) Simple Salts

Both relaxation and chemical shift studies for simple salts of calcium have been studied by Lutz *et al.*[1,2] Their work has been extensively reviewed.[3-5] With increasing concentration of salt, the relaxation rate of calcium-43 is observed to increase. Different salts produce a different concentration dependence. Surprisingly, no study has been found in the literature concerning the concentration dependence of calcium-43 linewidths for different anions, although for magnesium-25 an anion sequence of increasing linewidth $Cl^- < ClO_4^- < Br^- < NO_3^-$ has been reported by Simeral *et al.*[6] and Heubel *et al.*[7]

The chemical shift of calcium-43 as a function of anion concentration was studied in detail by Lutz *et al.*[1,2] Considerable shift changes were observed for the calcium ion on addition of the anion. The halide ions were observed to produce a high-frequency shift, whereas oxy-anions were observed to produce a low-frequency shift, Fig 7.1. In fact, for anions studied by Lutz *et al.* the calcium-43 chemical shift influence of the anion was found to follow the sequence $[NO_3]^- < [ClO_4]^- < H_2O$ (infinite dilution) < $Br^- < Cl^-$. However, according to a similar study by Farmer and Popov,[8] the perchlorate and nitrate ions were found to change places in the above sequence.

It is assumed that the shielding of ions is affected by near-by solvent molecules and ions. The theory of Kondo and Yamashita,[9] originally put forward to explain ion shielding in crystals, is preferred by most workers to explain the shielding of cations.[4,10] According to this theory, the shielding depends on the overlap of the outer p-orbitals of the studied ion with the outer orbitals of other ions or solvent molecules. Thus, the difference between the chemical shift effects of oxy-anions and halides was described by Lutz *et. al.*[1,2] in terms of the amount of overlap of the outer p-orbitals of the calcium ion with the outer orbitals of the anions. The oxy-anions are expected to give a smaller overlap than the halide anions, the former have a substantial positive

charge at the centre which reduces the electron density at the peripherals. In terms of the Kondo-Yamashita theory, a decrease in the cation-anion overlap occurs with oxy-anions, therefore increasing the shielding. Thus, a low frequency shift. For the halide ions, an increased overlap between the outer orbitals of the halides and the p-orbital of the calcium ion occurs. The electrons are more spread out as a result. Hence, the calcium-ion is less shielded, i.e. a high-frequency shift is observed.

Unfortunately, no study has been found in the literature concerning the effect of pH on calcium-43 relaxation and chemical shift for simple salt solutions.

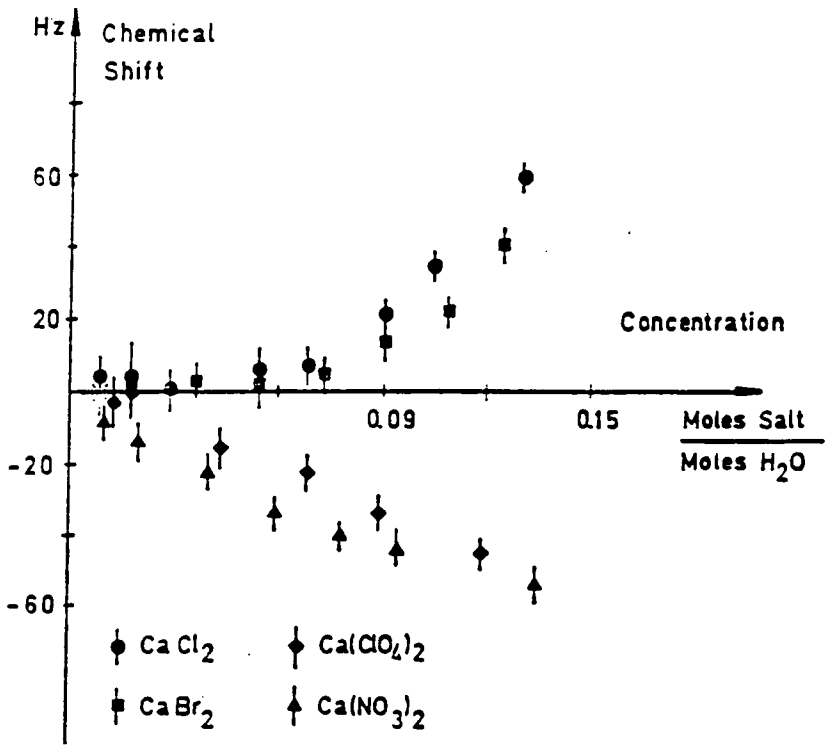

Fig 7.1 Chemical shifts of calcium-43 for aqueous solutions of calcium salts as a function of concentration. The reference is calcium chloride solution at infinite dilution.[2]

7.2) Complex Formation with Low Molecular Weight Ligands

Calcium forms complexes with a variety of ligands, for example, carboxylate groups, carbonyl groups, hydroxyl groups and water. The calcium ion, as reported by Forsén and Lindman,[3] is usually liganded by the oxygen atom.

The very first NMR study of calcium-43 in the biological field was made by Bryant[11] in 1968. He demonstrated the use of enriched calcium-43 (31.7 %) NMR for investigating complexing of Ca^{2+} with ATP and pointed to its usefulness in studies of calcium binding proteins. Only a single calcium-43 signal was observed for the Ca-ATP system, leading to the assumption that fast exchange of Ca^{2+} ions takes place between the complexed and free calcium forms.

Robertson *et al.*[12,13] investigated the binding of calcium to γ-carboxyglutamic acid (Gla) containing tripeptides. The amino acid Gla is normally found in calcium binding proteins involved in blood coagulation and is considered to be responsible for binding the calcium ion. In their study, Robertson *et al.*[12] employed enriched calcium-43 (80 %) which allowed NMR studies to be performed at calcium ion concentrations of approximately 20 mM. The addition of di- and tri- peptides, each containing two neighbouring Gla residues, caused considerable changes in both calcium-43 linewidth and chemical shift. With increasing peptide concentration, an increase in the linewidth and a low-frequency shift, referenced to a calcium solution at infinite dilution, were observed. The amino acid Gla binds the calcium ion via an oxygen atom, and therefore it is expected to produce a low frequency shift according to the Kondo-Yamashita theory.

The interaction of calcium with diketo ligands (pentane-2,4-dione and hexane-2,5-dione) was investigated by Kraft *et al.*[14] using calcium-43 NMR. No isotopic enrichment was used, and studies were made on 1.0 mol dm^{-3} aqueous solutions of CaI_2 containing 0.02 mol dm^{-3} of the diketone ligand. Under these conditions an approximate 13 ppm shift of the calcium-43 resonance to low frequency was observed for both diketones. Similarly, low-frequency calcium-43 shifts in the presence of

several oxy-anions, for example formate, and lactate, have been observed by Lutz *et al.*[2]

Separate calcium-43 NMR signals from free and liganded Ca^{2+} have been observed in solutions containing excess EDTA.[3] EDTA has four carboxylic groups and two amine groups, therefore the affinity of this ligand for calcium ions is very high. As a result, slow exchange of calcium ions between complexed and free calcium takes place. Hence, two signals for calcium-43 are observed in the presence of EDTA. The chemical shift of the complexed calcium ion is observed to be at a higher frequency compared to that of the free calcium ion , as is shown in Fig 7.2. It is assumed that the two nitrogens of EDTA form strong covalent bonds with Ca^{2+}, resulting in a high-frequency shift as is observed experimentally.

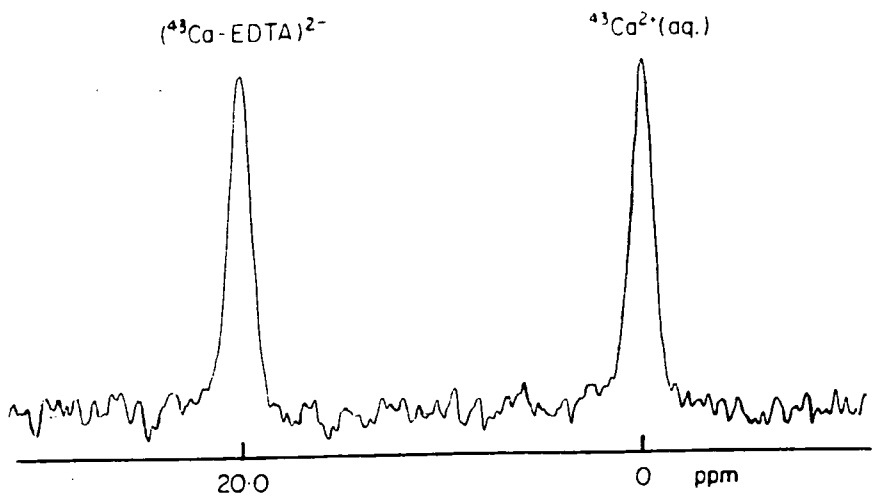

Fig 7.2 Calcium-43 NMR studies of an aqueous solution containing 4 mM Ca^{2+} and 2 mM EDTA at pH 7.[3]

7.3) Calcium-43 Binding to Polyions

In the biological field polyions such as nucleic acids and polysaccharides are considered to have vital structural and functional roles. To be effective it is important that these polyions bind simple cations, such as Na^+; Mg^{2+}, and Ca^{2+}.

Calcium-43 NMR studies of ion binding to polyions have been performed by Gustavsson.[3] However, the author has reported difficulties in interpreting the NMR data in detail. The complex relaxation behaviour of the spin 7/2 nuclei, and the complex exchange processes present in these systems have, according to Gustavsson, complicated data interpretation. Thus, relatively few examples of calcium-43 NMR studies of calcium-polyion systems have been found in the literature.

Nevertheless, a nice example of using calcium-43 NMR for investigating calcium-polyion interactions was provided by a study of calcium binding to DNA.[15] Calcium-43 linewidth at half-height was studied as a function of temperature, Fig 7.3. Up to a temperature of 70 °C the linewidth was observed to increase with increasing temperature, whereas at 80 °C and above, narrow calcium-43 lines were observed. These observations were explained in terms of a DNA transition from a double-stranded helical to a single-stranded random coil state between 70 and 80 °C. It was assumed that the conformational transition caused a considerable reduction in the number of calcium ions bound to DNA and as a result decreased the linewidth drastically.

Fig 7.3 Calcium-43 linewidth dependence on temperature for a solution of 7.1 mM DNA and 35 mM Ca^{2+} at pH 5.2.[15]

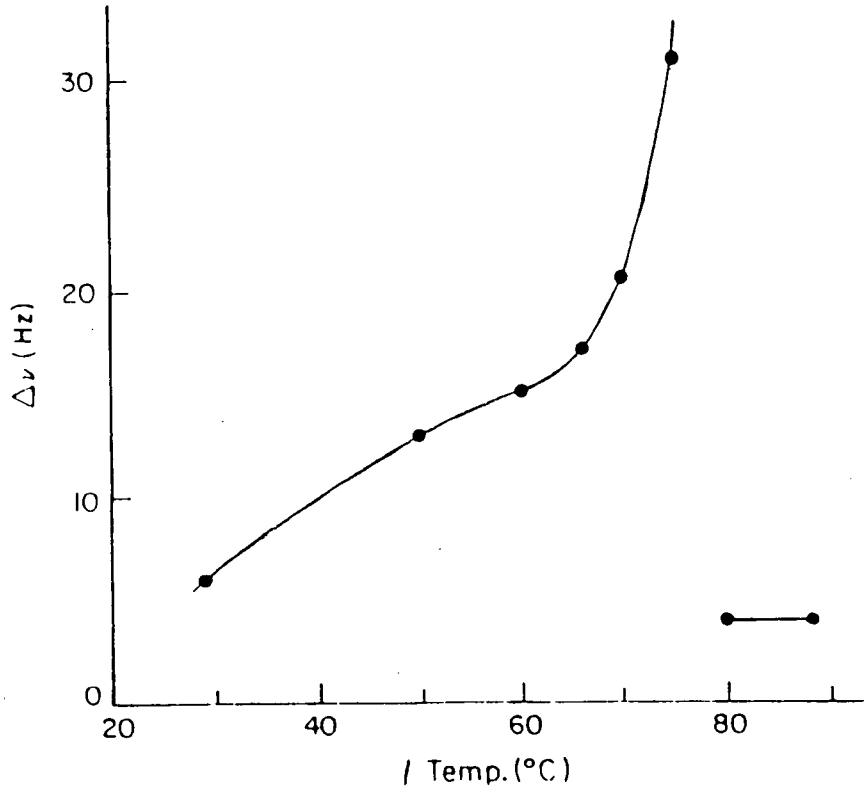

7.4) Calcium-43 Binding to Proteins

As mentioned before, calcium is necessary for the activity of a large number of enzymes, proteins and other biological macromolecules. Therefore, it was somewhat surprising to discover that detailed calcium-43 NMR studies of calcium-binding proteins have only been carried out since 1978 and not before.

In table 7.1, examples of some calcium-binding proteins are given. The molecular weight and the functional role of each protein as well as the reference are reported. It is important to note that for all examples cited, enriched calcium-43 material was used.

Protein	Molecular Weight / g	Functional Role	Reference
Parvalbumin	~ 11 500	buffer for intracellular Ca^{2+}	16
Prothrombin	~ 23 500	blood coagulation	17
Troponin C	~ 18 000	contraction of muscles	3
Calmodulin	~ 16 700	calcium regulation	18
α-lactalbumin	~ 16 000		19
Osteocalcin	~ 5 500	deposition of Ca^{2+} in bone	20
Hemocyanin	~ 4.5×10^5	oxygen transport	21
Trypsin	~ 24 000		22
Phosphodentine		deposition of Ca^{2+} in teeth	23
Calmodulin	~ 17 000	contraction of muscles	24,25
Phospholipase A_2	~ 14 000	catalysis	26

Table 7.1 Calcium-43 NMR studies of calcium-binding proteins

Generally, it was observed that for calcium-protein systems the relaxation or the linewidth of the calcium-43 signal was dependent on calcium ion exchange, the pH of the solution, and the temperature.

The temperature and pH dependence of calcium-43 NMR linewidth in the presence of parvalbumin was presented by Parello.[16] Very small calcium-43 linewidths were observed at room temperature and neutral pH, indicating slow chemical exchange of Ca^{2+} ions to calcium-binding sites of parvalbumin. However, significant line broadening was observed above 65 °C and at pH values exceeding 10.

The pH dependence of the calcium-43 linewidth for calcium prothrombin solutions was studied by Marsh.[17] At pH 3, very little calcium-ion binding was evident and as a result narrow lines were observed. However with increasing pH, the calcium-43 linewidth was observed to increase, with a pronounced inflection point at pH 3.7. Following a plateau at pH 5 - 6, a further increase was observed above pH 7, Fig 7.4

The calcium-43 linewidth in the presence of TnC and phospholipase A_2 as a function of temperature was studied by Forsén and Lindman[3] and Anderson *et al.*,[26] respectively. The results of each study are shown in Figs 7.5 and 7.6. At low temperatures, the linewidth was assumed to be dominated by the chemical exchange process, whereas at higher temperatures the linewidth was determined by the relaxation rate.

The interaction of calcium with calmodulin in the presence of trifluoperazine (TFP) was studied by Forsén *et al.*[18] TFP is known to strongly inhibit the biological activity of calmodulin.[3] The effect of adding TFP to a calcium-calmodulin solution on calcium-43 linewidth is shown in Fig 7.7. With increasing TFP concentration, the linewidth was observed to decrease. From temperature studies of calmodulin,[18] it was found that at room temperature the linewidth of calcium-43 was determined by the slow chemical exchange rate of calcium ions between the two calcium-ion binding sites of calmodulin. The addition of TFP was assumed to cause a considerable

decrease in the exchange rate, so that in the presence of TFP it seemed as though exchange did not take place. Hence, a decrease in calcium-43 linewidth was observed.

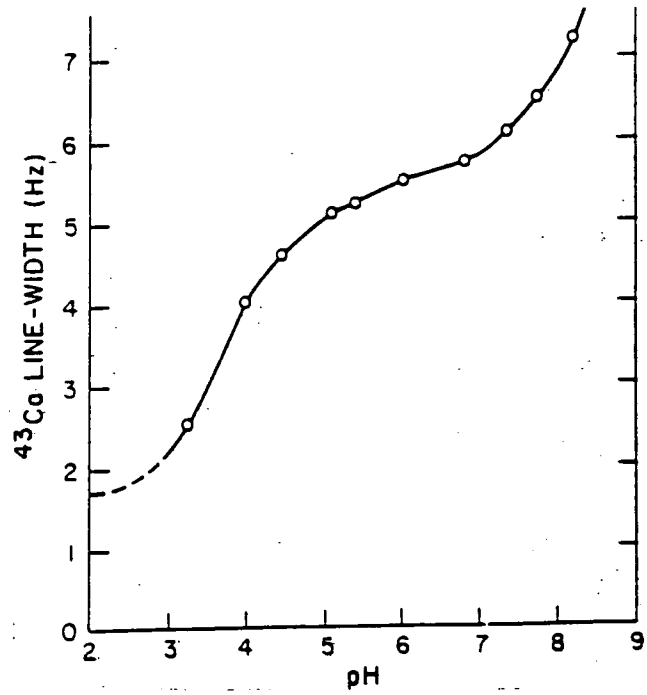

Fig 7.4 Calcium-43 linewidth dependence on pH for a solution of 21 mM Ca^{2+} and 53 mM prothrombin. The dotted line shows extrapolation to zero prothrombin concentration.[17]

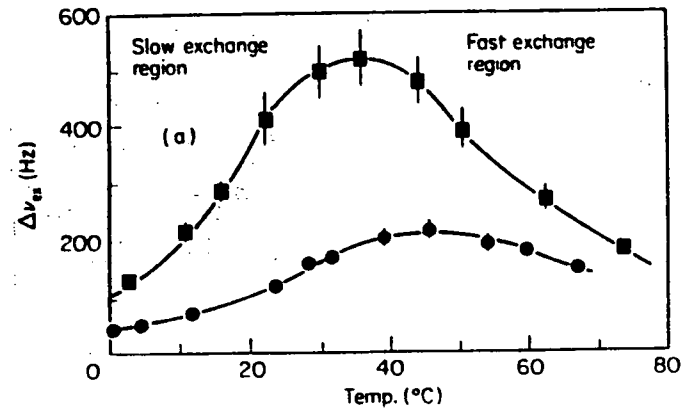

Fig 7.5 The temperature dependence of the calcium-43 linewidth in the presence of 0.86 mM TnC, 3.67 mM Ca^{2+}, pH 7.0 (■); and 0.75 mM TnC, 5.92 mM Ca^{2+}, pH 7.1 (●).[3]

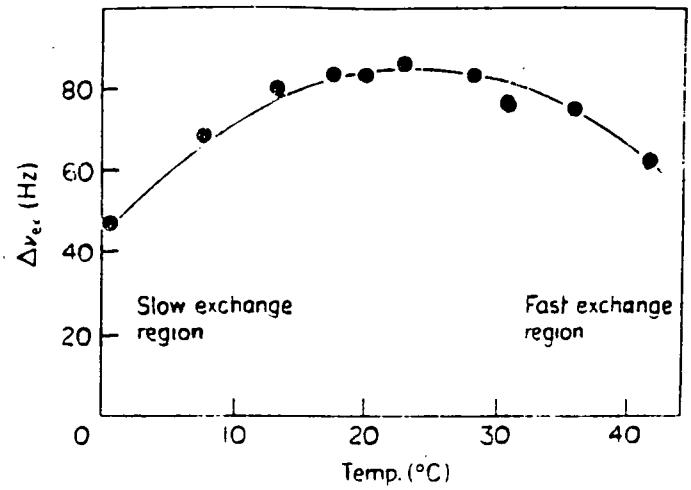

Fig 7.6 The temperature dependence of the calcium-43 linewidth for a solution of 1.7 mM phospholipase and 5.9 mM Ca^{2+} at pH 7.4 [26]

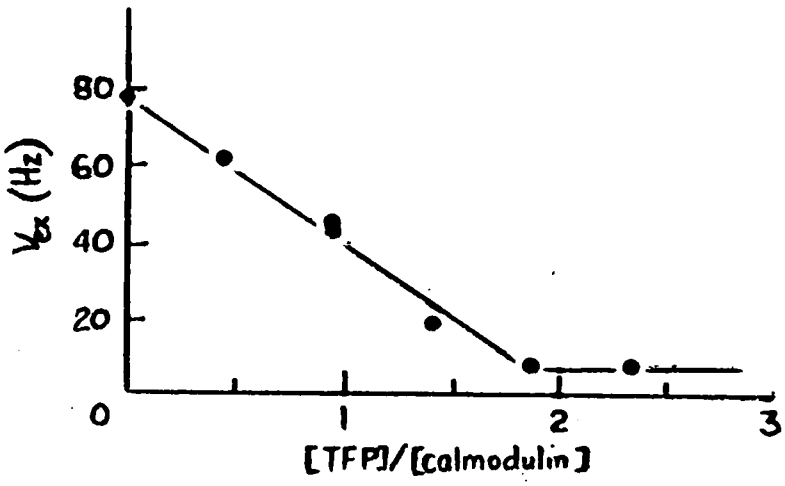

Fig 7.7 The effect of adding trifluoperazine (TFP) on calcium-43 linewidth in the presence of calmodulin. Conditions : 0.41 mM calf brain calmodulin, 2.96 mM Ca^{2+}, pH 7.1 at 23 °C.[18]

Some calcium binding proteins such as lactalbumin and parvalbumin have two calcium ion binding sites. In each binding site the calcium ion experiences small chemical shift changes but large broadening. In such a case, problems due to overlapping of resonances are encountered with very poor resolution between the peaks. In order to minimise these problems and to enhance resolution, attempts have been made to shift the resonance of the weakly bound and rapidly exchanging calcium ions.[27] Low-frequency shifts of up to -125 ppm and high-frequency shifts of up to +60 ppm have been induced for calcium ions using lanthanide-chelator complexes. The most effective were observed to be the Dy^{3+} and Tm^{3+} complexes with tripolyphosphate.[27] The introduction of the shift reagent to samples containing calcium-binding proteins with two calcium-binding sites shows a great improvement in the resolution. The resonance for weakly bound and rapidly exchanging calcium ions is shifted by the shift reagent, whereas for tightly bound and slow exchanging calcium ions the resonance remains unaffected, thus increasing the resolution. It is considered that the weakly bound calcium ions have a lower affinity for the protein than for the shift reagent, therefore the resonance for these ions is successfully shifted. However for situations where the affinity of calcium ions is greater for the protein than for the shift reagent or even similar, then shifting the resonance becomes very difficult.

7.5) NMR Studies using Substitution Probes for Calcium

The possibility of studying the interaction of calcium with large size macromolecules is usually not very favourable. The low natural abundance, low NMR sensitivity and receptivity, and signal broadening are all important factors which limit the NMR study of calcium-43. However, one possible solution to this problem is to substitute another metal ion, with more favourable NMR properties, for the calcium ion. Importantly, the probe should have approximately the same ionic radius and co-ordination properties as calcium. For biological interest, it is important that the probe behaves similarly to calcium when binding the protein or macromolecule.

The use of ^{113}Cd or ^{111}Cd as a probe for the calcium ion has been found to be very encouraging. The Cd^{2+} has been shown to replace Ca^{2+} specifically in several calcium-binding proteins and to give similar co-ordination properties. The NMR sensitivity of ^{113}Cd is more than 100 times better than that of ^{43}Ca at natural abundance. The relaxation of ^{113}Cd, being a spin 1/2, is expected to be slow even when bound to a macromolecule. Therefore, narrow lines are expected for ^{113}Cd compared to ^{43}Ca. The use of ^{113}Cd NMR to study calcium-binding proteins has been illustrated by Forsén *et al.*[28,29]

7.6) ^{1}H and ^{19}F NMR studies to Investigate Calcium Binding to Biological Molecules

A report published by Forsén and Lindman in 1981[3] on calcium-43 NMR studies of calcium binding to biological molecules concluded that calcium-43 NMR studies are not fruitful unless enriched calcium-43 material is used which, unfortunately, is very expensive. As an alternative and to reduce the cost, ^{1}H instead of ^{43}Ca NMR studies have been utilised to study interactions of calcium with biological molecules during the past decade.[30-37] The conformational changes that biological molecules undergo

upon calcium binding are studied by ^{1}H NMR. Such studies are still widely used in the biological field.

Fluorine-19 NMR has also been used to obtain information on calcium ions present in biological molecules. The concentrations of calcium ion in ferret heart and in cells (tissues) have been determined by Kirschenlohra *et al.*[38] and by Levy *et al.*[39], respectively using fluorine-19 NMR. In both cases, a fluorinated ligand with a high affinity for calcium was added to the heart or the cells. Two signals were observed. One signal corresponded to the free ligand whereas the other signal was assigned to the calcium complexed ligand. From the intensity ratio of the two signals the concentration of the calcium ions was evaluated.

REFERENCES

1) O. Lutz, A. Schwenk and A. Uhl, *Z. Naturforsch.*, 1973, **28a**, 1534

2) O. Lutz, A. Schwenk and A. Uhl, *Z. Naturforsch.*, 1975, **30a**, 1122

3) S. Forsén and B. Lindman, *Ann. Rep. NMR Spec.*(ed. G.A. Webb),1981, **11A**, 183

4) B. Lindman and S. Forsén, in *NMR and the Periodic Table* (ed. R.K. Harris and B.E. Mann), p.183, Academic Press, London, 1978

5) J.W. Akitt, in *Multinuclear NMR* (ed. J. Mason), p.189, Plenum, New York, 1987

6) L. Simeral and G. E. Maciel, *J. Phys. Chem.*, 1976, **80**, 552

7) P.H. Heubel and A.I. Popov, *J. Sol. Chem.*, 1979, **8**, 283

8) R.M. Farmer and A.I. Popov, *Inorg. Nucl. Chem. Lett.*, 1981, **17**, 51

9) J. Kondo and J. Yamashita, *J. Phys. Chem. Solids*, 1959, **10**, 245

10) B. Lindman and S. Forsén, in *Chlorine, Bromine and Iodine NMR - NMR Basic Principles and Progress* (ed. P. Diehl, E. Fluck and R. Kosfeld), Springer Verlag, Berlin-Heidelberg, 1976

11) R.G. Bryant, *J. Am. Chem. Soc.*, 1969, **91**, 1870

12) P. Robertson, Jr., R.G. Hiskey and K.A. Koehler, *J. Biol. Chem.*, 1978, **253**, 5880

13) P. Robertson, Jr., R.G. Hiskey and K.A. Koehler, *Biochem. Biophys. Res. Commun.*, 1979, **86**, 265

14) H.G. Kraft, P. Peringer and B.M. Rode, *Inorg. Chim. Acta*, 1981, **48**, 135

15) P. Reimarsson, J. Parello, T. Drakenberg, H. Gustavsson and B. Lindman, *FEBS Lett.*, 1979, **108**, 439

16) J. Parello, H. Lilja, A. Cavé and B. Lindman, *FEBS Lett.*, 1978, **87**, 191

17) H.C. Marsh, P. Robertson, Jr., M.E. Scott, K.A. Koehler and R.G. Hiskey, *J. Biol. Chem.*, 1979, **254**, 10268

18) E. Thulin, S. Forsén, T. Drakenberg, T. Andersson, J. Krebs and K. Seamon, in *Calcium-Binding Proteins and Calcium Function* (ed. F.L. Siegel, E. Carafoli and R.H. Wasserman), Elsevier/North Holland, New York, 1980

19) L.J. Berliner, R. Kaptein, K. Koga and G. Musci, in *NMR Applications to Biopolymers* (ed. J.W. Finlay, S.J. Schmidt and A. Serianni), Plenum, New York, 1990

20) H.J. Vogel, T. Drakenberg and S. Forsén, in *NMR of Newly Accessible Nuclei - Chemical and Biochemical Applications* (ed. P. Laszlo), p.157, Academic Press, New York, 1983

21) T. Andersson, E. Chiancone and S. Forsén, *Eur. J. Biochem.*, 1982, **125**, 103

22) T. Drakenberg and H.J. Vogel, in *Calcium-Binding Proteins in Health and Disease* (ed. F.L. Siegel, E. Carafoli and R.H. Wasserman), Elsevier, Amsterdam, 1983

23) A. Linde, M. Bhown and A. Butler, *J. Biol. Chem.*, 1980, **255**, 5931

24) T. Andersson, T. Drakenberg, S. Forsén, E. Thulin and M. Swärd, *J. Am. Chem. Soc.*, 1982, **104**, 576

25) T. Andersson, T. Drakenberg, S. Forsén and E. Thulin, *Eur. J. Biochem.*, 1982, **126**, 501

26) T. Andersson, T. Drakenberg, S. Forsén and T. Wieloch, in *Calcium-Binding Proteins and Calcium Function* (ed. F.L. Siegel, E. Carafoli and R.H. Wasserman), Elsevier/North Holland, New York, 1980

27) H.J. Vogel and W.H. Braunlin, *J. Mag. Res.*, 1985, **62**, 42

28) S. Forsén, T. Andersson, T. Drakenberg, E. Thulin and T. Wieloch, in *Advances in Solution Chemistry* (ed. Bertini *et al.*), Plenum, New York, 1980

29) M. Akke, S. Forsén and W. J. Chazin, *Mag. Res. Chem.*, 1993, **31**, 128

30) A. Pinter, A. Chollet, C. Bradshaw, A. Chaffotte, C. Cadieux, M.J. Rooman, K. Hallenga, J. Knowles, M. Goldberg and S.J. Wodak, *Biochemistry*, 1994, **33**, 11158

31) C. Johansson, M. Ullner and T. Drakenberg, *Biochemistry*, 1993, **32**, 8429

32) G.S. Shaw, R.S. Hodges and B.D. Sykes, *Biochemistry*, 1992, **31**, 9572

33) K. Török, A.N. Lane, S.R. Martin, J.M. Janot and P.M. Bayley, *Biochemistry*, 1992, **31**, 3452

34) L.E. Kay, W.D. McCubbin, C.M. Kay, and J.D. Forman-Kay, *Biochemistry*, 1991, **30**, 4323

35) S. Bagby, T.S. Harvey, K.E. Lewis, E.G. Susan, I. Sumiko and I. Mitsuhiko, *Biochemistry*, 1994, **33**, 2409

36) M.S. Sunnerhagen, M. Ullner, E. Persson, O. Telleman, J. Stenflo and T. Drakenberg, *J. Biol. Chem.*, 1992, **267**, 19642

37) G.S. Shaw, L.F. Golden, R.S. Hodges and B.D. Sykes, *J. Am. Chem. Soc.*, 1991, **113**, 5557

38) H.L. Kirschenlohr, A.A. Grace, S.D. Clarke, Y. Shachar-Hill, J.C. Metcalfe, P.G. Morris and G.A. Smith, *Biochem. Journal*, 1993, **293**, 407

39) L.A. Levy, E. Murphy, B. Raju and R.E. London, *Mag. Res. Chem.*, 1992, **30**, 723

8.1) Experimental

The relaxation of calcium-43 in calcium chloride, calcium bromide, calcium iodide, calcium nitrate, calcium acetate, and calcium ascorbate has been studied as a function of salt concentration. The variations of calcium-43 linewidth and chemical shift with concentration have also been analysed. The complexation and binding of calcium to sucrose and lysozyme were studied by analysing the effect of sucrose and lysozyme concentrations on calcium-43 relaxation and chemical shift.

Calcium chloride, calcium bromide, calcium iodide, and calcium nitrate were purchased from Sigma Chemical Co. Ltd. All were of analar grade and used without any further treatment. Sodium acetate and sodium ascorbate, both of analar grade, were bought from Sigma Chemical Co. Ltd and MTM Lancaster, respectively. They were also used without any further treatment. Lysozyme, purchased in the form of a powder, and sucrose were bought from Sigma Chemical Co. Ltd and were also used without any further treatment.

Calcium chloride, calcium bromide, calcium iodide, and calcium nitrate solutions were prepared by adding a weighed amount of the calcium salt to a pre-weighed amount of solvent. Different concentrations of the calcium salts were prepared and analysed. Unfortunately, both calcium acetate and calcium ascorbate have low solubilities in water at 20 °C. Thus, it is not possible to study high concentrations of these salts. In fact, the maximum concentrations that could be prepared were 1.5 mol dm^{-3} for calcium acetate and 1.0 mol dm^{-3} for calcium ascorbate. At these concentrations, it is almost impossible to observe a signal for calcium-43 at natural abundance. Therefore, to analyse the effect of acetate and ascorbate on calcium-43 longitudinal relaxation, linewidth at half-height, and chemical shift, a constant concentration of calcium chloride (1 mol dm^{-3}) solution was prepared. To this was added different amounts of sodium acetate and sodium ascorbate to increase the acetate and ascorbate concentration.

Likewise, the complexation and binding of calcium to sucrose and lysozyme was also analysed by preparing a constant concentration of calcium chloride (1 mol dm^{-3}) solution and adding to this different amounts of sucrose and lysozyme.

Calcium-43 relaxation, linewidth at half-height and chemical shift for calcium chloride, calcium nitrate, calcium acetate and calcium ascorbate solutions were also studied as a function of pH. A constant concentration of 1 mol dm^{-3} calcium chloride and calcium nitrate solutions was prepared for pH analysis, whereas calcium acetate and calcium ascorbate solutions were prepared by adding 1.0 mol dm^{-3} sodium acetate or 1.0 mol dm^{-3} sodium ascorbate to 1.0 mol dm^{-3} calcium chloride, respectively. The pH was altered by adding a small volume of either 1 mol dm^{-3} HCl or 1 mol dm^{-3} NaOH, or even a mixture of the acid and the base to the solution via a pipette. Normally, a very small volume of HCl or NaOH was required. For small changes of pH, the acid or the base were diluted before the addition to the calcium solution. The pH of the solution was in all cases measured by both litmus paper and an electronic pH meter (Jenway 3020 meter). The pH measurement by the electronic method was repeated at least twice and the reproducibility error was found to be approximately ±0.2 in most cases.

The interesting salts of calcium citrate and calcium phytate, known to be used in the food industry, could not be studied. The solubility of both these salts in water at 20 °C is very low. Increasing the temperature or altering the pH of the solutions to acidic or alkaline conditions did not make any difference to the solubility of these salts. Unfortunately, the solubility of both sodium citrate and sodium phytate salts is also very low in water at 20 °C. Therefore, it was not feasible to analyse the effect of citrate or phytate on calcium-43 signals by adding sodium citrate or sodium phytate to a constant concentration of calcium chloride.

The solvent for preparing calcium samples for analysis was always a mixture of 20 % D_2O and 80 % H_2O. D_2O was added so that a deuterium lock could be obtained which could then be used for shimming purposes. Both the Bruker AMX-500 and Varian VXR-600 spectrometers were shimmed using the lock signal.

The reference for chemical shift analysis was 1 mol dm^{-3} calcium chloride solution for all salts studied. Bulk susceptibility corrections were not carried out for any of the salts as these corrections made very little difference to the overall chemical shift.

The natural abundance of calcium-43 is 0.145 %. The possibility of observing a calcium-43 signal at low frequencies is almost impossible unless enriched material is used. Needless to say, great efforts were made to observe a calcium-43 signal on the Bruker MSL-300 spectrometer (SF = 20.195 MHz for ^{43}Ca) for a saturated calcium chloride solution at natural abundance of calcium-43. Unfortunately, a calcium-43 signal was not observed. Thus, calcium-43 studies at natural abundance were carried out only on Bruker AMX-500 and Varian VXR-600 spectrometers operating at frequencies of 33.659 MHz and 40.356 MHz, respectively. However, even for these spectrometers difficulties were encountered when observing a signal from very low concentrations of calcium ions. The minimum calcium chloride concentration that could be studied was 1 mol dm^{-3}. A reasonable signal-to-noise ratio was observed at this concentration after about 1000 transients.

The longitudinal relaxation times were measured using the inversion-recovery pulse sequence (see section 4.6), whereas the transverse relaxation times were obtained from the linewidth at half-height of the Fourier-transformed signal. For both spectrometers the probe was shimmed until the linewidth at half-height for protons was approximately 1 Hz. This meant that the contribution to calcium-43 linewidth due to field inhomogeneity was approximately 0.07 Hz, about 10 % of the experimentally measured linewidth for calcium-43 at low calcium salt concentration. Therefore the

contribution to calcium-43 linewidth from the field inhomogeneity (0.07 Hz) was considered to be significant and was, in all cases, subtracted from the experimentally measured linewidth. Thus the reported linewidths for calcium-43 are corrected for the field inhomogeneity contribution.

All measurements were done using a 10 mm probe and a temperature of 298 K on both spectrometers.

8.2) RESULTS

Calcium-43 has a spin number of 7/2 and is therefore quadrupolar. Thus, it is expected to undergo quadrupolar relaxation. In table 8.1 the NMR properties of calcium-43 are summarised.

The quadrupole moment of calcium-43, reported by Grundvik *et al.*[1], is -0.05×10^{-28} m^2. This value is quite small compared to those for other quadrupolar nuclei, for example magnesium-25 has a quadrupole moment of 0.22×10^{-28} m^2.[2] The small quadrupole moment of calcium-43 leaves a doubt in assuming that relaxation of calcium-43 is strongly dominated by quadrupolar relaxation. Possible contributions from other relaxation mechanisms may have to be considered, as mentioned by Forsén and Lindman.[2] However, to date studies of calcium-43 have considered quadrupolar relaxation to dominate. Unfortunately, possible contributions from other relaxation mechanisms have not been examined, although many scientists have reported this to be a worthy subject for study.

Woessner *et al.*[3] studied the relaxation of lithium-7 in H_2O and D_2O solutions. Lithium-7 has a spin of 3/2 and a quadrupole moment of -0.045×10^{-28} m^2 (comparable with the quadrupole moment of calcium-43). The relaxation rate of lithium-7 in H_2O was found to be greater than in D_2O. This was interpreted to mean that the relaxation of lithium-7 in H_2O has an extra contribution to relaxation that is not present in D_2O. In fact, in H_2O the extra contribution to relaxation is due to the ^7Li, ^1H magnetic dipole-dipole interactions which are not present in D_2O. Thus, in H_2O the relaxation is dependent on both magnetic dipolar and electric quadrupolar relaxation mechanisms. Since the magnetogyric ratio of deuterium is very small compared to that of the proton, the magnetic dipole-dipole interaction between the lithium nucleus and deuterium is negligible compared to that between lithium and proton. Thus, in D_2O quadrupolar relaxation is solely expected for lithium-7. Hence, a slower relaxation in D_2O is observed compared to H_2O.

isotope	*spin*	*natural abundance* %	*magnetic moment* μ / μ_N	*magnetogyric ratio* γ / 10^7 rad T^{-1} s^{-1}	*quadrupole moment* Q / 10^{-28} m^2	*receptivity* (^{13}C = 1.00)
^{43}Ca	7/2	0.145	-1.491	-1.80	-0.05	0.053

Table 8.1 Nuclear spin properties for calcium-43

Importantly, Woessner *et al.*[3] observed that relaxation of lithium-7 is not dominated by quadrupolar relaxation, although lithium-7 possesses a quadrupolar moment.

A similar experiment for 3 mol dm^{-3} calcium chloride solution in H_2O and D_2O revealed that in H_2O the longitudinal and transverse relaxation rates for calcium-43 were 2.0 and 4.2 s^{-1}, respectively, at a frequency of 33.659 MHz. However, in D_2O the longitudinal and transverse relaxation rates were found to be 2.5 and 5.3 s^{-1}, respectively at the same frequency.

Since, the relaxation of calcium-43 in D_2O is found to be faster than in H_2O, then it can be assumed that relaxation of calcium-43 is dominated by the quadrupolar relaxation mechanism. Any significant contribution from dipolar relaxation would have resulted in a faster relaxation rate in H_2O compared to D_2O, but this is not the case. The slight difference in the relaxation rates between the two solvents can be attributed to the difference in viscosity of the solvents and to experimental error. The viscosity ratio of D_2O : H_2O is approximately 1.23 at 25 °C.[4] Thus, a faster relaxation is expected in D_2O as is observed experimentally.

Under the assumption that quadrupolar relaxation is the dominant mechanism for calcium-43, the relaxation rate is expected to be given by equation 8.1. Within the extreme narrowing region, *i.e.* $\omega\tau_c << 1$, longitudinal and transverse relaxation rates are expected to be equal and exponential.

$$\frac{1}{T_1} = \frac{1}{T_2} = \frac{3\pi^2(2I+3)}{10I^2(2I-1)}\chi^2\left(1+\eta^2/3\right)\tau_c \qquad \text{eqn 8.1}$$

The various parameters are the same as those described earlier for water oxygen-17 studies.

In the non-extreme narrowing region, *i.e.* $\omega\tau_c \geq 1$, it is expected that $R_1 < R_2$. Thus the relaxation is no longer expected to be simple or exponential. In fact, a frequency dependence may be observed, and equation 8.1 may need to be modified to take this into consideration. However, experimentally it is very difficult to observe the non-exponentiality. No example of non-exponential relaxation of spin I =7/2 nuclei has been found in the literature. For calcium-43 experiments reported by Forsén and Lindman[2] on biological systems, the observed lineshapes were all Lorentzian to a very high degree. Non-exponentiality was not evident, although the reported T_1 and T_2 values were not equal due to non-extreme narrowing effects.

Non-exponentiality was not observed for any of the calcium solutions during this study. Even for the most concentrated calcium chloride solution (6 mol dm^{-3}) there was no evidence of non-exponential relaxation behaviour of calcium-43.

8.2.1) Calcium chloride

In table 8.2, the effect of salt concentration on calcium-43 relaxation, linewidth and chemical shift are reported for aqueous calcium chloride solutions at two different spectrometer frequencies.

With increasing calcium chloride solution, both the longitudinal and transverse relaxation rates of calcium-43 are observed to increase, Fig 8.1. As the concentration of the salt increases the motion of the system decreases. Thus the reorientational correlation time of calcium-43 increases and as a result the relaxation rates increase. In all cases, the transverse relaxation time is observed to be less than the longitudinal relaxation time. Thus, the transverse relaxation rate is greater than the longitudinal relaxation rate as may be expected.

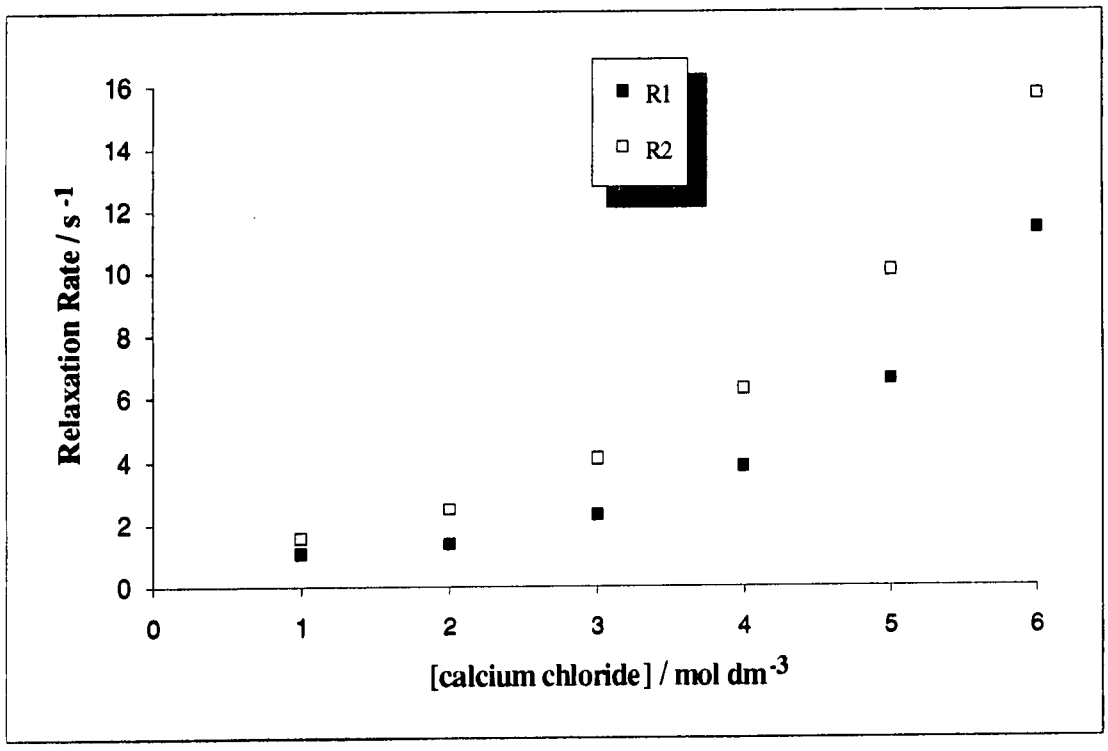

Fig 8.1 The variation of ^{43}Ca relaxation as a function of calcium chloride concentration for aqueous calcium chloride solutions. SF = 33.659 MHz

Concentration / mol dm^{-3}	pH	SF = 33.659 MHz			SF = 40.356 MHz		
		T_1 / ms	$\Delta\nu_{1/2}$ / Hz	δ / ppm	T_1 / ms	$\Delta\nu_{1/2}$ / Hz	δ / ppm
1.0	8.6	930 ± 50	0.5	0	950 ± 50	0.6	0
2.0	9.1	717 ± 30	0.8	+ 0.1	730 ± 30	0.9	0
3.0	9.2	428 ± 20	1.3	+ 0.1	454 ± 20	1.4	+ 0.1
4.0	9.4	259 ± 10	2.0	+ 1.0 ± 0.1	258 ± 10	2.1	+ 1.0 ± 0.1
5.0	9.5	152 ± 10	3.2	+ 2.4 ± 0.2	146 ± 10	3.2	+ 2.3 ± 0.2
6.0	9.6	88 ± 5	5.0	+ 5.0 ± 0.2	89 ± 5	5.1	+ 5.0 ± 0.2

Table 8.2 Experimental data for ^{43}Ca longitudinal relaxation time, linewidth at half-height, and chemical shift for aqueous calcium chloride solutions at two frequencies.

As expected the linewidth at half-height is also observed to increase with increasing salt concentration.

For calcium chloride solutions, a chemical shift of the calcium-43 signal is not observed up to a salt concentration of 3 mol dm^{-3}. At higher salt concentrations, a consistent shift towards high frequency is observed, Fig 8.2. As the salt concentration increases, the formation of a contact ion-pair between the cation and the anion becomes more likely. Thus, a greater chemical shift is expected with increasing salt concentration . The type of ion-pair formed between the cation and anion is very important for the chemical shift of the cation, as will be discussed later (see section 8.3).

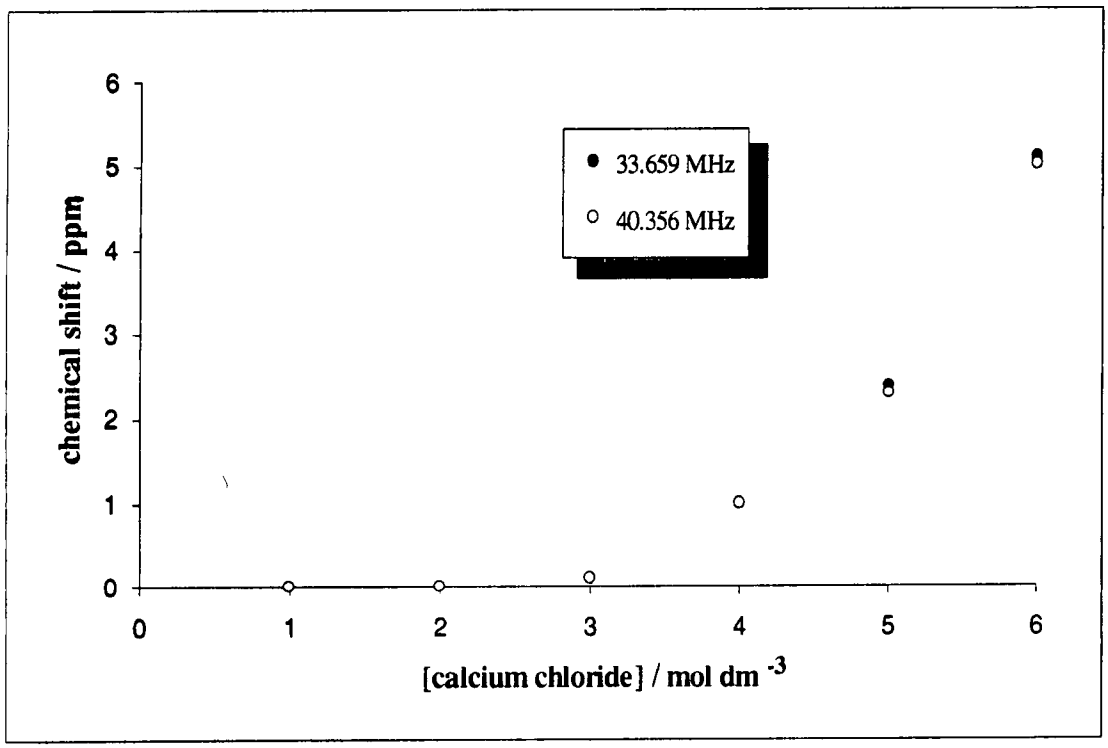

Fig 8.2 The dependence of ^{43}Ca chemical shift on calcium chloride concentration at two frequencies. The reference is 1.0 mol dm^{-3} calcium chloride solution. A positive sign indicates a high frequency shift.

Comparison of the results between the two spectrometer frequencies shows that there is very little difference in the linewidth at half height, table 8.2, the chemical shift, Fig 8.2, and the relaxation rates of calcium-43, Fig 8.3, at the two frequencies.

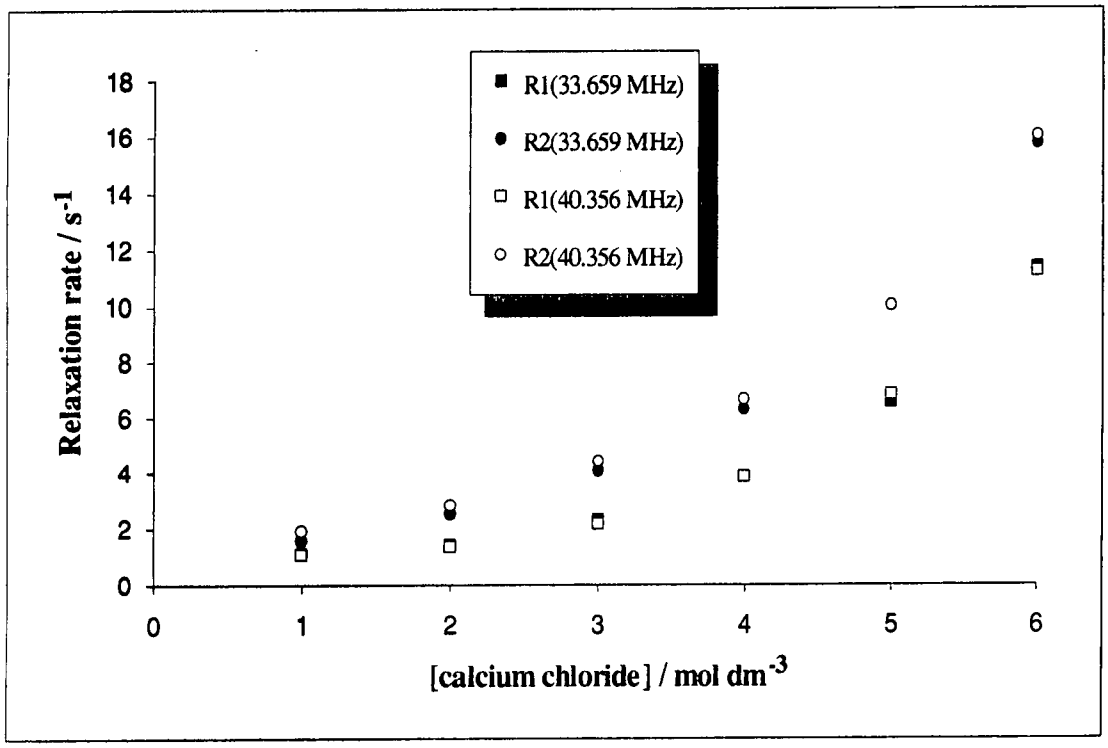

Fig 8.3 The variation of ^{43}Ca longitudinal and transverse relaxation rates as a function of calcium chloride concentration for aqueous calcium chloride solutions at two frequencies.

8.2.2) Calcium Bromide

The results for the effect of concentration of calcium bromide on calcium-43 relaxation, linewidth and chemical shift in aqueous calcium bromide solutions are reported in table 8.3.

Concentration / mol dm^{-3}	SF = 33.659 MHz		
	T_1 / ms	$\Delta\nu_{1/2}$ / Hz	δ / ppm
1	1200	0.4	0
2	800	0.6	0
3	440	1.0	0
4	270	1.7	+0.5
5	160	2.5	+1.7
6	90	4.2	+4.2

Table 8.3 Experimental data for ^{43}Ca longitudinal relaxation time, linewidth at half-height, and chemical shift for aqueous calcium bromide solutions

Both transverse and longitudinal relaxation rates increase with increasing salt concentration, Fig 8.4. As may be expected, the transverse relaxation rate is greater than the longitudinal relaxation rate.

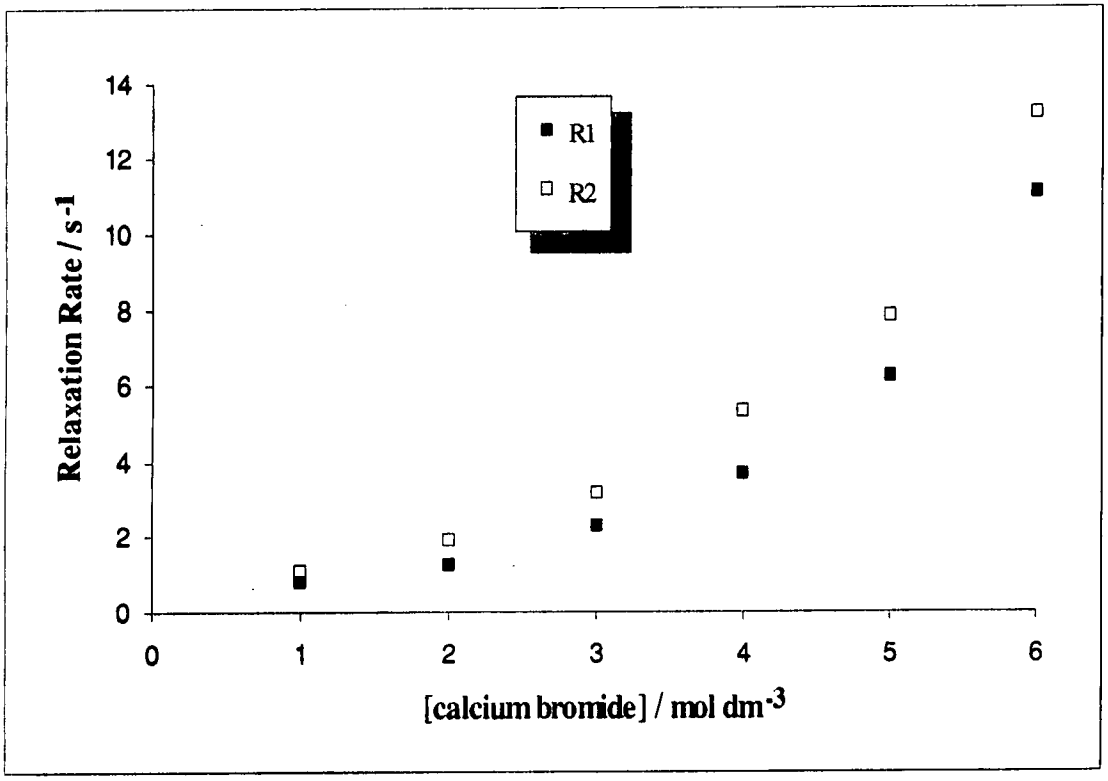

Fig 8.4 The variation of ^{43}Ca longitudinal and transverse relaxation rates as a function of calcium bromide concentration for aqueous calcium bromide solutions.

The linewidth at half-height and, thus the transverse relaxation rate, of the calcium-43 signal is observed to increase with increasing calcium bromide concentration. At low concentrations of calcium bromide, a narrow signal was observed. In fact, up to a salt concentration of 3 mol dm^{-3}, the linewidth at half-height was equal to 1 Hz or less. However, with increasing salt concentration, a large increase in the line width was seen.

Only at high concentrations of calcium bromide is a chemical shift difference from that of the reference observed for calcium-43. Like calcium chloride, no variation in chemical shift for calcium-43 is observed for calcium bromide solutions up to a concentration of 3 mol dm^{-3}, Fig 8.5

For concentrations greater than 3 mol dm^{-3} , the calcium-43 signal is observed to shift towards a higher frequency with increasing salt concentration. A large increase is observed with increasing salt concentration.

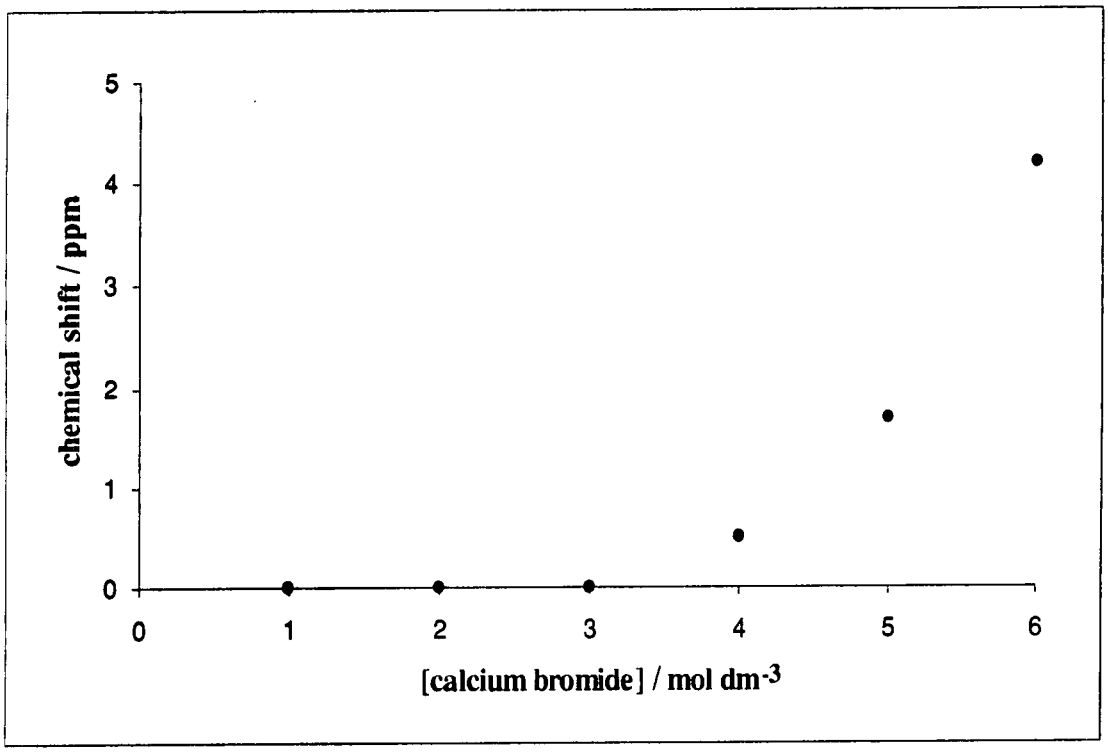

Fig 8.5 The dependence of ^{43}Ca chemical shift on calcium bromide concentration. The reference is 1.0 mol dm^{-3} calcium chloride solution. A positive sign indicates a high-frequency shift. No bulk susceptibility corrections were carried out

8.2.3) Calcium Iodide

The results for calcium iodide of the effect of concentration on calcium-43 relaxation, linewidth and chemical shift in aqueous calcium iodide solutions are reported in table 8.4

Concentration	SF = 33.659 MHz		
/ mol dm^{-3}	T_1 / ms	$\Delta\nu_{1/2}$ / Hz	δ / ppm
1	1310	0.3	0
2	880	0.6	0
3	490	1.0	0
4	300	1.6	0
5	170	2.7	+0.5
6	100	4.2	+2.0

Table 8.4 Experimental data for ^{43}Ca longitudinal relaxation time, linewidth at half-height, and chemical shift as a function of calcium iodide concentration for aqueous calcium iodide solutions.

An increase in both longitudinal and transverse relaxation rates is observed with increasing concentration as would be expected, Fig 8.6. With increasing salt concentration the difference between the two relaxation rates also increases. At the highest salt concentration, the inequality of the transverse and longitudinal relaxation rates suggests that the system is in the non-extreme narrowing region. However, even at this concentration, both relaxation processes are observed to be single exponential.

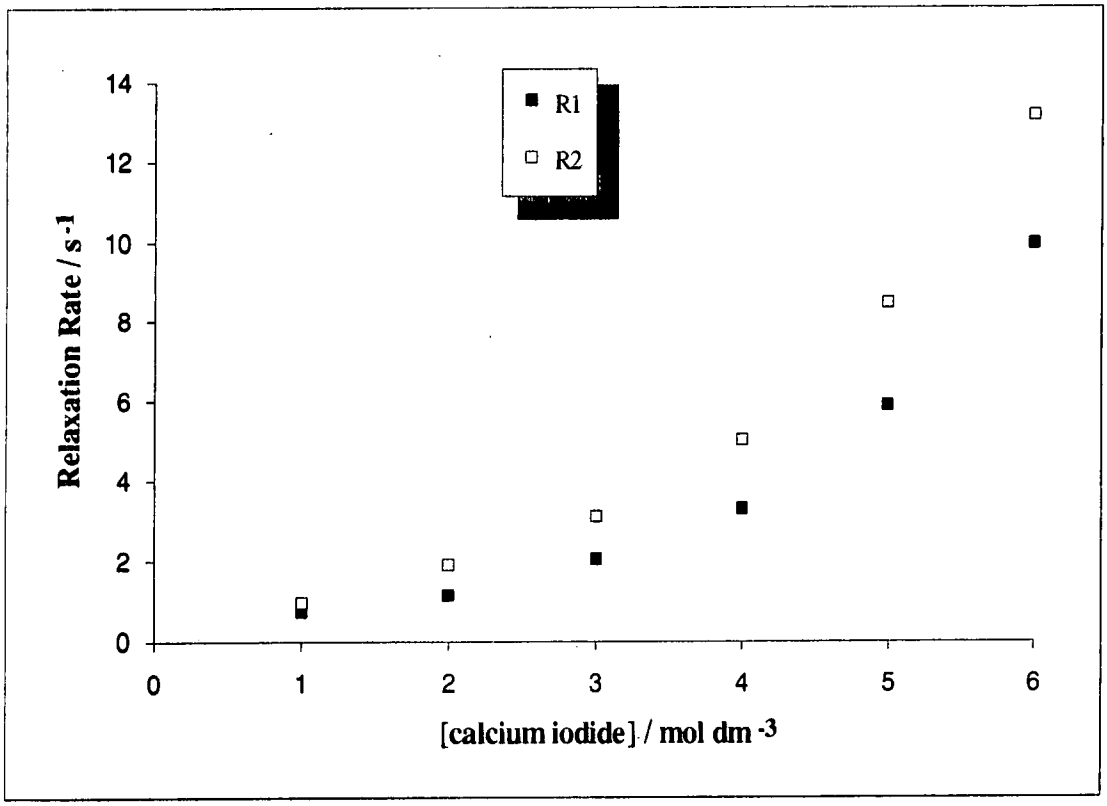

Fig 8.6 The dependence of ^{43}Ca longitudinal and transverse relaxation rates on calcium iodide concentration.

At low concentrations of calcium iodide, the calcium-43 signal is observed to be quite narrow. Up to calcium iodide concentrations of 2 mol dm^{-3}, the calcium-43 signal is observed to be less than 1 Hz in width. Thus the relaxation of calcium-43 is expected to be slow for these concentrations, as is observed. For 1 mol dm^{-3} calcium iodide solution, the relaxation time of calcium-43 is measured to be greater than 1 s.

The chemical shift (from that of the reference) for calcium-43 in calcium iodide solutions is observed to be small. For a concentration of 6 mol dm^{-3}, only a 2 ppm shift towards high frequency was observed. Up to and including a concentration of 4 mol dm^{-3}, calcium-43 chemical shifts could not be detected, Fig 8.7. However, for

concentrations greater than 4 mol dm^{-3} a chemical shift towards high frequency was observed.

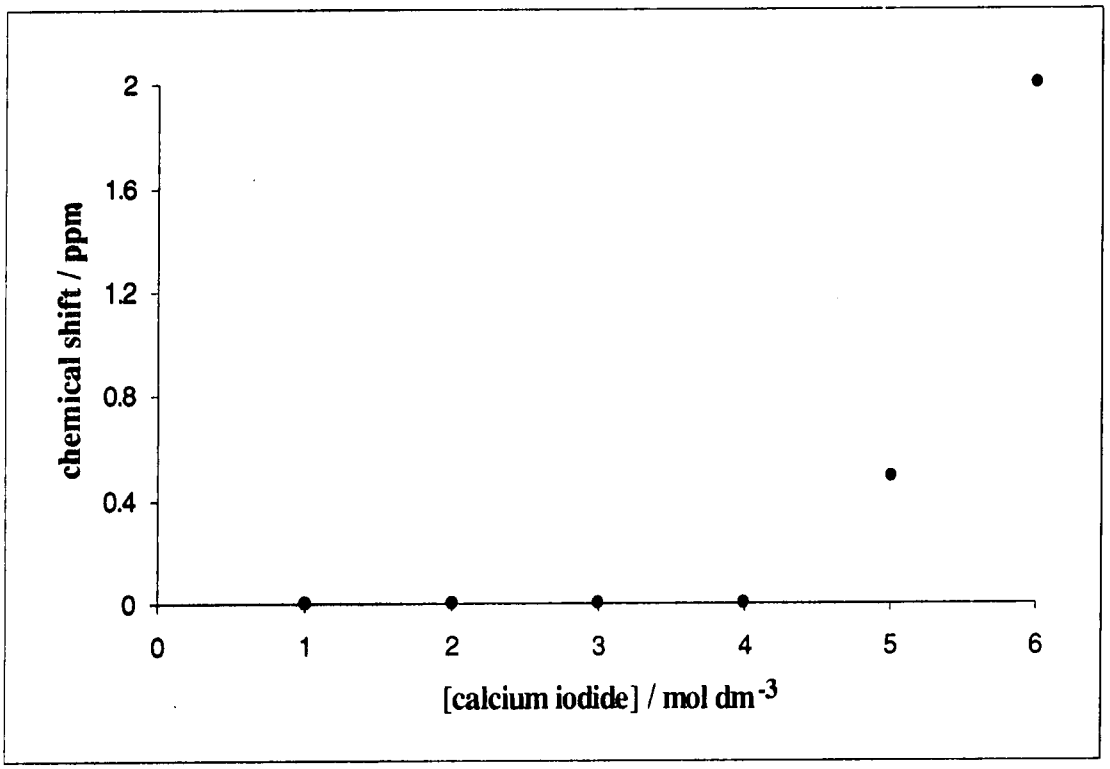

Fig 8.7 The dependence of ^{43}Ca chemical shift on calcium iodide concentration. The reference is 1.0 mol dm^{-3} calcium chloride solution. A positive sign indicates a high-frequency shift. No bulk susceptibility corrections were carried out.

8.2.4) Calcium Nitrate

The results of calcium nitrate concentration effect on calcium-43 relaxation, linewidth and chemical shift in aqueous calcium nitrate solutions are reported in table 8.5.

Concentration	SF = 33.659 MHz		
/ mol dm^{-3}	T_1 / ms	$\Delta\nu_{1/2}$ / Hz	δ / ppm
0.5	615	0.6	-1.6
1	398	1.1	-2.7
2	230	2.0	-4.2
3	158	2.9	-5.3
4	113	3.9	-6.4
5	85	4.9	-6.8

Table 8.5 Experimental data for ^{43}Ca longitudinal relaxation time, linewidth at half-height, and chemical shift for aqueous calcium nitrate solutions

With increasing calcium nitrate concentration, both the longitudinal and transverse relaxation rates of calcium-43 are observed to increase, Fig 8.8. However, the increase in both relaxation rates is observed to be linear for the concentration range studied. Again, a bigger difference between the two relaxation rates is observed with increasing salt concentration. For each concentration, both the transverse and longitudinal relaxation rates are observed to be single exponential to a very high degree.

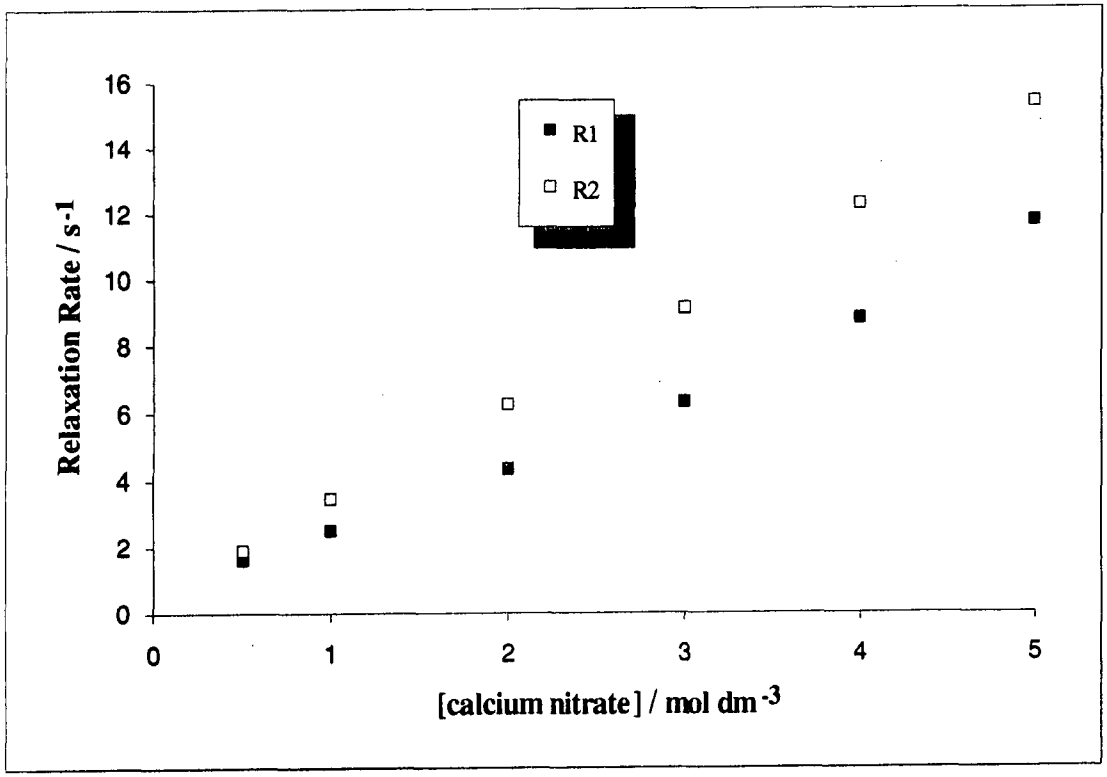

Fig 8.8 The variation of ^{43}Ca longitudinal and transverse relaxation rates as a function of calcium nitrate concentration for aqueous calcium nitrate solutions.

A low-frequency chemical shift for calcium-43 is observed in calcium nitrate solutions, Fig 8.9. The magnitude of the effect is observed to increase with increasing salt concentration *i.e.* as the salt concentration increases, the chemical shift towards lower frequency increases. The chemical shift is observed to increase up to a salt concentration of 4 mol dm^{-3} and then seems as though it levels off to a constant value for any further increase in calcium nitrate concentration.

Even at low concentrations of calcium nitrate, a considerable calcium-43 chemical shift from that of the reference was observed.

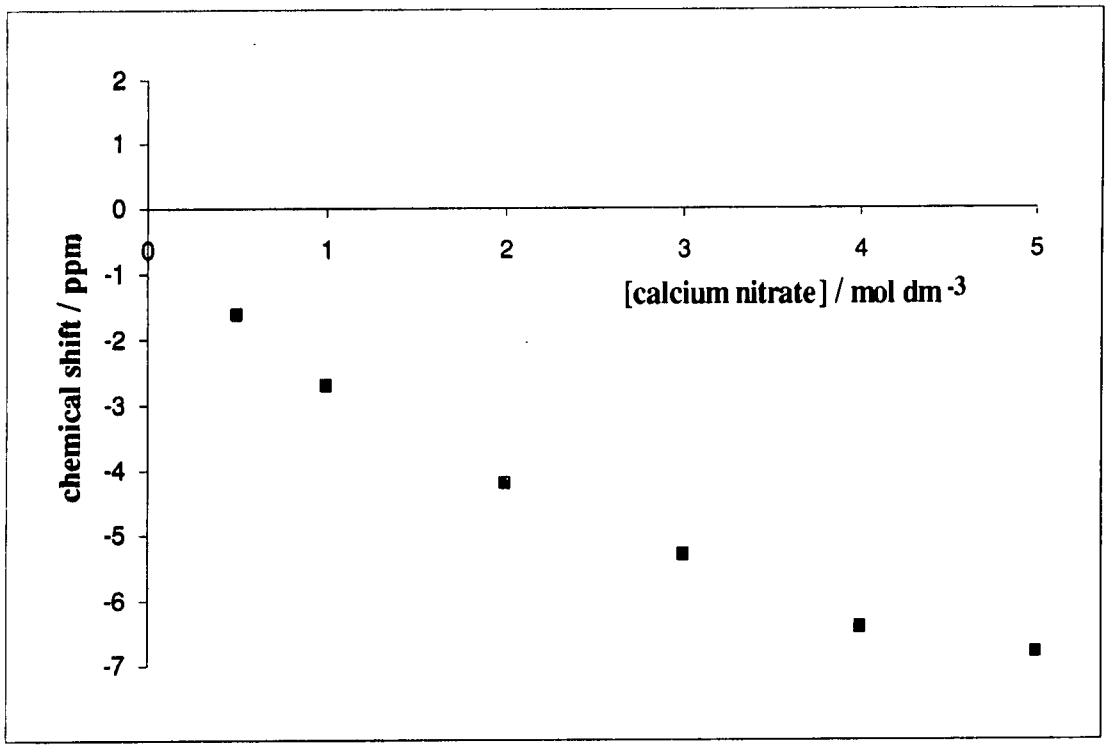

Fig 8.9 The dependence of ^{43}Ca chemical shift on calcium nitrate concentration for aqueous calcium nitrate solutions. The reference is 1.0 mol dm^{-3} calcium chloride solution. A negative sign indicates a low-frequency shift. No bulk susceptibility corrections were carried out.

8.2.5) Calcium Acetate

The effects of the acetate ion on calcium-43 relaxation, linewidth at half-height and the chemical shift are reported in table 8.6

[acetate] / mol dm^{-3}	[Ca^{2+}] / mol dm^{-3}	SF = 33.659 MHz		
		T_1 / ms	$\Delta\nu_{1/2}$ / Hz	δ / ppm
0.1	1	650	0.7	+0.1
0.5	1	450	1.0	+0.6
1	1	270	1.6	+1.2
1.5	1	190	2.2	+1.7
2	1	140	2.9	+2.4
3	1	90	4.4	+3.6
4	1	60	6.5	+4.5

Table 8.6 Experimental data for ^{43}Ca longitudinal relaxation time, linewidth at half-height, and chemical shift for 1.0 mol dm^{-3} calcium chloride + sodium acetate solutions.

The relaxation of calcium-43 in calcium acetate solutions is strongly dependent on the acetate ion concentration. With increasing acetate concentration, both the transverse and longitudinal relaxation rates are seen to increase, Fig 8.10. Even at low concentrations of acetate ion a significant change in calcium-43 relaxation is observed. For example, the presence of 0.1 mol dm^{-3} acetate ion in a 1 mol dm^{-3}

calcium chloride solution causes a significant change in the relaxation of calcium-43 compared to a 1 mol dm^{-3} calcium chloride solution with no added acetate.

For acetate ion concentrations greater than 4 mol dm^{-3}, broad calcium-43 signals were observed with fast relaxation. For an acetate ion concentration of 4 mol dm^{-3}, the linewidth at half-height of the calcium-43 signal was observed to be approximately 7 Hz, which is reasonably broad for a calcium ion signal. The longitudinal relaxation time was measured to be less than 0.1 s for the same sample.

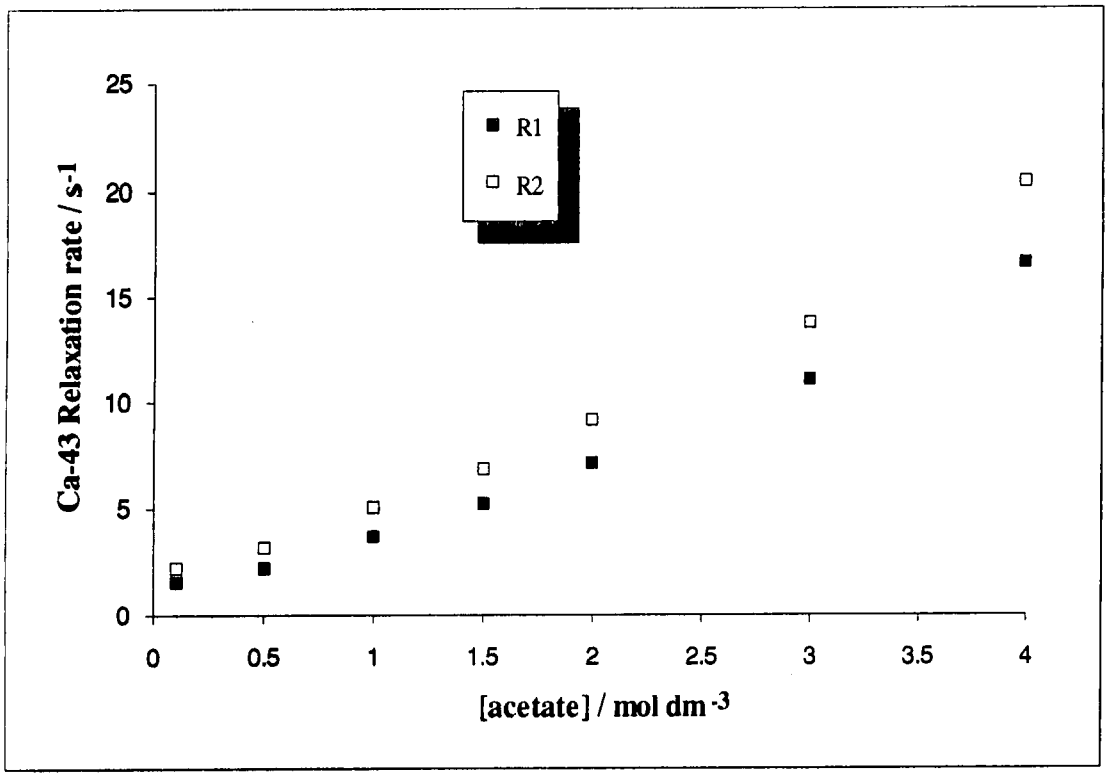

Fig 8.10 The dependence of ^{43}Ca longitudinal and transverse relaxation rates on acetate ion concentration for 1.0 mol dm^{-3} calcium chloride + sodium acetate solutions.

The chemical shift of calcium-43 is observed to be strongly dependent on the acetate ion concentration. With increasing acetate ion concentration, the calcium-43 signal is

seen to shift towards high-frequency, Fig 8.11. Even at low concentrations of acetate ion, a significant chemical shift effect can be observed.

For the acetate ion concentration range studied, the calcium-43 chemical shift seems to show a linear increase with increasing concentration, as can be seen from Fig 8.11.

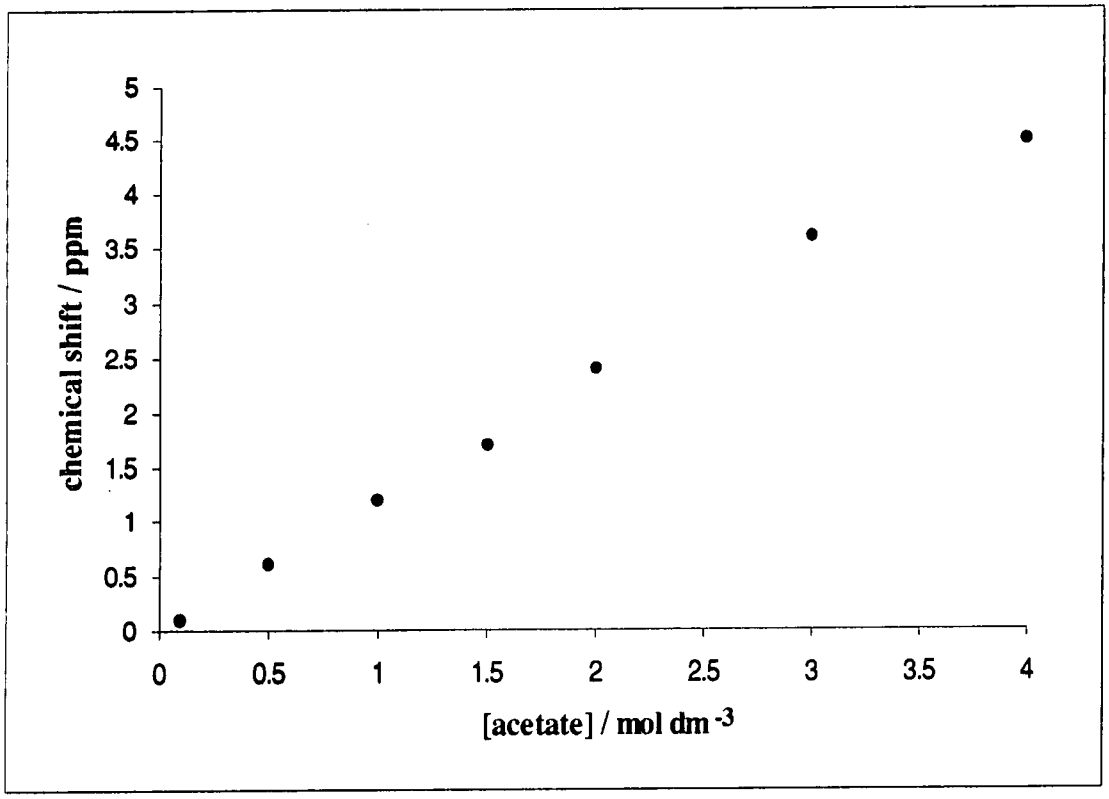

Fig 8.11 The variation of ^{43}Ca chemical shift as a function of acetate ion concentration for aqueous 1.0 mol dm^{-3} calcium chloride + sodium acetate solutions. The reference is 1.0 mol dm^{-3} calcium chloride solution. A positive sign indicates a high-frequency shift. No bulk susceptibility corrections were carried out.

8.2.6) Calcium Ascorbate

The effect of adding ascorbate ion to a 1 mol dm^{-3} calcium chloride solution on calcium-43 relaxation, linewidth at half-height and the chemical shift are reported in table 8.7

[ascorbate] / mol dm^{-3}	[Ca^{2+}] / mol dm^{-3}	SF = 33.659 MHz		
		T_1 / ms	$\Delta\nu_{1/2}$ / Hz	δ / ppm
0.1	1	500	0.9	0
0.5	1	230	2.6	0
1	1	80	6.0	-0.1
1.5	1	50	9.2	-0.2
2	1	33	13.1	-0.25
2.5	1	25	17.0	-0.3
3	1	19	22.0	-0.33

Table 8.7 Experimental data for ^{43}Ca longitudinal relaxation time, linewidth at half-height, and chemical shift for aqueous 1.0 mol dm^{-3} calcium chloride + sodium ascorbate solutions

The relaxation of calcium-43 shows a strong dependence on the ascorbate ion. With increasing ascorbate concentration, the relaxation rate is observed to increase, Fig 8.12. In fact, in the presence of ascorbate ion, relaxation of calcium-43 for a 1 mol dm^{-3} calcium chloride solution is observed to be extremely fast compared to the absence of ascorbate. At the highest ascorbate ion concentration studied (3 mol

dm^{-3}), the longitudinal relaxation time of calcium-43 is measured to be approximately 0.02 s.

The difference between transverse and longitudinal relaxation rates is seen to increase with increasing ascorbate ion concentration. At the highest ascorbate concentration, the difference between the two relaxation rates is approximately 20 s^{-1}.

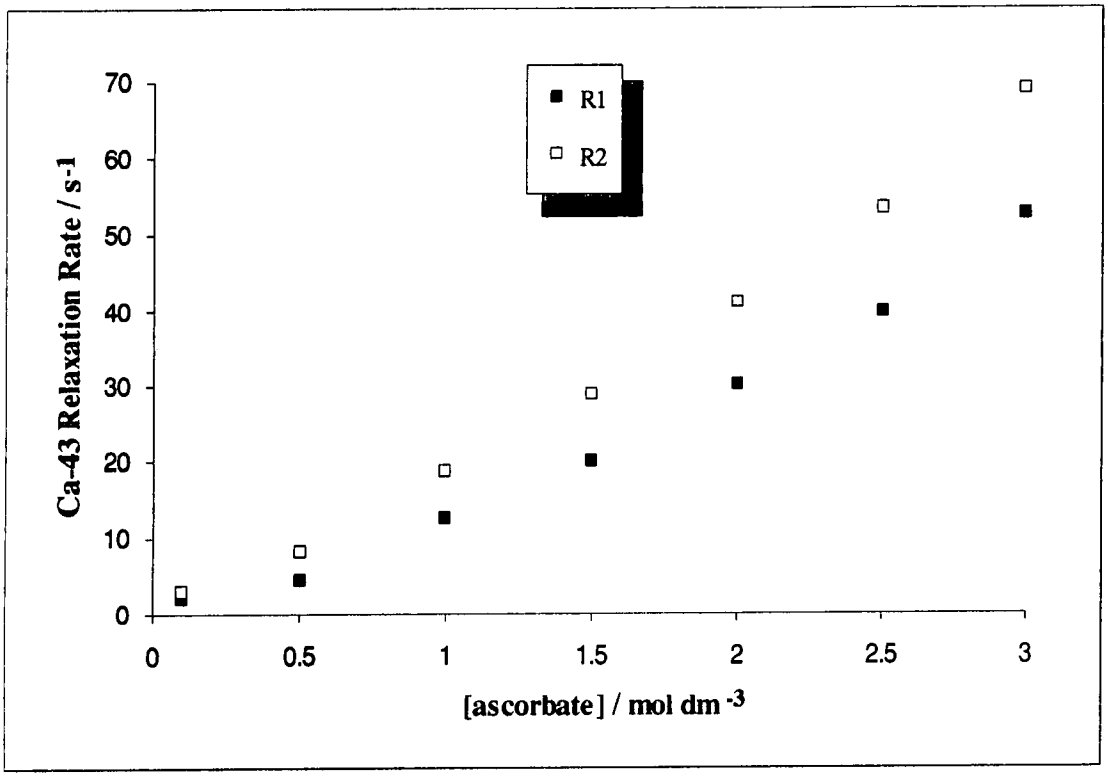

Fig 8.12 The dependence of ^{43}Ca longitudinal and transverse relaxation rates on ascorbate ion concentration for aqueous 1.0 mol dm^{-3} calcium chloride + sodium ascorbate solutions.

In the presence of ascorbate ion, calcium-43 signals are observed to be much broader than in the absence of ascorbate. For example, the linewidth of calcium-43 in 1 mol dm^{-3} calcium chloride solution is less than 1 Hz. However in the presence of 3 mol

dm^{-3} ascorbate ion the linewidth at half-height of the same sample was measured to be 22 Hz.

Surprisingly, the ascorbate ion has very little effect on the chemical shift of calcium-43. Very small changes in shift were observed for the ascorbate ion concentration range studied. In fact, up to an ascorbate ion concentration of 0.5 mol dm^{-3}, no significant shift was observed, Fig 8.13. However, above this concentration very small but low frequency shifts were observable. Even for the highest ascorbate ion concentration (3 mol dm^{-3}), a chemical shift of only 0.33 ppm was observed, which is exceptionally small for calcium-43.

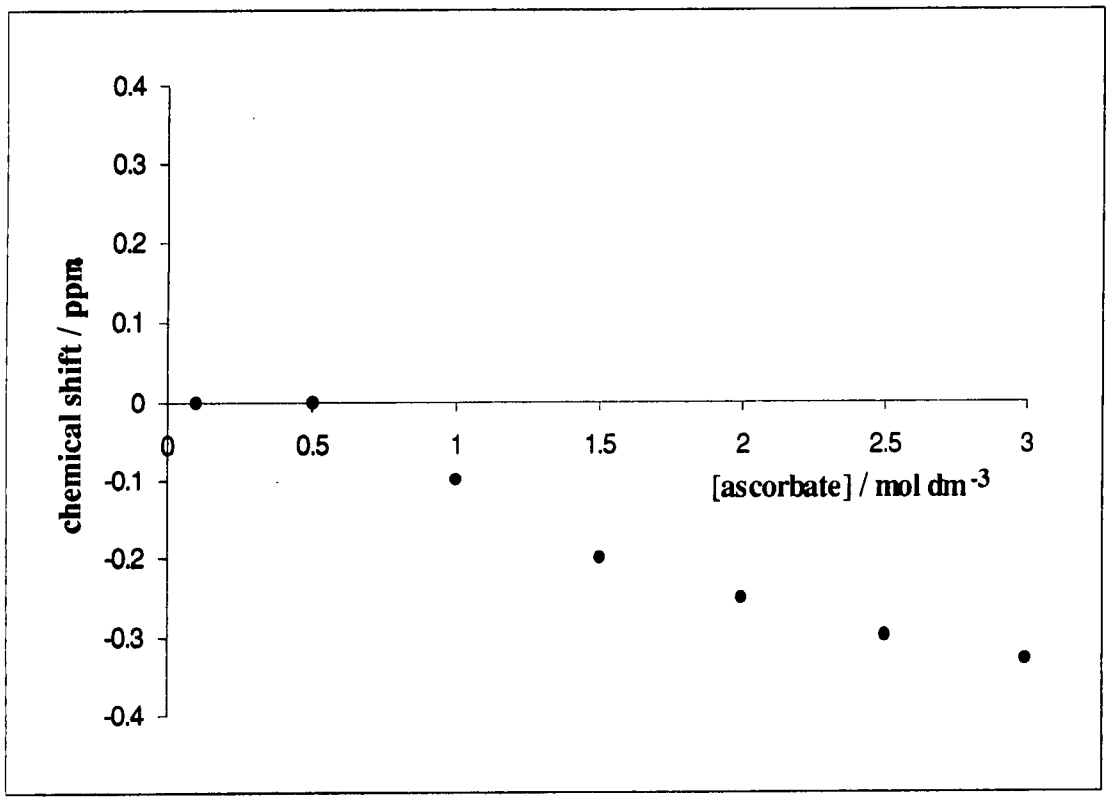

Fig 8.13 The dependence of ^{43}Ca chemical shift on ascorbate ion concentration for 1.0 mol dm^{-3} calcium chloride + sodium ascorbate solutions. The reference is 1.0 mol dm^{-3} calcium chloride solution. A negative sign indicates a low-frequency shift. No bulk susceptibility corrections were carried out.

8.2.7) Calcium - Sucrose

The effect of adding sucrose to a 1 mol dm^{-3} calcium chloride solution on calcium-43 relaxation, linewidth at half-height and the chemical shift are given in table 8.8

[sucrose] / mol dm^{-3}	$[Ca^{2+}]$ / mol dm^{-3}	SF = 33.659 MHz		
		T_1 / ms	$\Delta\nu_{1/2}$ / Hz	δ / ppm
0.1	1	500	1.1	-1.2
0.5	1	220	2.8	-3.4
1	1	82	6.5	-5.0
1.5	1	45	10.0	-5.7
2	1	30	15.5	-6.0

Table 8.8 Experimental data for ^{43}Ca longitudinal relaxation time, linewidth at half-height, and chemical shift for aqueous 1.0 mol dm^{-3} calcium chloride + sucrose solutions

The addition of sucrose to 1 mol dm^{-3} calcium chloride solution increases the relaxation rate of calcium-43. Both the transverse and longitudinal relaxation rates are observed to increase with increasing sucrose concentration.

The difference between the two relaxation rates also increases with increasing sucrose concentration. Even at the lowest sucrose concentration studied, a significant difference between the two relaxation rates can be observed, Fig 8.14.

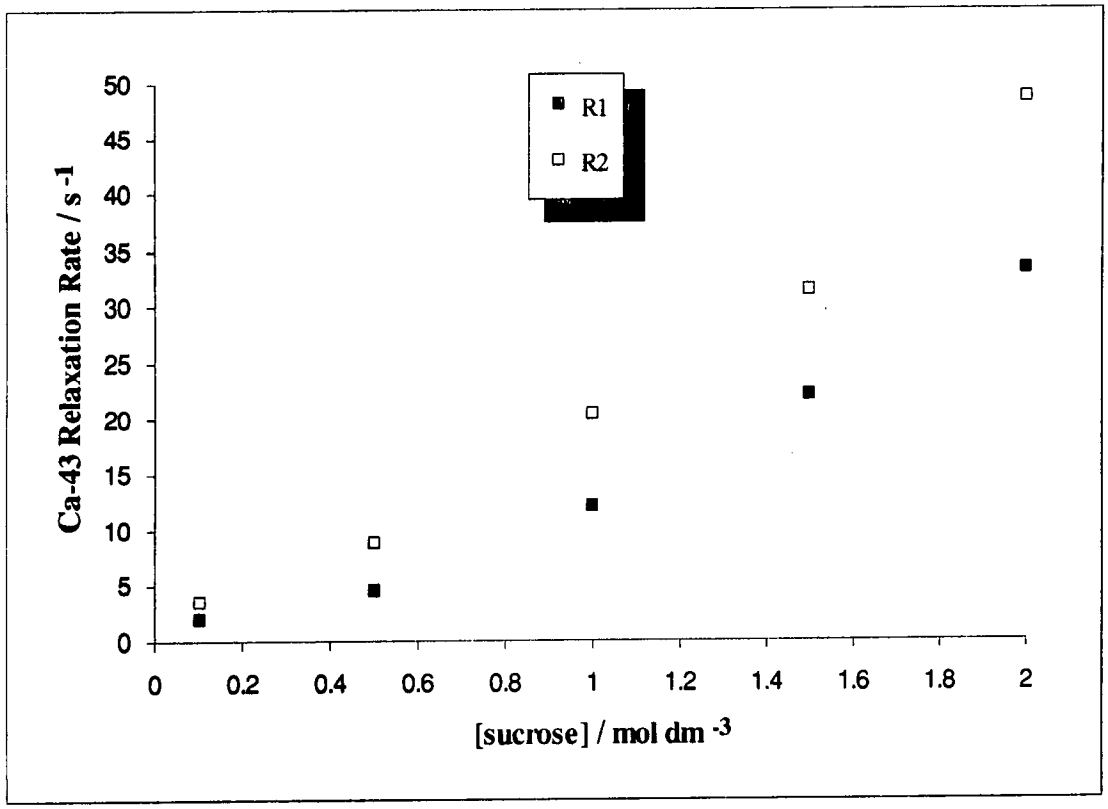

Fig 8.14 The dependence of ^{43}Ca longitudinal and transverse relaxation rates on sucrose concentration for 1.0 mol dm^{-3} calcium chloride + sucrose solutions.

For a sucrose concentration of 2 mol dm^{-3}, the line width at half-height was measured to be approximately 16 Hz. Any further increase in sucrose concentration excessively broadened the calcium-43 signal that it became very difficult to actually observe.

The chemical shift of calcium-43 from that of the reference is observed to be strongly dependent on sucrose concentration. With increasing sucrose concentration, a shift towards low-frequency was observed, Fig 8.15. Even at low concentrations of sucrose, a significant chemical shift was seen. The chemical shift towards low-frequency increases up to a sucrose concentration of 2 mol dm^{-3}. For more concentrated sucrose solutions, the chemical shift seems be independent of sucrose concentration as can be observed from Fig 8.15.

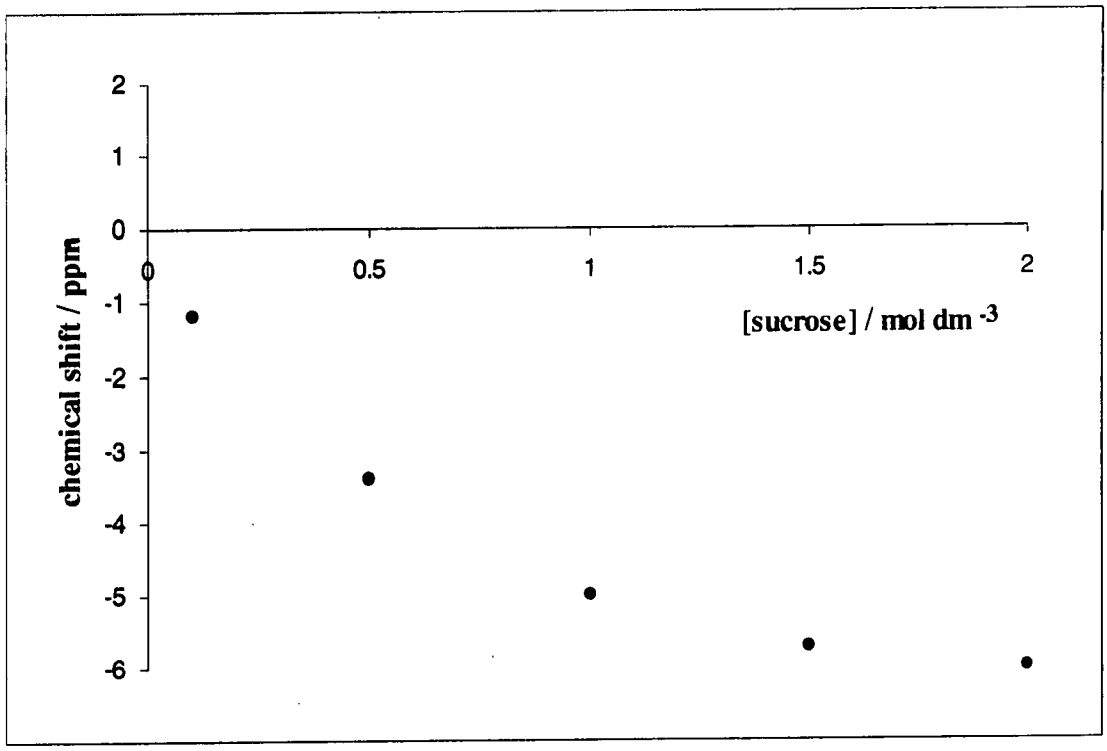

Fig 8.15 The dependence of ^{43}Ca chemical shift on sucrose concentration for 1.0 mol dm^{-3} calcium chloride + sucrose solutions. The reference is 1.0 mol dm^{-3} calcium chloride solution. A negative sign indicates a low-frequency shift. No bulk susceptibility corrections were carried out.

8.2.8) Calcium - Lysozyme Complex

The addition of lysozyme to a constant concentration of calcium chloride results in a strong complex being formed between the calcium ion and lysozyme. Lysozyme is reported[5] to have several calcium-binding carboxylate sites, the important one being in the active site of the protein. The active site of lysozyme contains two carboxylate residues which are reported to be approximately 0.81 nm apart. The presence of calcium causes the two carboxylate residues to move towards each other, as shown in Fig 8.16. In fact, the two carboxylate residues are expected to bind the calcium ion so strongly that the addition of calcium may alter the conformation of the active site.

For such a strong complex and at natural abundance of calcium-43, the observation of a signal from calcium-43 bound to lysozyme was very difficult. The slow motion of the lysozyme molecule and the strong interaction of the calcium ion with lysozyme causes the calcium ion signal to be so excessively broadened that it is impossible to actually observe the signal at natural abundance. Such problems were encountered when studying the effect of lysozyme on calcium ion even at the highest available frequency.

a) absence of calcium ion b) presence of calcium ion

Fig 8.16 The position of the two carboxylate residues in the active site of lysozyme in the absence and presence of calcium ion.

8.3) Discussion

8.3.1) Calcium-43 Relaxation

Fast relaxation for calcium-43 was observed for all calcium systems studied. Relaxation times of the order of ms were measured. Quadrupolar relaxation is expected to be the dominant relaxation mechanism in all cases.

Overall, there are two approaches to the quadrupole relaxation of ions *i.e.* two models which can give rise to electric field gradients, thus causing quadrupolar relaxation. One is the *electrostatic* approach of Hertz[6] and the other is the *electronic distortion* approach of Deverell.[7] In the electrostatic approach of Hertz, the field gradients at the relaxing ion are considered to be created from nearby ions, due to ion-ion interactions, and solvent molecules, modulated by their rotational and translational motion. The ionic contribution to electric field gradients is assumed to depend on the concentration of the ions causing relaxation and the distance of closest approach between two ions, as well as the mobility of the ions. The electric field gradients fluctuate with time as a result of molecular motion and cause relaxation. To simplify the analysis, the surrounding ions and solvent molecules are usually treated as point charges (monopoles) and dipoles, respectively. The approach of Hertz[6] is electrostatic in origin as it involves fluctuations of the electric environment of the relaxing ion with time.

In Deverell's model[7] the field gradients are assumed to arise from short range interactions due to collisions between the relaxing ion with solvent molecules, or with other solute particles. The collisions cause a distortion in the spherical symmetry of the electron cloud in the outer orbitals of the ion, thus creating electric field gradients. The approach taken by Deverell is not electrostatic, in that the field gradient is propagated by a transient rearrangement of the observed ion-electron distribution.

Out of the two models, the electrostatic approach of Hertz, is thought to be the most consistent[8,9] with observations. Reasonably good agreement has been obtained

between experimental data and the theoretical data using the Hertz model for alkali metal ions and halide ions.[10] An attempt to compare the experimental and theoretical data for alkaline earth metal ions was made by Forsén *et al.*[8] The observed relaxation rates were found to give good agreement with the predictions from the Hertz electrostatic model and therefore provided good support for this model.

8.3.2) Concentration Dependence of Relaxation

Various studies of calcium-43[4,11,12] in aqueous solutions have been carried out. However, owing to the difficulty in observing a signal at low concentrations, due to low natural abundance, and low receptivity of calcium-43, as well as the instrumental broadening in linewidth studies, there is still some uncertainty in obtaining the exact value of relaxation rates, R_1 & R_2, at infinite dilution. Forsén and Lindman[2] have obtained $R_1 = 0.75\ s^{-1}$ for 0.2 mol dm^{-3} calcium chloride solution and assumed this to be close to the infinite dilution value, R_1^o. In this study, R_1^o has been found to be 0.86 s^{-1} for calcium chloride solutions by extrapolation using Fig 8.3 (see section 8.2.1). Good agreement is observed between the R_1^o value obtained by Forsén and Lindman[2] and the value calculated in this study.

Little information has been found on the anion concentration dependence of calcium-43 relaxation in the literature. A possible reason, given by Hertz,[13-15] is that the anion effect on relaxation is very difficult to account for theoretically. For strongly solvated ions, where the calcium ion tends to have octahedral symmetry, the partial or total symmetry quenching of the field gradient, due to the solvent molecules, affects the surrounding anions in a way that is difficult to estimate. For weakly solvated solutions where a direct cation-anion interaction occurs it is important to consider quenching of those electric field gradients produced by the surrounding anions which are treated as point charges in the Hertz model. Hertz[13] has found that the previously ignored ion-ion correlations greatly affected the relaxation of ions by substantially

quenching the ionic contribution to electric field gradients through an ion cloud type of effect. This type of quenching is also difficult to estimate.

Unfortunately, for calcium solutions, no anion sequence has been found in the literature relating to the concentration and anion dependence of calcium-43 relaxation. Therefore, it was considered worthwhile to initially carry out a relaxation analysis for simple calcium salts.

In Figs 8.17 and 8.18 the anion dependence on calcium-43 relaxation for aqueous calcium systems analysed in this study is shown. The sequence for the longitudinal relaxation rate is observed to be

ascorbate > acetate > nitrate > halides

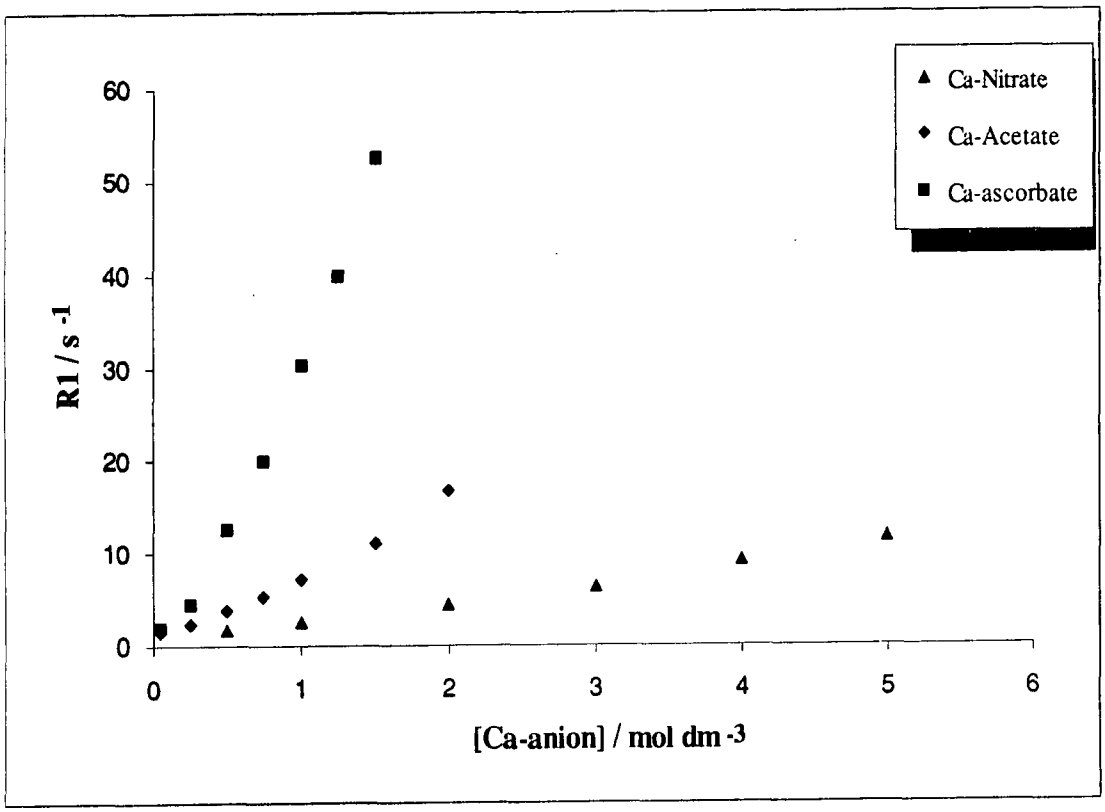

Fig 8.17 The dependence of the ^{43}Ca longitudinal relaxation rate for aqueous calcium systems on concentration.

The longitudinal relaxation rates of calcium-43 for the calcium halide salts studied are of very similar magnitude. Comparing the relaxation of the halide salts only, as in Fig 8.18, reveals that relaxation of calcium-43 is in fact, not equal at high concentrations of salt. The relaxation rate is observed to follow the sequence

$$Cl^- > Br^- > I^-$$

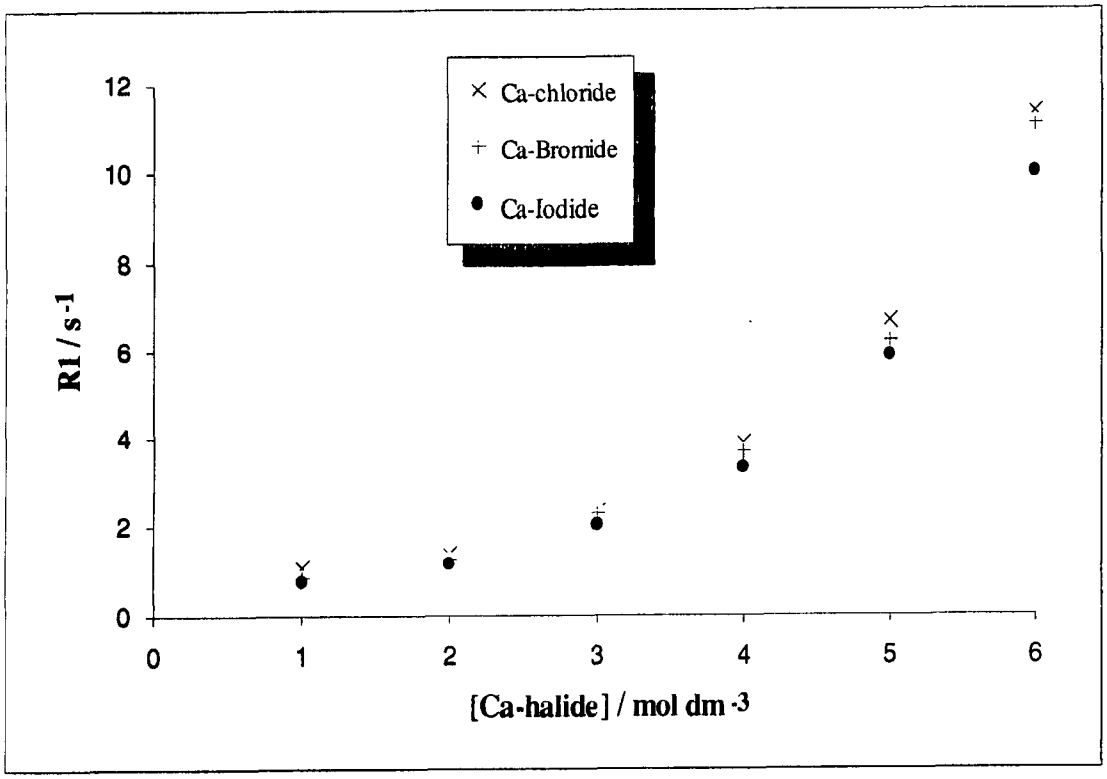

Fig 8.18 The dependence of the ^{43}Ca longitudinal relaxation rate on calcium halide concentration for aqueous calcium halide solutions.

Calcium-43 is observed to complex to sucrose. With increasing sucrose concentration, the relaxation rate of calcium-43 is observed to increase, Fig 8.19.

At low concentrations of sucrose and ascorbate ion, the relaxation rate of calcium-43 for both calcium-sucrose and calcium ascorbate solutions is observed to be equal,

within experimental error, as can be seen from Fig 8.19. However, at high concentrations of sucrose and ascorbate ion, calcium-43 relaxation for calcium-sucrose solutions is observed to be greater than that for calcium ascorbate solutions.

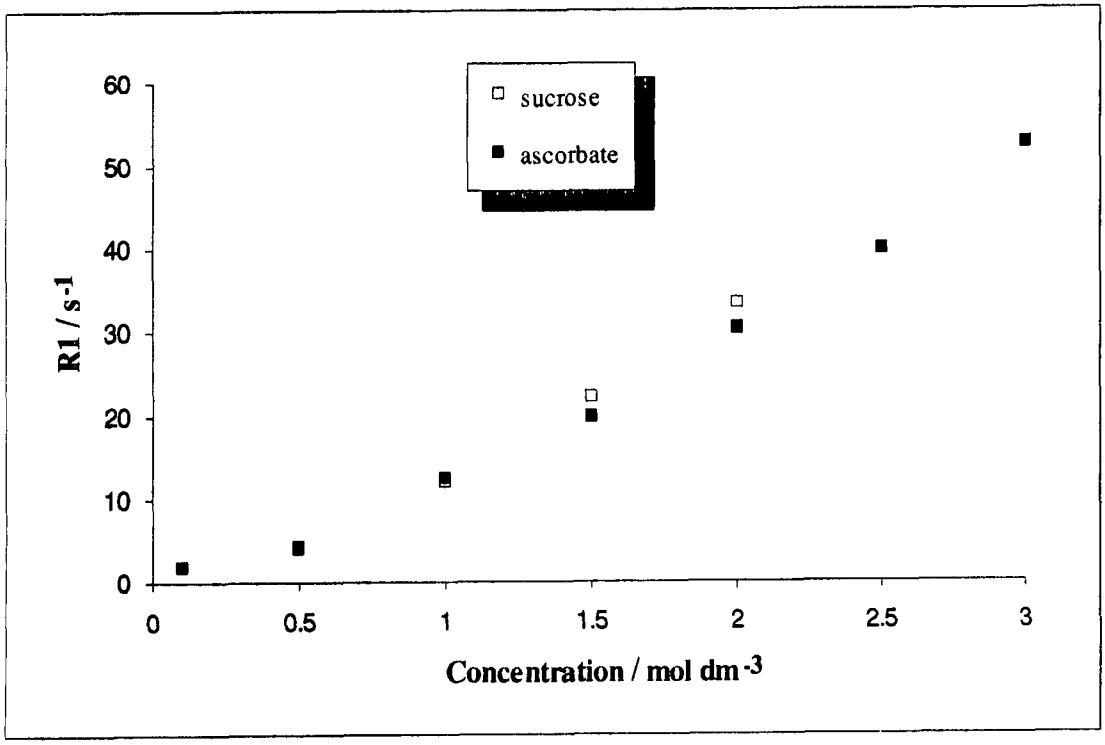

Fig 8.19 The dependence of ^{43}Ca longitudinal relaxation rates on sucrose and ascorbate ion concentrations for 1.0 mol dm^{-3} calcium chloride + sucrose/sodium ascorbate solutions

Thus, the overall anion sequence for calcium-43 relaxation is found to be

sucrose > ascorbate > acetate > nitrate > chloride > bromide > iodide

where sucrose gives the fastest relaxation rate and iodide gives the slowest relaxation rate.

The variation of calcium-43 linewidth for the different anions is similar to that of the longitudinal relaxation rate, see Figs 8.17 and 8.18. The sequence for increasing linewidth is observed to be

iodide ≈ bromide < chloride < nitrate < acetate < ascorbate < sucrose

The linewidth of the sucrose complex is in good agreement with the ascorbate salt, especially at low concentrations of sucrose and ascorbate. However, at high concentrations, the linewidth of the sucrose complex is observed to be greater than that of the ascorbate complex, Fig 8.20.

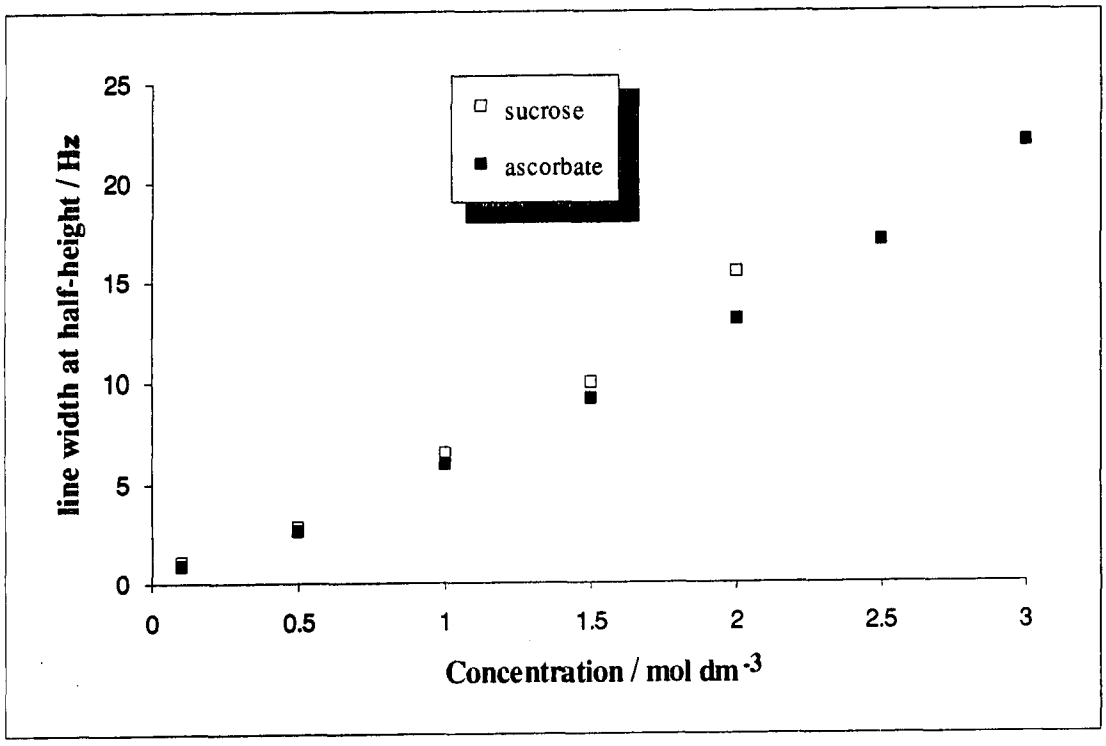

Fig 8.20 The dependence of ^{43}Ca linewidth at half-height on sucrose and ascorbate ion concentrations for 1.0 mol dm^{-3} calcium chloride + sucrose/sodium ascorbate solutions.

Sucrose is assumed to bind the calcium ion via the oxygen atoms of the hydroxyl groups. The relaxation rate of calcium-43 is observed to be extremely fast in the presence of sucrose. The ascorbate ion is expected to bind calcium via the oxygen atoms of the two carboxylate groups, which are assumed to form a strong bond with the calcium ion. Since both the oxygen atoms of each carboxylate group are likely to be involved in the binding process, then the octahedral symmetry of the calcium ion, expected for most aqueous calcium systems, will be distorted to some extent. The co-ordination number of the calcium ion in such a case is expected to be seven or eight. The relaxation of the calcium ion is then expected to be very fast as is observed experimentally.

The calcium-acetate complex also has two carboxylate groups bound to calcium. Again, both oxygens of each carboxylate group can bind the calcium ion, thus distorting the octahedral symmetry of the calcium ion and increasing the relaxation rate.

The effect of sucrose as well as ascorbate and acetate ions on calcium-43 relaxation can be quantified using equation 8.1 (see section 8.2). Assuming that the asymmetry parameter, η, for calcium-43 is small such that the term $\eta^2/3$ is negligible, then equation 8.1 may be simplified to

$$\frac{1}{T_1} = \frac{3\pi^2(2I+3)}{10I^2(2I-1)}\chi^2\tau_c \qquad \text{eqn 8.2}$$

The quadrupolar coupling constant, χ, for calcium-43 is calculated by Andersson *et al.*[16] to be 0.8 ± 0.1 MHz in the presence of prophospholipase A_2 ($PPLA_2$). Assuming that this value is reasonable and independent of the complexing anion, then it is possible to calculate the correlation time, τ_c, knowing T_1 from experimental data.

In table 8.9, the τ_c values calculated for calcium-43 in calcium-sucrose, calcium-ascorbate, calcium-acetate and free calcium chloride solutions are given.

Anion	R_1 / s	τ_c / s
Free $CaCl_2$	1.1	4.2×10^{-12}
Sucrose	33.3	12.9×10^{-11}
Ascorbate	30.3	11.7×10^{-11}
Acetate	7.1	2.7×10^{-11}

Table 8.9 τ_c values calculated for calcium-43 for in free $CaCl_2$, 1.0 mol dm^{-3} calcium chloride + 2 mol dm^{-3} sucrose, 1.0 mol dm^{-3} calcium chloride + 2 mol dm^{-3} ascorbate ion, and 1.0 mol dm^{-3} calcium chloride + 2 mol dm^{-3} acetate ion systems. Concentration of free calcium chloride corresponds to 1.0 mol dm^{-3} calcium chloride.

The addition of sucrose, ascorbate and acetate to 1.0 mol dm^{-3} calcium chloride considerably increases the correlation time of calcium-43 compared to that of free 1.0 mol dm^{-3} calcium chloride solution. It is assumed that in the presence of sucrose, as well as ascorbate and acetate, a fraction of calcium ions bind to the sucrose (ascorbate and acetate) molecules for a significant lifetime that the motion of these bound calcium ions is affected by the presence of sucrose. The large molecular size of sucrose is expected to reduce the motion of the bound calcium ions compared to that of free calcium ions resulting in an increase in the correlation time. However, since only one calcium-43 signal is observed for calcium-sucrose, calcium ascorbate and calcium acetate systems, then it is reasonable to assume that fast exchange of Ca^{2+} takes place between bound and free calcium states for these systems.

The slower relaxation rate of calcium-43 in the presence of the acetate ion compared to the ascorbate ion may indicate a weaker interaction between calcium and acetate compared to that between calcium and ascorbate. On the other hand, the slow relaxation rate observed for calcium acetate could be due to the small size of the acetate ion. For complexes with a significant lifetime, the interaction of the quadrupolar moment with the electric field gradient is modulated by the reorientation of the complex. For small-size complexes, the reorientation motion is expected to be fast resulting in a slow relaxation rate.

The relaxation of the calcium nitrate system is experimentally found to be faster than that for calcium halide systems. With increasing salt concentration, the relaxation is observed to increase in all cases. At low concentrations of salt, the symmetry of the calcium ion in aqueous calcium nitrate and calcium halide solutions is expected to be predominantly octahedral.[17] Thus, at low concentrations of salt, the asymmetry parameter, η, is expected to be low in both cases resulting in a small electric field gradient at the nucleus and, hence slow relaxation, as is observed experimentally. However with increasing salt concentration, deviations from octahedral symmetry may occur, thus increasing the relaxation rate. The distortion due to the nitrate ion is expected to be greater than that produced by the chloride ion. Like the carboxylate groups of the ascorbate and acetate ions, the nitrate ion also contains more than one oxygen atom which may bind to the calcium ion causing considerable distortion of the calcium ion symmetry. The high distortion effect of the nitrate ion compared to that of the chloride ion is thought to be responsible for the faster relaxation of the nitrate salt.

With increasing halide ion size, the relaxation rate of calcium-43 is observed to decrease as can be seen from Fig 8.18. For ionic solutions of the type involved in this study, the relaxation is also expected to be strongly dependent on the viscosity of the solution, as is reported by Simeral and Maciel[4] when studying simple salts of

magnesium . With increasing concentration, the viscosity of the solution is expected to increase, thus increasing the relaxation rate. The decrease in relaxation rate with increasing halide ion size is probably due to the effect of viscosity on relaxation. In the literature[18,19], the viscosity of the calcium-halide salts is reported to decrease with increasing halide ion size. The chloride ion is reported to show the biggest increase in viscosity with increasing halide concentration, followed by bromide and then by iodide.

8.3.3) Chemical Shift

Calcium-43 is known to undergo large chemical shift changes with the medium. Considerable changes in chemical shift occur upon calcium complexation. The reported chemical shift range for calcium-43 is in the region of 40 ppm.[12]

The concentration dependence on chemical shift has been studied in detail by Richards and co-workers.[20,21] These authors have concluded that the concentration dependence of the chemical shift is essentially determined by cation-anion interactions. Thus, the concentration dependence of the chemical shift is expected to follow the probability of cation-anion contact. The shift is thought to be caused as a result of the overlap of the cation-anion outer orbitals. Contributions from overlap of cation-solvent, namely water in this study, and cation-cation orbitals to chemical shift are also considered to be of importance. In fact, the measured chemical shift is considered to be the average of all possibilities in the molecular ensemble.

With increasing salt concentration, an increased chemical shift was observed for all calcium salts studied, as is shown in Fig 8.21. The magnitude and direction of the shift is dependent on the nature of the counterion *i.e.* on the overlap of the outer orbitals.

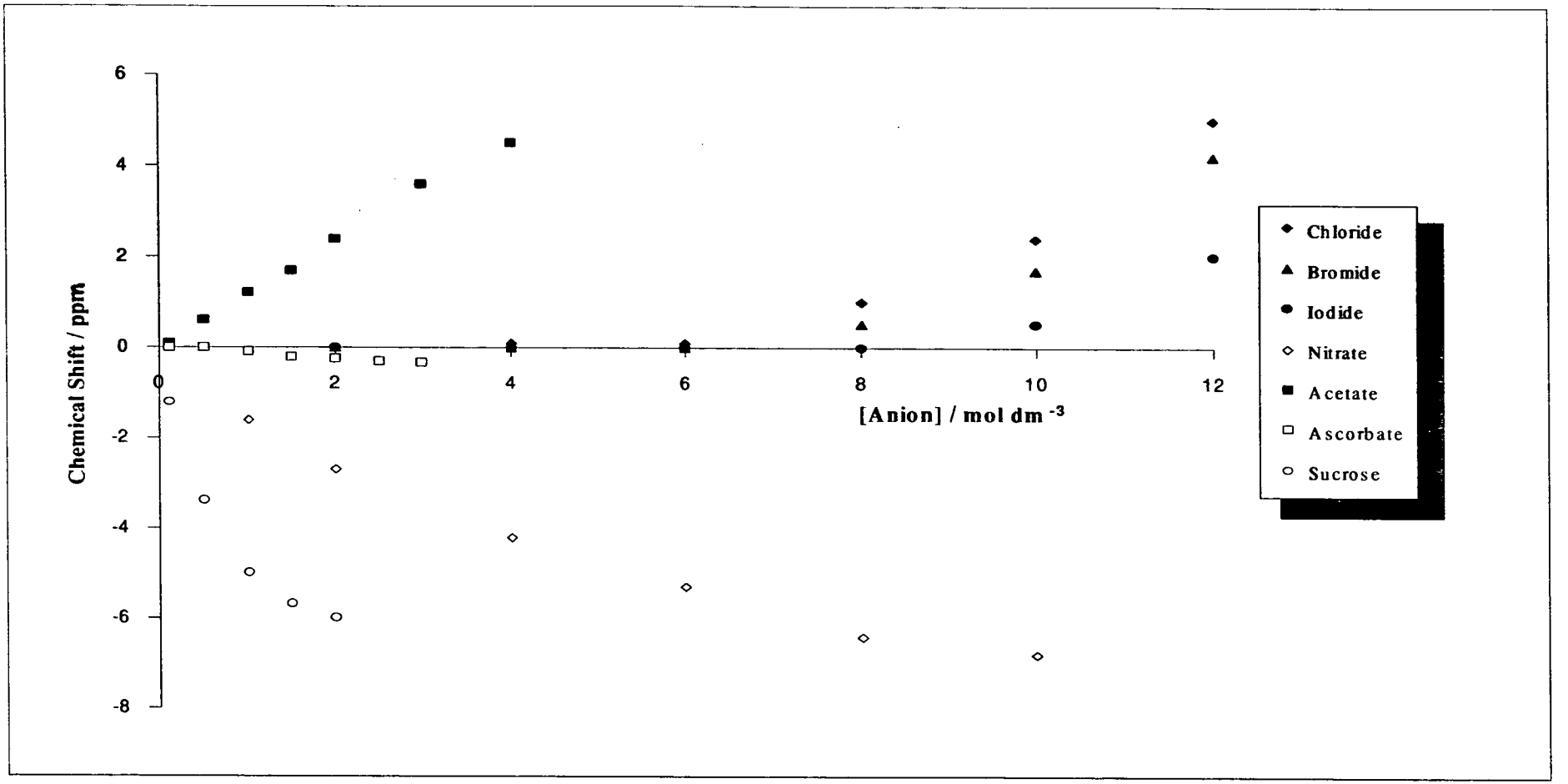

Fig 8.21 The dependence of the ^{43}Ca chemical shift on anion concentration for various aqueous calcium systems. The reference is 1.0 mol dm^{-3} calcium chloride solution. A positive sign indicates a high-frequency shift. No bulk susceptibility corrections were carried out.

High-frequency shifts were observed for the halide ions, whereas the oxyanions, except for the acetate ion, were observed to produce low-frequency shifts. As discussed by Lutz *et. al.*,[11,12] the direction of the chemical shift is strongly dependent on the overlap of the outer orbitals between the cation and the anion. The halide ions produce a significant overlap, thus the electrons are more spread out and hence less shielding of the calcium ion occurs, resulting in a high-frequency shift. On the other hand, the oxyanions have a smaller overlap with the calcium ion, resulting in greater shielding and low-frequency shifts.

Unfortunately, Lutz *et al.* only considered the diamagnetic shielding term to explain the effect of anion on calcium-43 chemical shift. Importantly, the authors failed to consider the paramagnetic term which, according to Ramsey,[24,25] has an important contribution to shielding. The overall shielding is reported by Ramsey to be the sum of the two terms

$$\sigma = \sigma_d + \sigma_p$$

where σ_d and σ_p are the diamagnetic and paramagnetic shielding terms, respectively.

Paramagnetic shielding is caused by the mixing of ground and excited electronic states by the electron orbital angular momentum. It becomes very large for an asymmetric distribution of *p* and *d* electrons close to the nucleus and for low-lying excited states with the correct symmetry for mixing to occur. However, the paramagnetic shielding term vanishes for electrons in *s*-orbitals which have zero angular momentum. The effect of the *p* and *d* electrons is to produce magnetic fields at the nucleus which when averaged over the molecular motion give a high-frequency shift, *i.e.* de-shielding, by reinforcing the applied field.

This type of paramagnetic shielding phenomena is usually referred to as *temperature-independent paramagnetism* (TIP).

The magnitude of the paramagnetic shielding term is reported[24-26] to be directly proportional to $\langle r^{-3} \rangle / \Delta E$ (where $\langle r^{-3} \rangle$ is the average inverse cube distance of the *p* or *d*

electron from the nucleus and ΔE is the average excitation energy). The values of $\langle r^{-3} \rangle$ for valence-shell orbitals of a particular atom are dependent on the effective charge on the atom. The increase in electron density at the atom leads to an orbital expansion (nephelauxetic effect) of the valence-shell electrons resulting in a decrease of $\langle r^{-3} \rangle$.

With increasing electronegativity the orbital expansion effect is assumed to decrease. As a result, the halides are expected to produce the smallest orbital expansion, and thus an increase in $\langle r^{-3} \rangle$. In such a case, the paramagnetic shielding term is expected to increase, resulting in de-shielding or a high-frequency shift, as is observed in Fig 8.21.

For the halide group, the orbital expansion is found to follow the sequence I > Br > Cl. The chloride ion has the smallest orbital expansion, and thus a high $\langle r^{-3} \rangle$ term. Therefore, one would expect significant paramagnetic shifts to high frequency for chloride, as are observed experimentally, Fig 8.21.

At low concentrations of halide ion, the chemical shift is observed to be constant and independent of concentration, *i.e.* the chemical shift of the calcium ion is essentially equal to that of the reference solution. At low concentrations of halide ion and high water content, the formation of solvent-shared or solvent-separated ion pairs between the calcium ion and the halide ion are highly likely. On the other hand, the possibility of forming a contact ion-pair between the cation and the anion at very low concentrations of the anion is, in fact, very unlikely. Since the chemical shift of the calcium ion is very sensitive to the interaction with the nearest neighbours, then the formation of solvent-shared or solvent-separated ion pairs is not expected to affect the chemical shift significantly. Experimentally it is observed that for the chloride and bromide ions, no calcium-43 chemical shift is seen up to a halide ion concentration of 6 mol dm^{-3}. For the iodide ion, the concentration range for which no chemical shift is observed is extended to 8 mol dm^{-3}, Fig 8.21.

At high concentrations of calcium-halide system, calcium-43 chemical shifts towards high frequency are observed. The formation of contact ion-pairs at high concentration

is highly possible, thus resulting in a significant chemical shift change. Comparison of the calcium-43 chemical shifts between the different halide ions reveals that the chemical shift decreases with increasing halide ion size. For the halide systems studied, the chloride ion is observed to produce the biggest chemical shift. The decrease in chemical shift with increasing halide ion size suggests that the calcium salts of the halides tend to be more hydrated for the larger halide ions. Thus, the probability of forming a contact ion-pair between a calcium ion and halide ion decreases with increasing halide ion size. The high electronegativity of the chloride ion makes it more likely to replace the water molecules, coordinated to the calcium ion, to form a contact ion-pair, compared to the bromide and iodide ions.

For the oxyanions, except for the ascorbate ion, a significant chemical shift is observed even at low concentrations of the anion. These calcium-oxyanion salts are probably less hydrated than the halide ions, and consequently they are much more likely to form contact ion-pairs compared to the halides.

Surprisingly, the chemical shift of calcium ascorbate solutions was experimentally observed to be very small. The fast relaxation and large linewidths of calcium ascorbate solutions indicated a strong interaction between the calcium ion and the ascorbate ion. Therefore, with increasing ascorbate concentration a large chemical shift towards low frequency was expected for calcium-43. However, as can be deduced from Fig 8.21, only small chemical shifts towards low frequency were observed for the ascorbate ion. For low concentrations of ascorbate ion, *i.e.* up to 0.5 mol dm^{-3}, the calcium-43 chemical shift was essentially equal to that of the reference. Even for higher concentrations of ascorbate ion, the chemical shift was seen to be very small. For an ascorbate concentration of 3 mol dm^{-3}, a shift of 0.33 ppm towards low frequency was observed. Similarly to calcium halide solutions of low halide ion concentration, the small chemical shifts observed for calcium-43 in calcium ascorbate solutions could be due to the formation of solvent-shared or solvent-separated ion pairs. The absence of contact ion-pairs for aqueous calcium ascorbate solutions

indicates that these solutions may have an extensive hydration sheath around the calcium ion..

For the acetate ion, high-frequency chemical shifts were observed, opposite to expectation. For the acetate ion concentration range studied, the chemical shift is seen to increase almost linearly with increasing concentration, Fig 8.21. Even at very low concentrations of acetate ion, a shift towards high-frequency can be observed, indicating a strong interaction between the calcium ion and the acetate ion with formation of contact ion-pairs. The high frequency shift for the acetate ion indicates a large overlap between the outer orbitals of the acetate and calcium ions, resulting in less shielding of the calcium ion.

Both the nitrate ion and sucrose produce low-frequency shifts. From the chemical shift data of calcium nitrate, it can be assumed that calcium and nitrate ions form contact ion-pairs even at low concentrations.

The large chemical shift observed for the sucrose shows that calcium complexes to sucrose and probably forms complexes with other carbohydrates too. The shift towards low frequency suggests that the oxygen atoms of sucrose (probably hydroxyl groups) are responsible for calcium ion binding. It can be assumed that contact ion-pairs between the calcium ion and sucrose are formed even at low concentrations of sucrose.

8.3.4) pH Effect

The pH analysis of calcium chloride and calcium nitrate revealed that for these salts the pH of the solution has very little effect on calcium-43 relaxation, chemical shift and the linewidth at half-height, table 8.10 and Fig 8.22.

However, for calcium acetate and calcium ascorbate complexes, calcium-43 relaxation, chemical shift, and the linewidth at half-height were observed to show a strong dependence on pH, table 8.11. The variation of the linewidth with pH showed three distinct stages. Below a pH of 3, the linewidth was observed to be independent of pH. Between pH range of 3 to 8, a sharp increase in the linewidth was observed. Finally, above pH of 8 the linewidth seemed to be constant and independent of pH, Fig 8.22.

The linewidth of the ascorbate complex showed a bigger pH dispersion than the acetate complex. This can be attributed to the large size of the ascorbate ion compared to the acetate ion.

The variation of calcium-43 longitudinal relaxation time, T_1, with pH also showed three regions, Fig 8.23. Up to pH of 4, the relaxation time decreases, but very slowly, with increasing pH. The relaxation was observed to be equal for both calcium acetate and calcium ascorbate solutions for this initial part of variation. Between pH of 4 and 7, the longitudinal relaxation time was observed to decrease sharply with increasing pH. Above pH of 7 the longitudinal relaxation time was observed to be constant and independent of pH.

concentration / mol dm^{-3}	pH	calcium chloride			calcium nitrate		
		T_1 / ms	$\Delta\nu_{1/2}$ / Hz	δ / ppm	T_1 / ms	$\Delta\nu_{1/2}$ / Hz	δ / ppm
5.0	0.5	154	3.4	+2.4	85	4.7	-6.8
5.0	1.0	153	3.4	+2.4	82	4.8	-6.8
5.0	2.0	155	3.3	+2.3	86	4.8	-6.8
5.0	3.0	154	3.3	+2.2	82	4.9	-6.8
5.0	4.0	154	3.3	+2.3	82	5.0	-6.7
5.0	4.5	154	3.5	+2.5	84	4.9	-6.8
5.0	5.0	156	3.6	+2.2	85	5.0	-6.8
5.0	5.5	155	3.4	+2.3	85	4.8	-6.7
5.0	6.0	154	3.5	+2.4	86	4.8	-6.7
5.0	6.5	152	3.4	+2.3	85	4.9	-6.7
5.0	7.0	152	3.4	+2.4	86	4.9	-6.8
5.0	7.5	153	3.3	+2.2	85	4.7	-6.8
5.0	8.0	151	3.4	+2.3	83	4.9	-6.7
5.0	9.0	154	3.3	+2.3	85	4.8	-6.7
5.0	10	151	3.2	+2.4	87	4.8	-6.7

Table 8.10 Experimental data for the dependence of ^{43}Ca longitudinal relaxation time, linewidth at half-height, and chemical shift on pH for aqueous calcium chloride and calcium nitrate solutions.

$[Ca^{2+}]$ / mol dm^{-3}	pH	Calcium Acetate				Calcium Ascorbate			
		[acetate] / mol dm^{-3}	T_1 / ms	$\Delta\nu_{1/2}$ / Hz	δ / ppm	[ascorbate] / mol dm^{-3}	T_1 / ms	$\Delta\nu_{1/2}$ / Hz	δ / ppm
1	1.0	1	875	0.5	0	1	860	0.6	0
1	2.0	1	840	0.6	0	1	825	0.7	0
1	3.0	1	813	0.7	+0.1	1	800	0.8	0
1	4.0	1	741	0.9	+0.2	1	735	1.3	0
1	5.0	1	676	1.2	+0.2	1	623	2.4	0
1	5.5	1	535	1.5	+0.3	1	441	3.1	0
1	6.0	1	370	1.7	+0.4	1	241	3.9	0
1	6.5	1	282	1.8	+0.5	1	153	4.6	0
1	7.0	1	247	1.9	+0.7	1	100	5.3	0
1	7.5	1	235	1.95	+0.8	1	80	5.7	-0.1
1	8.0	1	230	1.95	+0.9	1	65	6.0	-0.1
1	9.0	1	223	2.0	+1.1	1	60	6.2	-0.1

Table 8.11 Experimental data for the dependence of ^{43}Ca longitudinal relaxation time, linewidth at half-height, and chemical shift on pH for aqueous 1.0 mol dm^{-3} calcium chloride + 1.0 mol dm^{-3} sodium acetate and 1.0 mol dm^{-3} calcium chloride + 1.0 mol dm^{-3} sodium ascorbate solutions.

Fig 8.22 The variation of ^{43}Ca linewidth at half-height as a function of pH for aqueous calcium systems. ● and ■ are experimental data points for 1.0 mol dm^{-3} calcium chloride + 1.0 mol dm^{-3} sodium acetate and 1.0 mol dm^{-3} calcium chloride + 1.0 mol dm^{-3} sodium ascorbate solutions, respectively. ◊ and Δ are experimental data points for 5.0 mol dm^{-3} calcium chloride and calcium nitrate solutions, respectively.

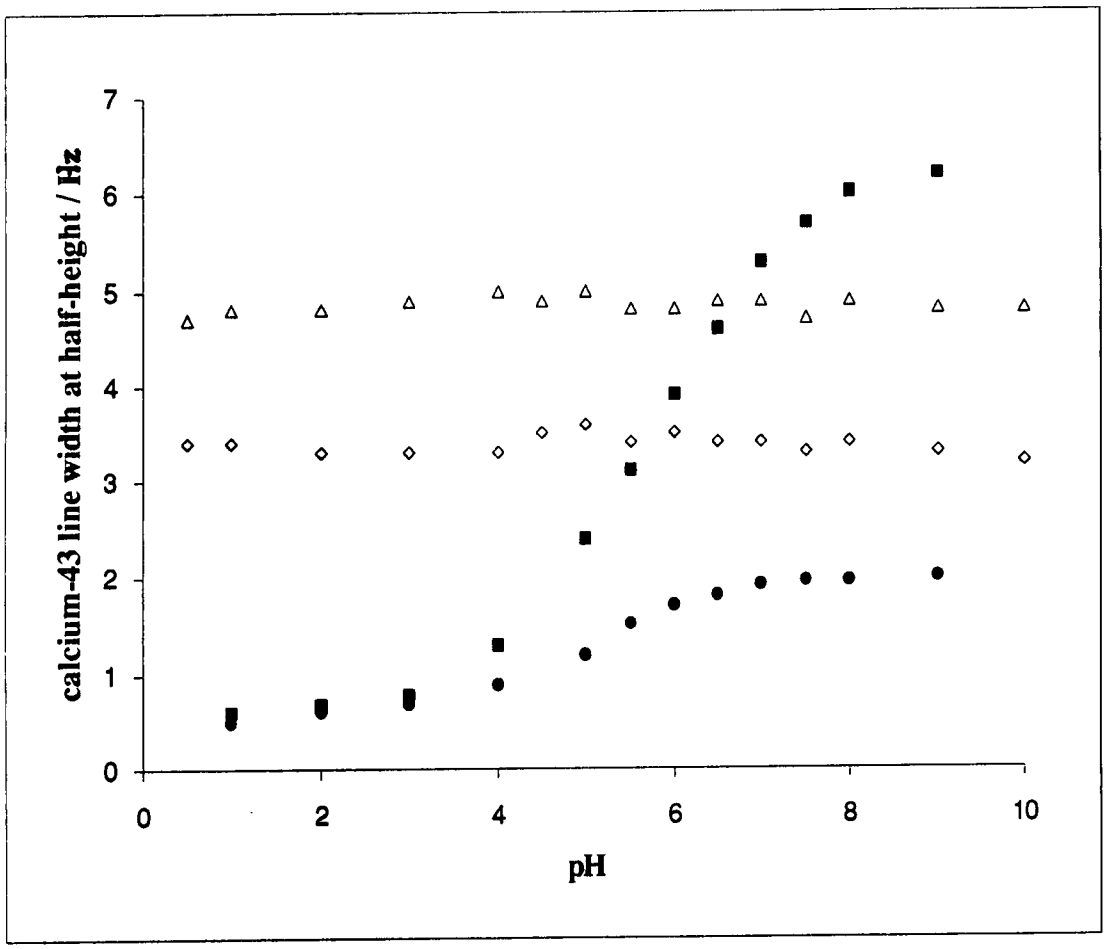

Fig 8.23 The dependence of the ^{43}Ca longitudinal relaxation time on pH for 1.0 mol dm^{-3} calcium chloride + 1.0 mol dm^{-3} sodium acetate and 1.0 mol dm^{-3} calcium chloride + 1.0 mol dm^{-3} sodium ascorbate solutions

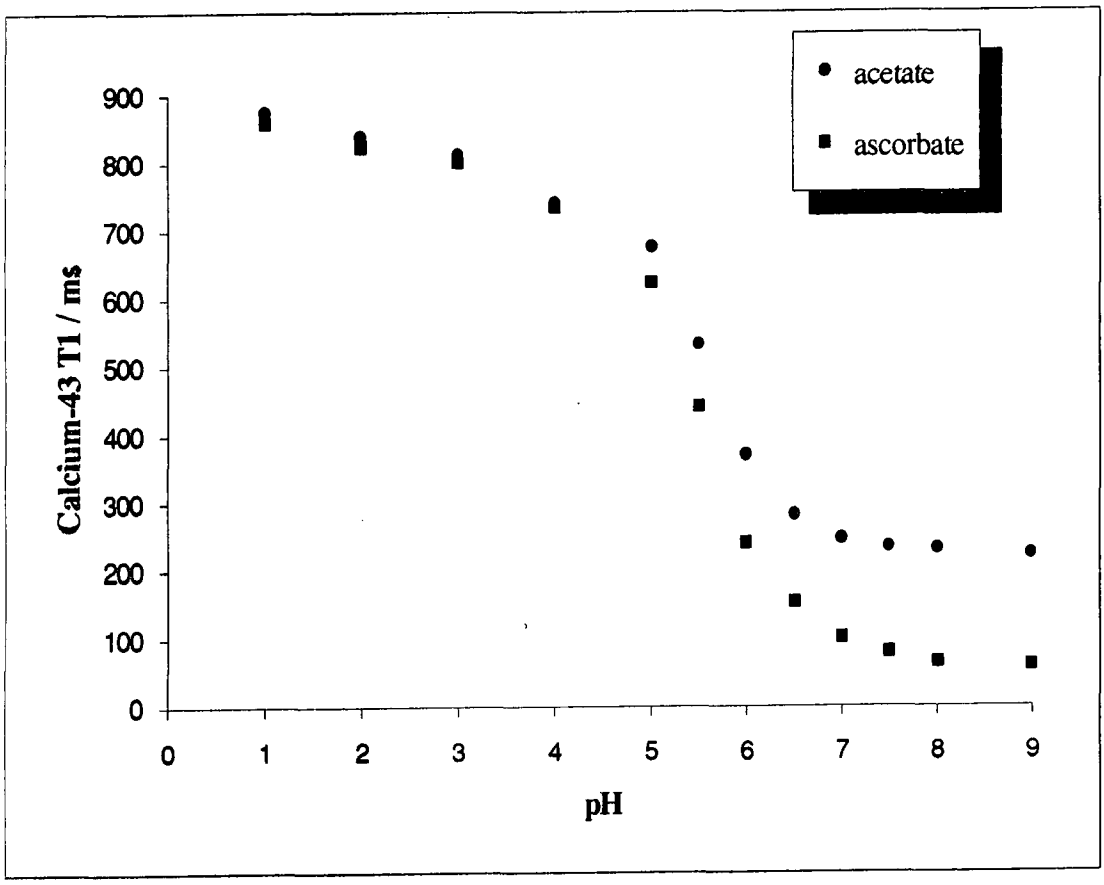

The variation of calcium-43 longitudinal relaxation time and linewidth at half-height with pH can be explained in terms of protonation of the carboxylate groups of the ascorbate and acetate ions. At low pH values, the carboxylate groups are expected to be extensively protonated, thus being incapable of binding the calcium ion. Therefore, the calcium ion behaves as a free ion with long relaxation times and narrow linewidths. However, as the pH increases, protonation of the carboxylate groups is expected to reduce. Hence, the ascorbate and acetate ions are able to complex/bind the

calcium ion, thus decreasing the longitudinal relaxation time and increasing the linewidth at half-height of calcium-43, as is observed experimentally.

The linewidth of calcium chloride and calcium nitrate salts is independent of pH because both the chloride and the nitrate ions are from strong acids that are expected to be strongly ionised with very little or no protonation.

Assuming that both acetic and ascorbic acids are weak acids and that only a single protonation step occurs for both, then the model suggested by Andersson *et al.*[16] (for a single protonation step) can be used to calculate the pK values for these acids. The suggested model is of the form

$$\Delta \nu = \frac{\Delta \nu_i}{1 + 10^{(pK_a - pH)}} + C \qquad \text{eqn 8.3}$$

where $\Delta\nu$ is the experimentally observed linewidth at a given pH, $\Delta\nu_i$ is the step in the linewidth (*i.e.* the difference between the high and low values of linewidth associated with the protonation step) and C is the contribution to the observed linewidth that is unaffected by pH (*i.e.* initial part of the curve).

The pK values calculated for both acetic and ascorbic acids are given in table 8.12 along with the literature values. Reasonably good agreement between the calculated pK value and that of the literature is obtained for acetic acid, within experimental error. However for ascorbic acid, the agreement between the calculated value and that of the literature is not very good. It is found in the literature that ascorbic acid has two pK values, $pK_1 = 4.1$ and $pK_2 = 11.8$, thus the assumption that protonation of ascorbic acid follows a single step is invalid and probably responsible for the discrepancy between the calculated pK value and that of the literature.

Acid	Calculated pK	Literature pK
Acetic	5.2	4.8 (reference 22)
Ascorbic	5.7	4.1 (reference 23)

Table 8.12 Comparison of the calculated and the literature values of pK for acetic and ascorbic acids

As was observed for calcium-43 chemical shift dependence on ascorbate ion concentration, a small chemical shift was seen for calcium ascorbate solutions as a function of pH. Up to a pH of 7, the calcium-43 chemical shift was observed to be equal to that of the reference. However, above pH of 7, a very small but low-frequency shift was observed, Fig 8.24. In contrast, the chemical shift for calcium acetate solutions showed a strong dependence on pH. Initially, no variation in chemical shift was observed for calcium acetate up to a pH of 3. However, above pH of 3, an increasing high-frequency chemical shift from that of the reference was observed with increasing pH, Fig 8.24.

The protonation of the acetate carboxylic groups in acidic conditions is thought to be responsible for the small chemical shift changes observed for the calcium acetate system up to a pH of 3. Above a pH of 3, deprotonation of carboxylic groups is expected to occur and as result acetate complexes to calcium. Therefore significant calcium-43 chemical shifts are observed with increasing pH, as may be expected.

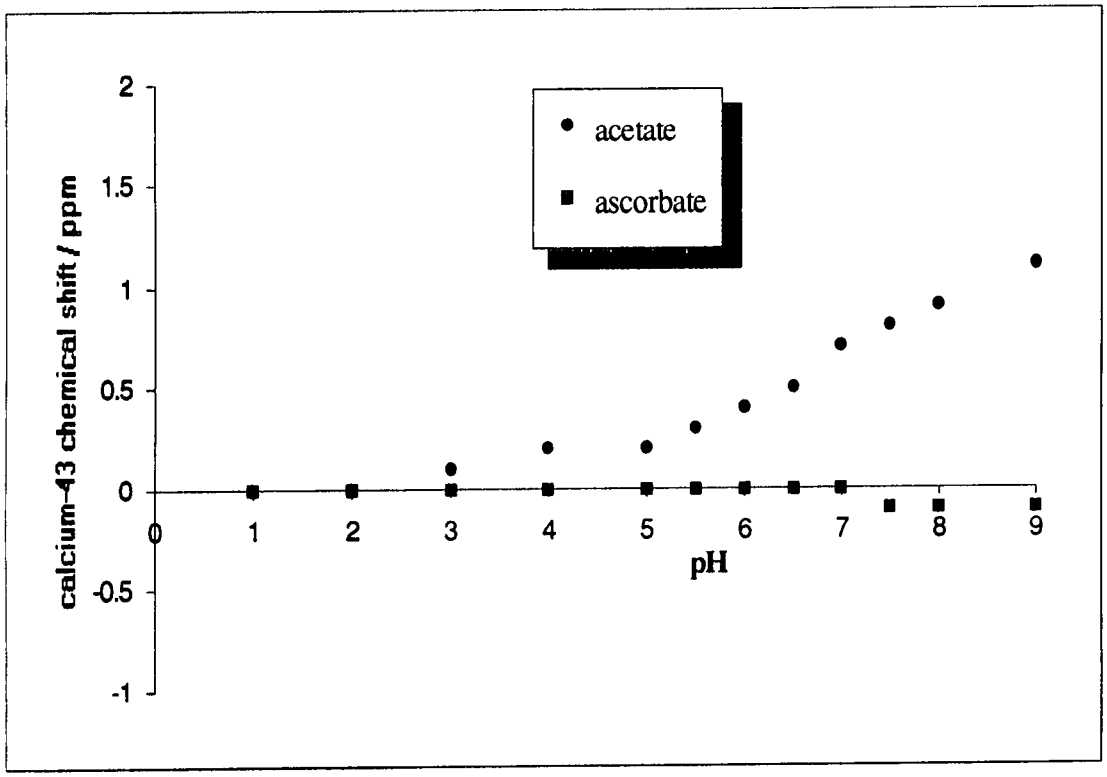

Fig 8.24 The dependence of ^{43}Ca chemical shift on pH for 1.0 mol dm^{-3} calcium chloride + 1.0 mol dm^{-3} sodium acetate and 1.0 mol dm^{-3} calcium chloride + 1.0 mol dm^{-3} sodium ascorbate solutions. The reference is 1.0 mol dm^{-3} calcium chloride solution. A positive sign indicates a high-frequency shift. No bulk susceptibility corrections were carried out.

8.4) CONCLUSION

Only one signal for calcium-43 was observed for all calcium salts studied. For halide and nitrate ions, no evidence of complexation with calcium was found in the literature. Therefore, only one calcium-43 signal was expected for calcium halide and nitrate salts as is observed experimentally. However, for the ascorbate ion, acetate ion, and sucrose, complexation by calcium is assumed to be possible. Even for these salts only one calcium-43 signal was observed, indicating that fast exchange of calcium ions takes place between complexed and free calcium.

Relaxation is strongly dependent on the viscosity of the solution as well as the symmetry of the calcium ion. At low concentrations of salt, especially aqueous halide and nitrate salts, the calcium ion is expected to be strongly hydrated. Thus, the symmetry of the calcium ion is expected to be high. For such a case, the relaxation of calcium-43 is expected to be slow. However, with increasing salt concentration the symmetrical environment of the calcium ion is expected to be distorted. The carboxylate and nitrate groups are assumed to produce a stronger distortion compared to the halide ions because these groups contain more than one oxygen atom which can bind the calcium ion. Thus, anions with more than one atom capable of binding the calcium ion are expected to have a faster relaxation rate compared to anions with only one atom for calcium binding. However, the relaxation of calcium-43 is also dependent on the size of the anion and the strength of the interaction between the calcium ion and the anion. Large anions and strong complexes are expected to produce fast relaxation.

The chemical shift of calcium-43 is strongly dependent on the interaction between the calcium ion and the anion. For strong calcium ion-anion interaction and formation of contact ion-pairs the chemical shift is expected to be large. The magnitude and direction of the chemical shift is dependent on the type of ion pair formed, and hence on the amount of overlap between the outer orbitals of the calcium ion and the anion.

Surprisingly, the chemical shift of calcium ascorbate solutions was found to be very small, suggesting the absence of contact ion-pair formation between the calcium and ascorbate ions. However, the relaxation of calcium ascorbate solutions was found to be extremely fast. The fast relaxation of calcium ascorbate solutions is assumed to be a direct result of the calcium ion symmetry distortion by the carboxylate groups of the ascorbate ion rather than a strong interaction between the calcium and ascorbate ions. If, however, a strong interaction between the calcium and ascorbate ions did take place then it is highly likely that contact ion-pairs would have been formed and as a result large chemical shifts would have been observed.

The possibility of studying the interaction of calcium with proteins is low unless enriched calcium-43 solutions are used. These, of course, are very expensive. Problems were encountered for observing the signal from a calcium ion complexed to lysozyme. The low natural abundance and low receptivity of calcium-43 as well as the line broadening effect on complexed calcium due to the lysozyme molecule made it impossible to observe the signal.

The low solubility of food systems in an aqueous medium has been found to be a major drawback for studying the interaction of these systems with calcium. Unfortunately, the interactions of calcium with citrate and phytate could not be studied due to the solubility problem.

REFERENCES

1) P. Grundvik, M. Gustavsson, I. Lindgren, G. Olsson, L. Robertson, A. Rosén and S. Svanberg, *Phys. Rev. Lett.*, 1979, **42**, 1528

2) S. Forsén and B. Lindman, *Ann. Rep. NMR Spec.* (ed. G.A. Webb), 1981, **11A**, 183

3) D.E. Woessner, B.S. Snowden, Jr. and A.G. Ostroff, *J. Chem. Phys.*, 1968, **49**, 371

4) L. Simeral and G.E. Maciel, *J. Phys. Chem.*, 1976, **80**, 552

5) *Calcium in Biological Systems*, Symposia of the Society for Experimental Biology, Symposium XXX, p.14, Cambridge University Press, Cambridge, 1976

6) H.G. Hertz, *Ber. Bunsenges. Phys. Chem.*, 1973, **77**, 531

7) C. Deverell, *Prog. NMR Spectroscopy*, 1969, **4**, 235

8) B. Lindman, S. Forsén and H. Lilja, *Chem. Scr.*, 1977, **11**, 91

9) M. Holz, S. Günther, O. Lutz, A. Nolle and P.G. Schrade, *Z. Naturforsch*, 1979, **34a**, 944

10) B. Lindman and S. Forsén, in NMR and the Periodic Table (ed. R.K. Harris and B.E. Mann), p.185, Academic Press, London, 1978

11) O. Lutz, A. Schwenk and A. Uhl, *Z. Naturforsch.*, 1973, **28a**, 1534

12) O. Lutz, A. Schwenk and A. Uhl, *Z. Naturforsch.*, 1975, **30a**, 1122

13) H.G. Hertz, *Ber. Bunsenges. Phys. Chem.*, 1973, **77**, 688

14) H.G. Hertz, M. Holz, R. Klute, G. Stalidis and H. Versmold, *Ber. Bunsenges. Phys. Chem.*, 1974, **78**, 24

15) H.G. Hertz, M. Holz, G. Keller, H. Versmold and C. Yoon, *Ber. Bunsenges. Phys. Chem.*, 1974, **78**, 493

16) T. Andersson, T. Drakenberg, S. Forsén, T. Wieloch and M. Lindström, *FEBS Lett.*, 1981, **123**, 115

17) D. Abbott, *Inorganic Chemistry*, p.252 & 254, Mills and Boon Ltd., London, 1971

18) *International Critical Tables*, **5**, p.14, McGraw-Hill Book Co., New York, 1929

19) R.H. Stokes and R. Mills, *Viscosity of Electrolytes and Related Properties*, Pergamon Press, London, 1965

20) J.D. Halliday, R.E. Richards and R.R. Sharp, *Proc. R. Soc. London*, 1969, **313A**, 45

21) C. Hall, R.E. Richards and R.R Sharp, *Proc. R. Soc. London*, 1974, **337A**, 297

22) P.W. Atkins, *Physical Chemistry*, p.368, 2nd Ed., Oxford University Press, London, 1982

23) R.C. Weast, *CRC Handbook of Chemistry and Physics*, p.8-35, 71st Ed., Chemical Rubber Co., Boca Raton, 1990/91

24) J. Mason and C.J. Jameson, in *Multinuclear NMR* (ed. J. Mason), p.51, Plenum Press, New York, 1987

25) R.G. Kidd and R.J. Goodfellow, in *NMR and the Periodic Table* (ed. R.K. Harris and B.E. Mann), p.195, Academic Press, London, 1978.

26) J.W. Emsley, J. Feeney and L.H. Sutcliffe, *High Resolution NMR Spectroscopy*, **2**, p.871, Pergamon Press Ltd., London, 1966

APPENDIX

Oral Presentations

Interactions of Water with Food Components, Studied by NMR.

Depertment of Chemistry, University of Durham, May 1994.

Poster Presentations

Interactions of Water with Food Components, Studied by NMR.

ICI Poster Competition, University of Durham, December 1993.

Colloquia, Lectures and Seminars from Invited Speakers

* *denotes attendance by the author.*

1991

October 17	Dr. J. A. Salthouse, University of Manchester Son et Lumiere - a demonstration lecture.
October 31	Dr. R. Keely, Metropolitan Police Forensic Science Modern Forensic Science.
* November 6	Prof. B. F. G. Johnson, University of Edinburgh Cluster-Surface Analogies.
November 7	Dr. A. R. Butler, St. Andrews University Traditional Chinese Herbal Drugs.
November 13	Prof. D. Gani, St. Andrews University The Chemistry of PLP Dependent Enzymes.
* November 20	Dr. R. More O'Ferrall, Dublin Some Acid-Catalysed Rearrangements in Organic Chemistry.
November 28	Prof. I. M. Ward, Leeds University The Science & Technology of Orientated Polymers.
December 4	Prof. R. Grigg, Leeds University Palladium Catalysed Cyclisation and Ion Capture Processes.
December 5	Prof. A. L. Smith, ex Unilever Soap Detergents and Black Puddings.
* December 11	Dr. W. A. Cooper, Shell Research Colloid Science, Theory, and Practice.

1992

January 16	Dr. N. J. Long, University of Exeter Metallocenophanes-Chemical sugar-tongs.
* January 22	Dr. K. D. M. Harris, University of St. Andrews Understanding the Properties of Solid Inclusion Compounds.
January 29	Dr. A. Holmes, University of Cambridge Cycloaddition Reactions in the Service of the Synthesis of Piperidine and Indolizidine Natural Products.
January 30	Dr. M. Anderson, Sittingbourne Research Centre, Shell Research Recent Advances in the Safe and Selective Chemical Control of Insect Pests.
* February 12	Dr. D. E. Fenton, University of Sheffield Polynuclear Complexes of Molecular Clefts as Models for Copper Biosites.
February 13	Dr. J. Saunders, Glaxo Group Research Limited Molecular Modelling in Drug Discovery.
* February 19	Prof. E. J. Thomas, University of Manchester Application of Organo-Stannanes to Organic Synthesis.

February 20	Prof. E. Vogel University of Cologne The Musgrave Lecture: Porphyrins, Molecules of Interdisciplinary Interest.
February 25	Prof. J. F. Nixon, University of Sussex Phospha-alkynes, New Building Blocks in Inorganic and Organometallic Chemistry.
* February 26	Prof. M. L. Hitchman, University of Strathclyde Chemical Vapour Deposition.
March 5	Dr. N. C. Billingham, University of Sussex Degradable Plastics- Myth or Magic?
* March 11	Dr. S. E. Thomas, Imperial College London Recent Advances in Organoiron Chemistry.
March 12	Dr. R. A. Hann, ICI Image Data Electronic Photography - An Image of the Future
March 18	Dr H. Maskill, University of Newcastle Concerted or stepwise fragmentation in a deamination-type reaction.
April 7	Prof. D.M. Knight, Philosophy Department, University of Durham Interpreting experiments: the beginning of electrochemistry.
May 13	Dr. J.-C. Gehret Ciba Geigy, Basel Some aspects of Industrial Agrochemical Research.
October 15	Dr. M. Glazer, Oxford University, & Dr. S. Tarling, Birbeck College, London It Pays to be British! - The Chemist's Role as an Expert Witness in Patent Litigation
October 20	Dr. H. E. Bryndza, Du Pont Central Research Synthesis, Reactions and Thermochemistry of Metal (Alkyl) Cyanide Complexes and Their Impact on Olefin Hydrocyanation Catalysis
October 22	Prof. A. Davies, University College London The Ingold-Albert Lecture: The Behaviour of Hydrogen as a Pseudometal
* October 28	Dr. J. K. Cockcroft, University of Durham Recent Developments in Powder Diffraction
October 29	Dr. J. Emsley, Imperial College, London The Shocking History of Phosphorus
November 4	Dr. T. P. Kee, University of Leeds Synthesis and Co-ordination Chemistry of Silylated Phosphites
November 5	Dr. C. J. Ludman, University of Durham Explosions, A Demonstration Lecture
* November 11	Prof. D. Robins, Glasgow University Pyrrolizidine Alkaloids: Biological Activity, Biosynthesis and Benefits
November 12	Prof. M. R. Truter, University College, London Luck and Logic in Host-Guest Chemistry
November 18	Dr. R. Nix, Queen Mary College, London Characterisation of Heterogeneous Catalysts
November 25	Prof. Y. Vallee. University of Caen Reactive Thiocarbonyl Compounds

November 25	Prof. L. D. Quin, University of Massachusetts, Amherst Fragmentation of Phosphorous Heterocycles as a Route to Phosphoryl Species with Uncommon Bonding
November 26	Dr. D. Humber, Glaxo, Greenford AIDS- The Development of a Novel Series of Inhibitors of HIV
* December 2	Prof. A.F. Hegarty, University College, Dublin Highly Reactive Enols Stabilised by Steric Protection
December 2	Dr. R. A. Aitken, University of St. Andrews The Versatile Cycloaddition Chemistry of $Bu_3P.CS_2$
December 3	Prof. P. Edwards, Birmingham University The SCI Lecture: What is Metal?
December 9	Dr. A. N. Burgess, ICI Runcorn The Structure of Perfluorinated Ionomer Membranes

1993

* January 20	Dr. D. C. Clary, University of Cambridge Energy Flow in Chemical Reactions
* January 21	Prof. L. Hall, Cambridge NMR- Window to the Human Body
January 27	Dr. W. Kerr, University of Strathclyde Development of the Pauson-Khand Annulation Reaction: Organocobalt Mediated Synthesis of Natural and Unnatural Products
January 28	Prof. J. Mann, University of Reading Murder, Magic and Medicine
February 3	Prof. S. M. Roberts, University of Exeter Enzymes in Organic Synthesis
* February 10	Dr. D. Gillies, University of Surrey NMR and Molecular Motion in Solution
February 11	Prof. S. Knox, Bristol University The Tilden Lecture: Organic Chemistry at Polynuclear Metal Centres
February 17	Dr. R. W. Kemmitt, University of Leicester Oxatrimethylenemethane Metal Complexes
February 18	Dr. I. Fraser, ICI Wilton Reactive Processing of Composite Materials
* February 22	Prof. D. M. Grant, University of Utah Single Crystals, Molecular Structure, and Chemical-Shift Anisotropy
February 24	Prof. C. J. M. Stirling, University of Sheffield Chemistry on the Flat-Reactivity of Ordered Systems
March 10	Dr. P. K. Baker, University College of North Wales, Bangor 'Chemistry of Highly Versatile 7-Coordinate Complexes'
March 11	Dr. R.A.Y. Jones, University of East Anglia The Chemistry of Wine Making
* March 17	Dr. R.J.K. Taylor, University of East Anglia Adventures in Natural Product Synthesis

March 24	Prof. I. O. Sutherland, University of Liverpool Chromogenic Reagents for Cations
* May 13	Prof. J. A. Pople, Carnegie-Mellon University, Pittsburgh, USA The Boys-Rahman Lecture: Applications of Molecular Orbital Theory
May 21	Prof. L. Weber, University of Bielefeld Metallo-phospha Alkenes as Synthons in Organometallic Chemistry
June 1	Prof. J. P. Konopelski, University of California, Santa Cruz Synthetic Adventures with Enantiomerically Pure Acetals
June 2	Prof. F. Ciardelli, University of Pisa Chiral Discrimination in the Stereospecific Polymerisation of Alpha Olefins
June 7	Prof. R. S. Stein, University of Massachusetts Scattering Studies of Crystalline and Liquid Crystalline Polymers
June 16	Prof. A. K. Covington, University of Newcastle Use of Ion Selective Electrodes as Detectors in Ion Chromatography
June 17	Prof. O. F. Nielsen, H.C. Ørsted Institute, University of Copenhagen Low-Frequency IR- and Raman Studies of Hydrogen Bonded Liquids
September 13	Prof. Dr. A.D. Schlüter, Freie Universität, Berlin, Germany Synthesis and Characterisation of Molecular Rods and Ribbons
September 13	Dr. K.J. Wynne, Office of Naval Research, Washington, USA Polymer Surface Design for Minimal Adhesion
September 14	Prof. J.M. DeSimone, University of North Carolina, Chapel Hill, USA. Homogeneous and Heterogeneous Polymerisations in Environmentally Responsible Carbon Dioxide
September 28	Prof. H. Ila, North Eastern Hill University, India Synthetic Strategies for Cyclopentanoids via Oxoketene Dithioacetals
October 4	Prof. F.J. Feher, University of California, Irvine, USA Bridging the Gap between Surfaces and Solution with Sessilquioxanes
* October 14	Dr. P. Hubberstey, University of Nottingham Alkali Metals: Alchemist's Nightmare, Biochemist's Puzzle and Technologist's Dream
* October 20	Dr. P. Quayle, University of Manchester Aspects of Aqueous ROMP Chemistry
October 21	Prof. R. Adams, University of South Carolina, USA Chemistry of Metal Carbonyl Cluster Complexes: Development of Cluster Based Alkyne Hydrogenation Catalysts
October 27	Dr. R.A.L. Jones, Cavendish Laboratory, Cambridge Perambulating Polymers
* November 10	Prof. M.N.R. Ashfold, University of Bristol High Resolution Photofragment Translational Spectroscopy: A New Way to Watch Photodissociation
* November 17	Dr. A. Parker, Rutherford Appleton Laboratory, Didcot Applications of Time Resolved Resonance Raman Spectroscopy to Chemical and Biochemical Problems

November 24	Dr. P.G. Bruce, University of St. Andrews Structure and Properties of Inorganic Solids and Polymers
November 25	Dr. R.P. Wayne, University of Oxford The Origin and Evolution of the Atmosphere
December 1	Prof. M.A. McKervey, Queen's University, Belfast Synthesis and Applications of Chemically Modified Calixarenes
* December 8	Prof. O. Meth-Cohn, University of Sunderland Friedel's Folly Revisited- A Super Way to Fused Pyridines
December 16	Prof. R.F. Hudson, University of Kent Close Encounters of the Second Kind

1994

January 26	Prof. J. Evans, University of Southampton Shining Light on Catalysts
* February 2	Dr. A. Masters, University of Manchester Modelling Water Without Using Pair Potentials
February 9	Prof. D. Young, University of Sussex Chemical and Biological Studies on the Coenzyme Tetrahydrofolic Acid
February 16	Prof. K.H. Theopold, University of Delaware, USA Paramagnetic Chromium Alkyls: Synthesis and Reactivity
February 23	Prof. P.M. Maitlis, University of Sheffield Across the Border: From Homogeneous to Heterogeneous Catalysis
* March 2	Dr. C. Hunter, University of Sheffield Noncovalent Interactions between Aromatic Molecules
* March 9	Prof. F. Wilkinson, Loughborough University of Technology Nanosecond and Picosecond Laser Flash Photolysis
March 10	Prof. S.V. Ley, University of Cambridge New Methods for Organic Synthesis
March 25	Dr. J. Dilworth, University of Essex Technetium and Rhenium Compounds with Applications as Imaging Agents
April 28	Prof. R.J. Gillespie, McMaster University, Canada The Molecular Structure of some Metal Fluorides and Oxofluorides: Apparent Exceptions to the VSEPR Model
May 12	Prof. D.A. Humphreys, McMaster University, Canada Bringing Knowledge to Life